

**STATISTICAL AND BIOMECHANICAL PREDICTION
OF AUTOMOBILE DRIVING POSTURE**

by

Matthew Paul Reed

**A dissertation submitted in partial fulfillment
of the requirements for the degree of
Doctor of Philosophy
(Industrial and Operations Engineering)
in The University of Michigan
1998**

Doctoral Committee:

**Professor Don B. Chaffin, Co-chair
Senior Research Scientist Lawrence W. Schneider, Co-chair
Senior Research Scientist James A. Ashton-Miller
Professor W. Monroe Keyserling**

UMI Number: 9825331

**UMI Microform 9825331
Copyright 1998, by UMI Company. All rights reserved.**

**This microform edition is protected against unauthorized
copying under Title 17, United States Code.**

UMI
300 North Zeeb Road
Ann Arbor, MI 48103

© Matthew Paul Reed 1998
All Rights Reserved

For Miriam

ACKNOWLEDGMENTS

I am going to break with the traditional order of dissertation acknowledgments to begin by thanking my most tireless champion and supporter, Miriam Manary. As a gifted fellow researcher, she supervised the conduct of several of the studies that were sources of data for this work and contributed, through her ideas and suggestions, to some of the best parts of this thesis. But, even more, she had the great courage to marry me, a Ph.D. candidate who had not even an outline of a draft. She bolstered my spirits when the data were uncooperative, tugged me gently back when I drifted beyond my scope, and nudged me forward when my ambition exceeded my endurance. I will be always grateful to her for being my steady friend through this process.

I am deeply indebted to Larry Schneider, my mentor and supervisor at UMTRI, who grew me from seed, so to speak, nurturing a garden-variety mechanical engineering graduate into a biomechanics researcher. He has provided the ideal environment for me to discover and apply my abilities, giving me the freedom to grow in new directions and the supportive framework to be successful. Larry initiated and encouraged my foray into graduate school with the funding and flexibility that I needed to be able to work and study. His leadership in obtaining support from industry meant that there were many concurrent studies from which I could draw data for this research. Finally, his friendship and perspective through the sometimes-arduous doctoral process has maintained my optimism for the post-doctoral future.

Don Chaffin, my IOE advisor and committee co-chair, has inspired me with the depth of his experience and the breadth of his accomplishment, instilling in me the focus and determination necessary for a successful dissertation. His encouragement to consider the interrelation between my research and other areas of biomechanics greatly improved

the cohesiveness and applicability of the thesis. It has been a privilege to work and study with him. The other two members of my committee, Monroe Keyserling and James Ashton-Miller, provided unique insight and asked thought-provoking questions that steered me toward more productive experiments and analyses. Monroe's focus on academic rigor, and James' encouragement to develop my models more fully, spurred me to strive toward a higher standard.

I would like to thank the many other people within the IOE department who helped me along my path. Although my home base was at UMTRI, rather than in the IOE labs, the IOE faculty and staff were ever willing to help. Some of the many faculty and staff who contributed to my very enjoyable graduate education were John Birge, Fran Bourdas, Jim Foulke, Gary Herrin, Bernard Martin, and Chuck Wooley. Because I spent most of my time at UMTRI, I missed out on much of the camaraderie among the other students at the Center for Ergonomics, but I'd like to acknowledge three former graduate students from whom I learned, and continue to learn, a great deal. Ulrich Raschke was one of the first fellow students to engage me in discussing my research, a daring enterprise not for people who need to be anywhere anytime soon. Through many long discussions of hypotheses and experiments and models, he became a good friend and trusted advisor. His assistance in interpreting the previous posture modeling work enabled me to put my own research into context. Maury Nussbaum, who has the patient temperament of a good teacher, piqued my interest in innovative modeling strategies and provided his torso model, along with a personal tutorial, for use in this research. Xudong Zhang, who preceded me at the Center in studying in-vehicle postures, contributed some important ideas and analysis strategies through his dissertation work.

I could not have conducted this research or written this dissertation without the tremendous assistance of the many talented people with whom I work at UMTRI. Every one of the research projects leading to this dissertation was truly a team effort. Brian Eby, Jim Whitley, and Stewart Simonett constructed accurate and functional laboratory

fixtures from my vague sketches and instructions, and Tracey Melville produced photo documentation of every phase of the research. I am deeply grateful to Beth Eby and Cathy Harden, who collected much of the posture data. Their efficiency, accuracy, and attention to detail were essential to the success of these studies. My sincere thanks go to Leda Ricci, who has been my friend and confidant throughout my years at UMTRI. Her substantive contributions to this work include helping to edit the manuscript and to coordinate much of the research, but she has also provided me with the personal support and encouragement that I needed to see this effort through.

Two of my fellow researchers at UMTRI deserve special mention, because I draw continually on their knowledge and experience to help me find my way through difficult problems. Carol Flannagan's office is my statistical mountain top; I seek her wisdom when my data are heteroscedastic, my contrast is insignificant, and my mien is weighted. She is a knowledgeable guide for an engineer who persists in applying mechanistic principles to processes for which the best models leave a quarter of the variance unexplained. She is able to draw for me a well-annotated blueprint of the theoretical structure that undergirds the analyses on which I rely. Ron Roe recently joined UMTRI after retiring from General Motors, having established himself as a world-leading expert in occupant packaging. Ron's incredibly complete knowledge of packaging practices and the data on which they are based is a tremendous resource for someone like me who is fairly new to these issues. I thank Ron for his patient tutelage in the often arcane world of industry practice.

I am also grateful to two colleagues from Germany who have done much to further my understanding of posture prediction in automobiles. Andreas Seidl's work in the development of the posture prediction algorithms underlying the RAMSIS software manikin was truly innovative, and provided considerable inspiration to me in my work. Much of my knowledge of Andreas' research came through many long and fruitful

discussions with Hartmut Speyer, who I thank for his intelligent and frank discussions of so many posture prediction issues.

Research costs money, and particularly research with large numbers of subjects and expensive test equipment, like automobiles. I and my fellow researchers in the UMTRI Biosciences Division have had the privilege of conducting research for many different corporations and organizations. The work in this thesis was supported in part by grants to ASPECT, a research and development program producing new tools for vehicle and seat design. ASPECT participants are Atoma, BMW, Chrysler, Ford, General Motors, Johnson Controls, Lear, PSA, Toyota, Volkswagen, and Volvo. The American Automobile Manufacturers Association also supported part of the research through grants to UMTRI to support the development of new industry-standard packaging models. Special thanks goes to two groups who provided the early seed money needed to initiate my dissertation research, and who supported much of the analysis and writing. Herman Miller, Inc., through the leadership of Bill Dowell and Jim Long, and the Great Lakes Center for Truck and Transit Research, under the direction of Tom Gillespie, gave the project a critical boost with their support.

TABLE OF CONTENTS

DEDICATION	ii
ACKNOWLEDGMENTS	iii
LIST OF FIGURES	x
LIST OF TABLES	xiv
CHAPTER	
1. INTRODUCTION	1
1.1 Thesis Statement	1
1.2 Applied Problem	1
1.3 Theoretical Problem	3
1.4 Research Objectives and Goals	10
1.5 Dissertation Organization	11
1.6 References	13
2. A TECHNIQUE FOR REPRESENTING AUTOMOBILE OCCUPANT POSTURE USING A KINEMATIC MODEL BASED ON SURFACE BODY LANDMARK LOCATIONS	17
2.1 Introduction	17
2.2 Kinematic Model	20
2.3 Experimental Method	26
2.4 Body Landmarks	27
2.4 Calculation of Joint Locations	30
2.5 Calculation Diagrams for All Joints	41
2.6 Discussion	50
2.7 References	51
3. THE EFFECTS OF PACKAGE, SEAT, AND ANTHROPOMETRIC VARIABLES ON DRIVING POSTURE	53
3.1 Abstract	53
3.2 Introduction	53
3.3 Methods	55
3.4 Results	65
3.5 Summary and Discussion	72
3.6 Conclusions	74
3.7 References	75

4.	THE EFFECTS OF FORWARD VISION RESTRICTION ON DRIVER POSTURE	77
4.1	Abstract	77
4.2	Introduction	77
4.3	Methods — Laboratory Study	79
4.4	Methods — Vehicle Study	86
4.5	Results — Laboratory Study	88
4.6	Results — Vehicle Study	94
4.7	Discussion and Conclusions	94
4.8	References	96
5.	DEVELOPMENT AND EVALUATION OF STATISTICAL POSTURE-PREDICTION MODELS FOR AUTOMOBILE DRIVING	98
5.1	Abstract	98
5.2	Introduction	98
5.3	Data Sources	101
5.4	Body Segment Scaling	103
5.5	General Model Formulation	104
5.6	Specific Model Formulations	111
5.7	Model Comparison	124
5.8	Model Assessment: Original Data	126
5.9	Model Assessment: Vehicle Data	132
5.10	Discussion and Conclusions	134
5.11	References	139
6.	FORCES EXERTED ON THE STEERING WHEEL IN NORMAL DRIVING POSTURES	142
6.1	Abstract	142
6.2	Introduction	142
6.3	Methods	143
6.4	Results	146
6.5	Discussion and Conclusions	154
6.6	References	156
7.	BIOMECHANICAL ANALYSIS AND PREDICTION OF NORMAL AUTOMOBILE DRIVING POSTURE	157
7.1	Abstract	157
7.2	Introduction	157
7.3	Methods	164
7.4	Effects of Seatback Angle and Sitting Procedure on Trunk Posture	172
7.5	Muscle Activity Analysis	176
7.6	Driving Posture Simulations	184
7.7	Discussion and Conclusions	197
7.8	References	202

8.	SUMMARY AND RECOMMENDATIONS	205
8.1	Review of Objectives	205
8.2	Summary of Findings	205
8.3	Principal Contributions	218
8.4	Recommendations for Future Research	220
	APPENDIX: VEHICLE PACKAGING TERMINOLOGY AND PRACTICES	224
	BIBLIOGRAPHY	228

LIST OF FIGURES

Figure	Page
1.1. Schematic of the hypothesized posture selection process.	5
2.1. Kinematic model showing segments used to represent posture.	23
2.2. Joints in kinematic model used to represent vehicle occupant posture.	24
2.3. Body landmarks used to calculate internal joint locations and segment orientations.	29
2.4. Illustration of pelvis scaling dimensions: pelvis width (PW), pelvis height (PH), and pelvis depth (PD).	33
2.5. Location of the hip joint in the sagittal plane relative to the ASIS and pubic symphysis landmarks.	34
2.6. Method used to estimate lower lumbar joint (L5/S1) location from the data in Reynolds et al. (1981).	36
2.7. Acromion location comparison between current definition (N = 12 midsize males) and Robbins (N = 25 midsize males).	40
2.8. Calculation techniques for upper neck joint.	42
2.9. Calculation method for lower neck joint and upper lumbar joint.	43
2.10. Calculation method for the shoulder joint.	44
2.11. Pelvis coordinate system, adapted from Reynolds et al. (1981).	45
2.12. A sagittal view of surface and bone pelvis coordinate systems based on measured landmark locations (not to scale).	46
2.13. Location of hip and lower lumbar joints in XZ plane relative to bone coordinate system (not to scale).	47
2.14. Calculation procedure for knee and ankle joints.	49
2.15. Calculation procedure for elbow joint.	50
3.1. Vehicle package geometry.	57
3.2. Schematic of vehicle mockup, showing adjustment axes.	59

3.3.	SW-BOFX versus seat height in 158 production vehicles.	61
3.4.	Seat cushion angle distribution for 65 production vehicles.	61
3.5.	Kinematic linkage representation of driving posture.	64
3.6.	Illustration of posture variables.	65
3.7.	Steering-wheel-position and seat-cushion-angle effects on HipX in Phases 1 and 2, Configurations 1 through 10.	66
4.1.	Subject in vehicle mockup.	80
4.2.	Vehicle mockup dimensions (mm).	81
4.3.	Simulator road scene projection schematic.	82
4.4.	Typical simulator road scene showing obstruction (cow) in right lane (displayed in color).	83
4.5.	Kinematic linkage representing driving posture.	85
4.6.	Vehicle dimensions (mm).	87
4.7.	Illustration of variable definitions.	89
4.8.	Illustration of the effects of instrument panel height condition and gender on posture variables.	93
4.9.	Illustration of average posture change resulting from a 150-mm increase in instrument panel height.	93
5.1.	Vehicle package geometry.	104
5.2.	Definitions of kinematic linkage and posture measures.	107
5.3.	Schematic of Cascade Prediction Model (CPM).	113
5.4.	Schematic of Independent Prediction Model (IPM).	118
5.5.	Schematic of Optimization Prediction Model (OPM).	120
5.6.	Posture variables used in OPM.	121
5.7.	Empirical posture likelihood (arbitrary units) as a function of knee angle and torso angle for midsize-male anthropometry in a mid-range vehicle package.	124
5.8.	Comparison of model predictions for a midsize male at two steering wheel positions for a mid-seat-height vehicle.	125
5.9.	Comparison of model predictions for a small female and a large male in a typical high-seat-height vehicle.	126

5.10.	Observed eye locations and predictions using three models.	128
5.11.	Observed-predicted eye locations for the CPM, showing marginal histograms and a 95 percent bivariate normal density ellipse.	129
5.12.	Illustration of CPM 95% confidence ellipsoids in the XZ (side-view) plane for the mean and individual observations of eye location.	131
6.1.	Load cell mounting in steering column and load cell coordinate system.	144
6.2.	Upper-extremity posture variables.	145
6.3.	Diagram for determination of Y-axis hand moment.	147
6.4.	Horizontal force on the steering wheel for 10 subjects.	149
6.5.	Vertical force on the steering wheel for 10 subjects.	149
6.6.	Y-axis moment on the steering wheel for 10 subjects.	149
6.7.	Schematic of planar, rigid-body upper-extremity model (scale in mm).	150
6.8.	Simulated horizontal forces on the steering wheel from both arms for loose-arm-hang (dashed) along with subject data from Figure 6.4.	151
6.9.	Predicted elbow (—) and shoulder (--) moments when average observed steering wheel forces are applied to the model of average upper-extremity segment lengths and masses (single arm).	152
6.10.	Triceps muscle activity versus elbow angle (five data points per subject), including second-order curve fits to each subject's data.	153
6.11.	Comparison of thorax moments due to upper extremities in loose-arm-hang simulation (— —) and in simulation with average measured hand forces (—).	154
7.1.	Schematic of proposed posture selection process.	158
7.2.	Laboratory vehicle mockup.	165
7.3.	Posterior electrode locations.	166
7.4.	Back SEMG normalization trial.	167
7.5.	Posterior (left) and anterior (right) neck normalization trials.	168
7.6.	Typical unsupported slump posture.	169
7.7.	Schematic illustration of posture variables.	173
7.8.	Between subjects comparison of seatback angle effects on head angle and abdomen angle.	176
7.9.	NEMG from three back sites with two hand positions.	178

7.10.	NEMG from three back sites with two hand positions versus seatback angle, with two high-responding subjects excluded.	179
7.11.	NEMG (%) at the T12 electrode site by seatback angle for preferred and prescribed sitting procedure trials.	181
7.12.	Log NEMG at the T12 electrode site, showing means and standard error bars.	182
7.13.	Neck muscle NEMG by head position condition.	183
7.14.	Effects of steering wheel position changes on anterior deltoid and triceps muscle activity.	184
7.15.	Effects of elbow angle changes on anterior deltoid and triceps muscle activity.	184
7.16.	Schematic of planar linkage model of driver, showing segments and centers of mass.	185
7.17.	Free-body diagram of the thorax in the average preferred driving posture.	186
7.18.	Illustration of average torso segment kinematics with changes in seatback angle, from -10 degrees with respect to the mean preferred seatback angle (22.5 degrees) to +10 degrees.	188
7.19.	Eye height versus net moment at T12/L1 due to steering wheel interaction and upper-body mass.	189
7.20.	Thoracolumbar extensor activity (T12 electrode site) versus T12/L1 moment predicted by the biomechanical model.	189
7.21.	Preferred driver posture (thick lines), contrasted with posture X from Figure 7.19 (thin lines).	190
7.22.	Preferred driver posture (thick lines) contrasted with preferred passenger posture (thin lines).	190
7.23.	Passive lumbar moments relative to lumbar flexion adapted from Nyquist and Murton (—), Dolan et al. (— —), and Nussbaum and Chaffin (— —).	193
7.24.	Average unsupported slump posture (sitting).	194
7.25.	Three alternative relationships between lumbar flexion relative to standing and passive T12/L1 moment.	195
7.26.	Driving posture analysis presented in Figure 7.19 with available passive extension moment included, using the scaled Dolan et al. flexion/moment relationship (center), the linear relationship (right), and the bilinear relationship (left).	196
8.1.	Schematic of proposed posture-selection process.	206

LIST OF TABLES

Table		
2.1	Definitions of Body Landmarks	28
2.2	Data Sources Used by Robbins (1985a) to Estimate Joint Locations	32
2.3	Comparison of Hip Joint Location Methods: Mean Scaling Relationships	34
2.4	Scaling Relationships for L5/S1 from Reynolds et al. (1981)	36
2.5	Landmarks Used To Define and Scale Joint Location Vectors	38
2.6	Flesh Margin Correction Vectors in the Surface Pelvis Coordinate System	46
2.7	Mean Hip Joint Scaling Relationships from Seidel et al. (1995)	48
2.8	Mean Lower Lumbar Joint Scaling Relationships Using Data from Reynolds et al. (1981)	48
3.1	Subject Pool	56
3.2	Test Conditions	60
3.3	Posture Variable Definitions	64
3.4	Effects of Steering Wheel Position and Seat Cushion Angle	66
3.5	Regression Equations Predicting Posture Variables	70
3.6	Range Estimates Using Regression Equations	70
4.1	Subject Anthropometric Summary — Laboratory Testing	79
4.2	Tested Instrument Panel Heights	83
4.3	Subject Anthropometric Summary — Laboratory Testing	86
4.4	Possible Behaviors to Compensate for a Forward Vision Restriction	89
4.5	Repeatability of Driving Posture	90
4.6	Summary of IP Height Effects: Mean of All Subjects	92
4.7	Summary Results from Vehicle Study (N=32)	94

5.1	Subject Pool	102
5.2	Test Conditions by Phase	102
5.3	Segment Length Scaling Fractions	103
5.4	Package Geometry Inputs	106
5.5	Regression Models	110
5.6	Regression Models	110
5.7	Average Change in Segment Orientation with Change in Eye-to-Hip-Vector Angle	115
5.8	Overall Average Torso Segment Angles	115
5.9	Angle Distribution Parameters for OPM	122
5.10	Covariance Matrix (Σ)	123
5.11	Comparison of Model Predictions vs. Observed Eye Locations in Original Data	127
5.12	Prediction Error Standard Deviations by Stature Group for CPM	130
5.13	Vehicle Characteristics	132
5.14	Comparison of Model Predictions vs. Observed Eye Locations in Vehicle Data	133
6.1	Subject Anthropometric Measures	144
6.2	Average Forces and Moments Exerted by the Hands On the Steering Wheel	148
6.3	Estimated Mean Segment Lengths and Masses	150
7.1	Subject Anthropometric Measures	164
7.2	Posture Variables	173
7.3	Effects of Seatback Angle and Sitting Procedure on Driving Posture	174
7.4	Test Variable Effects on Log NEMG by Electrode Site	180
7.5	Starting Segment Orientations and Motion Distribution Parameters	187

CHAPTER 1

INTRODUCTION

1.1 Thesis Statement

The driving posture selection process can be better understood by examining the effects of vehicle and seat design factors on posture in vehicle mockups. Posture prediction models based on laboratory posture measurements can accurately predict in-vehicle driving postures, and can demonstrate the quantitative tradeoffs drivers make when selecting a posture. A biomechanical model using a muscle activity reduction criterion can accurately predict average driving posture and provide insight into the posture selection process.

1.2 Applied Problem

Vehicle interior design is now performed primarily in computer software, using computer-aided design (CAD) tools to create three-dimensional renderings of proposed component shapes and positions. In the recent past, interiors were laid out on full-size paper drawings, using articulated plastic templates to represent the driver and passengers. These two-dimensional tools have been adapted to the three-dimensional CAD world, but are increasingly seen as anachronistic holdovers from an era when a design did not exist in three dimensions until it was mocked up out of wood and metal. Now, three-dimensional, whole-body human representations can be placed in a software mockup of a vehicle to simulate a wide range of activities. These new human models have the potential to revolutionize vehicle design by allowing the designer to test a prototype without ever constructing hardware, reducing the design time and potentially improving the comfort and accommodation of the users.

Porter et al. (1993) briefly reviewed the features of 13 human modeling systems in use prior to 1993 with potential application to vehicle design. Software development moves rapidly, however, and some of the systems that are commercially available as of this writing, including Genicom SafeWork, TecMath RAMSIS, and Transom Jack, are not included in the Porter et al. review. Most of the commercially available human models include substantial anthropometric scaling capability, allowing the model to be configured to represent geometrically the exterior dimensions of a wide range of potential vehicle occupants, but only RAMSIS is known to include any significant prediction capability for vehicle occupant postures (Seidl, 1994).

There are relatively few published studies applicable to posture prediction for vehicle occupants. In most studies of driver positioning, data are presented only in the aggregate or in terms of a population distribution, so the findings are not applicable to human-model posture. Studies have addressed eye location (Meldrum, 1965; Devlin and Roe, 1968; Hammond and Roe, 1972; Mourant et al., 1978; Arnold et al., 1985; Parkin et al., 1993) and driver-selected seat position (Schneider et al., 1979; Phillipart et al., 1985) but none of these studies allow simultaneous prediction of seat position and eye location for a particular vehicle and driver.

Posture prediction for drivers is often discussed in terms of comfortable joint angles (Babbs, 1979; Bohlin et al., 1978; Rebiffe, 1980; Grandjean, 1980; Weichenrieder and Haldenwanger, 1986; Asano et al., 1989; Judic et al., 1993). The assumption of this approach is that people will tend to choose joint angles that are close to the center of the range of motion for the joint, where comfort is assumed to be greatest. However, there is usually no discussion of how deviations from the optimal joint angles should be traded off in the usual case in which the optimal angles are kinematically inconsistent with the task constraints. In general, the comfort-angle approach is applicable to selecting component locations in design, but is ill-suited for posture prediction in a given design without a systematic strategy for dealing with deviations from the target values.

Seidl (1994) has presented the most complete approach to whole-body driving posture prediction to date. Using posture data collected in a laboratory vehicle mockup, he developed an optimization-based approach that is now used with the RAMSIS human model. Seidl's approach selects a posture consisting of the set of joint angles that is empirically most likely within the specified kinematic constraints. This technique relies on posture data collected from three vehicle configurations, and can be interpreted as representing an analog of the driver's inherent posture-selection process, but there are several important limitations. The data on which the predictions are based are proprietary, and cannot, without considerable effort, be applied to a human model having a different linkage. Because the optimization approach does not lend itself to a closed-form statement, the accuracy of the predictions cannot be assessed without use of the RAMSIS manikin. More importantly, the posture prediction method itself, while an innovative approach for predicting postures in novel situations, may be difficult to use as accurately as other methods in well-studied situations, such as normal driving postures.

1.3 Theoretical Problem

Empirical studies of task postures, such as those presented in this dissertation, provide evidence that there is an internal, largely unconscious process that governs posture selection. When asked to choose a comfortable driving posture, people do not choose randomly from among the feasible postures, but rather appear to trade off task performance capability and comfort in a complex way to achieve a suitable posture. Understanding this posture adaptation process is critical to improving the fit between humans and tasks so that comfort, safety, and performance can be improved.

The driving task can be divided into functional subtasks, each concerned with one aspect of the process. At a basic level, the driver must perform, simultaneously, each of the following functions:

- lane tracking,
- speed control,
- obstacle avoidance, and
- navigation.

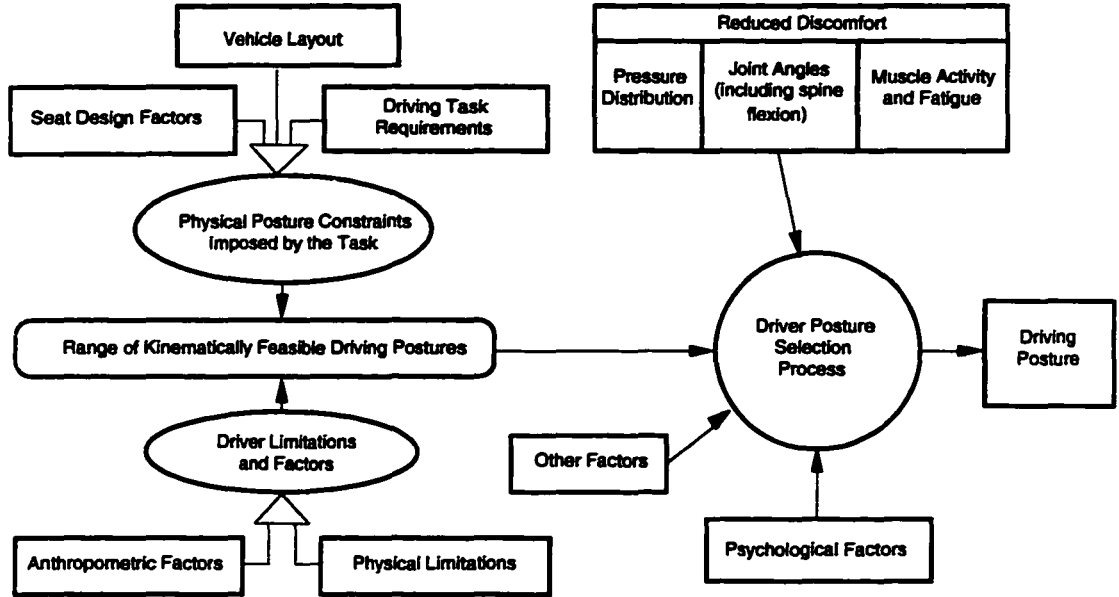
With regard to posture analysis, the primary importance of these functional subtasks lies in the physical restrictions that they place on driving posture. From this perspective, the driving task imposes the following physical requirements:

- vision to the external environment,
- manipulation of steering wheel,
- manipulation of pedal controls,
- vision to internal displays, and
- manipulation of shifters and other hand controls.

These requirements place physical restrictions on the locations of the hands, feet, and eyes of the driver. The first four restrictions are nearly constant during most driving scenarios, and hence are of primary importance. The driver must be able simultaneously to see out of the vehicle, manipulate the pedal controls, and turn the steering wheel. Thus, a driving posture must be kinematically consistent with exterior vision, particularly in front of the vehicle, hand reach to the steering wheel, and foot reach to the pedals.

Figure 1.1 describes in detail the hypothesized process of driving posture selection. The vehicle interior design, including the control layouts, seat design, and adjustments provided to the driver, represent a set of kinematic constraints on the posture. The driver has a particular body size and physical limitations, such as strength and joint range of motion, that interact with the kinematic constraints imposed by the vehicle to determine the range of feasible driving postures. These are postures that meet the physical eye, hand, and foot position requirements of driving within the driver's limitations. For a small person, the foot position on the pedals, combined with short lower extremities, may require a forward seat position that brings the torso so close to the steering wheel that there is only a small range of feasible seat positions. The range of torso recline available to small drivers is often limited by forward vision restrictions. For tall drivers, the range of seat-track travel frequently limits fore-aft hip position, and headroom restricts torso posture. The range of feasible postures is generally largest for people who are close to anthropometric means and smallest for those at the extremes, with some people unable to drive particular vehicle designs. While the range of

SCHEMATIC OF THE HYPOTHESIZED POSTURE SELECTION PROCESS



Factors Potentially Affecting Driving Posture

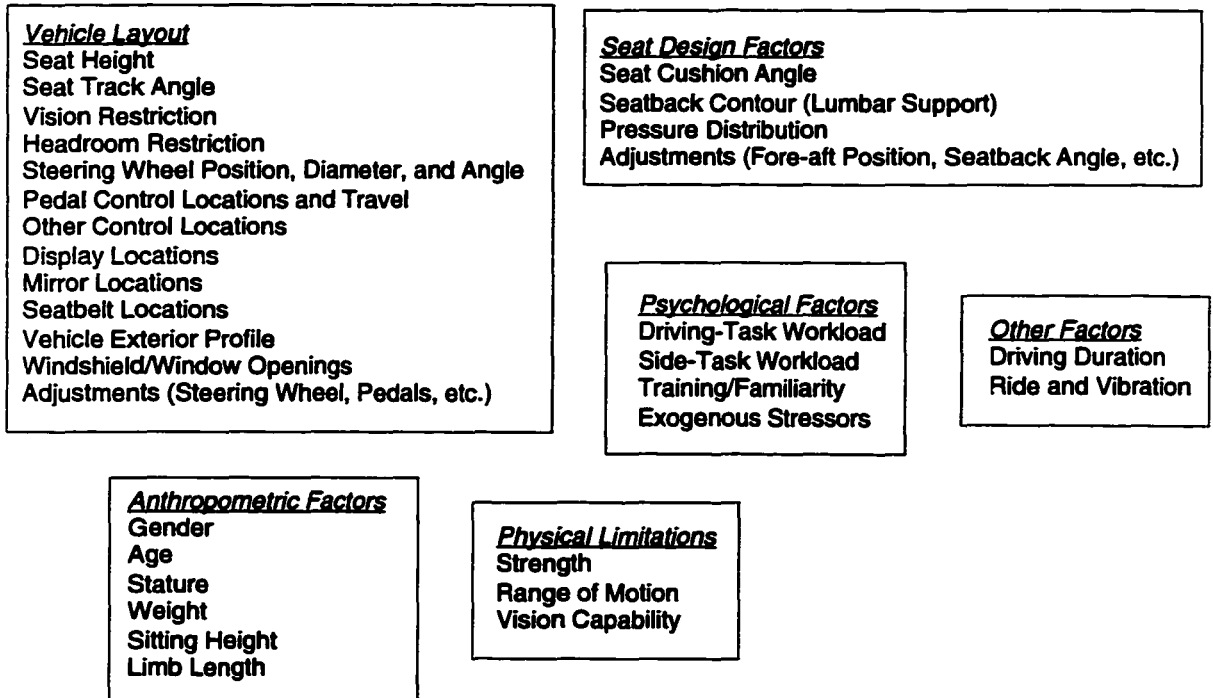


Figure 1.1. Schematic of the hypothesized posture selection process.

kinematically feasible postures can readily be determined by manipulating an anthropometrically scalable manikin, it quickly becomes apparent that for most body sizes there is a fairly broad range of feasible postures. How, then, do people choose their driving postures from within the feasible range?

Previous research has documented posture selection behavior under a variety of driving conditions and provides some guidance for the current work. Among the many factors listed in Figure 1.1, some are more important than others in determining driving posture, and some have been addressed in previous research. Vehicle geometric factors have received the most research attention. Parameters of the population distribution of eye locations have been predicted primarily by seat height (Devlin and Roe, 1968). Schneider et al. (1979) identified steering wheel position and seat height as important factors affecting driver-selected seat position. Phillipart et al. (1984) developed a model of driver-selected seat position using seat height as the sole predictor variable. Phillipart et al. (1985), using a more carefully controlled experimental design, found that steering wheel position and header location, in addition to seat height, affect driver-selected seat position. Recently, Flannagan et al. (1996) presented a more complex model of seat position that includes seat height, fore-aft steering wheel position, seat cushion angle, and transmission type.

The role of comfort or discomfort in driving postures has received considerable attention (see Reynolds, 1993, and Reed et al., 1994 for reviews). Most researchers have found it to be most useful to consider discomfort, rather than comfort, and to quantify the means by which discomfort can accrue (Branton, 1969). The primary sources of discomfort can be divided into three interrelated categories: pressure distribution, joint angles, and muscle activity.

The distribution of pressure at the interface between the sitter and seat can contribute to tissue ischemia and discomfort related to mechanical stress on the tissues. Pressure distribution measurement has recently been widely adopted for automobile seat

evaluation, but there are few published quantitative models relating pressure distribution to posture or comfort (Matsuoka and Hanai, 1988; Treaster and Marras, 1989; Matsushashi, 1991; Gross et al., 1993; Pywell, 1993). Reed et al. (1995) and Reed and Schneider (1996) studied the postural responses of drivers to changes in lumbar support prominence, and found that large changes in seatback contour cause only small changes in driving posture. Since the changes in lumbar support prominence were accompanied by considerable changes in peak pressure in the lumbar area, pressure distribution alone may not be an important determinant of driving posture.

Posture has been frequently addressed in relation to discomfort, particularly with regard to joint angles (Lay and Fisher, 1940; Babbs, 1979; Bohlin et al., 1978; Rebiffe, 1980; Grandjean, 1980; Weichenrieder and Haldenwanger, 1986; Asano et al., 1989; Judic et al., 1993; Verriest and Alonzo, 1986; Seidl, 1994). Muscle activity in driving and its potential relation to fatigue have also been examined, generally in relation to posture (Andersson et al., 1974b; Hosea et al., 1986; Sheridan et al., 1991). The interrelation of these factors is apparent, as a posture change will often change both the distribution of pressure and the muscle activity.

Although relationships between muscle activity and posture have been examined in many ergonomic studies relating to general seating situations (see Chaffin and Andersson, 1991, for a review), relatively few studies have examined muscle activity in driving postures (Andersson et al., 1974b; Hosea et al., 1986; Sheridan et al., 1991). In general, low muscle activity is assumed to be a desirable attribute of work postures (Chaffin and Andersson, 1991), and seat designs and orientations that produce lower muscle activity levels are recommended (Andersson et al., 1974b; Hosea et al., 1986). Sheridan et al. (1991) found evidence of fatigue in postural muscle activity during four-hour driving sessions. Other researchers have documented fatigue associated with sustained, low-level static exertions (Jorgensen et al., 1988), suggesting that driving

postures with less muscle activity may be less fatiguing and more comfortable, particularly for long-duration driving.

In other areas of biomechanical ergonomics, muscle-activity related criteria have been proposed as part of schemes to predict the muscle recruitment strategies associated with various work tasks and postures. Researchers have suggested that muscle recruitment strategies follow a global optimization model (Crowninshield and Brand, 1981). Bean et al. (1988) proposed an optimization-based procedure for allocating muscle effort in lifting tasks. There is an intuitive appeal to the idea that postures and movements should be performed in such a manner that the effort expended, whether in terms of muscle force or energy, is minimized. However, it has been demonstrated that muscle recruitment patterns, particularly in the trunk, often do not follow simple minimization criteria for a range of lifting-type tasks. In particular, concurrent contraction in antagonists and the involvement of muscles with a range of efficacies for a particular movement have been observed, and new models accounting for these relationships have been developed (Nussbaum, 1994; Raschke, 1994).

In spite of the known limitations of simple optimization criteria for predicting muscle recruitment patterns in lifting tasks, the less-strenuous seated driving task may be amenable to a simpler analysis. In this research, muscle activity reduction is proposed as a general selection criterion for driving postures. Within the constraints of the task, the chosen posture is hypothesized to be the one requiring the least muscle exertion. This research aims to illuminate this process by examining the effects of perturbations in the kinematic constraints imposed on the driver. This is analogous to determining the mechanical transfer function of a system by imposing a measured disturbance and analyzing the resulting output. In this case, the objective is a quantitative model of the posture-selection process, and an improved understanding of the underlying mechanisms.

The advantages of muscle activity reduction are a decrease in metabolic cost, avoidance of fatigue, and the reduction in control requirements. A posture that is

maintained through static muscle exertion will eventually lead to fatigue in the involved muscles, even at low levels of exertion (Jorgensen et al., 1988). While metabolic cost may not be an important issue for typical driving postures, the control requirements for an actively maintained posture may be significant, particularly in a moving vehicle environment. If a posture is maintained primarily through active muscle exertion, the muscle forces must be modulated dynamically as the postural loads change due to accelerations transmitted through the seat.

Among the kinematically feasible driving postures, some postures are better than others with respect to the requirements of the driving task. Postures that allow better vision to the environment and displays, and postures that allow better reach for manipulation of the controls, are preferred. In general, more upright postures with higher eye locations relative to the hips and greater forward reach will be preferred from the standpoint of task performance. In contrast, more reclined postures with direct support for the entire body will allow minimal muscle activity.

The hypothesized posture selection process chooses the posture that is most suitable for the task, that is, most upright, while maintaining muscle activity at near-resting levels. In passenger car seats, support for the head and neck is generally not provided, so an unsupported head is assumed. This general hypotheses leads to some specific predictions concerning muscle activity in driving postures.

- 1. Driving postures will be characterized by low levels of muscle activity.**
- 2. Perturbing driving postures toward more upright postures will cause an increase in trunk muscle activity.**
- 3. Perturbing driving postures toward more reclined postures will result in the same low levels of trunk muscle activity measured in preferred postures.**
- 4. Perturbing head and neck posture away from the preferred posture will cause increases in neck muscle activity.**

Expressing the overall concept as a single predictive hypothesis that takes into account the kinematics of torso recline,

5. **Driving posture is predicted to be the posture that is kinematically consistent with the task requirements and has the highest eye location with respect to the hips that can be obtained while back extensor activity is near resting levels.**

This hypothesis, if valid, provides considerable insight into driving posture, but potentially has broader applicability. People likely select their driving postures using the same internal processes that they use in selecting postures for many other tasks. If posture selection for the driving task is consistent with the stated hypotheses, exploring the applicability of this posture prediction concept to other tasks may well be fruitful.

1.4 Research Objectives and Goals

The research presented in this dissertation has the following principal goals:

1. **Develop a method of representing whole-body vehicle occupant posture using a kinematic linkage based on joint locations calculated from external body landmarks.**
2. **Determine the effects of anthropometric variables and changes in seat height, steering wheel position, instrument panel height, and seat cushion angle on driving posture over the relevant range for passenger vehicles.**
3. **Develop whole-body driving posture prediction models from laboratory data and assess their accuracy using in-vehicle posture data from a large number of drivers.**
- 4.. **Analyze driving posture from a biomechanical perspective, using muscle activity measurements and biomechanical simulations to determine if driving postures are consistent with a muscle-activity reduction hypothesis.**

The research is intended to be applicable to drivers of a wide range of body sizes driving production passenger cars for short time periods. The experiments, analysis, and models consider only the situation where the driver is provided with a fore-aft seat adjustment, seatback angle adjustment, and a steering wheel angle adjustment, but no other capability to manipulate the vehicle or seat geometry.

The posture prediction models are intended to have well-defined accuracy and precision, and to be superior in that regard to existing models. As noted above, there are

currently no published models for whole-body driving posture prediction, and consequently there is no benchmark against which to judge the model accuracy. Rather, the predictions from these models, developed with laboratory data, are compared directly to in-vehicle driving postures obtained in five vehicles with 120 drivers per vehicle. This comparison is believed to represent a good quantitative test of model performance. The comparison among the models, developed using three different prediction strategies, provides a measure of the robustness of the individual model assumptions.

1.5 Dissertation Organization

The body of this dissertation consists of six research papers, each presenting a particular experimental study or analysis related to the goals of the dissertation.

Chapter 2 presents a method of depicting and analyzing driving posture using a kinematic model representation of the body. Three-dimensional body landmark locations are measured using a coordinate measurement system such as the GP8-3D sonic digitizer or the FARO Arm. The landmark locations are used to calculate internal joint locations that define a kinematic linkage. This chapter is a critical synthesis of a number of previous studies and some additional data collected for this purpose.

Chapters 3 and 4 present two studies of the influence of vehicle and seat geometry on driving posture. Chapter 3 presents a three-phase laboratory study of the effects of seat height, steering wheel position, seat cushion angle, and seat type on driving posture. Sixty-eight men and women selected their preferred driving postures in a total of 18 different combinations of the test factors. The posture data were analyzed to determine the effects on driving posture, and the potential for interactions between the effects and anthropometric variables. Chapter 4 describes the influence of forward, downward vision restriction on driving posture. Five instrument panel heights were presented to 16 men and women in a driving simulator. The posture findings are compared with data from a vehicle in which 32 men and women drove a road route with and without a mask

obscuring part of the lower windshield. The findings are assessed with regard to the importance of vision restrictions for posture prediction.

Chapter 5 presents the development and evaluation of three posture prediction models based on the laboratory studies presented in Chapters 3 and 4. These prediction models are specifically designed for use with CAD human models, and are assessed with respect to the applications of such models. The three posture prediction models, each based on a different framework, are compared to each other and to the original data. The accuracy of the three models for prediction of posture in novel situations is assessed using posture data from 120 drivers in each of five production vehicles. The findings are discussed in the context of CAD human model usage, and one of the three models is recommended for general use in vehicle design.

Chapters 6 and 7 present a detailed investigation of driving posture using a large number of test measurements from 10 midsize-male drivers. In Chapter 6, the forces and moments exerted by the drivers on the steering wheel in a standardized driving posture are examined for a range of elbow angles. The results are interpreted to develop an appropriate method of simulating steering wheel interaction in biomechanical models and to gain a better understanding of drivers' strategies for posture selection and maintenance. Chapter 7 presents a study in which driver's preferred postures are perturbed in a number of different ways to determine if driving postures are consistent with the muscle-activity reduction hypothesis advanced in the preceding discussion. The drivers' postures and muscle activity were recorded with five different seatback angles, two different sitting procedures, and with the head and hand locations perturbed at five different levels. A simple biomechanical model is used in conjunction with the experimental data to explore the posture-selection hypotheses. The findings are interpreted with regard to the strategies underlying driving posture selection.

Chapter 8 presents a summary and discussion of the dissertation, including an assessment of how well the goals of the research were met. Recommendations for future work arising from the findings are presented.

Appendix A contains a brief overview of current vehicle design practice and terminology adapted from Roe (1993). Although these concepts are reviewed in various parts of the text, readers are encouraged to consult the Appendix to clarify automobile-specific terminology.

1.6 References

- Andersson, G.B.J., and Örtengren, R. (1974). Lumbar disc pressure and myoelectric back muscle activity during sitting. II. Studies on an office chair. *Scandinavian Journal of Rehabilitation Medicine* 6(3): 115-121.
- Andersson, G.B.J., Örtengren, R., Nachemson, A., and Elfström, G. (1974a). Lumbar disc pressure and myoelectric back muscle activity during sitting. I. Studies on an experimental chair. *Scandinavian Journal of Rehabilitation Medicine* 6(3): 104-114.
- Andersson, G.B.J., Örtengren, R., Nachemson, A., and Elfström, G. (1974b). Lumbar disc pressure and myoelectric back muscle activity during sitting. IV. Studies on a car driver's seat. *Scandinavian Journal of Rehabilitation Medicine* 6(3): 128-133.
- Arnold, A.J., Ferrara, R.A., and Kuechenmeister, T.J. (1985). Driver eyellipses produced by minimum deflection seats and by U.S. adult population changes. In *Proc. of the 29th Annual Meeting of the Human Factors Society, Volume I*, ed. R.W. Swezey, L.B. Strother, T.J. Post, and M.G. Knowles, 447-451. Santa Monica, CA: Human Factors Society.
- Asano, H., Yanagishima, T., Abe, Y., and Masuda, J. (1989). *Analysis of primary equipment factors affecting driving posture*. SAE Technical Paper 891240. Warrendale, PA: Society of Automotive Engineers, Inc.
- Babbs, F.W. (1979). A design layout method for relating seating to the occupant and vehicle. *Ergonomics* 22(2): 227-234.
- Bean, J.C., Chaffin, D.B., and Schultz, A.B. (1988). Biomechanical model calculation of muscle contraction forces: a double linear programming method. *Journal of Biomechanics* 21(1): 59-66.
- Bohlin, N., Hallen, A., Runberger, S., and Aasberg, A. (1978). *Safety and comfort-- Factors in Volvo occupant compartment packaging*. SAE Technical Paper 780135. Warrendale, PA: Society of Automotive Engineers, Inc.
- Branton, P. (1969). Behaviour, body mechanics and discomfort. *Ergonomics* 12(2): 316-327.

- Chaffin, D.B. (1973). Localized muscle fatigue-definition and measurement. *Journal of Occupational Medicine* 15:346.
- Chaffin, D.B., and Andersson, G.B.J. (1991). Guidelines for seated work. In *Occupational Biomechanics, Second Edition*, 335-375. New York: John Wiley and Sons, Inc.
- Crowninshield, R.D., and Brand, R.A. (1981). A physiologically based criterion of muscle force prediction in locomotion. *Journal of Biomechanics* 14(11): 798-801.
- Devlin, W.A., and Roe, R.W. (1968). *The eyellipse and considerations in the driver's forward field of view*. SAE Technical Paper 680105. New York, NY: Society of Automotive Engineers, Inc.
- Flannagan, C.A.C., Schneider, L.W., and Manary, M.A. (1996). Development of a new seating accommodation model. SAE Technical Paper 960479. In *Automotive Design Advancements in Human Factors: Improving Drivers' Comfort and Performance (SP-1155)*, 29-36. Warrendale, PA: Society of Automotive Engineers, Inc.
- Grandjean, E. (1980). Sitting posture of car drivers from the point of view of ergonomics. In *Human Factors in Transport Research. Volume 2 - User Factors: Comfort, the Environment and Behaviour*, ed. D.J. Osborne and J.A. Levis, 205-213. New York: Academic Press.
- Gross, C.M., Goonetilleke, R.S., Menon, K.K., Banaag, J.C.N., and Nair, C.M. (1993). The biomechanical assessment and prediction of seat comfort. In *Hard Facts About Soft Machines: The Ergonomics of Sitting*, ed. R. Lueder and K. Noro, 231-253. London: Taylor and Francis.
- Hammond, D.C., and Roe, R.W. (1972). *Driver head and eye positions*. SAE Technical Paper 720200. New York, NY: Society of Automotive Engineers, Inc.
- Hosea, T.M., Simon, S.R., Delatizky, J., Wong, M.A., and Hsieh, C.-C. (1986). Myoelectric analysis of the paraspinal musculature in relation to automobile driving. *Spine* 11(9): 928-936.
- Jørgensen, K., Fallentin, N., Krogh-Lund, C., and Jensen, B. (1988). Electromyography and fatigue during prolonged low-level static contractions. *European Journal of Applied Physiology* 57:316-321.
- Judic, J.M., Cooper, J.A., Truchot, P., Effenterre, P.V., and Duchamp, R. (1993). *More objective tools for the integration of postural comfort in automotive seat design*. SAE Technical Paper 930113. Warrendale, PA: Society of Automotive Engineers, Inc.
- Lay, W.E., and Fisher, L.C. (1940). Riding comfort and cushions. *SAE Journal* 47(5): 482-496.
- Matsushashi, K. (1991). Improvement of seating comfort. In *Proc. of the 6th International Pacific Conference on Automotive Engineering, Volume 1*, 625-633. Seoul: Korea Society of Automotive Engineers.
- Matsuoka, Y., and Hanai, T. (1988). *Study of comfortable sitting posture*. SAE Technical Paper 880054. Warrendale, PA: Society of Automotive Engineers, Inc.

- Meldrum, J.F. (1965). *Automobile driver eye position*. SAE Technical Paper 650464. New York, NY: Society of Automotive Engineers, Inc.
- Mourant, R.R., Pak, T., and Moussa-Hamouda, E. (1978). *Dynamic eye positions by vehicle type. Final report of the Second Generation Eyellipse Project*. Detroit, MI: Wayne State University, Department of Industrial Engineering and Operations Research.
- Nussbaum, M.A. (1994). *Artificial neural network models for analysis of lumbar muscle recruitment during moderate static exertions*. Ph.D. dissertation, University of Michigan, Ann Arbor.
- Parkin, S., Mackay, G.M., and Cooper, A. (1993). How drivers sit in cars. In *Proc. of the 37th Annual Conference of the Association for the Advancement of Automotive Medicine*, 375-388. Des Plaines, IL: Association for the Advancement of Automotive Medicine.
- Philippart, N.L., Kuechenmeister, T.J., Ferrara, R.A., and Arnold, A.J. (1985). *The effects of the steering wheel to pedal relationship on driver-selected seat position*. SAE Technical Paper 850311. Warrendale, PA: Society of Automotive Engineers, Inc.
- Phillipart, N.L., Roe, R.W., Arnold, A.J., and Kuechenmeister, T.J. (1984). *Driver selected seat position model*. SAE Technical Paper 840508. Warrendale, PA: Society of Automotive Engineers, Inc.
- Porter, J.M., Case, K., Freer, M.T., and Bonney, M.C. (1993). Computer-aided ergonomics design of automobiles. In *Automotive Ergonomics*, ed. B. Peacock and W. Karwowski, 43-77. London: Taylor and Francis.
- Pywell, J. F. (1993). Measuring seat comfort. *Automotive Engineering* 101(7): 25-29.
- Raschke, U. (1994). *Lumbar muscle activity prediction under dynamic sagittal plane lifting conditions: Physiological and biomechanical modeling considerations*. Ph.D. dissertation, University of Michigan, Ann Arbor.
- Rebiffe, R. (1980). General reflections on the postural comfort of the driver and passengers: Consequences on seat design. In *Human Factors in Transport Research. Volume 2 - User Factors: Comfort, the Environment and Behaviour*, ed. D.J. Osborne and J.A. Levis, 240-248. New York: Academic Press.
- Reed, M.P., and Schneider, L.W. (1996). Lumbar support in auto seats: Conclusions from a study of preferred driving posture. SAE Technical Paper 960478. In *Automotive Design Advancements in Human Factors: Improving Drivers' Comfort and Performance (SP-1155)*, 19-28. Warrendale, PA: Society of Automotive Engineers, Inc.
- Reed, M.P., Schneider, L.W., and Eby, B.A.H. (1995). Some effects of lumbar support on driver seated posture. SAE Technical Paper 950141. In *Human Factors in Vehicle Design: Lighting, Seating and Advanced Electronics (SP-1088)*, 9-20. Warrendale, PA: Society of Automotive Engineers, Inc.
- Reed, M.P., Schneider, L.W., and Ricci, L.L. (1994). *Survey of Auto Seat Design Recommendations for Improved Comfort*. Technical Report UMTRI-94-6. Ann Arbor, MI: University of Michigan Transportation Research Institute.

- Reynolds, H.M. (1993). Automotive seat design for sitting comfort. In *Automotive Ergonomics*, ed. B. Peacock and W. Karwowski, 99-116. London: Taylor and Francis.
- Roe, R.W. (1993). Occupant packaging. In *Automotive Ergonomics*, ed. B. Peacock and W. Karwowski, 11-42. London: Taylor and Francis.
- Schneider, L.W., Anderson, C.K., and Olson, P.L. (1979). *Driver anthropometry and vehicle design characteristics related to seat positions selected under driving and non-driving conditions*. SAE Technical Paper 790384. Warrendale, PA: Society of Automotive Engineers, Inc.
- Seidl, A. (1994). Das Menschmodell RAMSIS: Analyse, Synthese und Simulation dreidimensionaler Körperhaltungen des Menschen [The man-model RAMSIS: Analysis, synthesis, and simulation of three-dimensional human body postures]. Ph.D. dissertation, Technical University of Munich, Germany.
- Sheridan, T.B., Meyer, J.E., Roy, S.H., Decker, K.S., Yanagishima, T., and Kishi, Y. (1991). *Physiological and psychological evaluations of driver fatigue during long term driving*. SAE Technical Paper 910116. Warrendale, PA: Society of Automotive Engineers, Inc.
- Treaster, D.E., and Marras, W.S. (1989). *Seat pressure: Measurement and analysis*. SAE Technical Paper 890849. Warrendale, PA: Society of Automotive Engineers, Inc.
- Verriest, J.P., and Alonzo, F. (1986). A tool for the assessment of inter-segmental angular relationships defining the postural comfort of a seated operator. SAE Technical Paper 860057. In *Passenger Comfort, Convenience and Safety: Test Tools and Procedures*, 71-83. Warrendale, PA: Society of Automotive Engineers, Inc..
- Weichenrieder, A., and Haldenwanger, H.G. (1985). *The best function for the seat of a passenger car*. SAE Technical Paper 850484. Warrendale, PA: Society of Automotive Engineers, Inc.

CHAPTER 2

A TECHNIQUE FOR REPRESENTING AUTOMOBILE OCCUPANT POSTURE USING A KINEMATIC MODEL BASED ON SURFACE BODY LANDMARK LOCATIONS

2.1 Introduction

The human body is commonly represented in ergonomic and biomechanical investigations as an open chain of rigid segments. The number of segments and the nature of the joints between segments varies widely depending on the application of the resulting kinematic model. A classic representation of the body for design purposes by Dempster (1955) divided the body in 13 planar segments, including single segment from the hips to the top of the head. A contrasting model is presented by Nussbaum and Chaffin (1996) who used multiple rigid, three-dimensional segments to simulate torso kinematics. There are many other whole- and partial-body models in the literature, with a wide range of complexity.

For automotive applications, two kinematic representations of the body have been most widely used. The Society of Automotive Engineers (SAE) J826 H-point manikin (SAE, 1997) provides four articulating segments (foot, leg, thigh/buttocks, and torso) to represent a vehicle occupant's posture. A two-dimensional template with similar contours is used with side-view design drawings. The joints of the H-point manikin and the two-dimensional template have a single degree of freedom, pivoting in a sagittal plane. These two tools are the standard occupant representations of vehicle interior design (Roe, 1993).

The other widely used kinematic representation of vehicle occupants is that embodied in the Anthropomorphic Test Devices (ATDs), or crash dummies, used to

assess impact protection. The current standard ATD, the Hybrid-III, has many more degrees of freedom and body segments than the SAE H-point manikin or two-dimensional template, including three degrees of freedom at each hip, shoulder, and ankle (Backaitis and Mertz, 1994). The lumbar and cervical spine are represented by flexible structures that allow flexion or extension in any plane. In a more recent development, Schneider et al. (1985) presented new anthropometric data for an advanced family of crash dummies that were subsequently used in the development of a new ATD thorax that adds additional complexity to the shoulders, thoracic spine, and ribcage to obtain a more realistic interaction with restraint systems (Schneider et al., 1992).

Software representations of both the SAE J826 and ATD linkages are now widely used in the vehicle design process. The design tools are intended for kinematic analysis only, but models of the ATDs are intended for dynamic use, i.e., crash simulation. In both vehicle ergonomics and impact protection, commercial human body representations are now available that provide models with additional complexity (Seidl, 1994; Maltha and Wismans, 1980). The JOHN model, a three-dimensional kinematic tool intended for use in auto seat design, uses a six-joint lumbar spine to provide complex spine motions linked to changes in external contour (Haas, 1989). Bush (1993) developed a two-dimensional seat design template with similar kinematics using a fixed motion distribution between two lumbar joints

The objectives of the current work are:

1. to develop a kinematic representation of vehicle occupant posture for vehicle interior ergonomics applications relating to normal riding and driving postures while providing continuity with existing occupant protection tools, and
2. to develop techniques for measuring and representing posture using the kinematic model.

This work is primarily a review and synthesis of previous studies. The emphasis here is on the efficient representation of vehicle occupant posture, using the smallest amount of information necessary to describe the posture to a level of detail sufficient for vehicle ergonomic applications relating to normal riding and driving postures.

It is useful to define “normal driving posture” as sagittally symmetric, with the sagittal plane aligned with the vehicle or seat side-view (XZ) plane. A large body of experimental data in vehicles and laboratory vehicle mockups has demonstrated that drivers, when instructed to sit with a “normal, comfortable driving posture,” choose a torso posture that largely conforms to this definition. Asymmetric limb postures are resolved by recording the posture of only the right side of the body, since the right foot interaction with the accelerator pedal ensures that the right-leg posture is related to the driver’s adaptation to the workspace. The techniques presented here are readily applied to either or both legs or arms, so that the sagittal symmetry requirement for the limbs can be relaxed if desired. By accepting this somewhat restrictive definition of normal driving (or riding) posture, the resulting kinematic constraints can be exploited to reduce the amount of body position information that is necessary to describe the posture.

As noted above, one of the objectives of the current work is to provide continuity between ergonomic applications and impact protection. This process has been facilitated by extensive use of the data and analysis on which the new family of frontal crash dummies is based. Robbins (1985a, 1985b) used three-dimensional surface landmark data from seventy-five drivers in three size categories to estimate the locations of anatomical joints that define a kinematic linkage. In the current analysis, ambiguities among various sources relating to joint locations have been resolved in favor of consistency with Robbins’ analysis, except where the preponderance of evidence suggests that an alternative approach will significantly improve the location estimate.

Unfortunately, there is much less publicly available data for determining the relationship between surface anatomical landmarks and interior skeletal geometry than one might expect, given the importance of these calculations for so many ergonomic and biomechanical studies. The landmark studies in this area include Dempster (1955), who used cadaver dissections to propose a kinematic model for human-factors analysis, and Snyder et al. (1972), who used cadaver dissection and radiographs of male volunteers in a

variety of postures to obtain data on surface-landmark-to-skeleton transformations. The risks of radiography for healthy people have made such investigations unlikely to be performed today. Recently, Reynolds (1994) conducted radiographic studies with a small number of human cadavers, but additional useful linkage data from healthy people in normal postures will probably have to be derived from MRI or other low-risk imaging techniques.

2.2 Kinematic Model

The choice of the segments and joints for the kinematic model was based on an assessment of the needs for posture data in vehicle interior design. A vehicle occupant's posture can be represented in a number of ways, each of which has some advantages and disadvantages for use in vehicle design. In current SAE practice, the distribution of drivers' eye locations is predicted from vehicle geometry using statistical summaries of eye-position data collected from a large number of people (SAE Recommended Practice J941, SAE, 1997). The distribution of drivers' selected seat positions, which is closely related to their hip locations, is similarly predicted using a statistical summary of a large body of data (SAE Recommended Practice J1517, SAE, 1997). Both of these currently used models predict the spatial distribution of a single body landmark for an occupant population. The data on which they are based are, of course, the measured locations of these landmarks for a suitable population of drivers. Hence, one of the ways of representing vehicle occupant posture data is by statistical summaries of the locations of body landmarks for appropriately selected subjects. If these data are collected for a carefully selected range of vehicle interior geometries, then the resulting percentile accommodation models can accurately predict these landmark locations for a range of vehicles (Roe, 1993).

Recently, however, the use of three-dimensional software manikins to represent occupants in the vehicle design process has made more complete and integrated techniques necessary for representing occupant posture. To be useful in design, these

manikins must not only represent appropriate combinations of anthropometric variables, but also must accurately represent the likely posture of an occupant with the specified body dimensions. Most currently available statistical summaries of driving posture, such as those represented by the SAE eye position (J941) and driver-selected seat position (J1517) practices, are severely limited for use in positioning CAD manikins, because they predict parameters of the population distribution of landmark locations, rather than the most likely landmark locations for a specific size of occupant. So, for example, the J941 eyellipse centroid represents a prediction of the average eye position for the U.S. population, but does not provide useful information about the most likely eye location for a person who is 1650 mm tall.

A primary emphasis in the current work is the representation of posture data in a way that can be readily interpreted to determine appropriate postures for CAD manikins of different sizes. There are many different ways of representing body posture, including body landmark locations, external body contours, and kinematic-linkage-model representations. While body-landmark data are directly useful, particularly for prediction of eye and hip location, independent, simultaneous prediction of many individual landmark locations is inadequate for posturing CAD manikins, because the relative positions of the predicted landmark locations can be inconsistent with the kinematic constraints imposed by the manikin's internal linkage. A method for interpreting postures in terms of a kinematic linkage is required.

Seidl (1994) developed an innovative approach to representing posture using a kinematic linkage that is aligned using a person's external body contours in video images. The resulting posture analysis techniques were used to develop the RAMSIS software manikin, which is currently the only CAD manikin primarily intended for auto interior design that includes significant posture prediction capability. A limitation of the external contour fitting approach is that it does not generate external body landmark locations. Instead, the only representation of posture is in terms of the specific kinematic linkage

used in the model. In the case of the RAMSIS model, the joints in the torso of the RAMSIS manikin are not intended to relate to specific anatomical joints, so the posture data from this approach cannot be readily generalized to other manikin linkages.

In the current work, a posture representation method has been developed that uses external body landmark locations to estimate the locations of joints that define the end points of body segments. The joints and segmentation scheme have been chosen because they provide the minimum complexity believed to be necessary to simulate the motions typical of changes between different vehicle occupant postures, while preserving an anatomically defined relationship between the external landmarks and the internal joints that define the linkage. This procedure is believed to allow findings reported using these techniques to be readily generalized to CAD manikins with a wide range of kinematic complexity. Using fewer segments would provide inadequate mobility, and using more segments, or using segments without explicit anatomical referents, would increase the difficulty in presenting and using posture data.

The kinematic model is depicted in Figures 2.1 and 2.2. The choice of the limb segments is straightforward. Individual hand, forearm, arm, thigh, leg, and foot segments are joined on each side of the body. In practice, the hand and forearm segments are considered as a single segment for representing normal riding and driving postures, since the complexities of hand movement relative to the arm are unimportant in that context. In the torso, the lumbar and cervical regions of the spine are each represented by a single segment and two joints. It appears from analysis of changes between different vehicle occupant postures that this approach represents sufficient kinematic complexity for representing normal riding and driving postures, and corresponds to the linkage most commonly used for dynamic crash victim simulation (Maltha and Wismans, 1980). The key determinant of model complexity for this application is that the linkage must adequately represent within-subject posture changes resulting from changes in vehicle layout and seat design within the rotational degrees-of-freedom of the linkage, i.e.,

without changing segment lengths. This is a necessary condition for interpreting the data using a limited-degree-of-freedom CAD manikin. For example, eye-to-hip distance varies significantly with changes in lumbar support prominence (Reed and Schneider, 1996). The selected linkage must allow this change in distance without violating the kinematic constraints. Analysis presented in Chapter 7 demonstrates that the model presented here is kinematically adequate for representing normal driving postures.

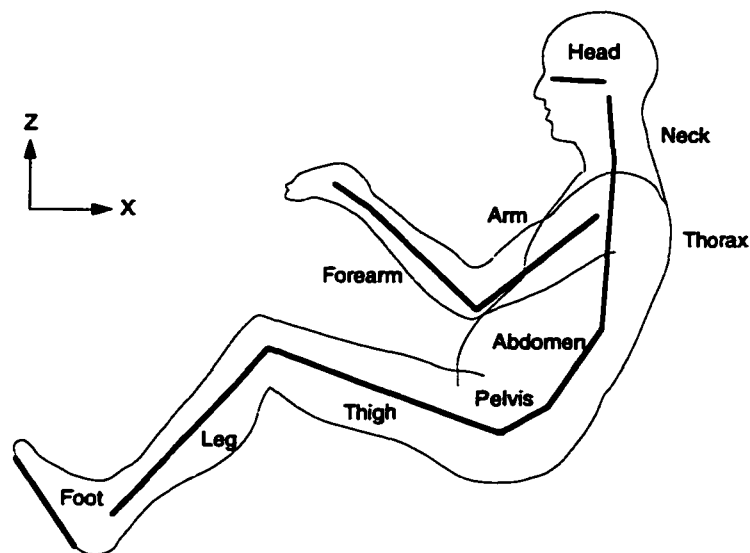


Figure 2.1. Kinematic model showing segments used to represent posture.

The joints in the model shown in Figure 2.2 correspond to approximate centers of rotation between adjacent bones and are located near the geometric center of particular anatomical joints. Some additional clarification of the nature of these joint locations may reduce potential confusion about their usage. The selected anatomical reference points correspond to joints in the kinematic model of human posture, and are generally located near the estimated anatomical center of a joint between bones, but are not necessarily at the actual center of rotation of the adjacent bones. As has been noted by many researchers, the instantaneous center of rotation between adjacent bones (or helical

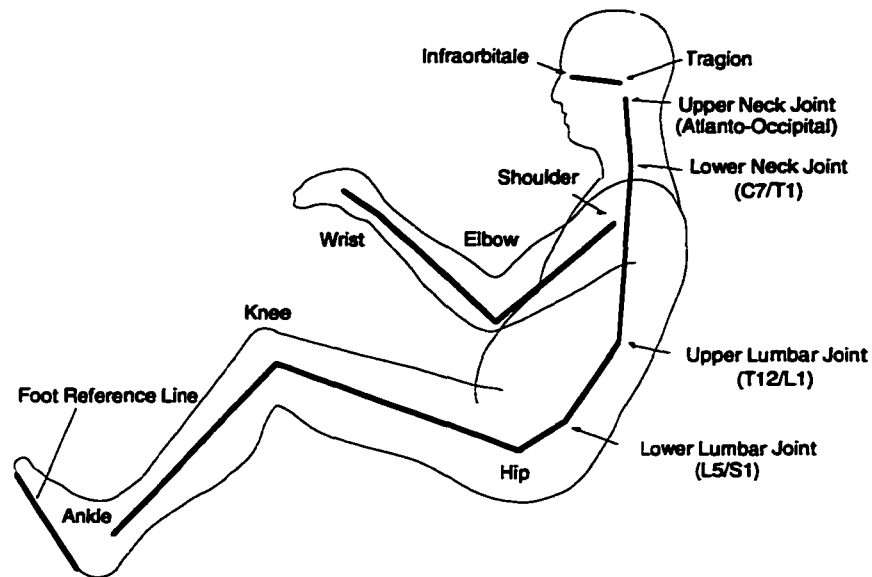


Figure 2.2. Joints in kinematic model used to represent vehicle occupant posture.

axis for three-dimensional rotation) changes position relative to the bones as the adjoining body parts are moved through their ranges of motion. This means that there is no single kinematic joint center at which all rotation between adjacent segments occurs.

However, for representation of normal vehicle occupant posture, the range of motion of interest at each joint is usually small; that is, the range of postures associated with different seats and packages is small relative to the range of possible human postures, so the potential for movement of the kinematic joint centers relative to the body segments is also small. Where posture changes can be large, such as at the knee and elbow, the adjoining segments are long relative to the potential discrepancies between the actual and estimated joint centers, so kinematic errors associated with joint location estimates will also be small.

However, data represented using the techniques presented here may be applied to computer models that are used over much wider posture ranges, e.g., for reach assessments or ingress/egress studies. These models may rely on linkages that have joints located differently relative to the skeleton, or may have different linkages with more or fewer joints. Since the potential requirements of future models cannot be

completely anticipated, the kinematic model joints in the current approach are anatomically defined, rather than kinematically defined. These joints are fixed in relation to skeletal landmarks and represent approximations of the center of rotation between adjacent bones. The relationships between these internal points (kinematic model joints) and external landmarks are thoroughly described in the following sections, so that the posture data reported using these techniques can be used in the future to estimate the location of any other bony reference point of interest, or to identify a joint location that is more suitable for a particular purpose. This approach is believed to provide a high level of generalizability for future modeling applications.

The orientation of the terminal segments (hands, feet, and head), are defined by vectors within the segments connecting landmarks of interest. Because the hands in normal driving and riding postures are, by definition, either on the steering wheel or resting on the thighs, the hand segment is assumed to be aligned with the forearm with whatever orientation (forearm pronation or supination) is appropriate to the task. For other occupant tasks, such as reaching, additional data on hand position and orientation could be collected.

An important distinction should be made between the use of this kinematic model for representing posture and for simulating posture changes. The model is used to represent posture when the posture is reported in terms of the lengths and orientations of the specified body segments. The corresponding posture can be reconstructed from this information and the model topology. Posture change for a particular subject can be represented by changes in orientation of model segments that were initially scaled to match the subject in a specific posture, or by a recalculation of each of the joint locations from new landmark data, resulting in different segment lengths and orientations. The latter approach has been used exclusively in this research for two reasons. The complexity of fitting a particular kinematic model to a new set of body landmark data is avoided, but, more importantly, the kinematic model has been found to be a sufficiently

accurate representation of the human body linkage that the changes in apparent segment length between different sitting postures are small (see Chapter 7). Thus, the differences between the segment orientations obtained by fitting a single kinematic model to all of a particular subject's postures and those obtained by direct calculation of joint locations for each posture are also small.

For this approach to posture representation, the number of joint degrees of freedom are unimportant, because the lengths of segments are allowed to vary as needed. However, for simulations of posture changes using this model, the model segment lengths are fixed and articulated according to movement relationships developed from data. In simulations, the joint degrees of freedom are specified in the particular set of posture prediction functions that are used, which may vary depending on the application. Thus, for prediction of normal driving posture, the wrist may be assigned zero degrees of freedom, but for other tasks, two or more degrees-of-freedom may be simulated.

One substantial difference between the current kinematic model and other similar models is that the shoulder joint is not connected by a rigid link to the thorax. Instead, the position of the shoulder (glenohumeral) joint in a thorax-based coordinate system is reported. This allows the arm position resulting from complex motion of the clavicle and scapula to be described without reference to a mechanical linkage. This approach is believed to result in greater generality, particularly because the treatment of the shoulder complex varies widely among kinematic models of the body.

2.3 Experimental Method

A driver's posture is recorded by measuring the three-dimensional locations of body landmarks with respect to a vehicle coordinate system. The surface landmark locations are used to calculate the joint locations that define the kinematic model posture. These data may be obtained by many different techniques, including: photogrammetry of targets applied to the subject's skin or clothing, automated marker tracking systems, or by direct recording with three-dimensional coordinate measuring equipment, such as the

FARO arm or SAC sonic digitizer. Each technique has advantages and disadvantages relating to accuracy, equipment cost, ease of use in vehicle and laboratory environments, and data processing requirements. In studies presented in this dissertation, landmark locations were measured using a Science Accessories Corporation GP8-3D sonic digitizer probe or a FARO Arm coordinate measurement device. Using both tools the experimenter first locates the landmark by direct palpation, then places the measuring probe at the landmark location to record the location. The pubic symphysis landmark is located by the subject. Each subject is trained to palpate down the midline of the abdomen until locating the symphysis. Assessments of the precision of pelvis landmark measurements using these techniques suggest that they are sufficiently reliable for characterizing pelvis location and orientation (Reed et al., 1995).

2.4 Body Landmarks

The experimenter palpated each landmark individually for each measurement to accurately locate the landmark and avoid the problems associated with movement of targets relative to the underlying bone. This technique also eliminated the need for target-to-landmark transformation calculations.

Table 2.1 and Figure 2.3 define and illustrate the body landmarks that are used to represent sitting posture with the kinematic model. These definitions are adapted from those in Schneider et al. (1985), and are mostly identical or similar to those used in previous studies (e.g., Snyder et al., 1972; McConville et al., 1980). Note that some of these landmarks are not accessible when the subject is sitting in a vehicle seat. They can, however, be collected when the subject is standing or sitting in a specially designed laboratory seat.

Table 2.1
Definitions of Body Landmarks

Landmark	Definition
Glabella	Undepressed skin surface point obtained by palpating the most forward projection of the forehead in the midline at the level of the brow ridges.
Infraorbitale	Undepressed skin surface point obtained by palpating the most inferior margin of the eye orbit (eye socket).
Tragion	Undepressed skin surface point obtained by palpating the most anterior margin of the cartilaginous notch just superior to the tragus of the ear (located at the upper edge of the external auditory meatus).
Occiput	Undepressed skin surface point at the posterior inferior occipital prominence. Hair is lightly compressed.
Corner of Eye	Undepressed skin surface point at the lateral junction of the upper and lower eyelids.
C7, T8,* T12*	Depressed skin surface point at the most posterior aspect of the spinous process.
Suprasternale (manubrium)	Undepressed skin surface point at the superior margin of the jugular notch of the manubrium on the midline of the sternum.
Substernale (xyphoid process)	Undepressed skin surface point at the inferior margin of the sternum on the midline.
Anterior-Superior Iliac Spine (ASIS - right and left)	Depressed skin surface point at the anterior-superior iliac spine. Located by palpating proximally on the midline of the anterior thigh surface until the anterior prominence of the iliac spine is reached.
Posterior-Superior Iliac Spine* (PSIS - right and left)	Depressed skin surface point at the posterior-superior iliac spine. This landmark is located by palpating posteriorly along the margin of the iliac spine until the most posterior prominence is located, adjacent to the sacrum.
Pubic Symphysis	Depressed skin surface point at the anterior margin of pubic symphysis, located by the subject by palpating inferiorly on the midline of the abdomen until reaching the pubis. The subject is instructed to rock his or her fingers around the lower margin of the symphysis to locate the most anterior point.
Lateral Femoral Condyle	Undepressed skin surface point at the most lateral aspect of the lateral femoral condyle. Measured on the skin surface or through thin clothing.
Wrist	Undepressed skin surface point on the dorsal surface of the wrist midway between the radial and ulnar styloid processes.
Acromion	Undepressed skin surface point obtained by palpating the most anterior portion of the lateral margin of the acromial process of the scapula.
Lateral Humeral Condyle	Undepressed skin surface point at the most lateral aspect of the humeral condyle.
Lateral Malleolus	Undepressed skin surface point at the most lateral aspect of the malleolus of the fibula.
Medial Shoe Point	Point on the medial aspect of the right shoe medial to the first metatarsal-phalangeal joint (approximately the ball of the foot).
Shoe Heel Contact Point	Point on the floor at the center of the right shoe heel contact area with the foot in normal driving position contacting the accelerator pedal.

*These points are not accessible when the subject is sitting in a conventional vehicle seat, but are recorded in other sitting and standing experimental situations to characterize the subject's torso geometry. See text for details.

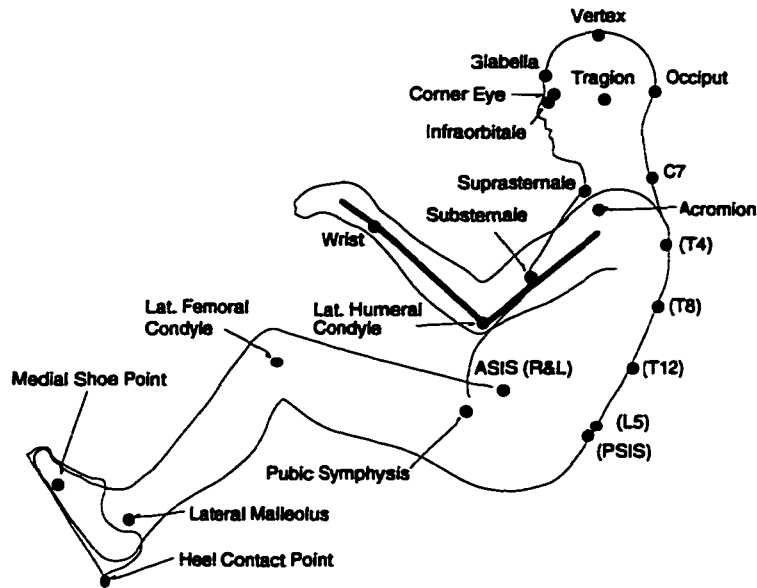


Figure 2.3. Body landmarks used to calculate internal joint locations and segment orientations.

One important difference between these definitions and the conventional definitions is for the acromion landmark. In McConville et al. (1980), the acromion landmark is defined as “the most lateral point on the lateral edge of the acromial process of the scapula.” The definition used in Schneider et al. (1985) is identical to McConville et al. (1980). This landmark definition is somewhat ambiguous because, on most subjects, the lateral margin of the acromion process extends for 10 to 20 mm in a sagittal plane, making a precise identification of the landmark in that plane difficult. For the current work, the definition of the acromion landmark has been refined to be the most anterior corner of the lateral margin of the acromion process. This bony point can be identified precisely on most subjects, and provides a more stable reference for shoulder location.

The landmark set is sparse with regard to limb landmarks, reflecting the practical constraints of measuring vehicle occupant postures. Medial landmarks on the limbs are often difficult to reach with the measurement probes or to view with automated marker tracking systems, and the need to measure each subject in a large number of vehicle and seat conditions (in a typical study design) provides incentive to reduce the number of

landmarks to shorten test times. However, because vehicle driving and riding postures are highly constrained, sufficient information to describe the posture is available with a sparse landmark set.

2.4 Calculation of Joint Locations

The kinematic model used to describe posture has joints that correspond to anatomical locations inside of the body. Calculation methods are needed to translate the exterior landmark locations to interior joint locations. This problem is common to any attempt to represent the body by a kinematic linkage, but is complicated because joint locations can be measured directly only with cadavers or through the use of x-rays or other internal imaging technology. Dempster (1955) conducted the first large-scale effort to address this problem. He performed dissections of cadavers and made systematic measurements for the specific purpose of developing scalable linkage models of the human body for use in human factors analysis. Snyder et al. (1972), in another important study, used radiography of male volunteers to study the locations and movements of the joints for a wide variety of seated and standing postures. Their specific emphasis was to determine the relationship between the motions of skin-mounted surface targets and the underlying joints.

Many researchers are currently performing biomechanical analysis of human activity using linkage models, and there are almost as many techniques for estimating internal joint locations from external, measurable locations of body landmarks to internal joints. In each case, the type of transformation chosen is dependent on the needs of the research. This section presents the calculation methods that have been selected based on the requirements of posture representation for automotive interior design using three-dimensional CAD manikins.

Data Sources

The landmark-to-joint transformation methods described here are based largely on the data and analysis presented by Schneider et al. (1985) and Robbins (1985a, b). This three-volume publication describes a detailed study of passenger-car drivers conducted to develop anthropometric specifications for crash-dummy design. Body landmark locations in a driving posture were recorded for 25 subjects in each of three size/gender groups: small females (approximately 5th-percentile U.S. by stature and weight), midsize males (approximately 50th-percentile U.S. by stature and weight), and large males (approximately 95th-percentile U.S. by stature and weight). The seated landmark data were supplemented by a large number of standard anthropometric measures and some developed specifically for automotive postures.

Robbins used the external landmark data to estimate internal joint locations, using skeleton geometry data from several sources. Table 2.2 shows the references for each of the model joints. In the current work, the original reference materials have been consulted to verify that the methods and estimates in Robbins (1985a) are valid. In the case of the upper lumbar and lower neck joints (T12/L1 and C7/T1), the data presented by Snyder et al. (1972), on which Robbins relied, support a number of different location estimates, both because there is considerable variability in the data and because the data are presented in a number of different ways. A reexamination of the Snyder data indicated that the Robbins estimates were among the reasonable interpretations, so the location methods for these joints were selected to be consistent with Robbins. The only area in which the current methods differ substantially from Robbins is in the calculation of the hip and lower lumbar (L5/S1) joints. Robbins' analysis contains some discrepancies in regard to pelvis location that have been resolved by an analysis of data from several sources, including data from recent studies that were not available to Robbins.

Table 2.2
Data Sources Used by Robbins (1985a) to Estimate Joint Locations

Joint	Reference	Type of Data
Upper Neck (atlanto-occipital)	Ewing and Thomas (1972)	Kinematic analysis of head/neck motion
Lower Neck (C7/T1)	Snyder et al. (1972)	Radiographic study of torso movement
Upper Lumbar (T12/L1)	Snyder et al. (1972)	Radiographic study of torso movement
Wrist	Dempster (1955)	Cadaver dissection
Elbow	Dempster (1955)	Cadaver dissection
Knee	Dempster (1955)	Cadaver dissection
Ankle	Dempster (1955)	Cadaver dissection
Shoulder (glenohumeral)	Snyder et al. (1972)	Radiographic study of torso movement

Hip Joint Calculations

The location of the pelvis in the Robbins analysis has been criticized because of the large apparent flesh margin under the ischial tuberosities. Recent data from Reynolds (1994) suggest that a typical flesh margin at the ischial tuberosities for a midsize-male cadaver on a rigid seat is about 16 mm, compared with about 42 mm in the Robbins analysis. The discrepancy appears to relate to the interpretation of the anterior-superior iliac spine (ASIS) landmarks relative to the ilia, which Robbins may have located too low on his pelvis reconstruction. Further, Robbins did not apparently include any flesh margin in the relationship between the measured ASIS location and the bone, which may have contributed to the discrepancy.

Because of these concerns about Robbins' estimates of the pelvis joint locations, the hip and lower lumbar joint (L5/S1) locations are estimated using pelvis landmark data with scaling methods developed from several other sources. Reynolds et al. (1981) presented data on the positions of a large number of landmarks on pelvis from a skeleton collection. Data were summarized for large male, midsize male, and small female pelvis, categories selected so that the data would be applicable to the design of crash dummies of

those sizes. Bell et al. (1989) suggest using the distance between the anterior-superior iliac spine landmarks as a scaling dimension. A similar method was used by Manary et al. (1994) in a study of driver hip joint locations. Recently, Seidel et al. (1995) demonstrated that the use of other pelvis dimensions in addition to inter-ASIS breadth would improve the estimate of the hip joint center location. Data from each of these sources have been examined to determine the best method for calculating the hip joint locations.

Seidel et al. define three pelvis dimensions, illustrated in Figure 2.4: pelvis width (PW), which is the inter-ASIS distance; pelvis height (PH), which is the length of a line perpendicular to the inter-ASIS line to the pubic symphysis; and pelvis depth (PD), which is the distance from the ASIS to the posterior-superior iliac spine on the same side of the pelvis. They present the mean hip joint coordinates for 65 pelvises relative to these dimensions. Table 2.3 compares the Seidel et al. scaling with that proposed by Bell et al. from radiographic measurements, and that obtained from the Reynolds et al. data. Figure 2.5 illustrates the X and Z coordinates. The Y coordinate is measured perpendicular to the midsagittal plane.

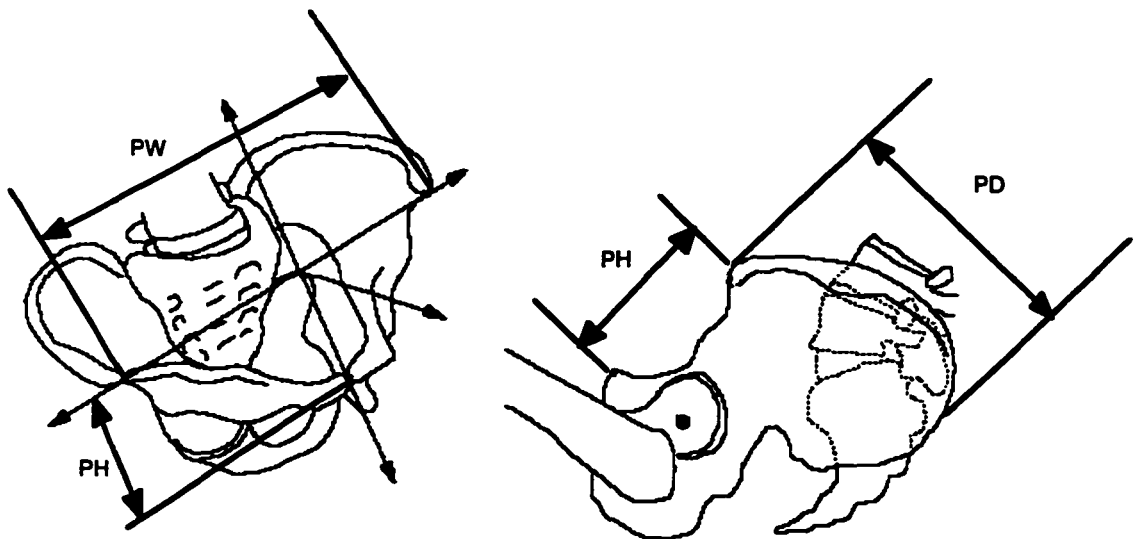


Figure 2.4. Illustration of pelvis scaling dimensions: pelvis width (PW), pelvis height (PH), and pelvis depth (PD).

Table 2.3
Comparison of Hip Joint Location Methods: Mean Scaling Relationships

Measure*	Seidel et al. (1995)	Bell et al. (1989)	Reynolds <i>et al.</i> (1981)†	Location Error Estimates** (mm)
Hip-X/PW	24%	22%	22%	4.9 (3.4)
Hip-Y/PW	36%	36%	37%	5.8 (4.2)
Hip-Z/PW	30%	30%	29%	7.5 (5.6)
Hip-X/PD	34%	—	32%	3.0 (2.3)
Hip-Z/PH	79%	—	83%	3.5 (2.8)

*The ratio of the coordinate value to the scaling dimension.

†Data from Reynolds *et al.* are the averages of values for small-female, midsize-male, and large-male pelvises.

** Mean (standard deviation) of prediction error from Seidel *et al.* (1995), N = 65 except N = 35 for Hip-X/PD.

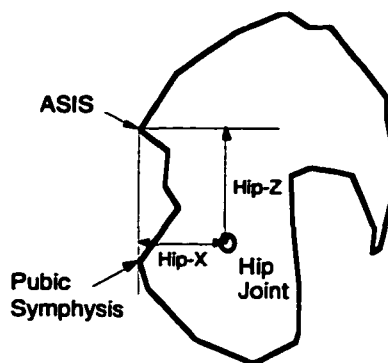


Figure 2.5. Location of the hip joint in the sagittal plane relative to the ASIS and pubic symphysis landmarks, showing the X and Z dimensions listed in Table 2.3.

The scaling relative to pelvis width (inter-ASIS breadth) is very similar in the three studies, varying most in the X coordinate. There are larger discrepancies in the scaling based on pelvis height and pelvis depth. The four-percent difference between Seidel and Robbins in Hip-Z/PH produces a difference in estimated hip joint location of about 3 mm for a midsize-male pelvis. The two-percent difference in Hip-X/PD also amounts to a difference of about 3 mm.

Seidel *et al.* demonstrated no statistically significant relationship between pelvis width and Hip-Z, suggesting that if pelvis width is the only available dimension, a constant value for Hip-Z, rather than the scaled value, could be used for all subjects. In

contrast, Seidel et al. showed a significant relationship between Hip-Z and pelvis height, indicating that pelvis height would be a suitable scaling dimension for that coordinate. The improved performance of the pelvis-height scaling was demonstrated by a smaller mean estimation error (3.5 mm vs. 7.5 mm). Similarly, scaling Hip-X by pelvis depth produced a smaller mean error compared with scaling by pelvis width (3.0 mm vs. 4.9 mm). Notably, Seidel et al. also found no important differences between male and female pelvises in these scaling relationships.

The foregoing analysis led to the conclusion that the scaling relationships proposed by Seidel et al. should be used when the necessary data are available and reliable, meaning the locations of both ASIS, the pubic symphysis, and both PSIS landmarks. However, Seidel et al. analysis demonstrated that the difference in error magnitudes for the alternative scaling techniques is small, so any of the techniques should give similar results.

Lower Lumbar Joint (L5/S1) Calculations

The joint between the fifth lumbar vertebra and first sacral vertebra can be considered to be a joint on the bony pelvis if motions within the sacral vertebrae and at the sacroiliac joints are assumed to be negligible. For analysis of seated postures, this is a reasonable assumption (Andersson et al. 1979).

Reynolds et al. (1981) include two data points on the top edge of the first sacral vertebra (S1) in the midsagittal plane. An offset vector of 10 mm, constructed perpendicular to the center of the line segment connecting the two S1 data points, was used to estimate the joint location, as shown in Figure 2.6.

The findings of Seidel et al. with respect to the superior scaling performance of pelvis height and pelvis depth for hip joint location suggest using those measures for estimating lower lumbar joint location as well. Table 2.4 shows scaling percentages from Reynolds et al. for L5/S1 location estimated as described in Figure 2.6. Although there are differences between the small-female, midsize-male, and large-male pelvises, they do

not appear to be systematically related to body size. Given the lack of important gender differences in the Seidel et al. analysis, the mean scaling values from Robbins were selected.

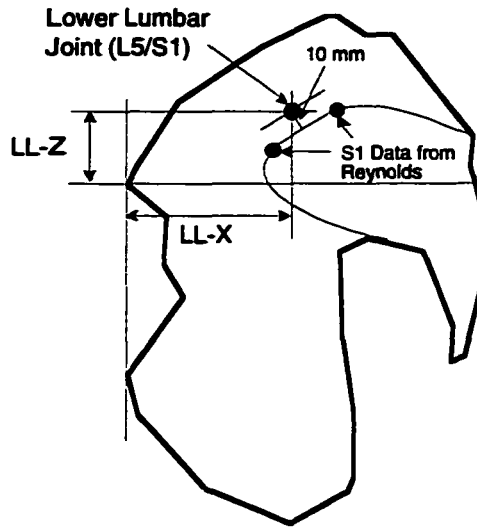


Figure 2.6. Method used to estimate lower lumbar joint (L5/S1) location from the data in Reynolds et al. (1981). Not to scale.

Table 2.4
Scaling Relationships for L5/S1 from Reynolds et al. (1981)

Measure	Small Female	Midsize Male	Large Male	Mean*
LL-X/PW	28.9%	26.4%	27.0%	27.4%
LL-Z/PW	17.2%	12.6%	15.1%	15.0%
LL-X/PD	42.5%	37.7%	39.4%	39.9%
LL-Z/PH	45.2%	39.9%	44.5%	43.2%

*Mean of small-female, midsize-male, and large-male values.

Flesh Margins

The preceding analysis of data relating to hip and lower lumbar joint location are based on landmarks on the pelvis bones. In live subjects, however, the landmark measurements are made through a thickness of compressed tissue. These flesh margin thicknesses are important to consider in calculating these joint locations. In previous analyses, Manary et al. (1994) and others at UMTRI have used estimates of compressed

flesh margin thickness of 5 mm at the ASIS and 15 mm at the pubic symphysis.

Recently, a small-scale, unpublished study was conducted in which the flesh margins at these landmarks were measured directly in 30 male and female cadavers, using a probe configuration similar to that used to record body landmark data. Flesh margins of 10 mm at the ASIS and 15 mm at the pubic symphysis were found to be good estimates for use with all subjects.

Landmark Selection and Scaling for Other Joints

As with the pelvis joints, the locations of other joints relative to the surface landmarks are calculated using simple linear scaling relationships. Since Robbins presents a large set of surface landmark locations along with the joint location estimates, it is possible to identify a number of different relationships among surface landmarks and joints that could be used to perform the transformations with new surface landmark data. The landmarks were selected to be as close as possible to those that were referenced in the original source materials listed in Table 2.2.

Since each joint lies some distance from the nearest measured landmark, a method must be developed to scale the vector relating the two, to account for differences in body size. In the current work, these joint location vectors are scaled by comparing the distance between two measured landmarks with the corresponding data for midsize males given by Robbins. This is analogous to the procedure used with pelvis landmarks. While the particular dimensions chosen may not be the ideal dimensions for scaling, they have been selected such that they are likely to be fairly well correlated with the vector magnitudes of interest. (In general, data on skeletal geometry necessary to test these assumptions are not available.) The scaling approach for all subjects uses the Robbins midsize-male data as the reference geometry because the underlying data on which the landmark-to-joint transformations are based (sources in Table 2.2) relied exclusively on male subjects. Table 2.5 lists the landmarks that define the location vectors and scaling measurements for each joint.

Table 2.5
Landmarks Used To Define and Scale Joint Location Vectors

Joint	Landmarks
Upper Neck (atlanto-occipital)	Infraorbitale, Trasion
Lower Neck (C7/T1)	C7, Suprasternale
Upper Lumbar (T12/L1)	T8, T12, C7, Suprasternale
Lower Lumbar (L5/S1)	ASIS, PS, PSIS
Hip	ASIS, PS, PSIS
Shoulder	Acromion, C7, Suprasternale
Knee	Lateral Femoral Condyle (plus Hip Joint and Lateral Malleolus)
Elbow	Lateral Humeral Condyle (plus Shoulder Joint and Wrist landmark)
Wrist	Wrist
Ankle	Lateral Malleolus (plus Lateral Femoral Condyle and Hip Joint)

Shoulder Joint

The shoulder joint of the kinematic model approximates the anatomical glenohumeral joint, the articulation of the humerus with the glenoid fossa of the scapula. As noted above, the acromion landmark definition used here is slightly different than that used in other studies, resulting in a measurement point that is anterior to that measured using the more conventional definition. As a consequence, the acromion-to-shoulder-joint relationship in Robbins' data is different from the relationship in data measured using the current methods.

Robbins estimated the glenohumeral joint location by orienting a midsize-male humerus according to the measured humeral landmarks (greater tubercle, lateral epicondyle, and medial epicondyle). This procedure was used because the Dempster definition referred to an arm position dissimilar to a normal driving posture. Snyder et al. (1972) report that the average sagittal-plane vector from the humeral head (approximately the glenohumeral joint center) to the acromion landmark is 52 mm long and oriented 42 degrees rearward from vertical, although there is considerable variability in both

measurements. Starting from the glenohumeral joint location calculated by Robbins and applying the vector from Snyder et al. results in an estimated acromion location about 10 mm forward and 16 mm above the landmark location reported by Robbins. Alternatively, starting at the acromion location given by Robbins, the Snyder et al. vector predicts a humeral head location 16 mm below and 10 mm forward of that reported by Robbins. It should be noted that these discrepancies are within the range of the vector length data and vector angle data reported by Snyder et al.

The potential effects of the revised acromion definition were assessed by comparing the relative sagittal plane locations of suprasternale, C7, and acromion landmarks in data collected using the current definition and those reported by Robbins. Figure 2.7 shows mean values for 12 midsize males in one typical vehicle package from a recent UMTRI study, using the revised acromion definition, and those from Robbins for midsize males, aligned at C7 and rotated so that the C7-to-suprasternale vectors are at the same angle. The mean distance from C7 to suprasternale is 130 mm for the recent subjects and 138 mm for the Robbins subjects, indicating that the overall thorax size is similar. The acromion location reported by Robbins is considerably rearward and lower than the acromion location recorded using the revised landmark definition. The differences in the definitions may account for the more forward position, but no explanation is apparent for the vertical difference.

Since Robbins generated the glenohumeral joint location by using a humerus aligned with data from humeral landmarks, i.e., without relying on potentially lower-precision transformations from points on sternum or scapula, Robbins' joint location is assumed to be reasonably accurate. A transformation was developed to relate the revised acromion landmark to Robbins' glenohumeral joint location relative to C7 and suprasternale. Figure 2.7 shows that the glenohumeral joint location in the sagittal plane can be estimated by constructing a vector 58 mm long at an angle of 67 degrees with respect to the C7-to-suprasternale vector. The Snyder et al. data are difficult to interpret

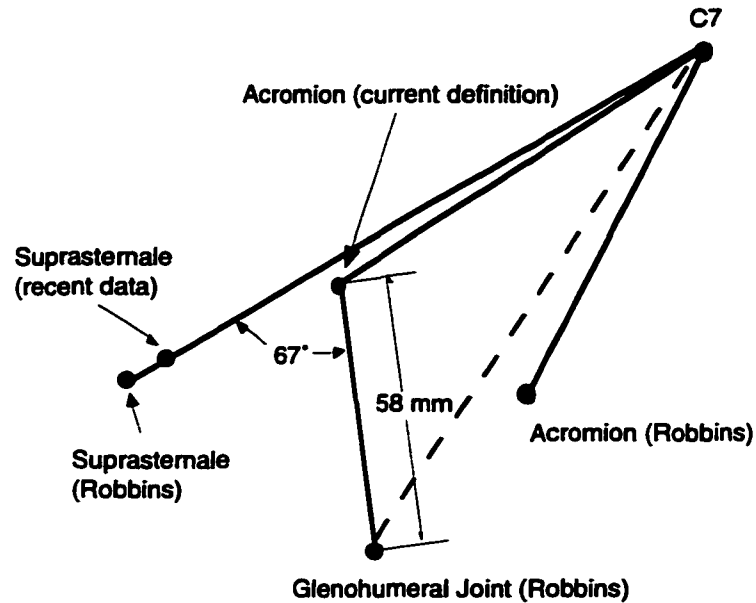


Figure 2.7. Acromion location comparison between current definition (N = 12 midsize males) and Robbins (N = 25 midsize males). Side-view data from Robbins have been aligned with the recent UMTRI data at C7 and rotated to align the C7-to-suprasternale vectors.

with regard to the necessity of scaling the acromion-to-humeral-head vector, because the data are not expressed in these terms. However, because it is reasonable to believe that the length of this vector will, on average, vary with body size, the length of the vector is scaled as a fraction of the C7-to-suprasternale vector, using the reference dimensions of 58 mm for acromion-to-glenohumeral-joint and 138 mm for C7-to-suprasternale, where the latter value is obtained from Robbins' midsize-male landmark data.

According to Snyder et al., the average angle from the center of the humeral head to the acromion landmark in the coronal (YZ) plane is only 2 degrees from vertical. Since the differences between the current and Snyder et al. acromion landmark definitions are believed to affect primarily the sagittal plane coordinates, the medial-lateral (Y-axis) coordinate of the shoulder (glenohumeral) joint will be taken to be the same as that of the acromion landmark.

This method for estimating the shoulder joint location for the kinematic model is based on fewer and less precise data than the methods for the hips and other extremity joints. However, the methods are likely to be sufficient for the intended applications.

Special Considerations for the Upper Lumbar Joint

The upper lumbar joint, which corresponds to the joint between the twelfth thoracic vertebra (T12) and the first lumbar vertebra (L1), is normally estimated, as indicated in Table 2.5, using the data from the T8 and T12 surface landmarks. However, these landmarks are not accessible when a subject is sitting in a normal automobile seat. Consequently, a method was developed to estimate the location of this joint from landmarks that are accessible in normal driving and riding postures.

Prior to posture measurement in the vehicle seat, the subject sits in a special laboratory seat that has approximately the same seatpan and seatback orientation as a normal vehicle seat, but has a 50-mm-wide slit in the center of the seatback that allows access to the spine. This seat is constructed with flat, rigid surfaces and is referred to as the “reference hardseat.” With the subject sitting in the hardseat, the locations of suprasternale, C7, T8, and T12 are recorded. The data from T8 and T12 are used to calculate the location of the upper lumbar joint using the scaling techniques described below. The data from C7 and suprasternale are also used to calculate the lower neck joint location (C7/T1). These two joints define the thorax segment for the subject. The length of the thorax segment (distance between the upper lumbar and lower neck joints) and the orientation of the vector between these joints relative to the C7-to-suprasternale vector is recorded for each subject. When analyzing subsequent test data from the subject in which T8 and T12 are not available, the location of the upper lumbar joint is calculated using the thorax geometry previously measured in the hardseat.

2.5 Calculation Diagrams for All Joints

This section contains detailed descriptions of the calculation procedures for each joint, along with figures depicting the scaling methods. As noted above, torso postures are restricted to being sagittally symmetric. Consequently, torso joint locations are calculated in the midsagittal XZ plane only, which is assumed to be parallel to the vehicle or seat XZ (sideview) plane. Extremity joints are located in three dimensions.

These landmark-to-joint transformations are presented in terms of rotated and scaled vectors. They could instead be presented in terms of segment-specific coordinate systems, but the current, equivalent procedure was judged to be simpler to present and closer to the manner in which such transformations would be implemented in computer software.

Upper Neck Joint

The upper neck joint corresponds anatomically to the atlanto-occipital joint. Figure 2.8 shows the technique for calculating the location of the upper neck joint from the infraorbitale and trasion landmarks, measured on the same side of the body. In the XZ plane, the upper neck joint center is located by rotating a vector from trasion to infraorbitale downward through 117 degrees. The vector length is 31 percent of the measured sagittal plane distance from trasion to infraorbitale. If a Y coordinate for the upper neck joint is required, it can be estimated by using the Y-coordinate of the mid-trasion or mid-infraorbitale point, i.e., centerline of head.

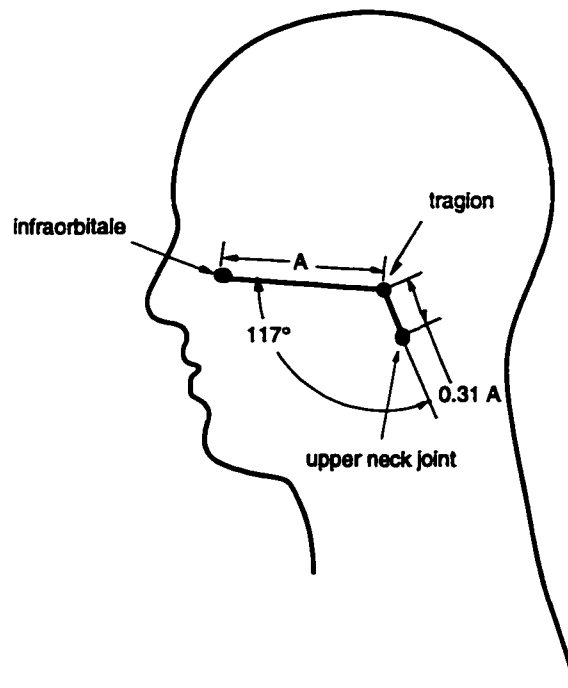


Figure 2.8. Calculation techniques for upper neck joint.

Lower Neck Joint

The lower neck joint corresponds anatomically to the C7/T1 joint. The location of this joint is calculated using the C7 and suprasternale surface landmarks, as shown in Figure 2.9. The vector from C7 to suprasternale is rotated upward 8 degrees and scaled to have a length equal to 55 percent of the measured sagittal-plane distance from C7 to suprasternale.

Upper Lumbar Joint

The upper lumbar joint corresponds anatomically to the T12/L1 joint. With the subject sitting in the reference hardseat, the locations of suprasternale, C7, T8, and T12 are recorded. The data from T8 and T12 are used to calculate the location of the upper lumbar joint, as shown in Figure 2.9.

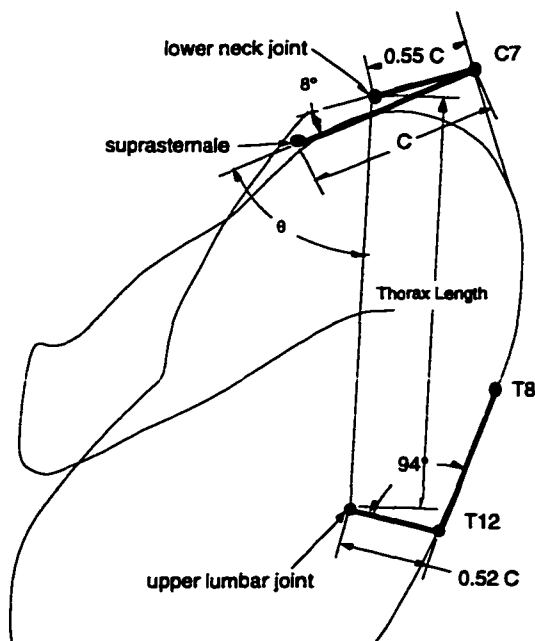


Figure 2.9. Calculation method for lower neck joint and upper lumbar joint.

Suprasternale and C7 data are used to calculate the lower neck joint location as described above. The thorax length (the distance from the lower neck joint to the upper lumbar joint) and the angle θ formed by the thorax segment and the C7-to-suprasternale vectors are recorded for the subject using data collected in the reference hardseat (see

above). These two values comprise the subject's thorax geometry for subsequent posture calculations.

When the subject's posture is measured in experimental vehicle conditions, the locations of suprasternale and C7 are used to calculate the lower neck joint location as described above. A thorax segment vector is then constructed and oriented relative to the C7-to-suprasternale vector based on the subject's thorax geometry obtained in the hardseat.

Shoulder Joint

The shoulder joint calculation in the sagittal plane is shown in Figure 2.10. The sagittal-plane distance from the shoulder joint to acromion landmark is 42 percent of the distance from C7 to suprasternale on a vector forming an angle of 67 degrees with the C7 to suprasternale vector. The Y-axis (medial-lateral) position of the shoulder joint is taken to be the same as the Y coordinate of the acromion landmark. Since the postures are restricted to sagittal symmetry, the contra-lateral shoulder joint has the same X and Z coordinate, and lies the same distance lateral from the C7 landmark.

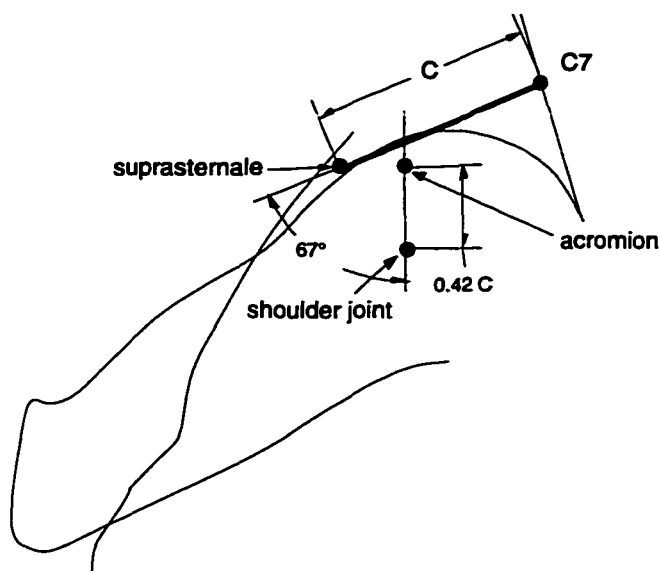


Figure 2.10. Calculation method for the shoulder joint.

Lower Lumbar Joint and Hip Joints

The hip joint and lower lumbar joint locations are calculated using the anterior-superior iliac spine (ASIS) landmarks (right and left), the pubic symphysis (PS) landmark, and the posterior-superior iliac spine landmark (PSIS). Calculations are conducted in three dimensions to obtain good estimates of both the left and right hip joint center locations for subsequent calculation of lower extremity posture. Although the measured postures are nominally sagittally symmetric and aligned with the package axes, a test subject's pelvis is sometimes tilted laterally or twisted relative to the package coordinate system. Consequently, the hip joint locations are calculated individually, then averaged in the XZ plane to obtain a mean hip joint location for use in calculating pelvis segment orientation (pelvis angle).

The lower lumbar and hip joint locations are calculated in a pelvis-centered coordinate system, which is then transformed to the desired global coordinate system. The pelvis coordinate system is shown in Figure 2.11. The Y axis is defined by the vector connecting the left and right ASIS. The Z axis is perpendicular to this line and passes through the pubic symphysis (PS). The X axis is mutually perpendicular to the Y and Z axes. Note that the coordinate system shown in Figure 2.11 is based on points on the bone, rather than surface landmarks. The flesh margins at the ASIS and PS landmarks are taken into account in the calculations.

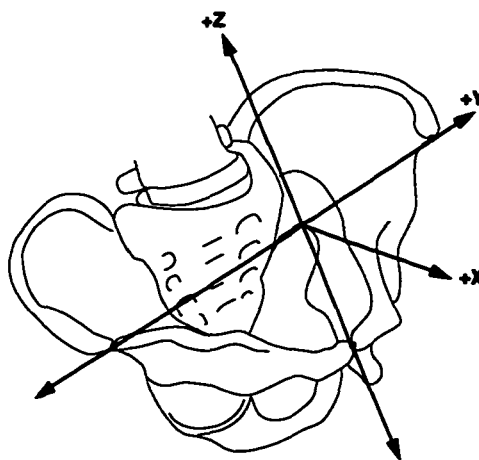


Figure 2.11. Pelvis coordinate system, adapted from Reynolds et al. (1981).

The first step in the calculation of pelvis joints is to account for flesh margins at the landmarks. According to recently collected cadaver data (unpublished), average flesh margin thicknesses is 10 mm at the ASIS and 15 mm at the pubic symphysis. Data are not available for the PSIS, but 5 mm is assumed. As shown in Figure 2.12, a preliminary surface pelvis coordinate system $\{X_s, Y_s, Z_s\}$ is established using the definition in Figure 2.11 with the ASIS and PS surface landmarks. The landmark points are then translated according to the flesh margins to obtain estimates of the underlying bony landmark location. The bone points are then used to define a pelvis bone coordinate system $\{X_b, Y_b, Z_b\}$ identical to that shown in Figure 2.11. Table 2.6 shows the flesh margin correction vectors in the surface pelvis coordinate system.

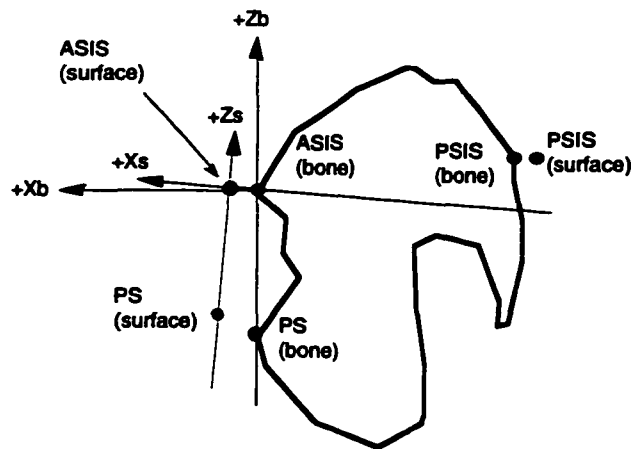


Figure 2.12. A sagittal view of surface and bone pelvis coordinate systems based on measured landmark locations (not to scale).

Table 2.6
Flesh Margin Correction Vectors
in the Surface Pelvis Coordinate System $\{X_s, Y_s, Z_s\}$
(mm)

Landmark	X	Y	Z
ASIS (right and left)	-10	0	0
PS	-10.6	0	-10.6
PSIS	5	0	0

The locations of the hip and lower lumbar (L5/S1) joints are calculated in the bone coordinate system $\{X_b, Y_b, Z_b\}$ using vectors scaled with reference to pelvis dimensions defined by the bone landmark locations. The reference dimensions, all measured in three-dimensions, are as follows:

- Pelvis Width (PW): Distance between right ASIS (bone) and left ASIS (bone).
- Pelvis Height (PH): Distance between PS (bone) and the midpoint of the line connecting left ASIS (bone) and right ASIS (bone).
- Pelvis Depth (PD): Distance between right ASIS (bone) and right PSIS (bone) or the distance between left ASIS (bone) and left PSIS (bone); if all four landmarks are available, use average of values from left and right sides.

Figure 2.13 shows the X and Z coordinates of the hip and lower lumbar joints. Tables 7 and 8 give the scaling relationships to be used. Note that the X and Z coordinates may be scaled using PW or PD and PH, respectively. The latter should be used when the required landmark data are available. The Y coordinate of the lower lumbar joint in the bone coordinate system is zero, i.e., equal to the Y coordinate of the midpoint of the line connecting right ASIS (bone) and left ASIS (bone). The Y coordinate of the hip joints are found by moving laterally right or left from the mid-ASIS point according to the scaling in Table 2.7.

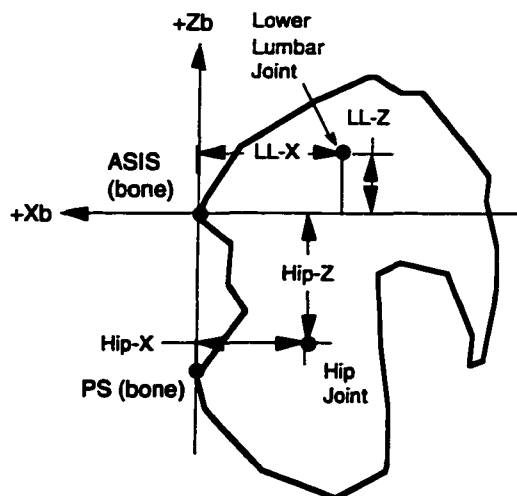


Figure 2.13. Location of hip and lower lumbar joints in XZ plane relative to bone coordinate system (not to scale). See Tables 2.7 and 2.8 for dimension scaling.

Table 2.7
Mean Hip Joint Scaling Relationships from Seidel et al. (1995)

Measure*	Scale Factor
Hip-X/PW	24%
Hip-Y/PW	36%*
Hip-Z/PW	30%
Hip-X/PD	34%
Hip-Z/PH	79%

*Y coordinate measured laterally from the mid-ASIS point.

Table 2.8
Mean Lower Lumbar Joint Scaling Relationships
Using Data from Reynolds et al. (1981)

Measure*	Scale Factor
LL-X/PW	27.4%
LL-Z/PW	15.0%
LL-X/PD	39.9%
LL-Z/PH	43.2%

Lower Extremity

The knee and ankle joint locations are calculated using simplifications of the techniques described by Dempster (1955) and adapted by Robbins (1985a). Both the Dempster and Robbins procedures locate these joints on vectors connecting landmarks on opposite sides of the limb. Because it is often difficult to measure the locations of medial landmarks with vehicle-seated occupants, the simplified procedures use data from only the lateral side of the limb to obtain reasonably similar results. The procedure is to project a vector a scaled distance perpendicular to the plane formed by two measured and one calculated landmark. The scaling was developed from data on limb breadth at the joints in Schneider et al. (1985). Figure 2.14 shows the procedure schematically.

To calculate the knee joint location, a plane is formed by the measured lateral malleolus and lateral femoral condyle locations, along with the calculated hip joint

location on the same side of the body. A vector is constructed perpendicular to this plane, passing through the lateral femoral condyle landmark. The knee joint is located on this vector medial to the lateral femoral condyle landmark by a distance equal to 11.8 percent of the measured distance between the lateral malleolus and the lateral femoral condyle landmarks.

The ankle joint location is calculated similarly. A vector is constructed perpendicular to the plane described above, and passing through the lateral malleolus landmark. The ankle joint is located medial to the lateral malleolus landmark by a distance equal to 8.5 percent of the distance between the lateral malleolus and the lateral femoral condyle landmarks.

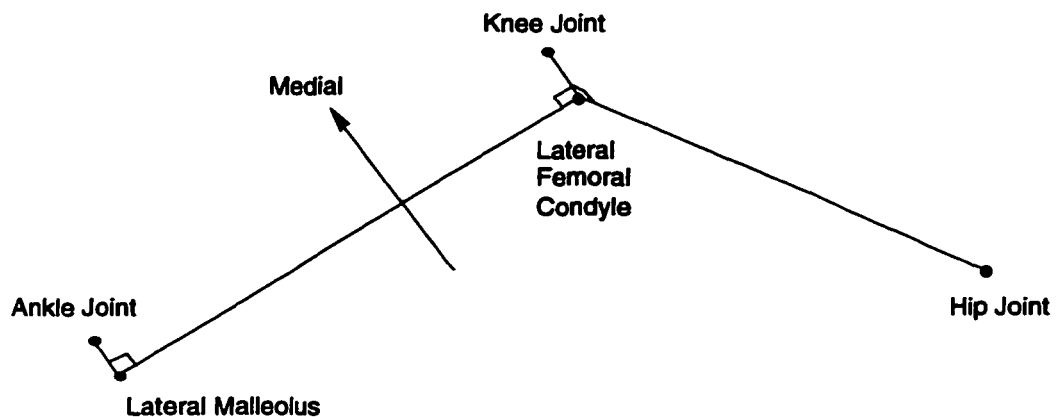


Figure 2.14. Calculation procedure for knee and ankle joints. Vectors from knee joint to lateral femoral condyle, and from ankle joint to lateral malleolus, are perpendicular to the plane formed by the hip joint, lateral femoral condyle, and lateral malleolus. See text for scaling length of vector from lateral femoral condyle to knee joint.

Upper Extremity

Calculations of upper extremity joint locations are similar to those for the lower extremity. Because of pronation and supination of the forearm, more than one wrist landmark would be necessary to use a method similar to the ankle technique to locate the wrist joint. However, a single point on the dorsal surface of the wrist is a sufficiently accurate estimate of the joint location for representing normal riding and driving postures. The measured wrist point is a skin surface point midway between the palpated radial and ulnar styloid processes.

The elbow location is calculated in a manner analogous to the knee, as shown in Figure 2.15. A plane is constructed that passes through the wrist landmark, lateral humeral condyle landmark, and the shoulder joint location on the same side of the body. A vector is constructed perpendicular to this plane, passing through the lateral humeral condyle landmark. The elbow joint is located medial to the lateral humeral condyle landmark a distance equal to 15.5 percent of the distance between the lateral humeral condyle and wrist landmarks. This scaling was determined from data on elbow width as a percentage of forearm length in Schneider et al. (1985).

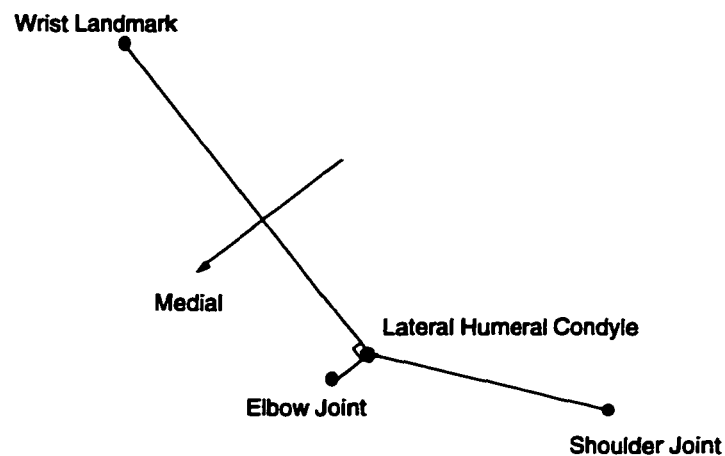


Figure 2.15. Calculation procedure for elbow joint. Vector from lateral humeral epicondyle to elbow joint is perpendicular to plane formed by the shoulder joint, lateral humeral epicondyle, and wrist landmark.

2.6 Discussion

These procedures provide a means of representing a vehicle occupant's posture as a kinematic linkage, using joint locations calculated from a sparse set of external body landmarks. The joint location calculation procedures are based on a review of the literature, with particular emphasis on a recent study of driver anthropometry used to formulate anthropometric specifications for a new family of crash dummies. In all cases, the joint calculations are believed to be sufficiently accurate for representing normal vehicle occupant postures. Computer software has been written to perform these calculations automatically from body landmark data. Using these techniques, the effects

of vehicle and seat design parameter as well as anthropometric factors on posture can be quantified and expressed in terms useful to the developers of ergonomic software.

2.7 References

- Andersson, G.B.J., Murphy, R.W., Örtengren, R., and Nachemson, A.L. (1979). The influence of backrest inclination and lumbar support on lumbar lordosis. *Spine* 4(1), 52-58.
- Backaitis, S.H., and Mertz, H.J., eds. (1994) *Hybrid III: The first human-like crash test dummy*. Special Publication PT-44. Warrendale, PA: Society of Automotive Engineers, Inc.
- Bell, A.L., Pedersen, D.R., and Brand, R.A. (1990). A comparison of the accuracy of several hip center location prediction methods. *Journal of Biomechanics* 23(6): 617-621.
- Bush, N.J. (1993). Two-dimensional drafting template and three-dimensional computer model representing the average adult male in automotive seated postures. Master's thesis, Michigan State University, East Lansing.
- Dempster, W.T. (1955). *Space requirements of the seated operator: Geometrical, kinematic, and mechanical aspects of the body with special reference to the limbs*. WADC Technical Report 55-159. Wright-Patterson AFB, OH: Wright Air Development Center.
- Ewing, C.L., and Thomas D.J. (1972) *Human head and neck response to impact acceleration*. NAMRL Monograph 21. Pensacola, FL: Naval Aerospace Medical Research Laboratory.
- Haas, W.A. (1989). Geometric model and spinal motions of the average male in seated postures. Master's thesis, Michigan State University, East Lansing.
- Maltha, J., and Wismans, J. (1980) MADYMO - Crash victim simulations, a computerised research and design tool. *Proc. 5th International IRCOBI Conference on the Biomechanics of Impact*, ed. J.P. Cotte and A. Charpenne, 1-13. Bron, France: IRCOBI.
- Manary, M.A., Schneider, L.W., Flannagan, C.C., and Eby, B.H. (1994). *Evaluation of the SAE J826 3-D manikin measures of driver positioning and posture*. SAE Technical Paper 941048. Warrendale, PA: Society of Automotive Engineers, Inc.
- McConville, J.T., Churchill, T.D., Kaleps, I., Clauser, C.E., and Cuzzi, K. (1980). *Anthropometric relationships of body and body segment moments of inertia*. Report no. AMRL-TR-80-119. Wright Patterson Air Force Base, OH: Aerospace Medical Research Laboratories.
- Nussbaum, M.A. and Chaffin, D.B. (1996). Development and evaluation of a scalable and deformable geometric model of the human torso. *Clinical Biomechanics* 11(1): 25-34.

- Reed, M.P., Schneider, L.W., and Eby, B.A.H. (1995). *The effects of lumbar support prominence and vertical adjustability on driver postures*. Technical Report UMTRI-95-12. Ann Arbor: University of Michigan Transportation Research Institute.
- Reynolds, H.M. (1994). *Erect, neutral, and slump sitting postures: A study of the torso linkage system from shoulder to hip joint*. Final Report AL/CF-TR-1994-0151. Wright Patterson Air Force Base, OH: Air Force Material Command.
- Reynolds, H.M., Snow, C.C., and Young, J.W. (1981). *Spatial Geometry of the Human Pelvis*. Memorandum Report AAC-119-81-5. Oklahoma City, OK: Federal Aviation Administration, Civil Aeromedical Institute.
- Robbins, D.H. (1985a). *Anthropometric specifications for mid-sized male dummy, Volume 2*. Final report DOT-HS-806-716. Washington, D.C.: U.S. Department of Transportation, National Highway Traffic Safety Administration.
- Robbins, D.H. (1985b). *Anthropometric specifications for small female and large male dummies, Volume 3*. Final report DOT-HS-806-717. Washington, D.C.: U.S. Department of Transportation, National Highway Traffic Safety Administration.
- Roe, R.W. (1993). Occupant packaging. In *Automotive Ergonomics*, ed. B. Peacock and W. Karwowski, 11-42. London: Taylor and Francis.
- Schneider, L.W., Robbins, D.H., Pflüg, M.A., and Snyder, R.G. (1985). *Development of anthropometrically based design specifications for an advanced adult anthropomorphic dummy family, Volume 1*. Final report DOT-HS-806-715. Washington, D.C.: U.S. Department of Transportation, National Highway Traffic Safety Administration.
- Seidl, A. (1994). *Das Menschmodell RAMSIS: Analyse, Synthese und Simulation dreidimensionaler Körperhaltungen des Menschen [The man-model RAMSIS: Analysis, synthesis, and simulation of three-dimensional human body postures]*. Ph.D. dissertation, Technical University of Munich, Germany.
- Seidl, G.K., Marchinda, D.M., Dijkers, M., and Soutas-Little, R.W. (1995). Hip joint center location from palpable bony landmarks--A cadaver study. *Journal of Biomechanics* 28(8): 995-998.
- Snyder, R.G., Chaffin, D.B., and Schutz, R. (1972). *Link system of the human torso*. Report no. AMRL-TR-71-88. Wright-Patterson Air Force Base, OH: Aerospace Medical Research Laboratory.
- Society of Automotive Engineers (1997). *Automotive Engineering Handbook*. Warrendale, PA: Society of Automotive Engineers, Inc.

CHAPTER 3

THE EFFECTS OF PACKAGE, SEAT, AND ANTHROPOMETRIC VARIABLES ON DRIVING POSTURE

3.1 Abstract

The effects of vehicle package, seat, and anthropometric variables on posture were studied in a laboratory vehicle mockup. Sixty-eight men and women selected their preferred driving postures in a total of 18 different combinations of seat height, fore-aft steering wheel position, and seat cushion angle. Two seats, differing in stiffness and seatback contour, were used in testing. Driving postures were recorded using a sonic digitizer to measure the three-dimensional locations of body landmarks. All of the test variables had significant, independent effects on driving posture. Drivers were found to adapt to changes in the vehicle geometry primarily by changes in limb posture while torso posture remained relatively constant. Stature accounts for most of the anthropometrically related variability in driving posture, and gender differences appear to be explained by body size variation. Large intersubject differences in torso posture, which are fairly stable across different seat and package conditions, are not closely related to standard anthropometric measures. The findings can be used to predict the effects of changes in vehicle and seat design on driving postures for people with a wide range of anthropometry.

3.2 Introduction

Accurate prediction of driving posture is essential for vehicle interior design. Optimal positioning of the controls, displays, and restraint systems depends on a detailed understanding of how and where drivers of widely varying sizes will sit. Early research into the problem of control and seat placement was concerned primarily with improving

the comfort of designs, rather than predicting how people would respond to particular vehicle and seat geometries (Lay and Fisher, 1940). Beginning in the late 1950s, designers began to use planar and three-dimensional manikins, based on the pioneering work of Dempster (1955), to assess leg room and control reach (Myal, 1958; Kaptur and Myal, 1961; Geoffrey, 1961). During the 1960s, the concept of a task-oriented percentile model was applied to vehicle design and driver posture prediction in a systematic way (Roe, 1993). Task-oriented percentile models describe the distribution of particular posture characteristics of interest in relation to a particular task. Meldrum (1965) developed the eyellipse, a statistical construct that predicts the distribution of driver eye locations. The eyellipse, documented in the Society of Automotive Engineers Recommended Practice J941 (SAE, 1997), has remained one of the most important interior design tools, even as it has been amended and its application broadened (Devlin and Roe, 1968; Hammond and Roe, 1972; Mourant et al., 1978; Arnold et al., 1985). The location of the eyellipse in vehicle space is calculated as a function of seatback angle with respect to the seating reference point location (see Appendix A for review of vehicle packaging terminology). Effectively, the driver eye location distribution is predicted as a function of seat height and seatback angle. However, almost all current driver seats are provided with seatback angle adjustment, making the validity of the eye location prediction dependent on the accurate selection of design seatback angle.

Another task-oriented percentile model has been developed to predict driver-selected seat position (Phillipart et al., 1984). This model, documented in SAE Recommended Practice J1517, predicts percentiles of the driver-selected seat position distribution as a function of seat height, although Phillipart et al. (1985) noted potential independent effects of steering wheel position and seat cushion angle. Recently, Flannagan et al. (1996) developed an improved model that includes effects of seat height, steering wheel position, seat cushion angle, and transmission type, each of which have significant, independent effects on driver-selected seat position.

While these tools have proven to be very useful in vehicle design, recent advances in computer technology have led to the development of software models of the entire human body that are increasingly used for vehicle design (Porter et al., 1993). Unfortunately, the task-oriented percentile models are not useful for positioning a human manikin that represents a particular body size. The seat position and eyellipse models predict the population distribution of their respective parameters, but do not provide a linkage between them, or to any individual set of anthropometric measurements.

The current study investigates the effects on whole-body driving posture of three variables that are known to have important effects on seat position. The analysis is intended to provide an understanding of the individual and interactive effects of seat height, steering wheel position, and seat cushion angle on all of the major posture characteristics of interest for vehicle interior design. The driving postures of sixty-eight subjects were measured in a total of 18 combinations of the test variables, using two different seats. Three-dimensional body landmark data were collected using a sonic digitizer to characterize the subjects' preferred driving postures. The data were analyzed using a kinematic linkage representation of the body to determine the postural effects of the test variables and subject anthropometry. These data and findings were used in a subsequent project to develop whole-body posture prediction methods suitable for use with computer software manikins (Chapter 5).

3.3 Methods

Subjects

This study was conducted in three phases, each of which used different subjects and a different set of conditions. A total of 68 licensed adult drivers participated in the study. Subjects were selected in gender-stature groups spanning more than 95 percent of the stature range in the U.S. population (Abraham et al., 1979). Table 3.1 summarizes the subject stature distribution by phase. Stratified sampling of this type ensures adequate representation at the upper and lower tails of the stature distribution, and also produces

adequate variance on other anthropometric measures of interest, such as weight and sitting height.

**Table 3.1
Subject Pool**

Subject Group	Stature Range (mm)	Gender	Phase 1 n	Phase 2 n	Phase 3 n	All n
0	under 1511	Female		3	3	6
1	1511 - 1549	Female	5	0	0	5
2	1549 - 1595	Female		3	3	6
3	1595 - 1638	Female	5	0	0	5
4	1638 - 1681	Female		3	3	6
5	1681 - 1722	Female		3	3	6
6	1636 - 1679	Male		3	3	6
7	1679 - 1727	Male		3	3	6
8	1727 - 1775	Male	5	0	0	5
9	1775 - 1826	Male		3	3	6
10	1826 - 1869	Male	5	0	0	5
11	over 1869	Male		3	3	6
Total			20	24	24	68

Facilities

Testing was conducted in a reconfigurable vehicle mockup that allowed the seat height, fore-aft steering wheel position, and seat cushion angle to be varied over a wide range. The seat and control layout, termed the vehicle “package,” was specified and measured using standard reference points and dimension definitions documented in Society of Automotive Engineers Recommended Practice J1100 and other related practices (see Appendix A for additional detail on vehicle package practices and terminology). Figure 3.1 illustrates these dimensions in a side view of a generic package. The X axis in the package coordinate system runs positive rearward, the Y axis positive to the driver’s right, and the Z axis positive vertically. The origin is defined by a different point on each axis. The origin X coordinate is defined by the Ball of Foot (BOF) reference point, while the origin Z coordinate is defined by the Accelerator Heel Point (AHP). In general terms, vertical dimensions are measured from the floor (heel

surface) and fore-aft dimensions are measured from a point on the accelerator pedal. For the current analysis, the origin Y coordinate is the centerline of the driver seat.

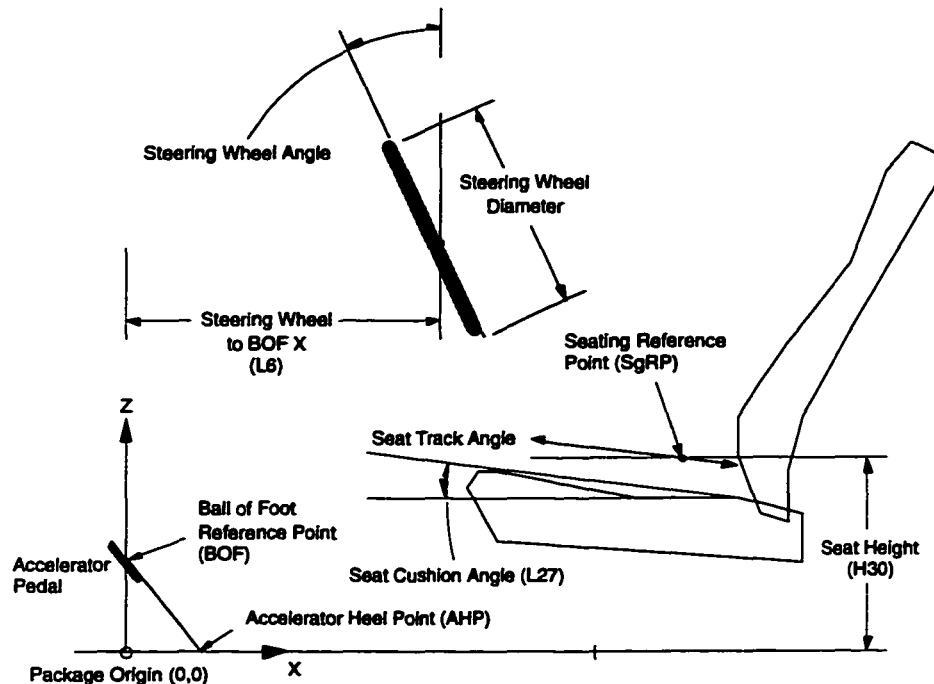


Figure 3.1. Vehicle package geometry. Expressions in parentheses are Society of Automotive Engineers nomenclature from SAE J1100 (SAE, 1997).

The weighted, contoured H-point manikin (SAE J826) measures a reference point on the seat known as the H-point (a hip-joint location estimate). When the seat is moved forward and rearward along its adjustment track, the orientation of the path of the H-point relative to the horizontal defines the seat track angle. The seating reference point (SgRP) is the H-point location that lies on the 95th-percentile selected seat position curve given by SAE J1517 (SAE, 1997). This curve is a second-order polynomial describing the horizontal position of the 95th-percentile of the seat position distribution as a function of seat height. Seat height is defined by the vertical distance between the SgRP and the AHP, and is termed H30, following the dimension definitions in SAE J1100.

Seat cushion angle (SAE L27) specifies the orientation of the lower part of the seat (seat pan) with respect to horizontal, and is measured using the H-point manikin with a procedure described in SAE J826. Seat cushion angle does not generally correspond to any measure of the unloaded centerline contour of the seat, but instead represents the deflected cushion orientation experienced by a standardized sitter (the H-point manikin). The steering wheel is characterized by the coordinates of the center of the front surface of the wheel, the angle of the front surface of the wheel with respect to vertical, and the diameter of the wheel. The horizontal distance from the center of the steering wheel to BOF is a key package dimension and is termed SW-BOFX.

Figure 3.2 illustrates the test mockup schematically. This is the same facility used in some of the research reported by Flannagan et al. (1996). The seat was mounted on a motorized platform allowing unrestricted fore-aft travel along a path inclined 6 degrees to the horizontal. Seat cushion angle was varied by pivoting the entire seat around a lateral axis. Seat height was set by adjusting the height of the heel surface relative to the seat. When the seat height was increased, the angle of the accelerator and brake pedals with respect to the horizontal was reduced, consistent with the pedal plane angle equation given in SAE J1516. In keeping with trends documented in vehicle fleet data, the steering wheel and instrument panel height were also lowered slightly with respect to the SgRP at higher seat heights (25 mm lower per 90 mm of seat height increase), and the steering wheel angle with respect to vertical was increased at higher seat heights (2 degrees per 90 mm of seat height increase). The fore-aft position of the steering wheel with respect to the pedals was varied by moving the pedals along a motorized horizontal track, rather than moving the steering wheel. This reduced the amount of seat track travel required and allowed the instrument panel and steering wheel to remain in a fixed relation.

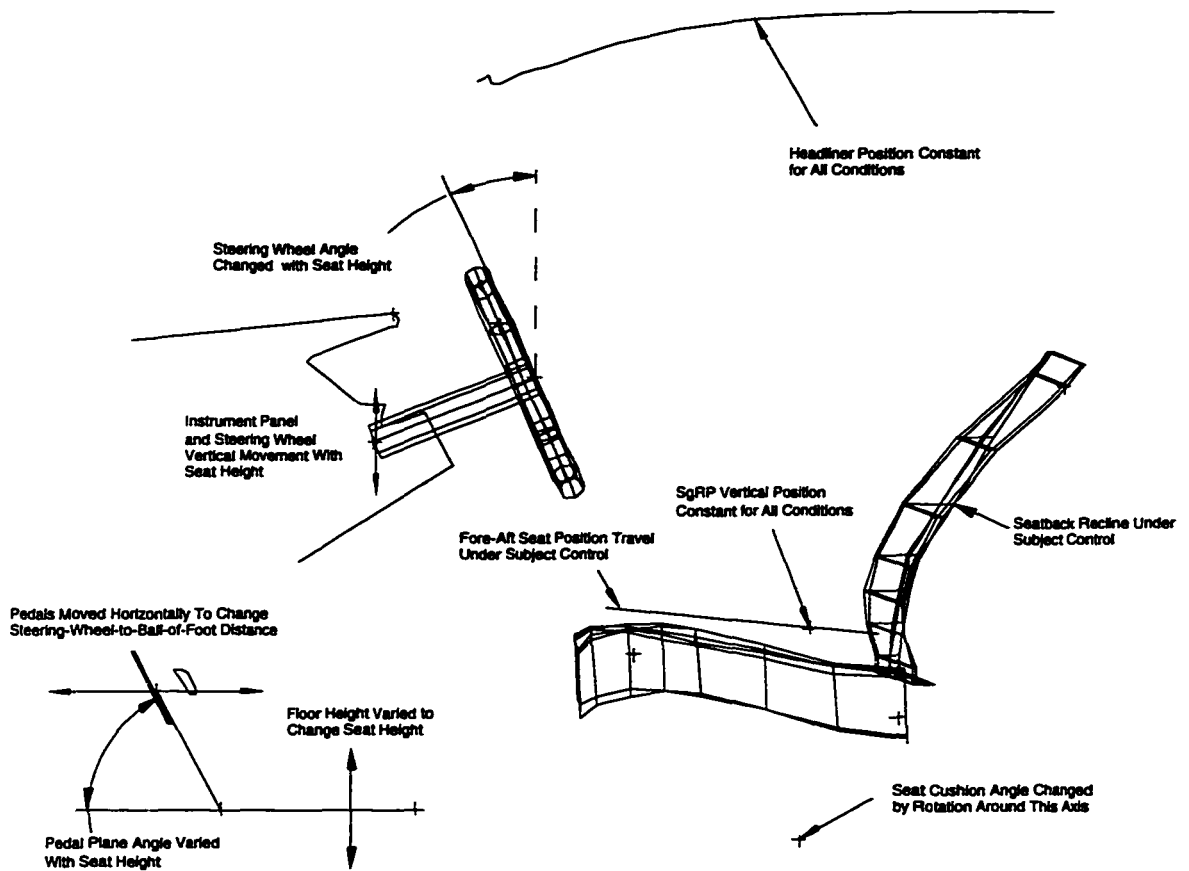


Figure 3.2. Schematic of vehicle mockup, showing adjustment axes.

Test Conditions

Three package and seat variables were manipulated independently, using a range of each variable intended to represent a substantial portion of the vehicle fleet. These variables were selected after reviewing the findings of a number of unpublished studies of driving posture conducted at UMTRI both in laboratory mockups and in vehicles. Table 3.2 lists the 18 configurations used in testing. Seat height (SAE H30) was set to 180, 270, and 360 mm, corresponding to a wide range of vehicle types from sporty cars to minivans. Seat cushion angle (SAE L27) was set to 11 and 18 degrees. The horizontal distance from the steering wheel center to the Ball of Foot reference point (SW-BOFX) was adjusted between 450 and 650 mm.

**Table 3.2
Test Conditions**

Configuration Number	N	Phase 1	Phase 2	Phase 3	Seat Cushion Angle (L27) (degrees)	Seat Height (H30) (mm)	SW-BOFX (mm)
1	44	x	x		11	270	450
2	68	x	x	x	11	270	500
3	68	x	x	x	11	270	550
4	68	x	x	x	11	270	600
5	44	x	x		11	270	650
6	44	x	x		18	270	450
7	68	x	x	x	18	270	500
8	68	x	x	x	18	270	550
9	68	x	x	x	18	270	600
10	44	x	x		18	270	650
12*	48		x	x	11	180	550
13	48		x	x	11	180	650
14	48		x	x	11	360	450
15	48		x	x	11	360	550
16	24			x	18	180	550
17	24			x	18	180	650
18	24			x	18	360	450
19	24			x	18	360	550

* Condition 11 included a modification to the seat. Data from condition 11 are excluded from this analysis.

Steering wheel position with respect to BOF is correlated with seat height in this experiment design, because it is not possible to manipulate both variables over a large range without correlation. At high seat heights, drivers tend to sit closer to the pedals, necessitating a more forward steering wheel position. In fact, across the vehicle fleet, a substantial correlation exists between these two variables. Figure 3.3 shows a plot of seat height and SW-BOFX for 158 recently produced vehicles, along with the test conditions used in this study. At each seat height level, the test conditions were selected to span a substantial fraction of the range of production vehicles. The correlation between seat height and steering wheel position in the experiment is addressed in the analysis, primarily by considering subsets of the test configurations for which the two variables are orthogonal. Figure 3.4 shows seat cushion angles for 65 vehicles, along with the two levels used in testing.

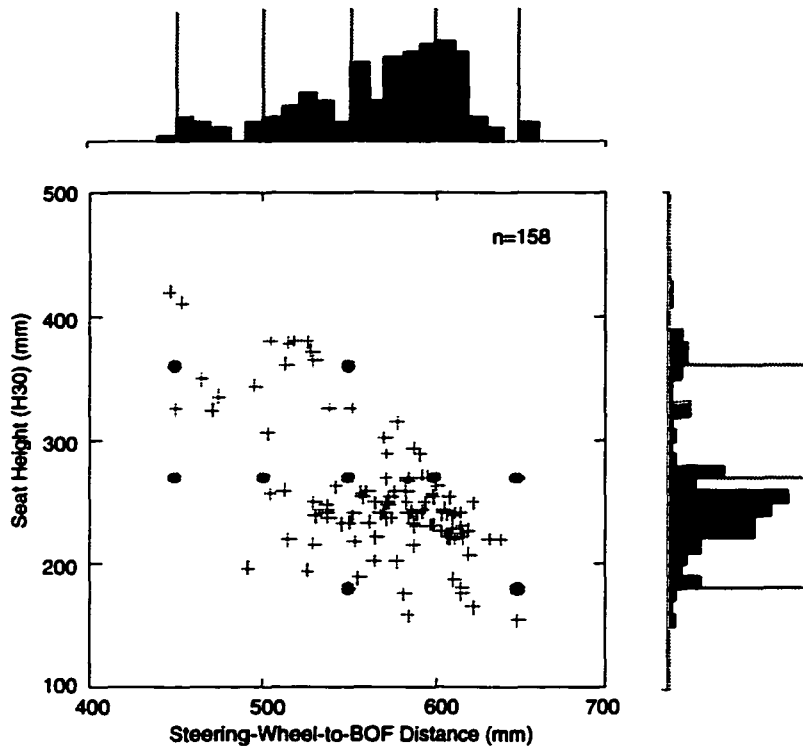


Figure 3.3. SW-BOFX versus seat height in 158 production vehicles. Large dots are test conditions used in the current study.

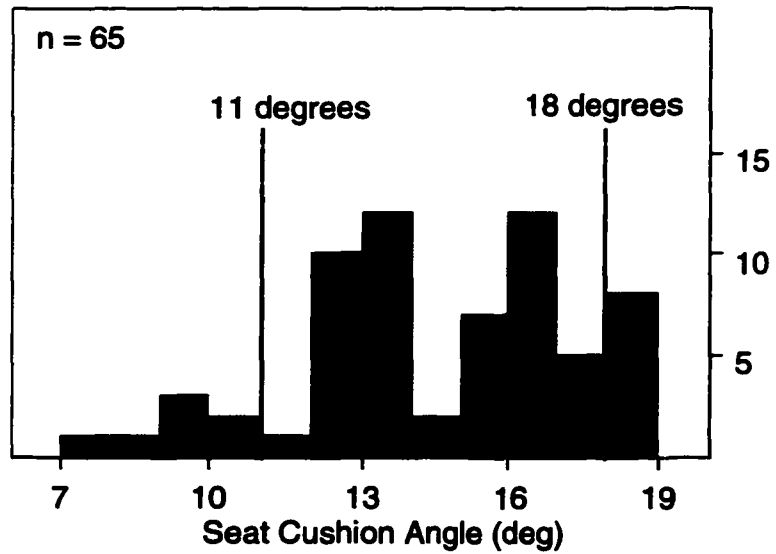


Figure 3.4. Seat cushion angle distribution for 65 production vehicles. Test conditions are shown with vertical lines. Vertical axis is count.

Phases 1 and 2 were conducted using a seat from a Ford Taurus, a typical midsize sedan seat that has minimal contouring or bolstering. The Dodge Neon seat used for Phase 3 testing was a sportier, bucket seat, with a firm, prominent lumbar support. The objective in switching seats was to evaluate whether the effects of seat height, steering wheel position, or seat cushion angle differed for the two seats.

Procedures

Subjects were recruited by advertisement and by word-of-mouth. All were licensed drivers with at least four years of experience. The study objectives were explained to each subject and written consent was obtained. The subject changed from street clothes into test garb, consisting of loose-fitting shorts and a short-sleeve shirt with a slit in the back to allow access to posterior spine landmarks. The subjects wore their own comfortable driving shoes.

Each subject's posture was measured in a standardized preliminary condition, using a sonic digitizer to record the location of palpated body landmarks (see Chapter 2). Landmark data were collected with the subject sitting in a laboratory hardseat that allows access to the posterior thoracic and lumbar spinous process landmarks. These data were used to quantify thorax geometry for calculation of the T12/L1 joint location using only landmarks that are accessible with the subject sitting in a vehicle seat (see Chapter 2).

The test conditions were presented to the subjects in random order. For each trial, the subject was screened from the vehicle mockup while the test conditions were set by the experimenter. The seat track position was adjusted to the estimated mean population seat position and the seatback angle was set to 23 degrees, using the SAE J826 manikin measure. The subject entered the mockup and adjusted the fore-aft seat position using a motorized control and adjusted the seatback recline angle using a manual adjuster. The subject was instructed to operate the pedals and steering wheel, and to continue to adjust until a "normal, comfortable driving posture" was obtained. A static road scene was displayed on a large screen in front of the drivers to provide consistent visual cues. In

Phase 1, the subjects were free to choose any hand position on the steering wheel. In Phases 2 and 3, subjects were instructed to place their hands on the steering wheel at the 10-o'clock and 2-o'clock positions. Although many other hand positions are possible in driving, the 10-o'clock and 2-o'clock positions are reasonable and standardizing the hand locations gives greater meaning to the elbow angles. There was, however, no significant difference in elbow angle for similar conditions in Phases 1 and 2.

After the subject obtained a comfortable driving posture, the experimenter recorded the body landmark locations using the sonic digitizer probe. The entire measurement required approximately 60 seconds, after which the subject exited the mockup to prepare for the next trial. Testing with each subject lasted approximately two hours.

Data Analysis

The body landmark data were used to calculate the locations of joints defining a kinematic-linkage representation of the body, illustrated in Figure 3.5. These procedures are described in detail in Chapter 2. The resulting body segment positions and orientations were analyzed to determine the effects of the experimental variables on driving posture. Six variables of primary interest are defined in Table 3.3 and illustrated in Figure 3.6. HipX is the horizontal location of the hip joint (average of right and left) aft of BOF. Hip-to-Eye Angle is the angle of a vector from mean hip to the Center-Eye point with respect to vertical, and is a measure of overall recline. The Center-Eye point (hereafter called the eye point) is an eye location estimate on the body centerline with the fore-aft coordinate of the infraorbitale landmark, the lateral coordinate of the glabella landmark, and the vertical coordinate of the corner-eye landmark.

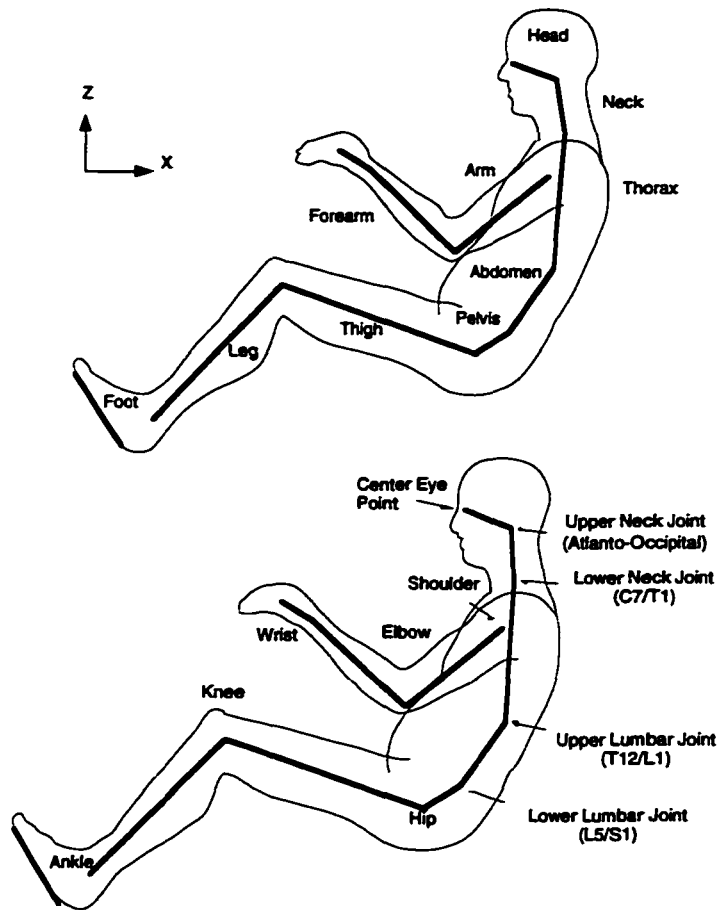


Figure 3.5. Kinematic linkage representation of driving posture.

Table 3.3
Posture Variable Definitions

Variable	Definition
HipX	Fore-aft distance from the mean hip joint location to the Ball of Foot reference point
Hip-to-Eye Angle	Angle in the side view (XZ) plane of the vector from the mean hip joint to the Center Eye point with respect to vertical
Center Eye Point	An eye location estimate on the body centerline with the fore-aft coordinate of the infraorbitale landmark, the lateral coordinate of the glabella landmark, and the vertical coordinate of the corner-eye landmark
Pelvis Angle, Thorax Angle, Head Angle	XZ (side view) plane angle of the respective segment with respect to vertical
Lumbar Flexion	Pelvis Angle minus Thorax Angle
Cervical Flexion	Head Angle minus Thorax Angle
Elbow Angle	Angle between the arm and forearm segments in the plane of the segments; smaller values indicate greater flexion
Knee Angle	Angle between the thigh and leg segments in the plane of the segments; smaller values indicate greater flexion

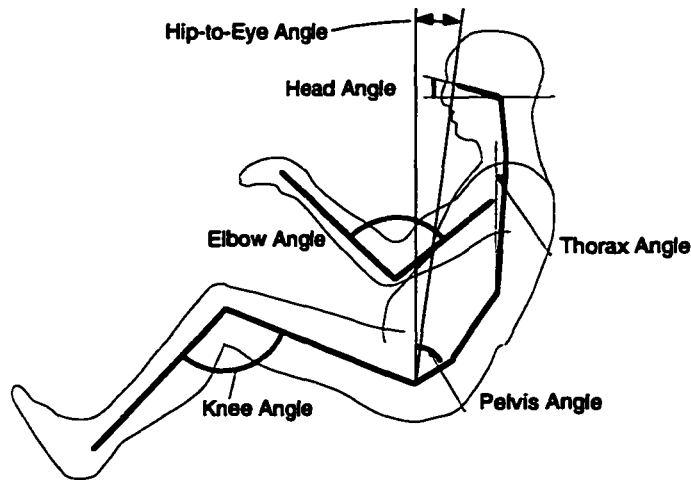


Figure 3.6. Illustration of posture variables.

3.4 Results

Data from Phases 1 and 2 for conditions 1 through 10, representing five steering wheel positions at two seat cushion angles, were extracted for initial analysis. Steering wheel positions were normalized by subtracting the midrange value at the 270-mm seat height (550 mm). Within-subject ANOVA identified highly significant effects of both test variables on most of the posture variables of interest. Table 3.4 summarizes effects that were significant with $p < 0.01$. In no case was the interaction between seat cushion angle and steering wheel position significant.

Table 3.4
Effects of Steering Wheel Position and Seat Cushion Angle:
Configurations 1 through 10 in Phases 1 and 2*

Variable	Normalized Steering Wheel Position (-100 to +100 mm)	Seat Cushion Angle (11° to 18°)
HipX (mm)	89.6	-6.0
Hip-to-Eye Angle	3.1	0.59
Lumbar Flexion	n.s.†	2.0
Cervical Flexion	n.s.	n.s.
Elbow Angle	-26.5	n.s.
Knee Angle	16.3	-3.6

*Listed values are mean differences between conditions. Positive values indicate the indicated change in the independent variable resulted in a rearward, more reclined, or more flexed dependent variable value. †n.s. indicates effect was not significant ($p > 0.01$).

Steering wheel position had a strong effect on fore-aft hip joint location (HipX). Moving the steering wheel rearward 200 mm from the most forward position resulted in an average rearward movement of the hip joint of about 90 mm. The rearward movement of the steering wheel reduced elbow angle by an average of 26.5 degrees while increasing knee angle by 16.3 degrees. Overall torso recline (hip-to-eye angle) increased about 3 degrees with the 200-mm increase in steering-wheel-to-pedal distance. The significant effects of steering wheel position were largely linear. Figure 3.7 illustrates the steering wheel and seat cushion angle effects on HipX. The effect of steering wheel position on hip location is approximately linear over a 200-mm range, and the steering wheel effect is very similar for the two seat cushion angles.

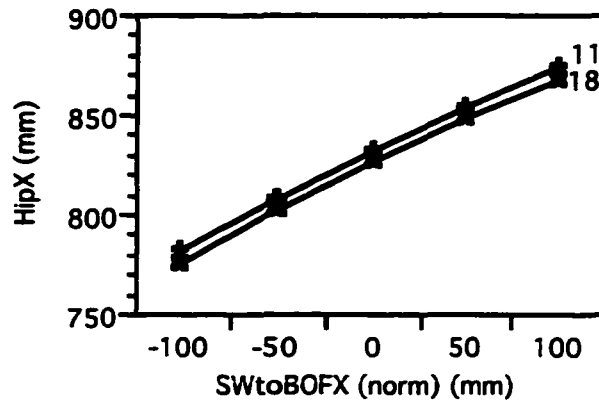


Figure 3.7. Steering-wheel-position and seat-cushion-angle effects on HipX in Phases 1 and 2, Configurations 1 through 10.

Changing the seat cushion angle from 11 to 18 degrees had significant but smaller average effects on posture. The higher cushion angle resulted in hip joint locations an average of 6 mm further forward, and increased overall torso recline by less than one degree. Net lumbar spine flexion increased by 2 degrees, but cervical flexion was not significantly affected. Elbow angles were not significantly affected, but knee angles were reduced an average of 3.6 degrees.

Seat Effects and Interactions

In Phase 3, six of the conditions tested in both Phase 1 and Phase 2 were repeated with different subjects and with a different seat. Data from these conditions (2, 3, 4, 7, 8, 9) were extracted to assess differences in posture between seats and potential interactions between the seat type and the steering wheel position or seat cushion angle.

There were two significant differences in average posture between the two seats, using a between-subjects comparison. The subjects in the Neon seat sat an average of 15 mm further forward (HipX) and with 3.4 degrees less lumbar flexion than the subjects in the Taurus. The difference in HipX is due partly to the fact that the Neon subjects were about 7 mm shorter, on average, than the Taurus subjects. Torso recline was not significantly different between the seats.

More importantly, however, the effects of the steering wheel position and seat cushion angle on the posture variables did not differ significantly between the seats ($p > 0.05$ for the interaction terms). This suggests that the effects of these two variables on posture do not depend on the seat.

Seat Height Effects and Interactions

In Phases 2 and 3, trials were conducted at three seat heights (180, 270, and 360 mm) and with two steering wheel positions at each seat height. Taking only the data from the Phase-3, 550-mm steering-wheel conditions (configurations 3, 8, 12, 15, 16, and 19) gives an orthogonal 3 x 2 design with seat height and seat cushion angle (24 subjects). In these data, there are no significant effects of seat height on lumbar flexion, cervical flexion, or hip-to-eye angle, nor any significant interactions between seat height and seat cushion angle. However, there is a significant, apparently nonlinear effect of seat height on HipX. The average hip location moved forward 9 mm as the seat height was raised from 180 to 270 mm, but moved forward 25 mm when the seat height was raised from 270 to 360 mm.

This analysis was expanded to examine potential interactions between steering wheel position and seat height. To eliminate the numerical correlation of the variables, steering wheel position was receded relative to the presumed neutral position at each seat height (600, 550, and 500 mm for the 180-, 270- and 360-mm seat heights, respectively). In the data from Phase 3, conditions 2, 4, 7, 9, and 12 through 19 form a 3 x 2 x 2 design in seat height, SW-BOFX, and seat cushion angle. Using a within-subject ANOVA, the main effects and interactions were tested for each of the dependent variables. None of the potential two-way interactions were significant, nor was the three-way interaction ($p > 0.10$ in all cases). The main effect estimates for the three variables were similar to those obtained using other analyses.

Gender Differences

Subject groups 4, 5, 6, and 7 contain men and women of similar stature. Using only these groups (24 subjects), and data from Phases 2 and 3, ANOVA was conducted to determine if the effects of the test variables differed between men and women. No significant interactions with gender were observed, indicating that the test variables affect the driving postures of men and women similarly.

Regression Analyses

The foregoing ANOVA analyses demonstrated that seat height, steering wheel position, seat cushion angle, and seat type have statistically significant but largely independent effects on driving posture. Steering-wheel-position effects appear to be substantially linear, but there are non-linear trends for seat height. Regression analysis was used to assess potential nonlinearities and also to determine the relationships between anthropometric variables and posture. Of particular interest was the potential for interaction between anthropometric variables and the test configuration variables. For example, do changes in steering wheel position affect the postures of tall people differently than short people?

Regression analyses were performed using step-wise procedures on the pooled data from all three phases. Potential regressors included all of the test variables and their two-way interactions, as well as stature and two derived measures of body dimension. The Body Mass Index (BMI) is calculated by dividing the body mass by stature squared (kg/m^2), and is intended to represent a measure of body mass that is less correlated with stature than mass. In these data, the correlation between BMI and stature is 0.32. Similarly, the ratio of sitting height to stature was used to account for differing trunk-to-limb proportions. The correlation between the ratio and stature is -0.42 in these data. The use of the less-correlated regressors allows the model coefficients to be interpreted more readily than would be the case if sitting height and mass were used directly, and reduces the importance of other statistical problems associated with collinearity.

Interactions between the three anthropometric variables and the test variables were also included as potential regressors. A second-order term for seat height was added to explore potential nonlinearities in that effect. An automated procedure was applied, using $p < 0.25$ to enter and $p > 0.10$ to leave, followed by an interactive procedure to obtain a more parsimonious model with an adjusted R^2 value within 0.02 of the full-model value. Table 3.5 shows the resulting models. All terms, and each model, are statistically significant with $p < 0.001$. Adjusted R^2 and root-mean-squared-error values are given in the table.

In no case did an interaction term contribute substantially to the fit. The second-order seat height term also did not add substantial predictive ability. Consequently, all of the models presented in Table 3.5 are linear, and contain only the three anthropometric variables and the three test variables.

The importance of the regression function terms can be evaluated more easily by multiplying each coefficient by the range of the independent measure that is present in the data. Table 3.6 shows the resulting values. For example, the range of stature in the data is 475 mm. Multiplying the coefficients from Table 3.6 by 475 mm indicates that the

effect on the fore-aft hip position of varying stature over this range is about 233 mm, while the effect on the hip-to-eye angle is about three degrees.

Table 3.5
Regression Equations Predicting Posture Variables*
 (all data)

Variable	HipX	Hip-to-Eye Angle	Lumbar Flexion	Cervical Flexion	Elbow Angle	Knee Angle
Stature	0.490	0.0067	0	0.0085	0.1267	0
Body Mass Index (Mass/Stature ²) (kg/m ²)	-2.51	0 [#]	0.956	-0.691	-0.561	-0.503
<u>Sitting Height</u> Stature	-441.6	115.1	59.2	0	404.6	59.5
Seat Height (mm)	-0.170	0	0	0	-0.037	-0.032
SW-BOFX (mm)	0.449	0.015	0	0.015	-0.135	0.083
Seat Cushion Angle (degrees)	-0.91	0.11	0.29	0	0	-0.56
R ² (adjusted)	0.80	0.21	0.10	0.07	0.46	0.48
Root Mean Square Error	34.8	3.9	11.0	9.4	17.1	7.4

*Values in tables are coefficients of the associated linear terms. The regression function is the sum of the products of the coefficients and the variable values, plus a constant intercept.

[#]A zero indicates that the model coefficient was not significantly different from zero.

Table 3.6
Range Estimates Using Regression Equations

Variable	Range	HipX	Hip-to-Eye Angle	Lumbar Flexion	Cervical Flexion	Elbow Angle	Knee Angle
Stature (mm)	475	232.8	3.2	0	4.0	60.2	0
Body Mass Index (kg/m ²)	16.7	-41.9	0	16.0	-11.5	-9.4	-8.4
<u>Sitting Height</u> Stature	0.08	-35.3	9.2	4.7	0	32.4	4.8
Seat Height (mm)	180	-30.6	0	0	0	-6.66	-5.8
Steering Wheel re BOF (mm)	200	89.8	3.0	0	3	-27	16.6
Seat Cushion Angle (degrees)	7	-6.4	0.8	2.0	0	0	-3.9
R ² (adjusted)*	--	0.80	0.21	0.10	0.07	0.46	0.48
Root Mean Square Error*	--	34.8	3.9	11.0	9.4	17.1	7.4

* Values repeated from Table 3.5.

[#]A zero indicate that the model coefficient was not significantly different from zero.

The range estimates, R^2 values, and root-mean-square-error (RMSE) values in Table 3.6 indicate the relative importance of the anthropometric and test variables in determining driving posture. The available variables account for a large percentage of the variance in HipX ($R^2 = 0.80$), with stature by far the most important determinant of hip position. Steering wheel position and seat height also have important effects, while seat cushion angle has a minor effect over the range studied.

In contrast, the overall torso recline is poorly predicted overall, with R^2 only 0.21. However, the RMSE is fairly small, indicating that the overall range of variability in the data is also small. The most powerful predictor of torso recline is the ratio of sitting height to stature. People with longer torsos relative to their stature tend to sit with more overall torso recline. Steering wheel position has a small effect, only about 3 degrees for a 200-mm range.

Lumbar and cervical spine flexion are largely unaffected by the test variables and are also not well predicted by the anthropometric variables. The RMSE values indicate that the range of spine flexion in the data is fairly large, but the R^2 values of 0.10 and 0.07, respectively, indicate poor relationships between the potential predictors and spine flexion.

Elbow and knee angles are predicted moderately well by the regressions. The ratio of sitting height to stature is an important determinant of elbow angle. Drivers having a larger sitting height for their stature (shorter limbs for their stature) tend to have larger elbow angles. Of the test variables, steering wheel position is most important, followed by seat height. Knee angle is not strongly related to any of the anthropometric variables, although there is a trend for people with larger BMIs to sit with smaller knee angles. However, knee angle is affected by all three test variables, most strongly by steering wheel position.

3.5 Summary and Discussion

A three-phase laboratory study was conducted to determine the effects of seat height, fore-aft steering wheel position, and seat cushion angle on driving posture. Analyses focused on three measures of torso posture and three measures of limb posture.

The principal observations are:

- Seat height, steering wheel position, and seat cushion angle each have significant, largely independent effects on posture.
- The effects of these three variables are independent of body size, proportion, and gender.
- Overall body size (stature) is the primary determinant of fore-aft hip position with respect to the pedals, but seat height, steering wheel position, and seat cushion angle all have significant effects.
- The ratio of sitting height to stature is an important predictor of hip-to-eye angle and elbow angle.
- Knee and elbow angles, the primary measures of limb posture, are strongly influenced by seat height and steering wheel position. Over the range studied, steering wheel position has the stronger effect.
- Seat cushion angle has a highly significant effect on both lumbar flexion and overall torso recline, but the importance of the effect is diminished by the restricted range of this variable in vehicle designs.

The most important observation from this study is that postural adaptations to changes in the layout of the driving task are accomplished mainly by changes in limb posture while torso posture remains largely unaffected. Instead, torso posture appears to be determined primarily by intersubject differences that are not closely related to overall anthropometric variables. A typical sitter's spine flexion does not vary substantially across different vehicle layouts, but may differ considerably from that of other sitters.

Of the three package and seat variables studied, the fore-aft steering wheel position is the most important. If the steering wheel is moved forward 100 mm, drivers respond by moving their hips about 45 mm closer to the pedals, accounting for about half the change in steering wheel position. The change in hip location is associated with an average reduction in knee angle of about 8 degrees. The more-forward steering wheel position (65 mm further in front of the hips) results in elbow angles that are larger by an

average of 13 degrees. In contrast to the relatively large changes in limb posture, hip-to-eye angle is reduced by less than two degrees.

The two seats that were tested produced different average postures, but the differences are difficult to interpret because different subjects were used. The seat with the subjectively more prominent lumbar support, the Neon, produced postures with less average spine flexion. This finding is consistent with previous studies (Reed et al., 1995; Reed and Schneider, 1996) in which prominent lumbar supports have been found to cause statistically significant but small reductions in the lumbar spine flexion of drivers. More importantly, however, the effects of seat height, steering wheel position, and seat cushion angle were not significantly different for the two seats, suggesting that these effects can be considered to be independent of seat type. A small non-linearity in the effect of seat height on fore-aft hip location did not contribute substantially to the overall regression prediction. Similar findings were reported by Flannagan et al. (1996) with regard to driver-selected seat position.

The findings of this study are directly applicable to vehicle interior design, for which the accurate prediction of occupant posture is of considerable importance. Although seat height is often set early in the design process and substantially constrained by exterior styling considerations, the fore-aft steering-wheel position and seat-cushion angle can be manipulated more readily to accomplish design goals. The findings from this study will help designers to predict more accurately the effects of these changes on driver posture.

This study was conducted in a laboratory mockup, without many of the spatial and visual cues that are present in an actual vehicle and that could affect posture, such as mirrors, doors, and seatbelts. However, other studies conducted in conjunction with this work have shown that these factors may not substantially reduce the generalizability of the findings. The study presented in Chapter 3 determined that forward vision restrictions do not affect driving posture in important ways. Further, comparison of

posture predictions derived from these laboratory data with in-vehicle driver postures indicate that the postures measured in this study can reliably be used to predict actual driving postures (Chapter 5).

The two most important restrictions on these findings pertain to the use of a two-way (one-degree-of-freedom) seat track. Although most vehicles are still designed initially using a two-way track, an increasing number of vehicles are being designed and sold with a larger range of adjustment, particularly six-way seat tracks that allow the seat height, seat cushion angle, and fore-aft seat position to be adjusted by the driver. Although research is presently underway to quantify driver behavior when these additional adjustments are available, the data from the current study should be understood to apply only to two-way tracks. Further, the seat track in this study allowed all subjects to select their preferred seat position without restriction. In many vehicles, the seat track length is insufficient to accommodate every driver at his or her preferred location, resulting in censoring of the seat position distribution, and potentially changing posture in ways that are not encompassed by the findings of the current study. In addition to seat-adjustment limitations, the postures measured in this study were obtained after the driver had been seated for only about one minute. Postures over a longer driving session could be different, although Reed et al. (1991, 1995) found only small changes in posture during long-term driving simulations. In dynamic, on-road driving, there appear to be small but important changes in eye location associated with driving duration, probably due to gradual compression of the seat foam (see Chapter 5). These findings are also limited by the health and age of the subjects. Although the subjects ranged in age from 21 to 75 years (average 35 years), the behavior of a geriatric population might differ from the relatively fit subjects used in this testing.

3.6 Conclusions

Drivers adapt to changes in the vehicle and seat geometry primarily through changes in limb posture, while torso posture remains fairly constant. Large differences in

torso posture between subjects are not well predicted by anthropometric differences. Seat height, steering wheel position, and seat cushion angle have effects on driving posture that are largely independent of body size and gender.

3.7 References

- Abraham, S., Johnson, C. L., and Najjar, M. F. (1979). *Weight by height and age for adults 18-74 years: United States, 1971-74, Vital and health statistics, Series 11, No. 208*. DHEW Publication No. 79-1656. Hyattsville, MD: U.S. Department of Health, Education, and Welfare.
- Arnold, A.J., Ferrara, R.A., and Kuechenmeister, T.J. (1985). Driver eyellipses produced by minimum deflection seats and by U.S. adult population changes. In *Proc. of the 29th Annual Meeting of the Human Factors Society, Volume I*, ed. R.W. Swezey, L.B. Strother, T.J. Post, and M.G. Knowles, 447-451. Santa Monica, CA: Human Factors Society.
- Dempster, W.T. (1955). *Space requirements of the seated operator: Geometrical, kinematic, and mechanical aspects of the body with special reference to the limbs*. WADC Technical Report 55-159. Wright-Patterson AFB, OH: Wright Air Development Center.
- Devlin, W.A., and Roe, R.W. (1968). *The eyellipse and considerations in the driver's forward field of view*. SAE Technical Paper 680105. New York, NY: Society of Automotive Engineers, Inc.
- Flanagan, C.A.C., Schneider, L.W., and Manary, M.A. (1996). Development of a new seating accommodation model. SAE Technical Paper 960479. In *Automotive Design Advancements in Human Factors: Improving Drivers' Comfort and Performance (SP-1155)*, 29-36. Warrendale, PA: Society of Automotive Engineers, Inc.
- Geoffrey, S.P. (1961). *A 2-D mannikin--The inside story. X-rays used to determine a new standard for a basic design tool*. SAE Technical Paper 267A. New York, NY: Society of Automotive Engineers, Inc.
- Hammond, D.C., and Roe, R.W. (1972). *Driver head and eye positions*. SAE Technical Paper 720200. New York, NY: Society of Automotive Engineers, Inc.
- Kaptur, V., and Myal, M. (1961). *The General Motors comfort dimensioning system*. SAE Technical Paper 267B. New York, NY: Society of Automotive Engineers, Inc.
- Lay, W.E., and Fisher, L.C. (1940). Riding comfort and cushions. *SAE Journal* 47(5): 482-496.
- Meldrum, J.F. (1965). *Automobile driver eye position*. SAE Technical Paper 650464. New York, NY: Society of Automotive Engineers, Inc.
- Mourant, R.R., Pak, T., and Moussa-Hamouda, E. (1978). *Dynamic eye positions by vehicle type. Final report of the Second Generation Eyellipse Project*. Detroit, MI: Wayne State University, Department of Industrial Engineering and Operations Research.

- Myal, M. (1958). A new method of accommodation dimensioning. Unpublished report to General Motors Styling Staff and General Motors Institute, Warren, MI.
- Phillipart, N.L., Kuechenmeister, T.J., Ferrara, R.A., and Arnold, A.J. (1985). *The effects of the steering wheel to pedal relationship on driver-selected seat position*. SAE Technical Paper 850311. Warrendale, PA: Society of Automotive Engineers, Inc.
- Phillipart, N.L., Roe, R.W., Arnold, A.J., and Kuechenmeister, T.J. (1984). *Driver selected seat position model*. SAE Technical Paper 840508. Warrendale, PA: Society of Automotive Engineers, Inc.
- Porter, J.M., Case, K., Freer, M.T., and Bonney, M.C. (1993). Computer-aided ergonomics design of automobiles. In *Automotive Ergonomics*, ed. B. Peacock and W. Karwowski, 43-77. London: Taylor and Francis.
- Reed, M.P., and Schneider, L.W. (1996). Lumbar support in auto seats: Conclusions from a study of preferred driving posture. SAE Technical Paper 960478. In *Automotive Design Advancements in Human Factors: Improving Drivers' Comfort and Performance (SP-1155)*, 19-28. Warrendale, PA: Society of Automotive Engineers, Inc.
- Reed, M.P., Schneider, L.W., and Eby, B.A.H. (1995). Some effects of lumbar support on driver seated posture. SAE Technical Paper 950141. In *Human Factors in Vehicle Design: Lighting, Seating and Advanced Electronics (SP-1088)*, 9-20. Warrendale, PA: Society of Automotive Engineers, Inc.
- Roe, R.W. (1993). Occupant packaging. In *Automotive Ergonomics*, ed. B. Peacock and W. Karwowski, 11-42. London: Taylor and Francis.
- Society of Automotive Engineers (1997). *Automotive Engineering Handbook*. Warrendale, PA: Society of Automotive Engineers, Inc.

CHAPTER 4

THE EFFECTS OF FORWARD VISION RESTRICTION ON DRIVER POSTURE

4.1 Abstract

A simulator study of the effects of the height of the top of the instrument panel on driving posture was conducted. Eight midsize men and eight small women drove an interactive simulator with a large-screen display under five different instrument-panel-height conditions. The three-dimensional locations of body landmarks were recorded to characterize their driving postures. In a confirmatory study, 32 men and women drove a sport-utility vehicle over a 15-minute road route with and without a mask that restricted part of the windshield above the instrument panel. These restrictions on drivers' forward vision had only small effects on driving posture. In the driving simulator, an increase in instrument panel height of 150 mm caused drivers to sit with their hips an average of 7 mm further forward with a hip-to-eye angle that was one degree more upright. There were no significant differences in postural response between the small-female and midsize-male subjects. In the vehicle, no significant effects of the windshield mask on posture were observed. These findings indicate that the vision restriction imposed by the instrument panel is unlikely to have an important effect on driving posture over the range of restriction that is reasonable for production vehicles, and that predictive models of driving posture do not need to include the effects of instrument panel height when the driver is not provided with a seat height adjustment.

4.2 Introduction

Driver eye location in vehicles is a key consideration in the design of vehicle interiors, and has been the subject of considerable study. Meldrum (1965) conducted the

first large-scale study of driver eye locations, leading to the development of the eyellipse, a statistical construction predicting the distribution of driver eye locations (Devlin and Roe, 1968). Hammond and Roe (1972) expanded on the earlier work to present eyellipses and head position contours applicable to a wide range of vehicles. Mourant et al. (1978) found that eye locations in a laboratory mockup were similar to those measured in a vehicle. These studies have contributed to the development of eye location prediction techniques used in contemporary vehicle design, documented in the Society of Automotive Engineers Recommended Practice J941 (SAE, 1997). This practice provides a method of predicting eyellipse location based on seat height and seatback angle. No other vehicle or seat factors are included in the prediction.

More recent research has demonstrated that factors in addition to seat height affect drivers' seat positions, and the near-universal use of adjustable-recline seatbacks for driver seats has called into question the use of fixed seatback angle for eye location prediction. Steering wheel position with respect to the pedals and seat cushion angle have been identified as important factors affecting fore-aft seat position and potentially other characteristics of driving posture (Flannagan *et al.*, 1996).

One factor that is not addressed in previously published research is the influence of vision restriction on driving posture. Previous studies have been conducted using production vehicles or vehicle mockups that have been adjusted to match typical vehicle geometry, but the forward vision restriction imposed by the instrument panel or other vehicle components has not been systematically investigated. If vision restriction has an important influence on posture, its inclusion in predictive models for eye location, seat position, and other characteristics of driving posture will be warranted. The effects of vision restriction on driving posture may also illuminate the manner in which drivers balance their comfort and the physical requirements of their task.

4.3 Methods — Laboratory Study

Overview

In this study, sixteen men and women operated an interactive laboratory driving simulator while sitting in a partial vehicle mockup. A generic visual obstruction was created at a horizontal position corresponding to a typical instrument panel location. The height of this simulated instrument panel was varied over a wide range to restrict the drivers' view of the road scene. Driving postures were recorded by collecting three-dimensional body landmark locations with a sonic digitizer. The data were analyzed to determine the manner in which restrictions on downward, forward vision affect driving posture.

Subjects

For the laboratory testing, eight male and eight female licensed drivers, ranging in age from 21 to 70 years, were selected for testing. Testing was conducted with two different stature groups to determine if instrument panel height and body size have interactive effects on driving posture. Table 4.1 summarizes several anthropometric measures for the two groups. The subjects in the small-female group were chosen for their small stature, which averages 1550 mm compared with 1755 mm for the midsize-male group. Each subject gave written consent to participate and was paid \$15 for approximately 90 minutes of testing.

Table 4.1
Subject Anthropometric Summary — Laboratory Testing
(min-mean-max)

Group	N	Stature (mm)	Mass (kg)	Erect Sitting Height (mm)
Midsize Male	8	1711-1755-1808	71-82-110	893-917-935
Small Female	8	1510-1550-1601	45-53-58	796-828-853

Facilities

The laboratory experiment was conducted in a partial vehicle mockup, shown in Figure 4.1, that simulates some interior features and dimensions typical of a minivan. The mockup includes an adjustable seat, a steering wheel, accelerator pedal, and brake pedal. The instrument panel (IP) is simulated by an angled piece of black sheet metal that presents a horizontally level vision obstruction. Figure 4.2 presents several key dimensions of the vehicle mockup. The seat height (SAE H30) is 335 mm (see Appendix A for a general discussion of vehicle dimensioning nomenclature). The center of the steering wheel is 400 mm behind and 709 mm above the Accelerator Heel Point (AHP). The SAE J941 95th-percentile eyellipse is shown to illustrate the approximate locations of driver's eyes (SAE, 1997). The apex of the IP is located 66 mm rearward of the AHP, and the vertical position is manually adjusted by the experimenter to the specified test condition. The vehicle mockup area in front of the IP is obscured by a black cloth drape. The seat can be adjusted by the subject fore-aft using a manual seat-track adjuster on track angled three degrees above horizontal. The seatback angle adjustment is motorized and is also controlled by the subject. The seatback includes a prominent lumbar support. The data showed that both the seat-track fore-aft adjustment range and the seatback angle adjustment range were adequate, as no censoring occurred when subjects selected their preferred postures.



Figure 4.1. Subject in vehicle mockup.

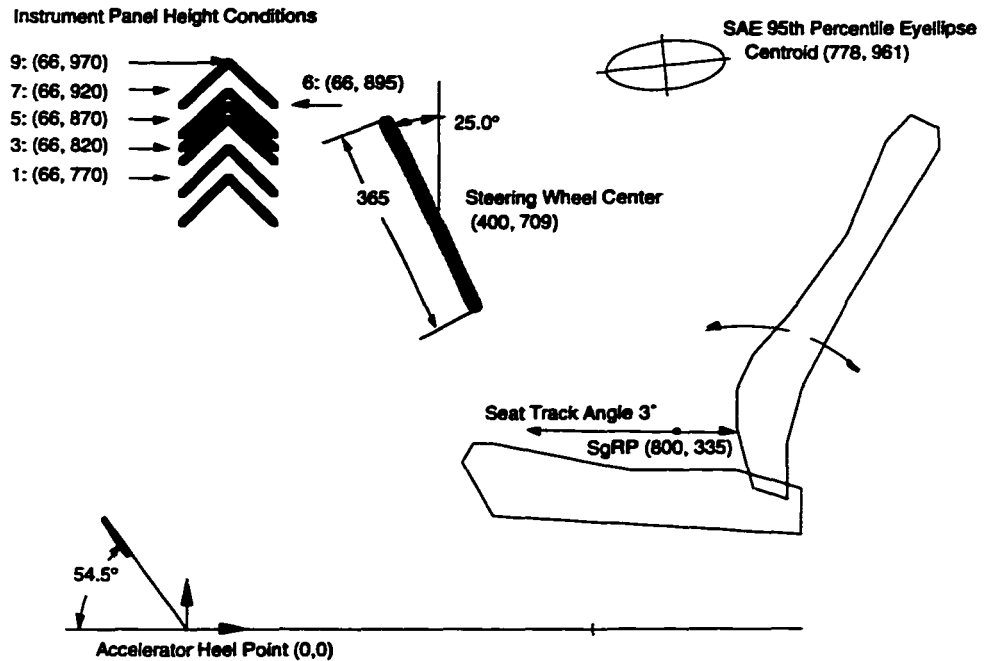


Figure 4.2. Vehicle mockup dimensions (mm).

The steering wheel, accelerator pedal, and brake pedal of the vehicle mockup are connected to a fixed-base, interactive driving simulator (MacAdam *et al.*, 1993). A computer-generated scene of a winding road is projected onto an angled screen located 3.4 m in front of the eyellipse centroid, as shown in Figure 4.3. The simulator scene of a two-lane road includes road edge markings, a panning horizon scene, and numerous roadside objects. The horizon of the road scene is located at the centroid of the SAE 95th-percentile eyellipse, or 961 mm above the heel surface. In the absence of vision restriction, the projected image occupies a lateral visual angle of 32 degrees and a vertical visual angle of 24.2 degrees, with 11.5 degrees above horizontal and 12.7 degrees below horizontal. Figure 4.4 shows a typical road scene from the simulator (displayed in color).

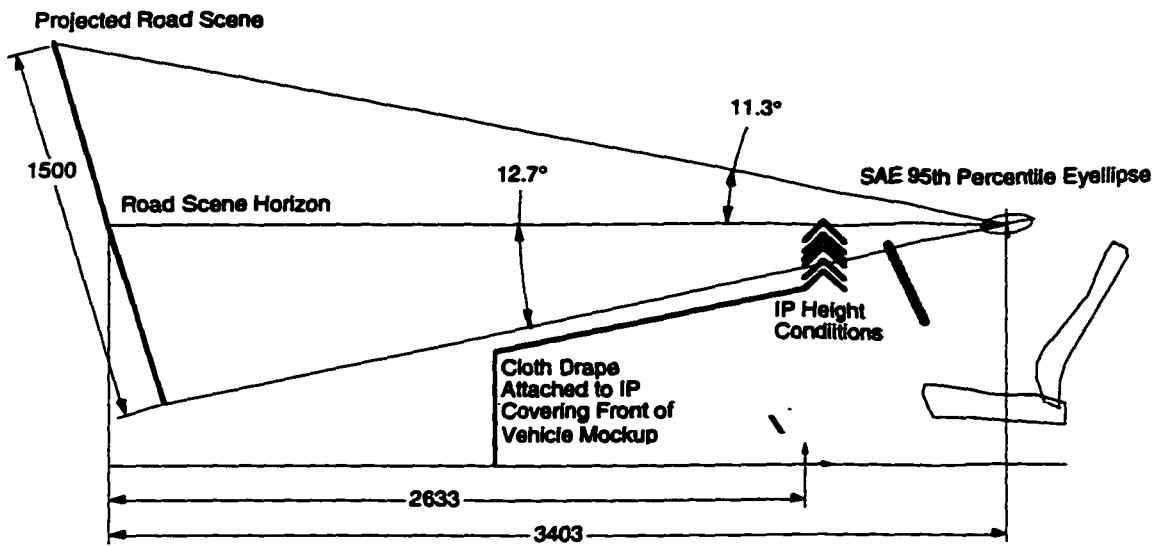


Figure 4.3. Simulator road scene projection schematic. Dimensions in millimeters IP positions (test conditions) from Figure 4.2 are illustrated.



Figure 4.4. Typical simulator road scene showing obstruction (cow) in right lane (displayed in color).

Laboratory Experiment Design

Laboratory testing was conducted with the simulated IP set to seven different heights above the heel surface. Table 4.2 lists the test conditions used with male and female subjects. Because of the smaller sitting height of the female subjects, an intermediate condition was substituted for the highest condition. Each subject was tested twice in each of the specified conditions. The order of presentation of the trials was randomized. As illustrated in Figure 4.3, the lowest IP height (condition 1) does not obstruct the scene as it would be viewed from the center of the SAE eyellipse. The

highest IP height (condition 9) places the apex of the IP at the same height as the centroid of the eyellipse, indicating that approximately 50 percent of the population would be expected to be unable to view the part of the road scene below the horizon in their normal driving posture.

Table 4.2
Tested Instrument Panel Heights

Condition Number	IP Height Above Heel Surface (mm)	Height re Condition 1 (mm)	Male Conditions	Female Conditions
1	770	0	x	x
3	820	50	x	x
5	870	100	x	x
6	895	125		x
7	920	150	x	x
9	970	200	x	

Test Procedures

The subject changed into loose fitting clothing provided by the experimenters to facilitate the measurement of body landmark locations. Each of these subjects had previously participated in another study in which standard anthropometric measures were taken and body landmark data from a standardized seated posture were recorded, so collection of those data was not required at these test sessions.

Prior to each measurement trial, the seat was placed in the full-rear position on the seat track and the seatback was adjusted to an SAE J826-referenced back angle of 21 degrees. This starting seatback angle is typical of the average seatback angle selected by drivers. The first trial for each subject was conducted with the IP adjusted to the lowest position, and was intended to familiarize the subject with the operation of the simulator. The subject was given verbal instructions to try to keep the simulated vehicle in the right lane of the road and to drive within a prescribed speed range. The simulator was started and the subject drove the simulator for about 5 minutes. Several of the subjects reported

feeling nauseous (simulator sickness), but only one subject was unable to complete the trials and was dropped from the study. The driving task was deliberately made more complex than a typical driving experience by constructing a simulated road with many irregular curves, and by placing objects in the right lane (see Figure 4.4). The subject was instructed to switch temporarily to the left lane to avoid these objects. Driving performance was not recorded, but the subjects all maintained attention to the road scene.

Following the initial familiarization trial, the subject stood up and turned away from the vehicle mockup while the experimenter adjusted the IP height to the specified condition and reset the seat position and seatback angle to the starting values. The subject sat in the seat and adjusted the fore-aft seat position and seatback angle to obtain a “comfortable driving posture” while looking at a fixed road scene. For each trial, the subject was instructed to place his or her hands on the steering wheel at approximately the 10 o’clock and 2 o’clock positions. When the subject’s initial adjustment was completed, the simulator was restarted and the subject drove for at least three minutes, or for 30 seconds after the last adjustment of the seat. During the drive, the subject was asked to continue to adjust the seat position and seatback angle to seek a maximally comfortable driving posture. If the subject asked for clarification, the experimenter told the subject to find a posture that would be comfortable for a long trip. Most subjects adjusted the seat once or not at all after starting the simulator.

The simulator was paused after instructing the subject to maintain his or her driving posture. Visual observation of the subjects confirmed that they were readily able to follow this instruction. The experimenter recorded body landmark and vehicle component locations using a Science Accessories Corporation GP8-3D sonic digitizer and the techniques described in Chapter 2. The posture measurement required approximately 90 seconds. After the posture was recorded, the subject stood up and again turned away while the IP height was adjusted and the seat reset. This process was

repeated until the subject had completed 10 trials (two each at five instrument panel heights).

Analysis

The body landmark data were reviewed quantitatively and visually to ensure that there were no anomalous points. The methods used to express the posture in a kinematic-linkage representation are described in Chapter 2. Figure 4.5 shows a side view of the driving posture formed by straight segments connecting joint locations calculated from the landmark data. A Center Eye point was defined from which several dimensions of interest were measured. The Center Eye point has the X (fore-aft) coordinate of the Infraorbitale landmark and the Z (vertical) coordinate of the Corner Eye landmark, and is intended to be an estimate of the driver's side-view eye location. The Center Eye point is the eye location referred to in subsequent discussion. The posture data, represented by the kinematic linkage, were examined graphically and statistically, using conventional ANOVA and regression techniques where appropriate. The IP height condition (5 levels) and subject group (two levels) were considered as independent variables affecting posture measures, including hip location, eye location, and hip-to-eye vector angle.

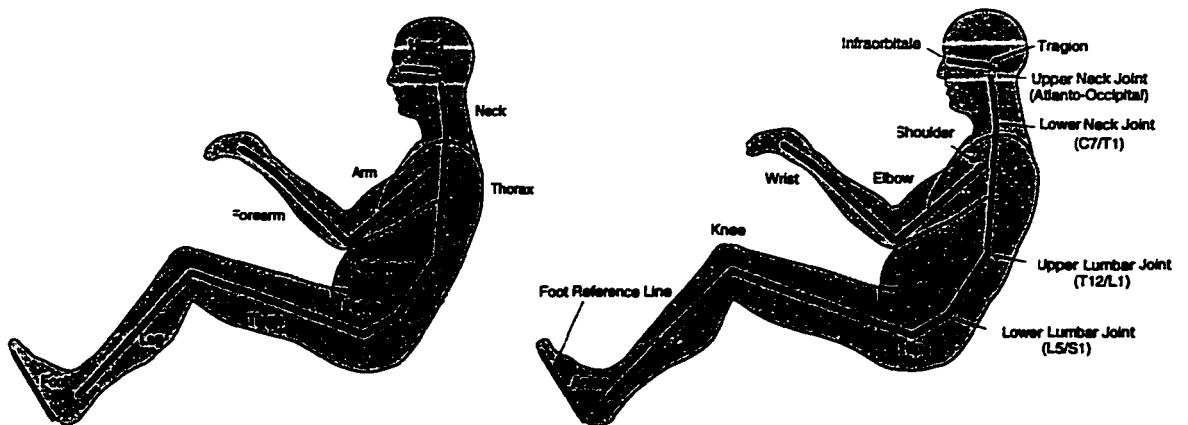


Figure 4.5. Kinematic linkage representing driving posture.

4.4 Methods — Vehicle Study

Overview

A confirmatory study was conducted in a vehicle, using a removable windshield mask to restrict downward, forward vision. Thirty-four men and women drove a sport-utility vehicle over a 15-minute road route with and without the mask. After returning from the drive, body landmark locations documenting their preferred driving postures were recorded using a coordinate measurement machine. The effects of in-vehicle vision restriction were compared to the laboratory results.

Subjects

Table 4.3 summarizes key anthropometric variables for the 32 vehicle-testing subjects. These subjects were chosen in sequence from people who were participating in another study of driver posture, and represent a wide range of male and female body sizes.

Table 4.3
Subject Anthropometric Summary — Laboratory Testing
(min-mean-max)

Group	N	Stature (mm)	Mass (kg)	Erect Sitting Height (mm)
Men	15	1648-1771-1952	68-83-114	840-925-988
Women	17	1450-1599-1711	56-68-86	776-849-895

Facilities

The on-road testing was conducted in a 1996 Jeep Grand Cherokee. Figure 4.6 summarizes the key vehicle dimensions. The vehicle was tested with a motorized fore-aft seat position adjuster that moved the seat on a straight path oriented 10 degrees above the horizontal. The subjects adjusted the seatback recline and tilt-wheel position manually.

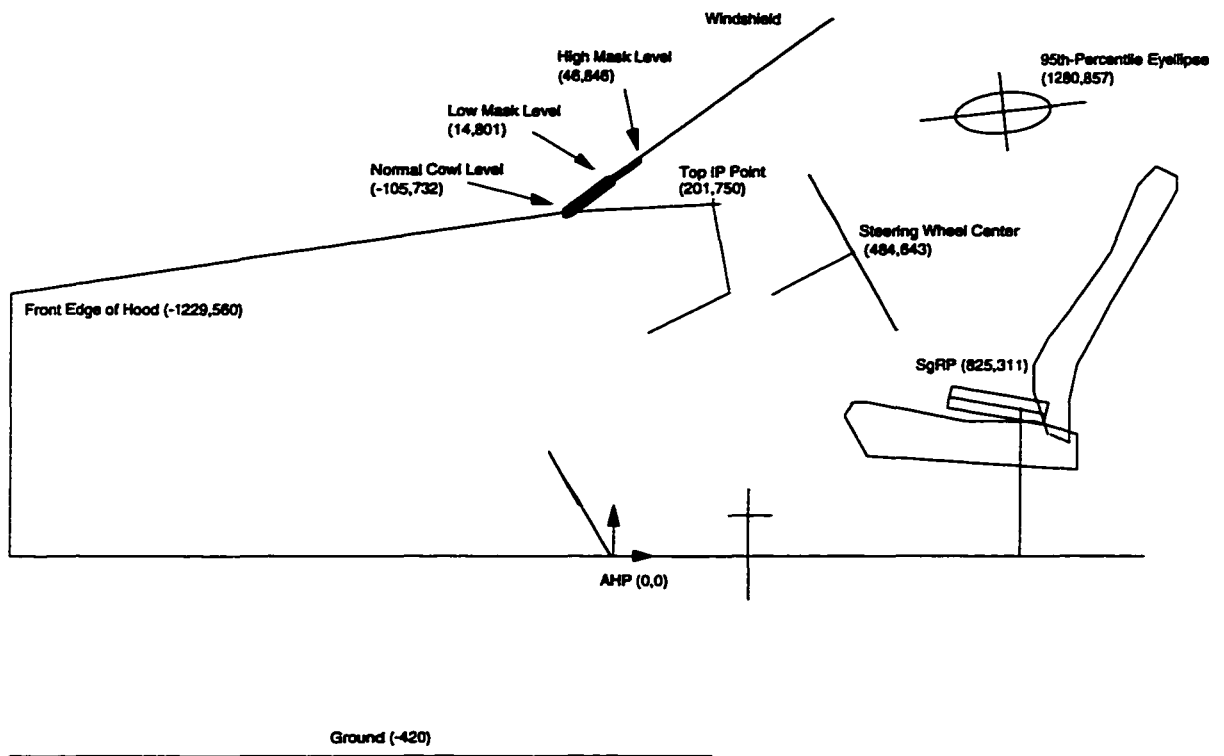


Figure 4.6. Vehicle dimensions (mm).

Field Experiment Design

For the on-road testing, subjects operated the vehicle in its normal configuration and with the addition of a cardboard mask placed against the inside of the windshield across the driver's side of the vehicle. Two masks were used: one for drivers who had erect sitting height measurements greater than 900 mm, and a lower one for drivers with sitting heights less than 900 mm. The 10 tallest subjects were tested with the more restrictive mask. Figure 4.6 shows the location of the masks relative to the normal vehicle geometry on the driver centerline plane. The height of the low and high masks above the seating reference point is comparable to conditions 3 and 5. More restrictive masks were not used because of concerns about driver safety.

Procedures

The subjects in the vehicle study were participating in a study of driving posture in which the subject drove each of three vehicles, including the Jeep Grand Cherokee,

over a 15-minute road route. After completion of each drive, the subject drove into a garage area and stopped the vehicle. The subject maintained his or her driving posture while the body landmark locations were measured using a FARO arm, a portable, three-dimensional coordinate measurement machine. Predefined landmarks on each vehicle allowed the body data to be expressed relative to the vehicle interior geometry. Although many landmarks were recorded, only the right and left ASIS, corner eye, infraorbitale, and glabella landmarks were used for analysis.

Analysis

Eye and hip joint locations in the XZ (side-view) plane were calculated for each in-vehicle trial. The calculation of the eye point was conducted in the same manner used with the simulator study data. However, hip joint location could not be estimated with the procedures used for the simulator study because the pubic symphysis landmark data were not collected. Instead, hip joint location in the XZ plane was estimated relative to the measured ASIS locations only. In the data from the simulator study, the estimated hip location in the XZ plane was unaffected by the IP height but was significantly related to subject stature. Regression equations predict the offset between the mean ASIS location and the mean hip locations as

$$\text{ASIS-Hip}(X) = -114.5 + 0.08195 \text{ Stature}$$

$$\text{ASIS-Hip}(Z) = 60.3 + 0.0152 \text{ Stature}$$

where stature is in millimeters. These offset equations were used to estimate the hip location for each in-vehicle posture measurement.

4.5 Results — Laboratory Study

When a driver's forward vision is obstructed by raising the instrument panel, the driver can compensate by moving his or her eyes forward and/or upward, thereby preserving the same view of the road scene. Table 4.4 lists four posture behaviors that accomplish this eye movement and some of the posture variables that are affected. In general, sitting further forward, sitting more upright, (less reclined), sitting with less

lumbar spine flexion, or sitting with a different head and neck posture will make more of the road scene visible above the IP. Figure 4.7 illustrates the definitions of the variables in Table 4.5.

Table 4.4
Possible Behaviors to Compensate for a Forward Vision Restriction

Behavior	Affected Variables	Definition
Sit further forward	HipX	horizontal coordinate of mean hip joint
Sit more upright (less reclined)	Hip-to-Eye Angle	angle with respect to vertical of a side-view line connecting the mean hip joint and the Center Eye point (see text).
Reduce lumbar spine flexion	Pelvis Angle – Thorax Angle	difference between the orientations of the pelvis and thorax segments; a measure of lumbar spine flexion
Change head and neck posture	Head Angle	angle with respect to horizontal of the line connecting the infraorbitale and trigion landmarks
	Thorax Angle - Head Angle	difference between the orientations of the head and thorax; a measure of cervical spine flexion

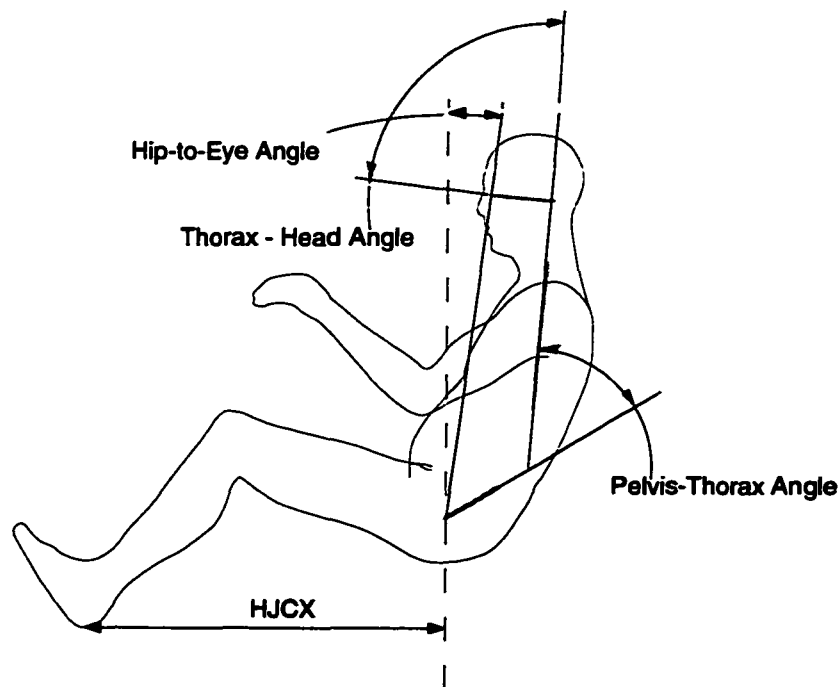


Figure 4.7. Illustration of variable definitions.

Repeatability

Each subject selected a driving posture twice for each IP height condition, allowing an assessment of the repeatability of the posture. Table 4.5 lists the mean and standard deviation of the absolute differences between repeated trials for the variables in Table 4.4. The average difference in fore-aft hip location for repeated trials was 11 mm, compared to the full range for all subjects of 248 mm. The two measures of torso recline showed average differences between trials of less than two degrees. Measurements of head angle and spine flexion were less repeatable, with average differences between trials of around 5 degrees. The posture repeatability, measured in this way, did not change significantly with changes in IP height.

Table 4.5
Repeatability of Driving Posture

Variable (degrees or mm)	Absolute Difference Between Repeated Trials (N=80)	
	mean	std. dev.
HipX (mm)	11.1	8.5
Hip-to-Eye Angle	1.3	1.0
Pelvis Angle – Thorax Angle	4.6	3.4
Head Angle	5.5	4.5
Thorax Angle - Head Angle	5.9	5.0

Effects of Gender and Body Size on Posture

As expected, there was a significant difference ($p<0.01$) in the fore-aft hip location (HipX) between subject groups (small females vs. midsize males), due to the large difference in average stature between the groups. There was also a significant difference ($p<0.01$) between groups in seatback angle (17.5 degrees for small females versus 25.2 degrees for midsize males). However, the hip-to-eye angles were not significantly different between the groups. This apparently contradictory finding is explained by the fact that the midsize male group sat with about 11 degrees more lumbar spine flexion, as measured by the Pelvis Angle – Thorax Angle variable. The greater

amount of spine flexion tends to reduce the hip-to-eye angle relative to a particular back angle. To obtain the same hip-to-eye recline angle, a person sitting with greater lumbar spine flexion requires a more reclined seatback angle. The same observation was made in a previous study (Reed et al., 1995).

There were no significant differences between the anthropometric groups in head angle or cervical spine flexion. Note that because there is no overlap between the groups in stature or other key anthropometric variables, it is not possible to determine whether the significant differences between groups are due to gender or anthropometric differences. However, other studies have shown that the apparent gender differences in fore-aft positioning and seatback angle can be attributed to anthropometric differences (see Chapter 3).

Instrument Panel Height Effects

Figure 4.8 shows posture variables versus IP-height condition. Separate lines are plotted showing small-female and midsize-male group means. In analyses of data from the four instrument panel heights that were tested with both subject groups (conditions 1, 3, 5, and 7), the interaction between Group and IP Height was significant only for hip-to-eye angle ($p < 0.001$). The plots in Figure 4.8 show that the average effects of IP height on the variables of interest are small.

Downvision angle in Figure 4.8 is the XZ (side-view) angle of the line from the eye point to the top of the IP, relative to horizontal. Smaller values indicate a reduced forward field of view. In condition 1, the least-restrictive condition, the subjects' average downvision angle was greater than 15 degrees. In the highest IP condition for each group (7 for the women, 9 for the men), the average IP downvision angle was about 5 degrees. Projection of the nearly linear trend suggests that the small-female group would have been, on average, unable to see below the road scene horizon at IP condition 9, an observation made during pilot testing.

In spite of these reductions in downvision angle, the drivers' postures did not change substantially. Table 4.6 summarizes the differences in average posture between conditions 1 and 7. On average, drivers sat with their hips (HipX) 7 mm further forward in condition 7 than in condition 1 ($p<0.01$). Interestingly, the average driver-selected seat position was about 13 mm further forward in condition 7 than in condition 1 ($p<0.001$), indicating that the subjects sat with their hips about 6 mm further rearward on the seat in condition 7. This effect is consistent with an attempt to sit more erect (less slumped), and is also seen in the orientation of the pelvis, which is about 4 degrees more upright in condition 7 than in condition 1 ($p<0.001$). The average lumbar spine flexion, as measured by the difference between the pelvis and thorax orientations, decreased by an average of 3.6 degrees, but the effect was less clear than the trend in the pelvis orientation ($p=0.02$). Head angles and cervical spine flexion were not significantly affected by the IP height. Overall recline, as measured by the hip-to-eye angle, was reduced by about one degree as the IP height was raised from condition 1 to condition 7. To put these small changes in posture in the context of the vehicle package, Figure 4.9 illustrates the average difference in hip and eye location between conditions 1 and 7.

Table 4.6
Summary of IP Height Effects:
Mean of All Subjects

Variable	Condition 1	Condition 7	Difference (7-1)
HipX (mm)	670.5	663.4	-7.1*
Hip-to-Eye Angle	9.2	8.2	-1.0*
Pelvis Angle – Thorax Angle	59.3	55.7	-3.6*
Head Angle	-2.1	-2.6	-0.5
Thorax Angle - Head Angle	6.3	6.1	0.2

*Difference is significant ($p<0.05$) using a paired t test.

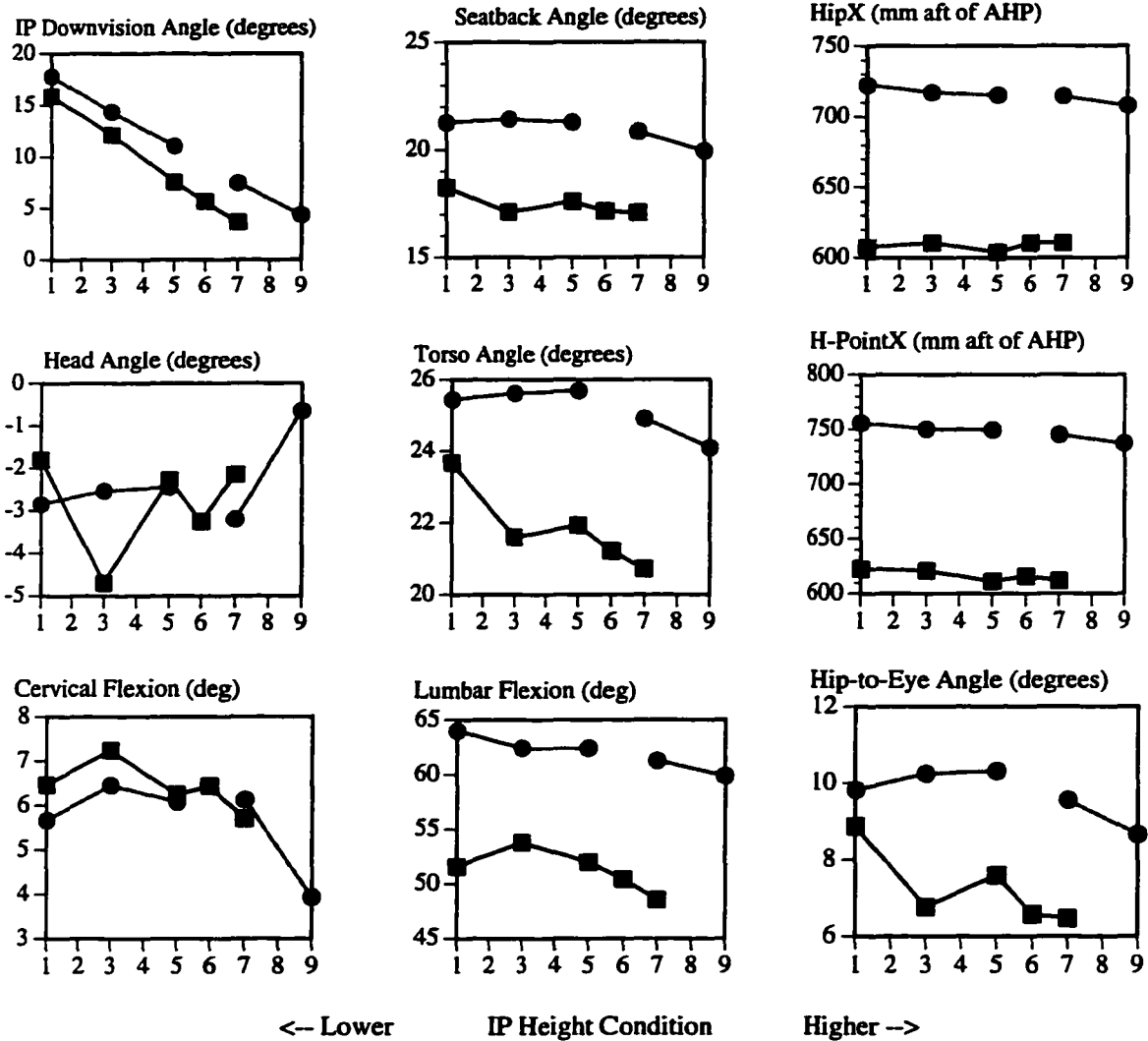


Figure 4.8. Illustration of the effects of instrument panel height condition and gender on posture variables. Horizontal axis shows IP condition number. See Table 4.2 for actual heights. Small Females = ■, Midsize Males = ●. Symbols represent condition means.

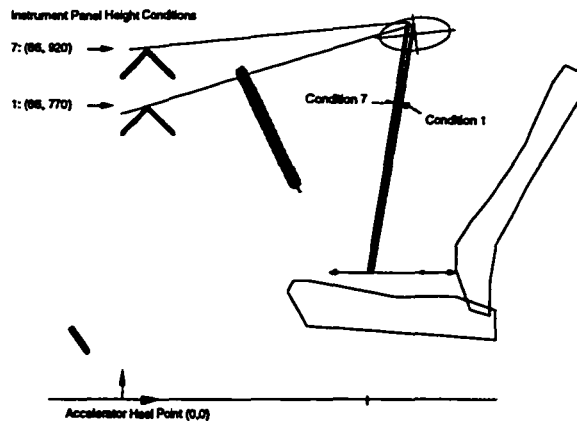


Figure 4.9. Illustration of average posture change resulting from a 150-mm increase in instrument panel height. Lines connect mean hip and mean eye locations for all subjects in IP height conditions 1 and 7. The SAE 95th-percentile eyellipse is also shown for reference.

4.6 Results — Vehicle Study

Drivers in the vehicle study did not significantly change either their fore-aft hip position or hip-to-eye angle when the mask was added. Table 4.7 shows the mean values for the two variables, along with a summary of the paired t tests comparing the mask and no-mask conditions. The least significant value is the radius of the confidence interval on the mean difference estimate, and is a measure of the sensitivity of the test. Given the observed variance in the measured postures, a difference in hip location of 6.8 mm or a difference in hip-to-eye angle of 0.7 degrees would have been found to be significant with $p = 0.05$. The trend in hip location is in the same direction as the response to vision restriction observed in the simulator study, but the effect is small. No trend is apparent in the hip-to-eye angle data.

Table 4.7
Summary Results from Vehicle Study (N=32)

Condition	HipX (mm) mean (std.dev.)	Hip-to-Eye Angle (degree) mean (std.dev.)
No Mask	759.8 (53.1)	8.9 (2.2)
Mask	754.3 (55.9)	9.0 (2.8)
Difference	5.5 (19.2)	-0.1 (2.1)
$t (p)^*$	-1.7 (0.11)	0.31 (0.76)
Least Significant Value (0.05)	6.8	0.7

*Paired t test, t value and probability \neq $|t|$.

4.7 Discussion and Conclusions

The drivers in this study changed their postures only slightly when a simulated instrument panel or a windshield mask obstructed their forward view. The changes were consistent with the expected behaviors to compensate for the vision restriction, but the effects on torso posture and eye position were small. The resulting downvision angles were nearly the same as those that would have resulted if the subjects had not changed their postures at all.

The design of this study limits to some extent the generalizability of this central finding, but the data are applicable to some important vehicle ergonomics problems. A primary limitation is that the drivers were provided with seats that did not have vertical (height) adjustment. Although most vehicles are currently manufactured with a seat having only fore-aft adjustment of the seat location, an increasing number of driver seats have height adjustment. Further study is needed to determine the effects of vision restriction on driving postures when such seat height adjustment is provided.

Only the drivers' static, normal driving posture was measured, but it is likely that some drivers in the vehicle study leaned further forward, off of the seatback, when performing visually demanding driving maneuvers. These subjects may have returned to a normal driving posture while being measured, in which case the measured posture would not be representative of all of their driving postures, although it probably represents the most prevalent posture. The subjects ranged in age from 21 to 73 years (average 42 years), but these findings may not be applicable to unusual population subgroups, such as those with age-related vision degradation. The experiment also did not consider the potential effects of high-stress driving situations, such as heavy traffic or poor weather.

Although the changes in posture resulting from vision restriction were small, many of the subjects complained of discomfort and driving difficulty in the more restrictive conditions, indicating that they were having difficulty seeing the road. Since the subjects were clearly made uncomfortable by the IP height, it is reasonable to believe that they would have changed their posture to reduce their discomfort if they were able to, that is, if a posture that improved the visibility of the scene was readily achievable. This suggests, then, that the typical vehicle layout and driving posture are such that substantial improvements in downvision angle are difficult to achieve while maintaining a driving posture.

This experiment was conducted with a fairly small number of subjects, but the posture-change behaviors were reasonably similar across subjects and between the two groups. This suggests that additional subjects would not have changed the findings substantially, although some of the smaller effects would likely reach statistical significance.

The evidence from this study suggests that the choice of IP height and forward vision restriction in laboratory studies of driving posture is not likely to affect the findings substantially. This has important implications for studies of control layout and seat design, since many such experiments cannot readily be conducted in vehicles. The findings further suggest that restrictions on forward vision are not important factors to consider in developing techniques to predict driving posture for vehicles equipped with fore-aft seat tracks.

4.8 References

- Devlin, W.A., and Roe, R.W. (1968). *The eyellipse and considerations in the driver's forward field of view*. SAE Technical Paper 680105. New York, NY: Society of Automotive Engineers, Inc.
- Flanagan, C.A.C., Schneider, L.W., and Manary, M.A. (1996). Development of a new seating accommodation model. SAE Technical Paper 960479. In *Automotive Design Advancements in Human Factors: Improving Drivers' Comfort and Performance (SP-1155)*, 29-36. Warrendale, PA: Society of Automotive Engineers, Inc.
- Hammond, D.C., and Roe, R.W. (1972). *Driver head and eye positions*. SAE Technical Paper 720200. New York, NY: Society of Automotive Engineers, Inc.
- MacAdam, C.C., Green, P.A., and Reed, M.P. (1993). An overview of UMTRI driving simulators. *UMTRI Research Review* 24(1): 1-8.
- Meldrum, J.F. (1965). *Automobile driver eye position*. SAE Technical Paper 650464. New York, NY: Society of Automotive Engineers, Inc.
- Mourant, R.R., Pak, T., and Moussa-Hamouda, E. (1978). *Dynamic eye positions by vehicle type. Final report of the Second Generation Eyellipse Project*. Detroit, MI: Wayne State University, Department of Industrial Engineering and Operations Research.
- Reed, M.P., Schneider, L.W., and Eby, B.A.H. (1995) *The effects of lumbar support prominence and vertical adjustability on driver postures*. Technical Report UMTRI-95-12. Ann Arbor: University of Michigan Transportation Research Institute.

Roe, R.W. (1993). Occupant packaging. In *Automotive Ergonomics*, ed. B. Peacock and W. Karwowski, 11-42. London: Taylor and Francis.

Society of Automotive Engineers (1997). *Automotive Engineering Handbook*. Warrendale, PA: Society of Automotive Engineers, Inc.

CHAPTER 5

DEVELOPMENT AND EVALUATION OF STATISTICAL POSTURE PREDICTION MODELS FOR AUTOMOBILE DRIVING

5.1 Abstract

Driving postures chosen by 68 men and women in 18 different vehicle package and seat conditions were used to create three alternative models to predict whole-body driving posture. The model predictions were compared to the original data and to the driving postures of 120 men and women in five vehicles. A model using multiple independent regression predictions was approximately as accurate as a model combining regression predictions with inverse kinematics, but the latter model provides greater generalization to alternative human models. Errors in mean eye location predictions in the vehicles for the two better models were typically less than 10 mm. Prediction errors were largely independent of anthropometric variables and vehicle layout. Although the average posture of a group of people can be predicted accurately, individuals' postures are poorly predicted due to intersubject posture variance that is unrelated to key anthropometric variables. The posture-prediction models developed in this research can be applied to posturing computer-rendered human models for vehicle interior ergonomic assessment.

5.2 Introduction

The design of passenger car interiors is increasingly assisted by the use of three-dimensional human representations that can be manipulated in a computer environment (Porter et al., 1993). These Computer-Aided-Design (CAD) human models have increased in sophistication in recent years with advances in computer hardware and

software, but their effective use is hampered by the lack of valid methods to posture the models in the simulated vehicle interior.

In the mid-1950s, Dempster (1955) introduced an approach to ergonomic assessment for seated vehicle occupants using an articulated, two-dimensional template. A similar template design and a weighted three-dimensional manikin for measurements in actual vehicles were standardized in the mid-1960s for passenger car interior design by the Society of Automotive Engineers in Recommended Practice J826 (SAE 1997). These two tools, the two-dimensional template and the three-dimensional H-point machine, are still widely used for designing vehicle interiors, but are supplemented by statistically based tools that predict the distributions of particular posture characteristics for the U.S. population. These task-oriented percentile models, based on posture data from a number of different studies, are available for driver-selected seat position (SAE J1517), eye position (J941), reach (J287), and head location (J1052). See Roe (1993) for a thorough review of the use of these tools in contemporary occupant packaging.

Although the existing task-oriented percentile models are very useful for vehicle design, they are not directly applicable to the posturing of human models because they address the population distribution of particular posture characteristics, rather than predicting the posture for any particular anthropometric category. For example, the SAE eyellipse provides a prediction of the mean and distribution of driver eye locations, but does not predict the eye location for women 1550 mm tall or men 1800 mm tall. This more detailed information is necessary to establish an accurate posture for a particular instance of a CAD human model, which necessarily represents a single set of anthropometric variable values.

As computer technology has developed, CAD models have been created to simulate the two- and three-dimensional physical manikins, supplemented by more complete three-dimensional human representations. Porter et al. (1993) briefly reviewed the features of 13 human-modeling systems in use prior to 1993 with potential application

to vehicle design. Software development moves rapidly, however, and some of the systems that are commercially available as of this writing, including Genicom SafeWork, TecMath RAMSIS, and Transom Jack, are not included in the Porter et al. review. Most of the commercially available human models include substantial anthropometric scaling capability, allowing the model to be configured to represent geometrically the exterior dimensions of a wide range of potential vehicle occupants, but only RAMSIS is known to include any significant prediction capability for vehicle occupant postures (Seidl, 1994). Without posture-prediction capability built into the model or available through other external data or statistical models, many of the most useful applications of the CAD human models are unreliable. For example, vision and reach assessments require an accurate starting posture for the particular manikin dimensions being used. In the absence of accurate posture prediction, CAD human models are valuable primarily for visualization rather than for assessment.

There are few published studies applicable to posture prediction for vehicle occupants. In many early studies, data are presented only in the aggregate or in terms of a population distribution, so the findings are not applicable to human-model posture (Meldrum, 1965; Hammond and Roe, 1972; Phillipart et al, 1984). Seidl (1994) presented the most complete approach to whole-body driving-posture prediction to date. Using posture data collected in a laboratory vehicle mockup, he developed an optimization-based approach that is now used with the RAMSIS human model. The Seidl approach selects a posture consisting of the set of joint angles that is empirically most likely within the specified kinematic constraints. This technique uses posture data collected from three vehicle configurations, and can be interpreted as representing an analog of the driver's inherent posture-selection process, but there are several important limitations. The data on which the predictions are based are proprietary, and hence cannot be independently assessed except through the use of the RAMSIS software, and cannot without considerable effort be applied to a human model having a different

linkage. More importantly, the posture-prediction method itself, while an innovative approach for predicting postures in novel situations, may be more difficult to use as accurately as other methods in well-studied situations, such as normal driving postures.

In the current research, three alternative posture-prediction models were developed using driving posture data obtained from a laboratory study of 68 men and women in vehicle and seat configurations that span a large range of passenger car interior geometry (Chapter 3). The Cascade Prediction Model (CPM) places the highest priority on accurate prediction of hip and eye locations, two of the posture characteristics that are most important for vehicle interior assessment. The Independent Prediction Model (IPM) predicts the whole-body posture using multiple, independent regression predictions, and is intended primarily as a contrast to the Cascade Prediction Model. The Optimization Prediction Model (OPM) uses a modified version of the Seidl approach in which the predicted posture is the posture identified as most likely among the kinematically feasible postures based on the observed distribution of joint angles.

The prediction accuracy of each of the three models was assessed using the original laboratory data and data from a separate study of driving posture in five vehicles. The vehicles were each driven by 120 men and women over a 15-minute road route, after which the drivers' postures were recorded. The comparisons demonstrate the overall accuracy of the three modeling approaches and lead to some important conclusions regarding the use of human models in vehicle design.

5.3 Data Sources

The posture-prediction models were developed using data from a laboratory study of driving posture which has been presented in detail elsewhere (Chapter 3). An anthropometrically diverse group of 68 men and women selected their preferred driving postures in a vehicle mockup that was configured to represent a wide range of vehicle interior conditions. The study was conducted in three phases, each of which used different subjects and test conditions. Table 5.1 summarizes the subject stature range and

Table 5.2 lists the test conditions by test phase. External body landmark data recorded with a sonic digitizer were used to calculate joint locations defining a three-dimensional kinematic-linkage representation of the body (Chapter 2). The resulting lengths, positions, and orientations of the linkage segments were used in the development of the posture prediction models.

Table 5.1
Subject Pool

Subject Group	Stature Range (mm)	Gender	Phase 1 n	Phase 2 n	Phase 3 n	All n
0	under 1511	Female		3	3	6
1	1511 - 1549	Female	5	0	0	5
2	1549 - 1595	Female		3	3	6
3	1595 - 1638	Female	5	0	0	5
4	1638 - 1681	Female		3	3	6
5	1681 - 1722	Female		3	3	6
6	1636 - 1679	Male		3	3	6
7	1679 - 1727	Male		3	3	6
8	1727 - 1775	Male	5	0	0	5
9	1775 - 1826	Male		3	3	6
10	1826 - 1869	Male	5	0	0	5
11	over 1869	Male		3	3	6
Total			20	24	24	68

Table 5.2
Test Conditions by Phase

Configuration Number	N	Phase 1	Phase 2	Phase 3	Seat Cushion Angle (L27) (degrees)	Seat Height (H-30) (mm)	SWtoBOFX (mm)
1	44	x	x		11	270	450
2	68	x	x	x	11	270	500
3	68	x	x	x	11	270	550
4	68	x	x	x	11	270	600
5	44	x	x		11	270	650
6	44	x	x		18	270	450
7	68	x	x	x	18	270	500
8	68	x	x	x	18	270	550
9	68	x	x	x	18	270	600
10	44	x	x		18	270	650
12*	48		x	x	11	180	550
13	48		x	x	11	180	650
14	48		x	x	11	360	450
15	48		x	x	11	360	550
16	24			x	18	180	550
17	24			x	18	180	650
18	24			x	18	360	450
19	24			x	18	360	550

* Condition 11 included a modification to the seat. The data are excluded from this analysis.

5.4 Body Segment Scaling

A key part of posture prediction is the creation of a kinematic linkage that is appropriate for the specified set of anthropometric variables. In general, posture-prediction methods are linkage-specific, although the Cascade Prediction Model developed in this work is intended to be applicable to any reasonable linkage. Scaling relationships to calculate body segment lengths from stature and sitting height were developed using the data from the laboratory study. Although there are a few significant gender differences in segment proportion, these differences are small enough to be neglected for posture prediction. Table 5.3 lists the scaling relationships. Note that torso segment lengths are scaled using sitting height, while limb dimensions are scaled using stature. This allows the ratio of sitting height to stature to be varied independently, simulating occupants with different body proportions. When only stature is supplied, the sitting height can be estimated by multiplying stature by 0.52. The scaling relationships in Table 5.3 differ slightly from those used with other linkage representations of the body (cf. Drillis and Contini, 1966). In particular, the ratio of thigh length to leg length is unusual. The implications of linkage differences in the context of posture prediction are considered in the Discussion, below.

Table 5.3
Segment Length Scaling Fractions*

Segment	Stature Fraction	Sitting Height Fraction
Head		0.105
Neck		0.143
Thorax		0.300
Abdomen		0.224
Pelvis		0.105
Pelvis Width		0.168
Thigh	0.257	
Leg	0.237	
Arm	0.162	
Forearm	0.147	
Hand	0.046	

* Limb segments are predicted as fractions of stature, torso segments as fractions of erect sitting height.

5.5 General Model Formulation

Vehicle Geometry Definitions and Model Inputs

Posture prediction is conducted in a vehicle package coordinate system, defined by several commonly used vehicle reference points. Complete definitions of these points can be found in Society of Automotive Engineers Recommended Practice J1100 and associated practices (SAE, 1997; see Appendix A for a brief review). The X axis in the package coordinate system runs positive rearward, the Y axis positive to the driver's right, and the Z axis positive up. The origin is defined by a different point on each axis. The origin X coordinate is defined by the Ball of Foot (BOF) reference point, while the origin Z coordinate is defined by the Accelerator Heel Point (AHP). In general terms, vertical dimensions are measured from the floor and fore-aft dimensions are measured from a point on the accelerator pedal. For the current analysis, the origin Y coordinate is the centerline of the driver seat. Figure 5.1 illustrates these reference points on a side-view schematic of the driver's station.

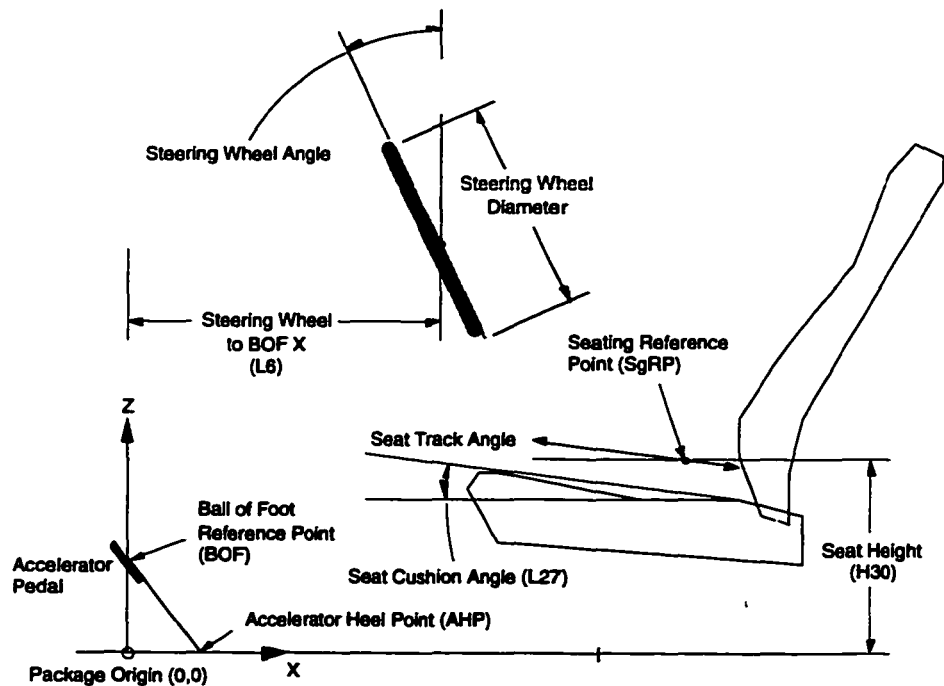


Figure 5.1. Vehicle package geometry. Expressions in parentheses are Society of Automotive Engineers nomenclature from SAE J1100 (SAE, 1997).

A number of vehicle package dimensions are used as inputs to the posture prediction models. These parameters have been varied systematically in testing or are those whose specification is necessary to sufficiently characterize the locations of components. The weighted, contoured H-point manikin (SAE J826) measures a reference point on the seat known as the H-point (a hip-joint location estimate). When the seat is moved forward and rearward along its adjustment track, the orientation of the path of the H-point relative to the horizontal defines the seat track angle. The seating reference point (SgRP) is the H-point location that lies on the 95th-percentile selected seat position curve given by SAE J1517 (SAE, 1997). This curve is a second-order polynomial describing the horizontal position of the 95th-percentile of the seat position distribution as a function of seat height. Seat height is defined by the vertical distance between the SgRP and the AHP, and is termed H30, following the dimension definitions in SAE J1100.

Seat cushion angle (L27) specifies the orientation of the lower part of the seat (seat pan) with respect to horizontal, and is measured using the H-point manikin with a procedure described in SAE J826. Seat cushion angle does not generally correspond to any measure of the unloaded centerline contour of the seat, but instead represents the cushion orientation experienced by a standardized sitter. The steering wheel is characterized by the coordinates of the center of the front surface of the wheel, the angle of the front surface of the wheel with respect to vertical, and the diameter of the wheel. The horizontal distance from the center of the steering wheel to BOF is a key package dimension and is termed SWtoBOFX.

Table 5.4 lists package geometry inputs to the posture prediction models in two categories: parameters that solely affect kinematic constraints imposed on the models, and those that are variables in the predictive equations. Only three variables are used in the posture prediction models: H30, SWtoBOFX, and L27. Notably, the vertical position of the steering wheel and the degree of forward vision restriction imposed by the instrument panel or vehicle cowl are not included. The vertical position of the steering

wheel is highly constrained in vehicle design, because of the conflicting requirements of sufficient leg space beneath the wheel and sufficient vision above the wheel. The leg depth of large drivers and the eye height of small drivers tends to constrain the vertical steering wheel position to a small range relative to the SgRP location. Restrictions on forward vision, in the range that is reasonable for vehicle design, do not have important effects on posture (Chapter 4).

Table 5.4
Package Geometry Inputs

Prediction Variables	Kinematic Constraints
Seat Height (H30)	Seating Reference Point (X,Y,Z)
SWtoBOFX	Steering Wheel Center (X,Y,Z)
Cushion Angle (L27)	Steering Wheel Angle
	Steering Wheel Diameter
	Seat Track Angle
	Center of Accelerator Pedal Y Coordinate (with respect to seat centerline).

The driver's characteristics are represented in the models using four parameters: gender, stature, weight, and sitting height. Additional anthropometric data, such as arm or leg lengths, do not provide substantially better prediction. Because stature, weight, and sitting height are highly correlated in the data set, two transformations of the variables were used as regressors. The ratio of sitting height to stature (SH/S), a measure of body proportion, was used in lieu of sitting height, and the Body Mass Index (BMI), the ratio of mass (kg) to stature (m) squared, was used instead of mass. Each of these two ratio variables is only moderately correlated with stature in this data set ($r = -0.34$ and 0.32 for SH/S and BMI, respectively). The predictive ability of the regressions using these variables, assessed using the adjusted R^2 value, was within 0.01 of the values obtained using sitting height and mass directly, while reducing the problems associated with correlated regressors.

Kinematic Model

Driving posture is represented using a kinematic linkage model of the human body. The linkage and its derivation from external body landmark data is described in detail in Chapter 2. Figure 5.2 shows the linkage and defines variables that are used in the posture-prediction models.

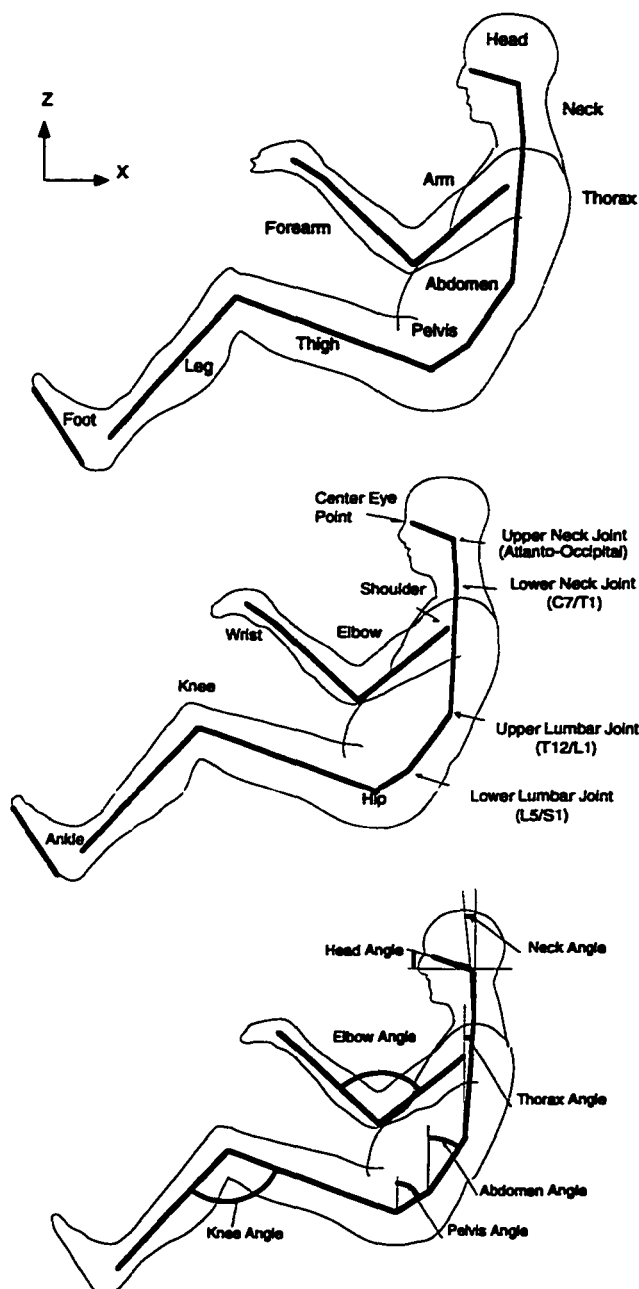


Figure 5.2. Definitions of kinematic linkage and posture measures. Angles referenced to horizontal or vertical are XZ (sagittal) plane angles. Angles between segments (elbow angle, knee angle, and ankle angle) are measured in the plane formed by the segments (included angles). Note: Neck angle is negative as shown. All other angles are positive as shown.

Model Simplifications and Restrictions

Several simplifying assumptions are made to reduce the model complexity. Normal driving posture is considered to be sagittally symmetric, with the posture of the left side of the body mirroring the right. In the data collection used to develop the models, subjects were asked to choose a “normal, comfortable driving posture” with their hands located at the 10-o’clock and 2-o’clock position on the steering wheel. By observation, the only important deviations from sagittal symmetry occurred when left lower-extremity postures did not match the right lower-extremity, which was constrained by the requirement of operating the accelerator pedal. Data from the right upper and lower extremities were used exclusively for developing the models, since the geometric task constraints imposed by the pedals operate solely through the right lower-extremity. The hand-position constraint in testing was imposed so that the elbow angle would be a reliable measure of the distance between the steering wheel and torso. The performance of the models in predicting postures measured in conditions with free hand placement suggests that this constraint provides useful upper-extremity posture data without otherwise affecting posture (see below).

To simplify limb kinematics calculations, the hands are assumed to be continuous with the forearms. Foot posture is neglected in favor of direct prediction of ankle joint location. Detailed information on foot posture that could be incorporated in these models can be found in Schneider et al. (1994).

The models are applicable to automatic transmission vehicles only (no clutch), and to the case where the driver may adjust only the fore-aft position of the seat along a linear track and the orientation of the seatback with respect to vertical (recline angle). The models may have utility when the driver is also provided with a steering-wheel-angle adjustment, such as in the validation vehicles, but additional research will be necessary to adapt the models for use in situations in which the seat height, seat cushion angle, fore-aft steering wheel position, or pedal locations can be adjusted by the driver.

Regression Equations

In all three of the model formulations, a number of degrees of freedom are predicted using regression equations developed from the laboratory study data. These equations were created by a stepwise process after a thorough analysis of the study data (see Chapter 3 for a summary of the study). Among the conclusions of the original analysis were that seat height, steering wheel position, and seat cushion angle all had important, independent effects on posture. There were also small differences in posture between the two seats tested, but these are neglected in the development of the posture-prediction models because appropriate tools to characterize seat differences beyond seat cushion angle remain under development.

Data from all subjects and conditions were pooled (68 subjects in a total of 916 trials) to create the prediction models. A stepwise-regression technique was applied with potential regressors stature, weight, sitting height, sitting height divided by stature, seat height, steering wheel to BOF distance, and seat cushion angle. An automated algorithm selected a model using $p < 0.25$ to enter and $p > 0.10$ to leave, after which manual selections were made to obtain a parsimonious model that maintains an adjusted R^2 value within 0.02 of the maximum value obtained by the automated procedure. Tables 5.5 and 5.6 summarize the regression models that are used in the three posture prediction models. All terms included in the models are significant with $p < 0.001$, as are the models themselves.

Some interesting observations can be made by examining the values in Tables 5.5 and 5.6. The fore-aft hip position (HipXreBOF) is a critical variable that is fairly well predicted, with $R^2 = 0.78$. However, considerable variance remains, evidenced by the root mean square error (RMSE) of 35.9 mm. Horizontal eye position is less well predicted, particularly with respect to the hip location. The large R^2 value for EyeZreAHP is due to the fact that seat height (tested at three levels) is the dominant term in that model. Note that the RMSE is approximately the same for EyeZreAHP and

EyeZreHip, while the R^2 value is lower, reflecting the remaining predictive ability after removing the effects of seat height. The hip-to-eye angle (XZ plane) is not well predicted ($R^2 = 0.20$), and has a fairly small RMSE, indicating that overall torso recline is only weakly affected by the vehicle geometry and the driver's body size. The lack of predictive ability for torso recline is also observed in the low R^2 of the EyeXreHip model.

Table 5.5
Regression Models*

Variable (mm or deg)	Stature (mm)	Sitting Height/Stature	H30 (mm)	SWtoBOFX (mm)	Cushion Angle (deg)	R^2_{adj}	RMSE
HipXreBOF	0.4659	-430.1	-0.1732	0.4479	-1.04	0.78	35.9
Hip-to-Eye Angle	0.00642	115.7		0.0147	0.11	0.20	3.9
EyeXreBOF	0.5842	916.6	-0.1559	0.6101		0.71	50.9
EyeZreAHP	0.3122	679.9	1.0319	0.0292		0.89	21.8
EyeXreHip	0.1187	1347.2		0.1563	1.15	0.23	41.7
EyeZreHip	0.3336	675.8		-0.0544		0.72	22.9
AnkleXreBOF	0.0400	467.6	0.1746	0.1358	1.3	0.32	18.0
AnkleYreAPedal	-0.0466					0.05	23.2
AnkleZreAHP	0.0312		0.1236		0.55	0.25	13.1
Knee Angle	-0.0071	61.3	-0.0321	0.0829	-0.59	0.44	7.7
Head Angle	0.00919	137.5				0.03	10.6
Neck Angle	-0.01197			0.0109		0.04	7.7
Thorax Angle	0.00497	45.2		0.0128		0.03	6.1
Abdomen Angle	0.0109	184.5		0.0222		0.09	9.7
Pelvis Angle	0.0102	90.2		0.0177	0.39	0.04	10.0

*Linear model created by multiplying each term in the table by the value of the column variable and adding a constant intercept.

Table 5.6
Regression Models*

Variable	Stature (mm)	Body Mass Index (kg/m^2)	H30 (mm)	SWtoBOFX (mm)	Cushion Angle (deg)	R^2_{adj}	RMSE
HipXreHPt	0.0482	-2.677			5.00	0.34	27.6
HipZreHPt		2.009	0.0700	0.1375	0.49	0.40	13.7

*Linear model created by multiplying each term in the table by the value of the column variable and adding a constant intercept.

Ankle position with respect to the pedal reference points is moderately associated with the regressor variables, except for the Y coordinate, which is not strongly affected by any of the regressors, but does show considerable residual variance. The ankle Y coordinate is not, however, very important in the predictive models. The individual torso segment orientations are poorly predicted, with R^2 values below 0.10 in all cases. The RMSE values show that considerable variance remains, but these intersubject differences do not appear to be explained by overall body size or proportion.

The XZ-plane hip location (average of right and left hip joints) with respect to the translated seat H-point is moderately well predicted. The residual variance is fairly small vertically, but larger horizontally, indicating that drivers sit with a range of fore-aft positions on the seat. These variables are independently affected by stature and BMI. Seat cushion angle strongly affects the horizontal hip position, while all three vehicle geometry variables have moderate effects on the vertical position. These equations illustrate that the H-point manikin measure of hip location is reasonably accurate, but that driver's hip locations differ relative to the H-point, depending on body dimensions and the vehicle and seat geometry.

5.6 Specific Model Formulations

In this section, three whole-body driving-posture-prediction algorithms are presented. Each uses combinations of the regression equations presented in Tables 5.5 and 5.6 along with inverse kinematics guided by additional information from the input data set. The Cascade Prediction Model (CPM) is intended to produce the best possible prediction of eye and hip locations, while potentially sacrificing some accuracy in other model degrees of freedom. The Independent Prediction Model (IPM) uses multiple, independent regression models to predict most degrees of freedom, and is intended primarily as a contrast to the CPM. The Optimization Prediction Model (OPM) uses an optimization-based approach to predict driving posture, without the use of regression equations to predict the primary degrees of freedom. With each model, the posture of the

trunk and the right limbs is predicted, after which the right-limb posture is reflected to the left side of the body, in keeping with the sagittally symmetric definition of normal driving posture.

Each model requires the input of certain driver descriptors and characteristics of the vehicle geometry, summarized in Table 5.4. As a first step for all three models, the supplied anthropometric variable values are used to scale the kinematic linkage, as described above. Linkage scaling is the only part of the procedure in which gender is a factor.

The vehicle geometry is used to establish kinematic constraints that are important for all three models. The hand grip location at 2 o'clock on the steering wheel is calculated geometrically from the supplied steering-wheel-center coordinates, steering-wheel angle, and steering-wheel diameter. Ankle position, used as the analogous kinematic constraint for the lower extremity, is predicted using the regression equations in Table 5. The SgRP and seat track angle define the seat centerline Y coordinate and the XZ-plane path of the H-point, which is used as a linear constraint on H-point location.

Cascade Model

The Cascade Prediction Model (CPM) is termed “cascade” because the predictions are obtained using a series of submodels, each based on the results of the previous model. The motivation for this approach is to provide the best possible prediction accuracy for the hip and eye locations, the posture characteristics that are most important for ergonomic assessments of the driver’s station. Hip location is closely related to seat position and lower-extremity posture, while eye location is critical for vision analyses.

Figure 5.3 depicts the CPM algorithm schematically. The fore-aft hip location (HipXreBOF) is predicted directly using the equation in Table 5.5. The hip-to-H-point offset vector is calculated using the equations in Table 5.6, yielding a hip travel path in the XZ plane corresponding to fore-aft seat position adjustment. The point along this line

with X value equal to the predicted fore-aft hip location is the predicted hip location in the XZ plane. The Y coordinate of the each hip joint is set so that each hip joint lies equidistant from the seat centerline, placing the torso segments in the XZ plane of the seat centerline.

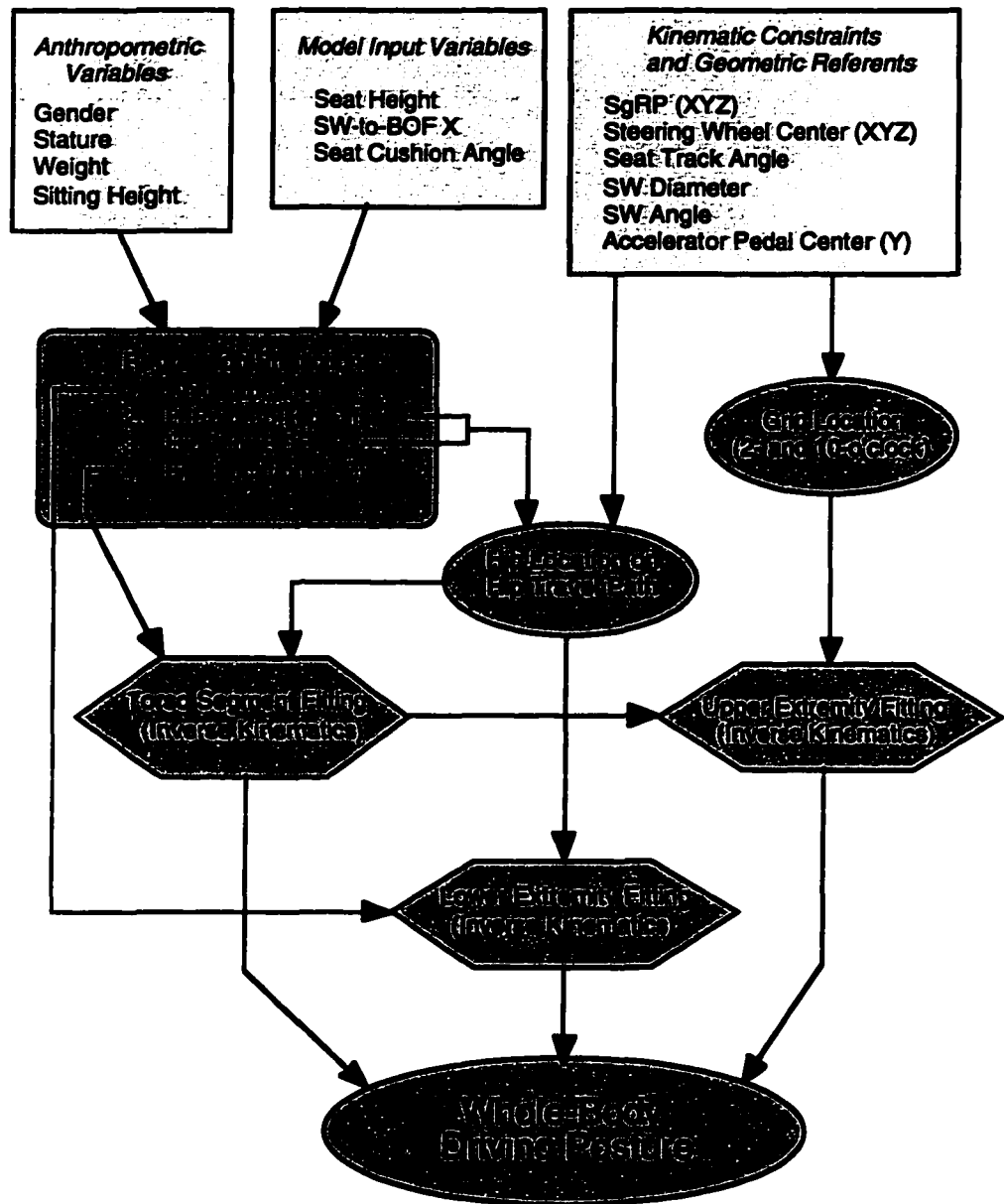


Figure 5.3. Schematic of Cascade Prediction Model (CPM).

Eye location with respect to the hip is then calculated using the regression equations in Table 5.5. With respect to the original data set, predicting the eye location relative to the hip location and relative to AHP/BOF give essentially identical results. However, the indirect procedure avoids potential errors associated with seat track angles different from the angle used in testing. The predicted eye location is the center-eye point, a point on the midline of the body that has a Z coordinate equal to the corner-of-eye landmark and an X coordinate equal to the infraorbitale landmark. This allows all torso segment calculations to be conducted in a plane.

Inverse-kinematics submodels are used to fit the kinematic-linkage representation of the torso to the predicted hip and eye locations. In the torso, previous analyses of these data found statistically significant but small effects of vehicle and seat geometry on torso segment orientations (Chapter 3). In particular, changes in steering wheel position tend to create small changes in overall torso recline, which are accompanied by flexion or extension motions at various levels of the spine. Reflecting these motion patterns in the fitting procedure for the torso segments will allow the resulting models to be used for realistic assessment of the effects of changing vehicle and seat parameters on spine flexion.

To assess the distribution of torso recline, regression analyses were performed using values of torso segment orientation and overall recline (hip-to-eye) angle after subtracting off subject means. The slopes of the regression functions estimate the average change in XZ-plane orientation of each torso segment with a change in overall recline. Table 5.7 shows the slope estimates. Head orientation does not change significantly with recline, while the neck and thorax change orientation at a slower rate than the overall recline measure. In contrast, the abdomen and pelvis show greater angle changes than the hip-to-eye vector.

Table 5.7
Average Change in Segment Orientation with Change in Eye-to-Hip-Vector Angle

Segment	Slope Estimate*	Std. Error	Gamma Value
Head	-0.62†	0.62	0
Neck	0.477	0.082	0.399
Thorax	0.739	0.046	0.617
Abdomen	1.437	0.052	1.199
Pelvis	1.198	0.067	1

*Estimated change in segment orientation (degree/degree)

†Head orientation slope is not significantly different from zero ($p = 0.32$). All other slope estimates are significantly different from zero with $p < 0.001$.

The values in Table 5.7 are used to determine the relative motion in the torso as the torso segments are manipulated to match the predicted hip and eye locations. The overall average torso segment angles (all subjects and conditions) are used as an initial posture. Table 5.8 lists the starting angles.

Table 5.8
Overall Average Torso Segment Angles

Segment	Angle Positive Rearward of Vertical (degrees)
Head	-68.5
Neck	2.0
Thorax	-3.6
Abdomen	32.9
Pelvis	63.4

An inverse-kinematics procedure is used to fit the scaled linkage, initially oriented according to the values in Table 5.8, to the predicted hip and eye locations. Since head orientation does not change significantly with torso recline in the range of interest, the location of the head-neck joint (upper neck joint) is first calculated using the scaled head segment length and the head angle from Table 5.8. The motion distribution given by the values of Table 5.7 can be expressed in terms of a segment motion distribution parameter

vector γ , where γ is rate of change of the segment with respect to a change in pelvis orientation. The γ values are obtained by dividing each slope value in Table 5.7 by the pelvis slope value. Use of the γ distribution parameter reduces spine motion to a single degree of freedom, denoted by variable α . Adding a second variable β that describes rotation of the whole torso around the hip, the coordinates of the head/neck joint with respect to the hip are given by

$$\text{HN}(X) = \sum_{i=1}^4 L_i \text{Sin}[\theta_i + \gamma_i \alpha + \beta] \quad [1]$$

$$\text{HN}(Z) = \sum_{i=1}^4 L_i \text{Cos}[\theta_i + \gamma_i \alpha + \beta] \quad [2]$$

where the L_i are the lengths of the four segments between the hip and head/neck joint and the θ_i are the starting segment orientations from Table 5.8. A fast gradient-based minimization procedure is used to determine the combination of alpha and beta that fits the head/neck and hip locations to within 0.01 mm. Values of α and β are generally less than five degrees. The predicted torso segment angles are then given by $\theta_i + \gamma_i \alpha + \beta$.

Once the torso segment orientations have been calculated using the inverse-kinematics procedure, the right shoulder (glenohumeral) joint location is calculated. Shoulder joint location with respect to the thorax segment did not vary significantly with the vehicle or seat variables studied, so the shoulder location on the thorax segment can be calculated with respect to anthropometric variables only. The height of the shoulder along the thorax segment is given by the regression function $-21.3 + 0.1128 \text{ Stature}$ ($R^2 = 0.60$, $\text{RMSE} = 11.1$), and the lateral (Y axis) position is predicted as 0.100 times stature. The fore-aft position of the shoulder joint with respect to the thorax is not a significant function of anthropometry, vehicle, or seat variables, and is represented by a constant 2.8 mm.

Given the right shoulder and right hand-grip locations, the forearm-hand and arm segments are fit using inverse kinematics. An arm splay angle prediction is used identify an elbow location from the locus of mathematically possible elbow positions. Arm splay angle is a weak function of elbow angle, predicted by $-9.9 + 0.156 \text{ Elbow Angle}$ ($R^2 = 0.12$, $RMSE = 9.8$).

Arm splay angle is the angle around the shoulder-to-grip vector that the elbow location would have to be rotated to lie in a vertical plane with the grip and shoulder points.

An analogous process is used to fit the thigh and leg segments to the predicted hip and ankle locations. Leg splay is taken as a constant, average value of 8.4 degrees. Leg splay is the angle around the hip-to-ankle vector that the knee location would have to be rotated to lie in a vertical plane with the ankle and hip joints. The limb postures are reflected to the left side of the body to complete the posture prediction.

Independent Prediction Model

The independent prediction model is a model that predicts many segment orientations using independent regression equations while respecting the kinematic restrictions of the linkage and vehicle geometry. Although there are many potential approaches of this type, the IPM described here appears to be the most practical model. Figure 5.4 illustrates the IPM approach schematically. After scaling the model and calculating the ankle location, grip location, and hip-travel path, knee angle is predicted using the regression equation in Table 5.5. Given the scaled leg and thigh segment lengths, the knee angle specifies a particular hip-to-ankle distance. The point on the right hip-travel path lying the specified distance from the ankle is the predicted hip location. The torso segments are then oriented using the regression equations in Table 5.5. The small coefficients result in predictions that deviate only slightly from the overall mean values given in Table 5.8. Shoulder, elbow, and knee locations are calculated by the same techniques used with the CPM.

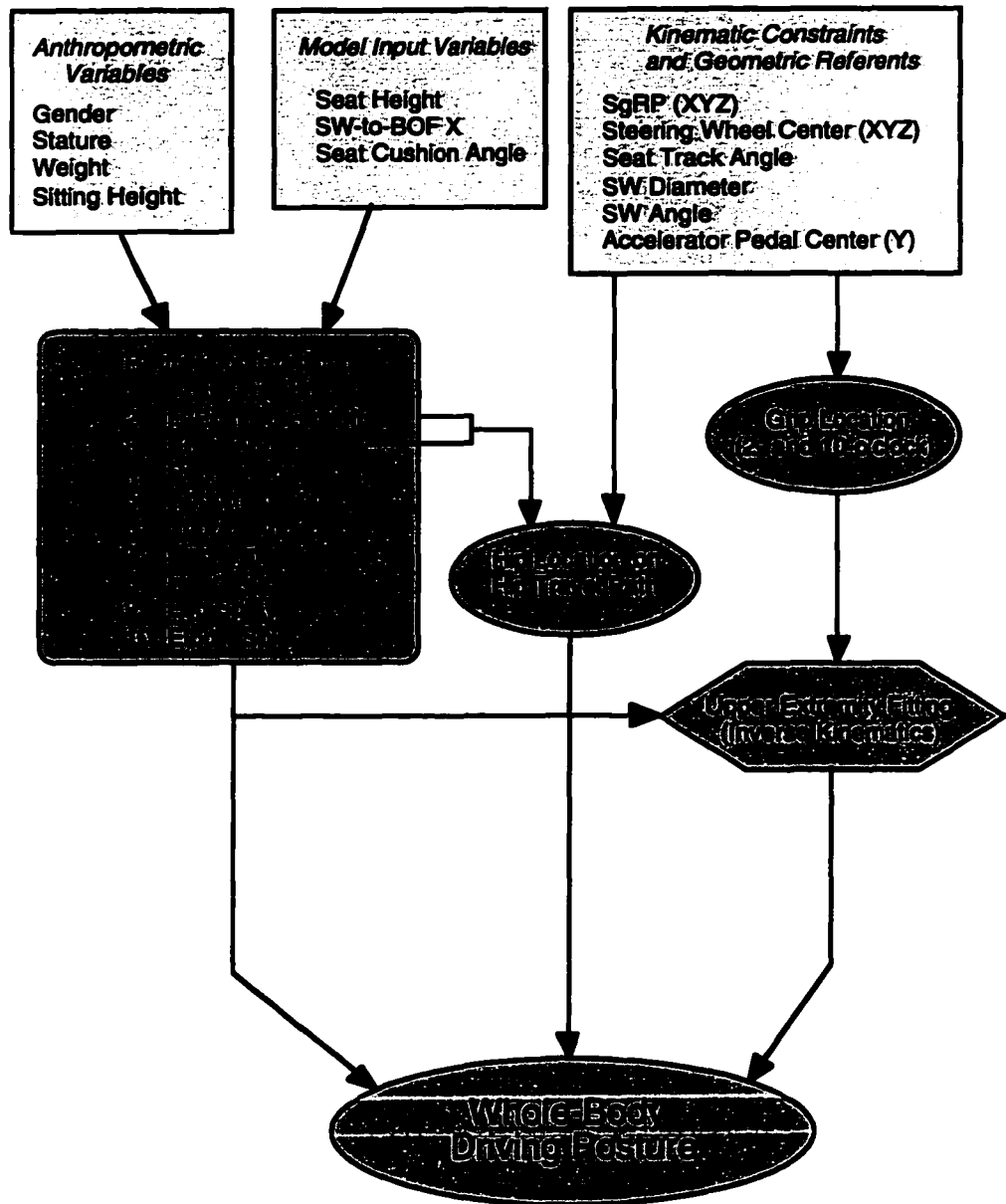


Figure 5.4. Schematic of Independent Prediction Model (IPM).

Optimization Prediction Model

The optimization prediction model represents a completely different approach to posture prediction from the regression-based methods described above that has antecedents in a number of previous posture prediction schemes. Many researchers have proposed that there are joint angles, various called comfort angles or neutral postures, that result when the moments across the joint are passively balanced (Babbs, 1979; Bohlin et

al., 1978; Rebiffe, 1980; Grandjean, 1980; Weichenrieder and Haldenwanger, 1986; Asano et al., 1989; Judic et al., 1993). If there are comfort costs associated with deviations from these angles, then posture might be predicted by assuming that people select postures that allow as many joints as possible to be close to these neutral angles (Weichenrieder and Haldenwanger, 1986). There are three essential components to this approach. The neutral angles, the cost functions associated with deviations from the neutral posture, and the manner in which these costs are traded off or optimized must be determined.

The neutral angles have been identified in a number of ways, most notably by observing postures underwater and in zero-g environments (Reynolds, 1993), and by assuming that the average postures observed over a wide range of task conditions represent the preferred or neutral posture (Verriest and Alonzo, 1986; Judic et al., 1993; Weichenrieder and Haldenwanger, 1986). The cost functions and optimization procedure, which are interdependent, have generally been parameterized *a priori*, using, for example, a minimization of the deviations from the neutral angles (Weichenrieder and Haldenwanger, 1986).

Recently, Seidl (1994) proposed a novel method of simulating the joint-angle comfort tradeoffs that are frequently assumed to underlie posture selection behavior. The actual distributions of joint angles measured over a range of task conditions (vehicle package geometries) are used to determine the joint cost functions. A posture is selected within those kinematically possible that simultaneously maximizes the likelihood of each of the joint angles with respect to the observed distributions. This procedure, embodied in the RAMSIS software manikin, applies this method globally to all joints in the model for each posture prediction.

The OPM uses a modified version of Seidl's approach, illustrated schematically in Figure 5.5. To begin, the kinematic linkage is scaled and the ankle location, grip location, and hip travel path are calculated as with the CPM and IPM. The OPM

algorithm calculates the most likely posture, based on the input data, that is consistent with the specified kinematic constraints. The model is made independent of specified package and seat geometry by predicting ankle location and the hip offset vector using average conditions ($H30 = 270$ mm, $SWtoBOFX = 550$ mm, cushion angle = 14.5 degrees). In practice, additional information on the vehicle geometry could be inferred from the kinematic constraints, but in the current analysis the goal was to minimize the usage of regression equations in the OPM.

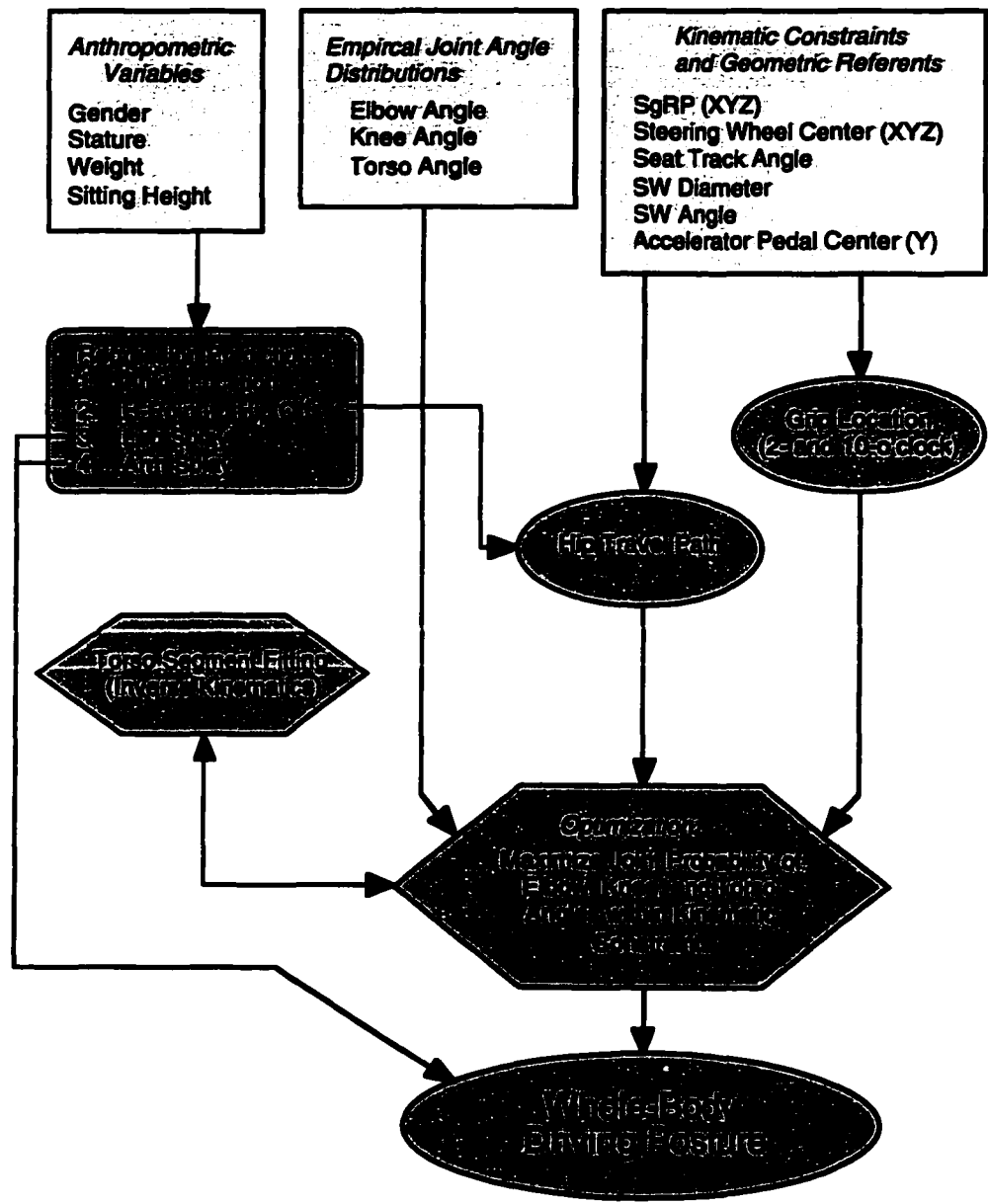


Figure 5.5. Schematic of Optimization Prediction Model (OPM).

The kinematic optimization is conducted using the three-dimensional linkage depicted in side view in Figure 5.6. Intersegment motion in the torso is governed by the same motion distribution parameter values used in the CPM and IPM. Three angles are used in the optimization process: elbow angle, knee angle, and torso angle. The elbow and knee angles are the angles formed by the adjacent model segments at the respective joints (larger angles represent greater extension), and torso angle is the XZ-plane angle of the vector from hip to shoulder with respect to vertical.

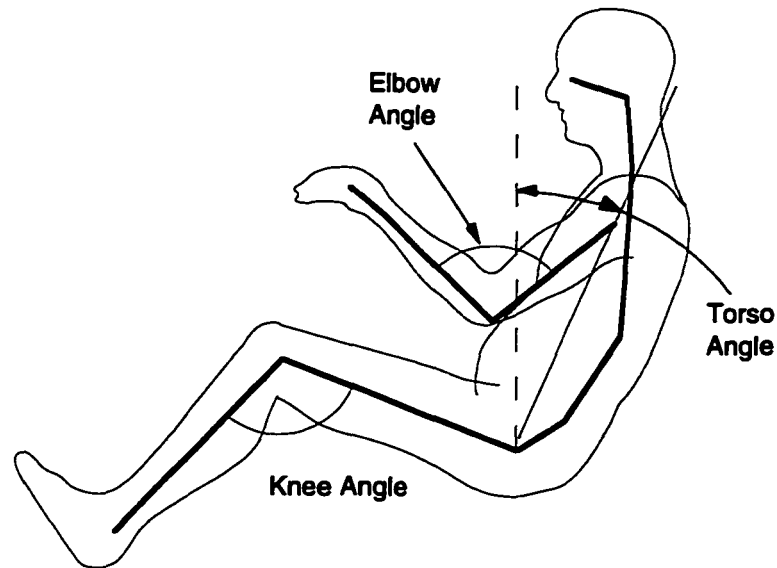


Figure 5.6. Posture variables used in OPM.

In the reference dataset, the mean values of knee angle and torso angle are not significantly related to the anthropometric variables, but mean elbow angle is a function of stature and the ratio of sitting height to stature. The mean values and predictive equation, used to determine the neutral values in the optimization, are given in Table 5.9. While Seidl used the pooled angle values from all subjects to model the distribution of angles, a more direct interpretation of the relative sizes of the angle distributions can be obtained by first subtracting off each subject's mean. The spreads of the resulting distributions reflect the average within-subject joint-angle tradeoffs. Shapiro-Wilk W-

test values given in Table 5.9 indicate that in each case the within-subject angle distribution is not significantly different from normal.

Table 5.9
Angle Distribution Parameters for OPM

Angle	Between-Subject Mean (degrees)	Within-Subject Standard Deviation (degrees)	Shapiro-Wilk Test for Normality (W, p)*
Torso Angle	23.8	2.8	0.994, 1.00
Knee Angle	118.0	7.9	0.986, 0.35
Elbow Angle	$-297.0 + 0.12 \text{ Stature} + 406.6 \text{ SH/S}^\dagger$	11.6	0.987, 0.63

*p values less than 0.05 (or some other Type-I error level) would support a conclusion that the distribution is not normal.

†Regression on stature (mm) and the ratio of sitting height to stature, $R^2 = 0.32$, $\text{RMSE} = 19$ degrees.

Using the within-subject analysis, the relative sizes of the angle distributions represent quantitatively the joint angle tradeoffs used by the subjects in adjusting to a wide range of vehicle and seat geometries. Angle changes at the elbow were largest, followed by knee angle, with only small angle changes occurring in the torso.

The objective of the OPM is to select, from the postures that meet the kinematic constraints, the posture that is most likely. This means choosing the vector of joint angles

$$\Phi = \{\text{knee angle, elbow angle, torso angle}\} = \{\phi_1, \phi_2, \phi_3\} \quad [3]$$

such that the joint (combined) probability of Φ is maximized. In the original approach developed by Seidl, the range of test conditions was restricted in a way which reduced the correlation among the variables to the point where they could be neglected. In that case, the combined probability is simply the product of the probabilities at the individual joints. However, in the broader dataset used for the development of the OPM, there are potentially important correlations among the joint angles, notably between the elbow and knee angles ($r = -0.39$). Therefore, the likelihood of a particular angle at one joint is dependent on the value of another joint. To compute the overall likelihood of a posture, it is necessary to consider the combined probability.

Using the marginal normality findings from Table 5.9, the three individual joint angle distributions can be considered as a single multinormal distribution characterized by mean vector μ and covariance matrix Σ . The probability density function for the random vector Y , where Y has multivariate normal distribution, is given by

$$f(\mu, \Sigma) = \frac{1}{(2\pi)^{r/2} \sqrt{|\Sigma|}} \text{Exp}\left[-\frac{1}{2} (Y - \mu)^T \Sigma^{-1} (Y - \mu)\right] \quad [4]$$

where μ is the mean vector, r is the dimension of Y (3, in this case), Σ is the covariance matrix, $|\Sigma|$ denotes the determinant of Σ , and Σ^{-1} denotes the inverse. For the knee, elbow and torso angles used in the OPM, the mean values are given by the expressions in Table 5.9 and the covariance matrix is given in Table 5.10. The optimization problem, then, is to find the vector $Y = \Phi$ that for which $f(\mu, \Sigma)$ is a maximum.

Table 5.10
Covariance Matrix (Σ)

	Knee Angle	Elbow Angle	Torso Angle
Knee Angle	62.41	-35.7396	5.0876
Elbow Angle	-35.7396	134.56	-1.2992
Torso Angle	5.0876	-1.2992	7.84

Because of the kinematic constraints imposed by the ankle location, grip location, hip travel path, and torso motion distribution, the kinematic linkage has only two degrees of freedom (neglecting arm and leg splay). If the knee angle and torso angle are given, the elbow angle can be computed from the constraints. This reduces the optimization problem to the search of a two-parameter space, and the objective function (posture likelihood) can be plotted as a surface, as shown in Figure 5.7. The single local maximum is also a global maximum, so a gradient-based approach is adequate to compute the posture.

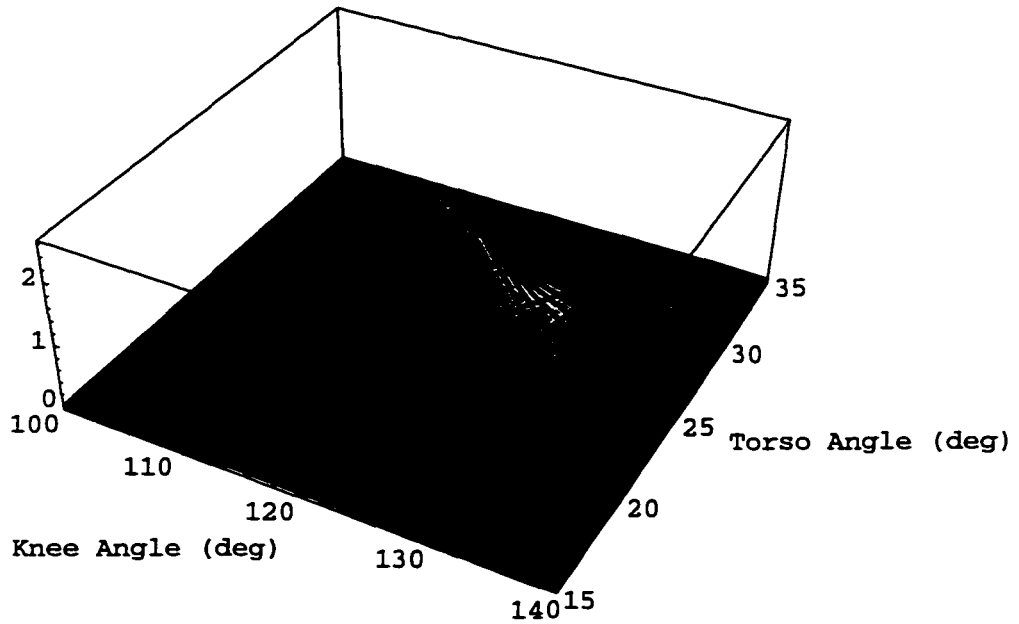


Figure 5.7. Empirical posture likelihood (arbitrary units) as a function of knee angle and torso angle for midsize-male anthropometry in a mid-range vehicle package.

Computation

Each of the models was implemented in *Mathematica* (Wolfram, 1996). The *Mathematica* function `FindMinimum[]`, which uses a gradient-based minimization algorithm, was used for the torso-segment inverse kinematics calculations for the CPM and OPM and for the optimization calculations in the OPM.

5.7 Model Comparison

The three model formulations (CPM, IPM, and OPM) were exercised on the conditions of the 916 trials present in the reference dataset and the predictions compared. In general, the predictions of the three models were very similar. Figures 5.8 and 5.9 show stick-figure representations of the body linkage oriented using the three models for two different anthropometric, vehicle, and seat conditions. The head segment in the illustrations extends from the head-neck joint to the center-eye point. In each figure, the steering wheel, SgRP, H-point travel path, accelerator pedal, and heel surface are

depicted schematically. The hip-to-H-point offset vector is also illustrated. The CPM predictions are shown with thick lines, the IPM with thin lines, and the OPM with dotted lines. For each condition, the predictions from the three models are quite similar, with the largest discrepancies appearing in the vertical locations of the hip and eye.

Figure 5.8 shows the effects of fore-aft steering wheel position on midsize-male driving posture. A more forward steering wheel position tends to cause drivers to sit with more extended elbows, more flexed knees, and slightly more upright torso posture.

Figure 5.9 shows the effects of body size, comparing the predicted postures for statures of 1550 and 1850 mm in a typical high-seat-height package. Note that the torso postures are very similar, but there are differences in limb postures that are nearly identically predicted by the three models.

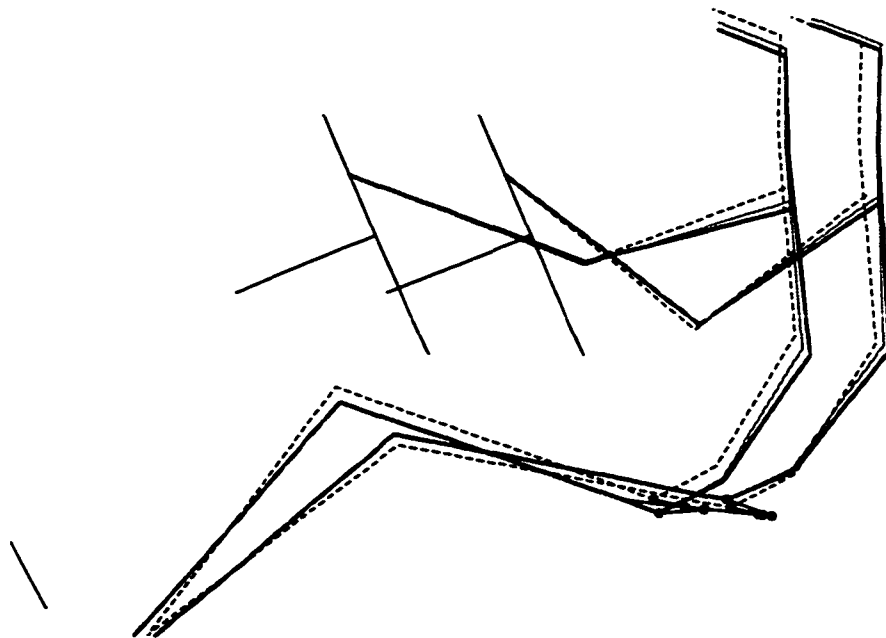


Figure 5.8. Comparison of model predictions for a midsize male at two steering wheel positions for a mid-seat-height vehicle. CPM: thick lines; IPM: thin lines; OPM: dotted lines.

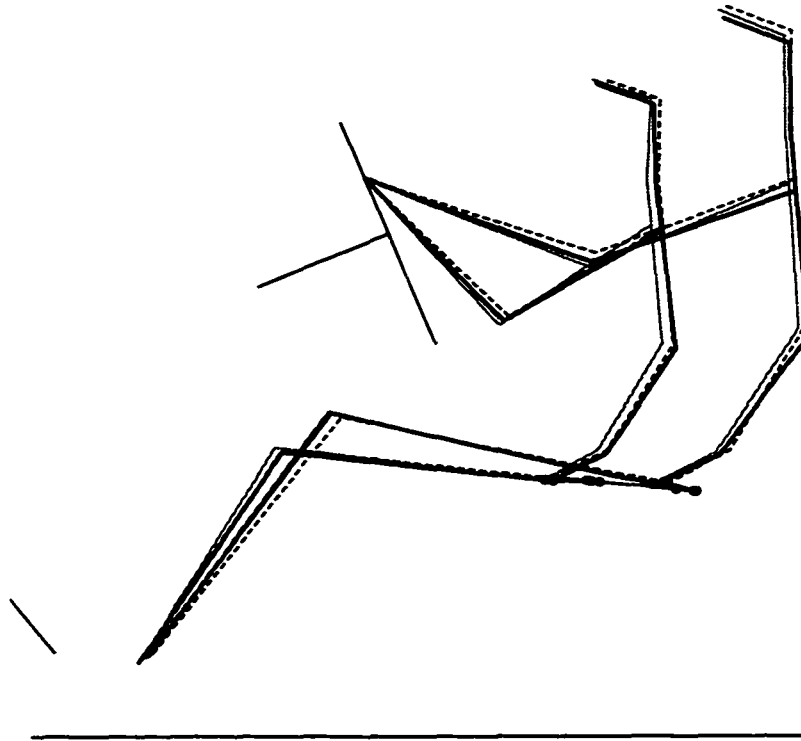


Figure 5.9. Comparison of model predictions for a small female and a large male in a typical high-seat-height vehicle. CPM: thick lines; IPM: thin lines; OPM: dotted lines.

5.8 Model Assessment: Original Data

There are two general areas of concern in assessing model performance. First, the ability of the models to match the original data used to construct the models is assessed. Second, the predictive ability of the models is evaluated using new data collected in vehicles.

It is clear from Figures 5.8 and 5.9 that the three models produce very similar predictions over a range of body sizes and vehicle layouts. There are, however, discrepancies in eye location predictions that are related to the model methods. Since eye location is one of the most important characteristics of the posture prediction, quantitative assessments of the models will focus on eye location.

Table 5.11 and Figure 5.10 compare the predicted eye locations with the observed locations in the original dataset for the three models. As expected, the CPM, which uses nearly direct prediction of eye location, has the best overall accuracy, with average errors

in the X and Z coordinate of eye location of less than 1 mm. The eye locations predicted by the IPM are slightly forward and below the observed, on average, with average errors of about 5 mm in each coordinate. The OPM is the least accurate of the three, with average errors of over 10 mm in each coordinate. Although some of the error in the OPM is due to the use of more restricted regression equations to predict ankle location and hip-to-H-point offset, the overall accuracy is not improved by using the more complex relationships (mean X error 11.3 mm, mean Z error -13.1 mm).

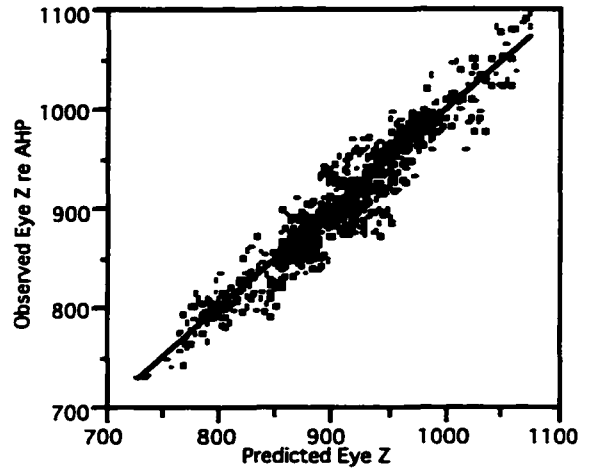
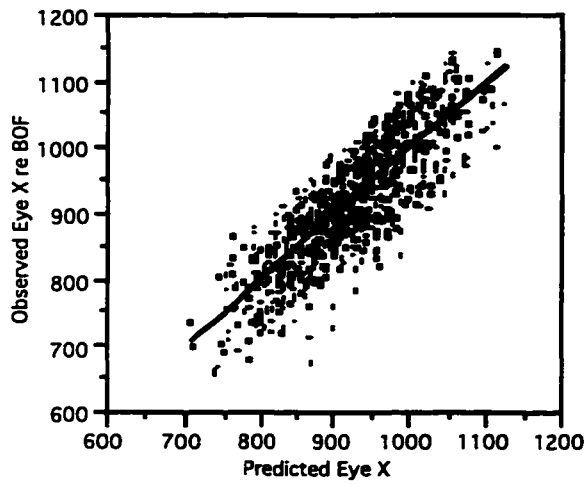
Table 5.11
Comparison of Model Predictions vs. Observed Eye Locations in Original Data

Measure	EyeX (mm)			EyeZ (mm)		
	CPM	IPM	OPM	CPM	IPM	OPM
Mean (Obs-Pred)	0.9	-5.1	9.9	-0.4	-5.7	-13.8
Standard Deviation (Obs-Pred)	50.5	52.6	51.4	19.9	19.8	21.5

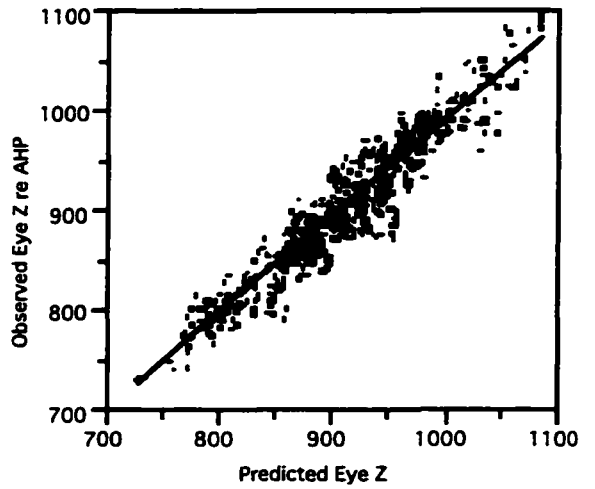
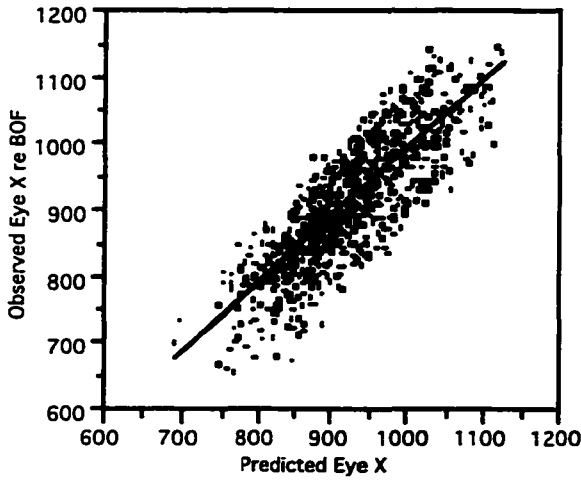
The standard deviation of the errors, a measure of the residual posture variance not accounted for by the model predictions, is similar for the three models, averaging about 51 mm for the X coordinate and about 20 mm for the Z coordinate. These values are similar to the root-mean-square-error values for the direct regression prediction of the eye location in Table 5.5, indicating that the prediction precision of each of these models is similar to the precision obtained by a direct prediction. In Figure 5.10, prediction errors are visible as deviations from the linear fit of predicted versus observed eye coordinate values.

As may be inferred from Figure 5.10, the eye locations predicted by the three models are highly correlated. In the original dataset, all intermodel correlations on the eye X and Z coordinates are greater than 0.96. The X and Z coordinates of the residual prediction errors in eye location are correlated with $r = -0.47$, -0.42 , and -0.43 for the CPM, IPM, and OPM, respectively. Figure 5.11 shows a plot of the CPM errors along

CASCADE



INDEPENDENT



OPTIMIZATION

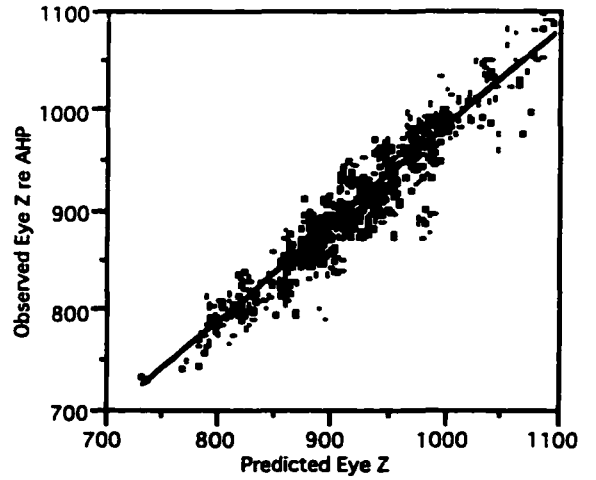
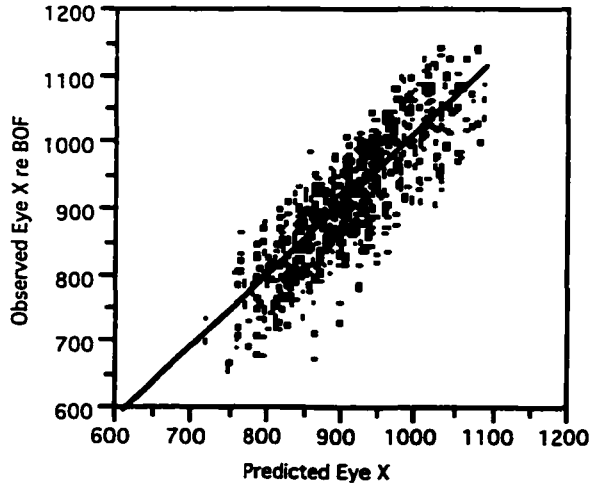


Figure 5.10. Observed eye locations and predictions using three models.

with a 95 percent density ellipse. The Z-axis errors are approximately normally distributed (Shapiro-Wilk W-test), but the X-axis errors have a broader-than-normal distribution. Nonetheless, the normal distributions overlying the marginal distribution plots in Figure 5.11 illustrate that the XZ-plane prediction error distribution can reasonably be approximated as bivariate normal.

The correlation among the errors is due to the effects of the principal ways in which the posture-selection behavior can deviate from the prediction. People can select a different seat position than predicted, or can choose a different recline angle. Both of these deviations tend to cause a movement of the eye along an inclined side-view path. Seat position prediction errors result in discrepancies along a path having the same slope as the seat track, and recline angle errors result in errors along a slightly more inclined path.

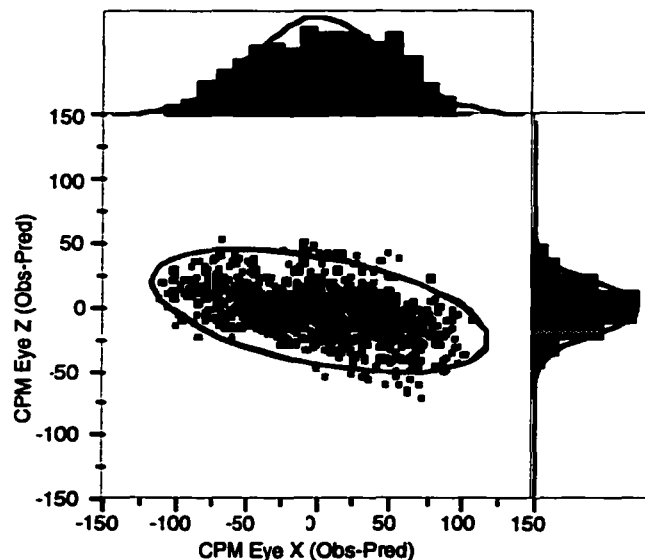


Figure 5.11. Observed-predicted eye locations for the CPM, showing marginal histograms and a 95 percent bivariate normal density ellipse. A normal distribution with equivalent variance is depicted overlying each histogram.

One important question concerning the prediction errors is whether the prediction precision varies substantially with the input variables. Is the prediction precision approximately the same for small people and large people, or for different seat heights? To address this issue, the subjects were divided into five stature groups using 100-mm

bins from 1550 to 1850 mm (three groups), and creating two groups from those with statures above 1850 and below 1550 mm. The number of subjects in each group ranged from 9 to 26. Table 5.12 lists the group definitions and the within-group error standard deviations. The error variance from the CPM was compared among the groups using Levene's test for homogeneity of variance. Levene's test is an ANOVA on the absolute differences between each observation and the group mean. No significant differences in variance were found among groups for X-coordinate errors, but there were small but significant differences in the distribution of Z-coordinate errors. However, the standard deviations in Table 5.12 indicate that there is not a consistent trend with body size, and the differences are small enough to be of minimal practical importance. Similar trends are observed for other variables (seat height, etc.) and the other models (IPM and OPM). These findings suggest that the precision of the model predictions can reasonably be approximated as constant throughout the range of the input data.

Table 5.12
Prediction Error Standard Deviations by Stature Group for CPM

Group	Stature Range (mm)	Subjects in Group	Eye X (Obs-Pred) Standard Deviation (mm)	Eye Z (Obs-Pred) Standard Deviation (mm)
1	<1550	11	48.9	16.0
2	1550 – 1650	13	47.2	18.5
3	1650 – 1750	26	50.5	22.4
4	1750 – 1850	9	55.9	16.2
5	>1850	9	47.7	21.2

The prediction precision can be assessed by constructing confidence intervals on the mean, based on the observed variance in the prediction errors. Assuming a bivariate normal distribution for XZ-plane errors, a $(1-\alpha)$ percent confidence ellipse on the mean is given by

$$(\mathbf{Y} - \boldsymbol{\mu})^T \boldsymbol{\Sigma}^{-1} (\mathbf{Y} - \boldsymbol{\mu}) = c \quad [5]$$

where Y is $\{x, z\}$, μ is the mean vector $\{\bar{x}, \bar{y}\}$, Σ is the covariance matrix, and c is a constant given by

$$c = \frac{2(n-1)}{n(n-2)} F_{\alpha, 2, n-2} \quad [6]$$

where n is the number of data points and $F_{\alpha, 2, n-2}$ is the α -th percentile of the F distribution with 2 and $n-2$ degrees of freedom (Box and Draper, 1987). The ellipse dimensions differ from the confidence intervals that would be constructed using the univariate approach based on the Student's t distribution, because the ellipse considers the joint probability of each coordinate value. Another, potentially more useful ellipse can be constructed that defines a region within which the next error observation would lie, with 95-percent probability. Using the convergence of the t distribution to the normal for large sample sizes, the ellipsoid is the 95-percent density ellipse for the bivariate normal distribution having the covariance matrix equal to the model-prediction error (sample) covariance matrix, and is shown in Figure 5.12.

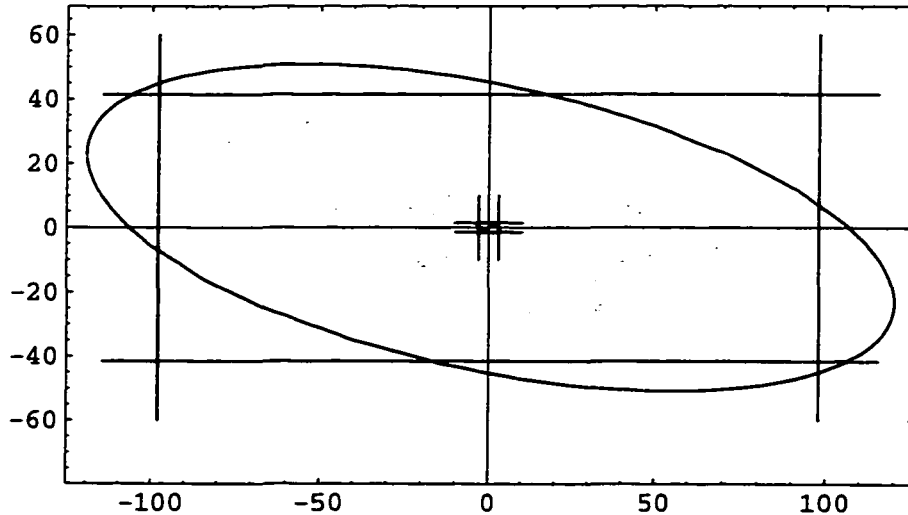


Figure 5.12. Illustration of CPM 95% confidence ellipsoids in the XZ (side-view) plane for the mean and individual observations of eye location. Lines indicate the 95% univariate confidence intervals for the mean and individual observations.

5.9 Model Assessment: Vehicle Data

A more important measure of the posture prediction model performance than the fit to the original data is the correspondence between the model predictions and the postures of drivers in actual vehicles. In a separate study, 120 men and women ranging in stature from 1441 to 1952 mm drove five vehicles over a 15-minute road route, adjusting the seat track position and seatback angle to obtain a comfortable driving posture. Each car was equipped with an automatic transmission and was tested with the seat track adjustment restricted to two-way (fore-aft) travel. After returning from the road route, the driver's preferred posture was recorded using a FARO coordinate measurement arm and procedures similar to those used in the laboratory (Chapter 2). Table 5.13 lists some of the characteristics of the vehicles. The vehicles were selected to represent a substantial part of the range of the interior geometry available in current passenger cars.

Table 5.13
Vehicle Characteristics

Vehicle	Seat Height (mm)	SWtoBOFX (mm)	Seat Cushion Angle (deg)
Plymouth Voyager	326	504	14.0
Chrysler LHS	250	597	17.7
Dodge Avenger	189	577	16.6
Jeep Grand Cherokee	298	607	11.3
Plymouth Laser	194	550	11.3

The posture-prediction models (CPM, IPM, and OPM) were exercised using the vehicle configurations and subject anthropometry. The resulting eye position predictions were compared with the observed eye positions to assess the model accuracy. Table 5.14 lists the means and standard deviations of the prediction errors by vehicle for each posture model.

Table 5.14
Comparison of Model Predictions vs. Observed Eye Locations in Vehicle Data:
Mean Observed minus Predicted (Standard Deviation)

Vehicle	EyeX (Obs - Pred) (mm)			Eye Z (Obs - Pred) (mm)		
	CPM	IPM	OPM	CPM	IPM	OPM
Voyager	0.7 (52.2)	-3.7 (53.9)	-1.2 (50.4)	-4.8 (20.6)	-11.2 (20.6)	-15.2 (20.4)
LHS	0.0 (46.5)	-4.7 (49.7)	9.2 (46.3)	-6.5 (18.1)	-9.2 (18.2)	-20.6 (18.3)
Avenger	2.5 (47.5)	1.5 (50.0)	20.0 (47.1)	-7.4 (18.8)	-11.3 (18.9)	-22.7 (19.7)
Jeep Grand Cherokee	5.9 (49.6)	-2.3 (50.6)	16.8 (50.3)	-13.6 (18.9)	-19.6 (18.8)	-22.9 (18.9)
Laser	8.7 (46.2)	-0.5 (46.7)	21.1 (45.0)	-2.2 (17.3)	-9.3 (17.5)	-24.9 (17.9)
Overall Mean	3.6 (48.4)	-1.9 (50.2)	13.2 (47.8)	-6.9 (18.7)	-12.1 (18.8)	-21.3 (19.0)
Dynamic Z Correction*	--	--	--	2.1	-3.1	-12.3
Overall Range	8.7	6.2	22.3	11.4	10.4	9.7

*Eye Z predicted location lowered by 9 mm (see text).

The CPM and IPM both predicted the mean eye location for the five vehicles with considerable accuracy. The predicted horizontal coordinate was within 10 mm in all cases, with average errors of 3.6 mm for the CPM and -1.9 mm for the IPM. On the vertical coordinate, the predicted mean eye locations were higher than observed in all cases. Pilot testing in three vehicles demonstrated that eye locations after the 15-minute drive were on average 9 mm lower than those measured immediately prior to the drive. The cause appears to be settling into the seat, rather than additional slumping, as the distance between the ASIS landmarks and the eye landmarks remained unchanged. Since the prediction models were generated from static, vehicle-mockup data, a 9-mm dynamic correction was made to the Z-coordinate predictions. With the correction, the average vertical error across vehicles is 2.1 mm for the CPM and -3.1 mm for the IPM. The range of prediction errors, a measure of the consistency of the models across vehicles, was under 10 mm for the X coordinate and about 10 mm for the Z coordinate for both the CPM and IPM. The OPM did not predict as accurately as the CPM and IPM, with average errors across vehicles of 13.2 and -12.3 mm, and ranges of 22.3 and 9.7 mm, for

the X and Z coordinates, respectively. The standard deviations of the errors, a measure of the individual prediction accuracy, were essentially identical to the standard deviations computed with the original vehicle mockup data, suggesting that the error distribution for the vehicle data is similar to that observed in the laboratory.

5.10 Discussion and Conclusions

Model Evaluation

Three models to predict driving posture were developed using posture data obtained in a laboratory vehicle mockup. The three models produce fairly similar predictions for the original data set, but the Cascade Prediction Model (CPM) and Independent Prediction Model (IPM) are more accurate than the Optimization Prediction Model (OPM) for predictions of vehicle postures. A good predictive model of driving posture will have a number of useful characteristics for any degree of freedom of interest. Taking the prediction of eye location as an example, the model will:

1. Be accurate and precise, on average, across vehicles, meaning that the mean predicted eye location will deviate only a small amount from the mean observed eye locations across vehicles. This implies both that the error in mean eye location prediction for each vehicle will be small, and also that the errors will offset so that, across vehicles, the average error is small.
2. Have the accuracy characteristics described in (1) for any population composition, e.g., for a group of small females or large males.
3. Have minimal error variance for individual predictions, meaning that the absolute deviations of individuals from the predictions for people with matching anthropometry on the key variables is small.

The CPM and IPM show good accuracy, based on criteria 1 and 2, but the error variance for individual predictions with all three models is fairly large (criterion 3). Individual prediction performance is constrained by the consistency of driving postures chosen by different people with similar anthropometry. In effect, the only opportunity for improving the model's ability to predict individuals is to add additional anthropometric descriptors as input to the models. However, such additions are not likely to be useful for general vehicle design, because the intended user population is anthropometrically

diverse, and hence cannot usefully be described by more than a few variables. For example, a vehicle that is to be driven by people from the 3rd to 97th percentiles of the U.S. population by stature will cover a similarly large range of other anthropometric variables of interest. Further, efforts to use additional measures such as arm or leg length have not yielded substantial improvements in prediction precision.

The observed error variance may be a measure of the variance in subject preference that cannot be attributed to useful subject descriptors and hence must be accounted for in predicting any individual's posture. The variance is large enough that the driving posture of an individual cannot effectively be predicted except within a large window. For vehicle design, this does not pose any particular problems, provided that the mean postures of population groups of interest can be accurately predicted, and the prediction error variance is kept always in mind. However, this finding indicates that a CAD manikin representation of a person sitting in a vehicle will be only one of a wide range of postures that a person with the specified dimensions might choose. The accommodation of people with diverse anthropometry will not be assessed accurately by a few manikin sizes, even if they are postured in ways that accurately represent the average postures of the corresponding anthropometric group.

The use of only a few anthropometric descriptors can cause seemingly anomalous results for extreme anthropometric cases. For example, using the CPM, a CAD human model configured with unusually short arms relative to other link lengths would not be predicted to sit any differently in the torso and legs. In relation to the potential occupant population, the variability in arm length is so closely related to stature that no relationship is found between posture and arm length that is not adequately predicted by stature. It is not possible to independently vary arm length experimentally, of course. Further, the utility of manipulating arm length independent of leg length is very limited, because these measures are highly correlated with each other and with stature in the population, and, for

individuals, the posture prediction variance is so large that meaningful evaluations are not possible.

A substantial advantage of the CPM over the IPM and OPM is that the accuracy of the former on the key posture variables of hip location and eye location is independent of the kinematic linkage of the human model with which it is used. With the IPM and OPM, the lengths of the body segments, particularly in the limbs, affect the predicted eye and hip locations. With the CPM, differences in limb segment scaling affect only the limb postures.

One of the substantial contributions of this work is the simplification of torso posture prediction by the use of empirical motion distribution parameters. The data demonstrate that torso recline can reasonably be reduced to a single degree of freedom while preserving the appropriate interrelation of the body segments as the recline angle is changed. This simplification makes possible the straightforward optimization method used with the OPM, and allows the CPM to accurately predict the manner in which torso segment orientations are affected by vehicle geometry. Although these small changes in spine flexion are of only minor importance for general accommodation applications, they may have importance for some comfort assessments and hence it is useful to have quantitative accuracy in the predicted spine movements.

OPM is dependent on the definition of the kinematic constraints (e.g., grip location) which must match those used in the original input set. More importantly, the accuracy of the OPM is strongly related to the range of vehicle conditions in the input data set. In particular, a smaller range of steering wheel positions relative to seat heights in the input data set will tend to cause greater weight to be put on deviations from the average elbow and knee angles relative to torso angles, since these angles are more strongly affected by steering wheel position than is torso angle. Another restriction is that some important factors, notably seat cushion angle, cannot be readily represented by

a kinematic constraint. It would be necessary to bias the optimization by altering the mean joint angles to account for seat cushion angle effects.

All of the models are dependent on accurate prediction of the offset vector between the hip and H-point. A previous study found that the H-point was a consistent predictor of hip location (constant offset) for people of various sizes in three seats (Manary et al., 1994), but the study was restricted to a single seat cushion angle and used imposed seatback angles with a single vehicle package. In the current study, the offset vector is affected substantially by several factors, most notably seat cushion angle. Considerably more research using different vehicle seats will be necessary to verify these relationships.

Restrictions and Limitations

There are important restrictions to the general application of these posture prediction models. In particular, the models are for use with seats that have two-way (fore-aft) seat-track adjustment and seatback angle adjustment, but without any seat height or seatpan angle adjustment. While the majority of production passenger cars still fall within this restriction, an increasing number are manufactured with height- or angle-adjustable seats. Further research will be necessary to expand the models to predict postures for vehicles with these seats. The models assume an automatic transmission (no clutch), which covers more than 85 percent of passenger cars sold in the United States. Recent research has suggested that drivers sit slightly further forward when driving a car with a manual transmission (Flannagan et al., 1996). The models also assume that seat track position is not censored, meaning that drivers are free to choose a fore-aft seat position without constraint from track travel limitations. The effects of censoring are generally important only for very large and very small people, but it is likely that the additional kinematic constraint changes posture adaptation.

The in-vehicle posture data used to evaluate the model performance were obtained from subjects after they returned from a fifteen-minute drive. Although the measured

postures probably represent the most prevalent, normal driving postures for these subjects, it is likely that they shifted their postures as they drove, so the results are not representative of all on-road postures. However, the variance associated with within-subject posture changes during the testing is likely to be very small relative to the between-subject variance and the effects of vehicle geometry.

The subjects whose postures were used to develop the model ranged in age from 21 to 75 years, but their behavior may not be representative of certain population segments, such as the very old or those with visual or other impairments. The short-duration sitting sessions used to develop the models also restrict the application of the models to prediction of short-term postures, although Reed and Schneider (1996) demonstrated that postures do not change substantially in long-term sitting.

Although the vehicle mockup testing leading to the development of these models was conducted without the use of seatbelts, the accuracy of the models in predicting in-vehicle postures, for which the drivers used the seatbelts, suggests that these restraints do not significantly affect posture. Observations of people selecting their driving postures in vehicles suggest that driving posture is generally selected before buckling the seatbelt.

The posture prediction models presented here do not include a number of additional factors that might affect driving posture. Restrictions to downward, forward, vision have been demonstrated to have negligible effects, within the range applicable to production vehicles (Chapter 4), but other vision restrictions could be important. For example, restrictions to lateral vision might cause posture changes. More research will be necessary to determine if these effects are important. The effects of headroom restriction have not been considered in the development of these models. For large drivers, particularly in sporty cars, headroom may have an important influence on posture. A large-scale study currently underway at UMTRI will determine the importance of headroom and restrictions to upward, forward vision on driving posture.

The current models consider only a single seat design factor, seat cushion angle. Previous research has shown that changes in seatback contour can have small but potentially important effects on lumbar spine flexion and the height of the eyes above the hips (Reed and Schneider, 1996). Seatback effects might account for some of the errors in the predictions of in-vehicle eye height. The effects of lumbar support prominence are not currently included in the posture prediction models because there is currently no suitable way of measuring seatback contour. However, a project is now underway to develop a new weighted manikin that will provide a useful measure of seatback contour, and will allow seatback effects to be included in the posture prediction models.

Conclusions

Whole-body posture driving postures can be predicted with considerable accuracy on average. Both the CPM and IPM predict vehicle postures with better accuracy than the OPM, but the CPM is preferred because the predictions of key degrees of freedom are independent from the kinematic model definition and linkage scaling. The model prediction errors are largely independent of body size and vehicle geometry, allowing a straightforward interpretation of prediction precision. The cascade model approach allows the most important degrees of freedom to be predicted directly, with reasonable accuracy on other degrees of freedom obtained using inverse kinematics assisted by motion distribution heuristics.

5.11 References

- Asano, H., Yanagishima, T., Abe, Y., and Masuda, J. (1989). *Analysis of primary equipment factors affecting driving posture*. SAE Technical Paper 891240. Warrendale, PA: Society of Automotive Engineers, Inc.
- Babbs, F.W. (1979). A design layout method for relating seating to the occupant and vehicle. *Ergonomics* 22(2): 227-234.
- Bohlin, N., Hallen, A., Runberger, S., and Aasberg, A. (1978). *Safety and comfort--Factors in Volvo occupant compartment packaging*. SAE Technical Paper 780135. Warrendale, PA: Society of Automotive Engineers, Inc.
- Box, G.E.P., and Draper, N.R. (1987). *Empirical model-building and response surfaces*. New York: Wiley and Sons, Inc.

- Dempster, W.T. (1955). *Space requirements of the seated operator: Geometrical, kinematic, and mechanical aspects of the body with special reference to the limbs*. WADC Technical Report 55-159. Wright-Patterson AFB, OH: Wright Air Development Center.
- Drillis, R., and Contini, R. (1966). *Body segment parameters* (PB174 945). University Heights, NY: New York University, School of Engineering and Science.
- Flannagan, C.A.C., Schneider, L.W., and Manary, M.A. (1996). Development of a new seating accommodation model. SAE Technical Paper 960479. In *Automotive Design Advancements in Human Factors: Improving Drivers' Comfort and Performance (SP-1155)*, 29-36. Warrendale, PA: Society of Automotive Engineers, Inc.
- Grandjean, E. (1980). Sitting posture of car drivers from the point of view of ergonomics. In *Human Factors in Transport Research. Volume 2 - User Factors: Comfort, the Environment and Behaviour*, ed. D.J. Osborne and J.A. Levis, 205-213. New York: Academic Press.
- Hammond, D.C., and Roe, R.W. (1972). *Driver head and eye positions*. SAE Technical Paper 720200. New York, NY: Society of Automotive Engineers, Inc.
- Judic, J.M., Cooper, J.A., Truchot, P., Effenterre, P.V., and Duchamp, R. (1993). *More objective tools for the integration of postural comfort in automotive seat design*. SAE Technical Paper 930113. Warrendale, PA: Society of Automotive Engineers, Inc.
- Manary, M.A., Schneider, L.W., Flannagan, C.C., and Eby, B.H. (1994). *Evaluation of the SAE J826 3-D manikin measures of driver positioning and posture*. SAE Technical Paper 941048. Warrendale, PA: Society of Automotive Engineers, Inc.
- Meldrum, J.F. (1965). *Automobile driver eye position*. SAE Technical Paper 650464. New York, NY: Society of Automotive Engineers, Inc.
- Phillipart, N.L., Roe, R.W., Arnold, A.J., and Kuechenmeister, T.J. (1984). *Driver selected seat position model*. SAE Technical Paper 840508. Warrendale, PA: Society of Automotive Engineers, Inc.
- Porter, J.M., Case, K., Freer, M.T., and Bonney, M.C. (1993). Computer-aided ergonomics design of automobiles. In *Automotive Ergonomics*, ed. B. Peacock and W. Karwowski, 43-77. London: Taylor and Francis.
- Rebiffe, R. (1980). General reflections on the postural comfort of the driver and passengers: Consequences on seat design. In *Human Factors in Transport Research. Volume 2 - User Factors: Comfort, the Environment and Behaviour*, ed. D.J. Osborne and J.A. Levis, 240-248. New York: Academic Press.
- Reed, M.P. and Schneider, L.W. (1996). Lumbar support in auto seats: conclusions from a study of preferred driving posture. SAE Technical Paper 960478. In *Automotive Design Advancements in Human Factors: Improving Drivers' Comfort and Performance (SP-1155)*, 19-28. Warrendale, PA: Society of Automotive Engineers, Inc.
- Reynolds, H.M. (1993). Automotive seat design for sitting comfort. In *Automotive Ergonomics*, ed. B. Peacock and W. Karwowski, 99-116. London: Taylor and Francis.

- Roe, R.W. (1993). Occupant packaging. In *Automotive Ergonomics*, ed. B. Peacock and W. Karwowski, 11-42. London: Taylor and Francis.
- Schneider, L.W., Langenderfer, L.S., Flannagan, C.A.C., and Reed, M.P. (1994). *Effects of seat height, cushion length, seatpan angle, and pedal force level on resting foot force and maximum comfortable displacement of the accelerator pedal*. Final Report. Technical Report UMTRI-94-38. Ann Arbor: University of Michigan Transportation Research Institute.
- Seidl, A. (1994). Das Menschmodell RAMSIS: Analyse, Synthese und Simulation dreidimensionaler Körperhaltungen des Menschen [The man-model RAMSIS: Analysis, synthesis, and simulation of three-dimensional human body postures]. Ph.D. dissertation, Technical University of Munich, Germany.
- Society of Automotive Engineers (1997). *Automotive Engineering Handbook*. Warrendale, PA: Society of Automotive Engineers, Inc.
- Verriest, J.P., and Alonzo, F. (1986). A tool for the assessment of inter-segmental angular relationships defining the postural comfort of a seated operator. SAE Technical Paper 860057. In *Passenger Comfort, Convenience and Safety: Test Tools and Procedures*, 71-83. Warrendale, PA: Society of Automotive Engineers.
- Weichenrieder, A., and Haldenwanger, H.G. (1985). *The best function for the seat of a passenger car*. SAE Technical Paper 850484. Warrendale, PA: Society of Automotive Engineers, Inc.
- Wolfram, S. (1996). *The Mathematica Book, Third Edition*. Champaign, IL: Wolfram Media.

CHAPTER 6

FORCES EXERTED ON THE STEERING WHEEL IN NORMAL DRIVING POSTURES

6.1 Abstract

The forces and moments exerted on the steering wheel in normal driving postures were measured for 10 men using an instrumented steering column in a vehicle mockup. The force and moment data for a range of elbow angles were analyzed to develop techniques for modeling the steering wheel interaction in biomechanical analysis of driving postures. The average vertical force applied by the hands to the steering wheel was 38 N (downward) and the average horizontal force was 8.4 N (rearward). A static biomechanical analysis indicated that drivers did not employ a loose-arm-hang strategy in interacting with the steering wheel, but rather generated extension moments at the elbow. Six of the ten subjects produced a net forward horizontal force on the steering wheel in at least one test condition, opposite of the expected rearward force. The findings suggest that drivers, when required to place both hands on the steering wheel, adopt a strategy that, on average, maintains lower flexion moments on the torso and lower grip forces than would be produced by alternative strategies.

6.2 Introduction

This study was conducted to determine the forces and moments that characterize the interaction between a driver's hands and the steering wheel in normal driving postures. This problem does not appear to have been addressed previously in the published literature. Woodson (1971) reviewed previous studies on control interaction and presented new data on the maximum control forces drivers can exert, but did not report normal resting forces. Sanders (1981) reported isometric hand forces exerted by

truck drivers on steering wheels, but also focused on maximal rather than resting-level forces.

This study addresses forces exerted by drivers in static driving postures with symmetrical hand positions, without the need to exert actual steering forces. This information is primarily useful for biomechanical modeling of the driver, but also provides some interesting insight regarding the tactics by which drivers maintain postural stability when sitting with both hands on the steering wheel.

6.3 Methods

Ten men participating in a larger study of driving posture sat in a partial vehicle mockup equipped with a six-axis load cell in the steering column. The mockup is an A-to-C-pillar passenger compartment from a 1993 Taurus sedan with a seat height (SAE H30) of approximately 270 mm. The standard Taurus seat includes a manually adjusted fore-aft seat track at a 6-degree angle to the horizontal and a manual seatback angle adjuster.

A six-axis, strain-gage load cell manufactured by JR3, Inc. is mounted rigidly to the steering wheel and the steering column just aft of the tilt-wheel mechanism. Figure 6.1 shows a detailed view of the load-cell and steering wheel geometry. The mounting of the load cell prevents the steering wheel from being rotated. The six load cell channels record forces and moments on three axes in a coordinate system aligned with the steering wheel. Data from the load cell were recorded using a personal-computer-based data acquisition system. The data were zeroed by subtracting readings obtained from the load cell without external loading.

Standard anthropometric measures were obtained from each subject. Table 6.1 summarizes the body size of the subjects, including several dimensions used for estimating the masses of the subject's upper extremities.

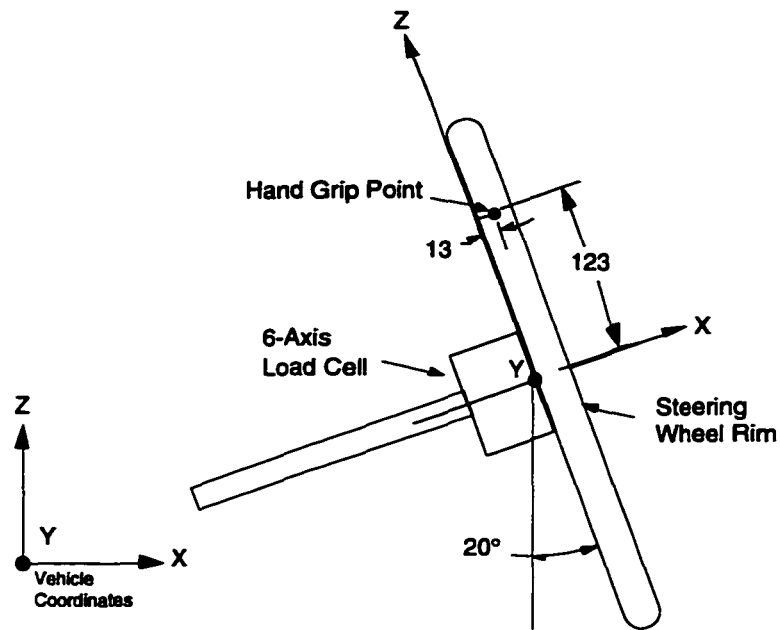


Figure 6.1. Load cell mounting in steering column and load cell coordinate system. Y axis in both systems is perpendicular into the page. Dimensions in mm.

Table 6.1
Subject Anthropometric Measures

Measure (mm or kg)	Mean	Standard Deviation
Stature	1729.2	51.3
Mass (kg)	78.6	7.3
Erect Sitting Height	906.8	35.4
Elbow Circumference	264.6	14.5
Hand Circumference	207.9	10.0
Biceps Circumference	305.7	24.7
Acromion-Radiale Length	324.1	25.2

The subject entered the mockup and selected a fore-aft seat position and seatback angle to find a “comfortable driving posture,” placing his hands on the steering wheel at the marked locations at approximately the 10-o’clock and 2-o’clock positions. The subject was asked to maintain this posture, looking straight ahead, while a 10-second sample at 10 Hz was recorded from the load cell channels. The signals were examined on the computer screen as they were collected to ensure that the load cell output was stable

during the trial. Trials with significant signal variability, indicating subject movement, were repeated and the original data discarded. While the subject maintained the posture, the orientations of the left forearm and arm relative to the horizontal were measured manually using an electronic inclinometer. To record the forearm orientation, the inclinometer was placed on an imaginary line connecting the center of the dorsal surface of the wrist with the palpated location of the lateral humeral epicondyle. Arm posture was recorded using the palpated locations of the surface landmarks at the lateral humeral epicondyle and the greater tubercle of the humerus. Figure 6.2 shows the definitions of the upper-extremity posture variables. Elbow angle, defined as the included angle between the arm and forearm, was used to represent the arm posture in the data analysis. Although the angle was measured in the plane formed by the arm and forearm, this plane was nearly vertical in all cases, allowing a planar analysis.

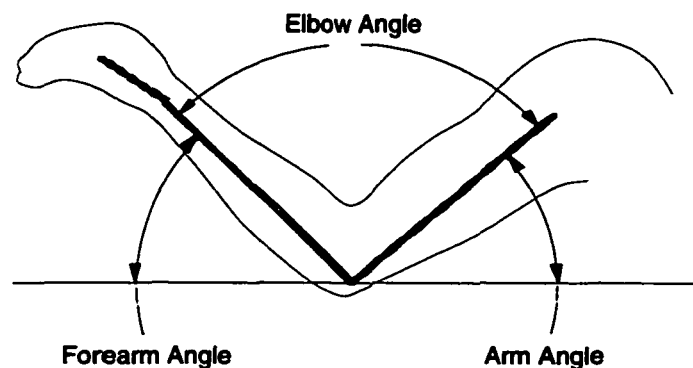


Figure 6.2. Upper-extremity posture variables.

Following the initial trial, the subject was asked to slide the seat forward slightly (one or two detents on the seat track) and to again find a comfortable driving posture without adjusting the seatback angle. The data-collection procedure was repeated at the new seat position. A total of 10 trials were conducted with each subject, using a variety of seat positions both forward and rearward of the subject's preferred seat position. The procedure resulted in data for a range of arm postures with the driver's preferred torso posture.

As part of another driving posture experiment with the same subjects (Chapter 7), muscle activity was measured at two sites on the right arm. As the subjects sat in their preferred driving postures, the steering wheel position was varied fore-aft, resulting in a range of elbow angles. Surface electromyography signals from the anterior deltoid and triceps regions of the arm were amplified and transformed using an analog root-mean-square filter with a 55-ms time constant. The mean of a 10-second sample at 100 Hz was computed for each electrode site at each of five steering wheel positions. These data were used in the current investigation to aid in the interpretation of the steering wheel force data.

6.4 Results

An initial step in the analysis was to determine if the subjects exerted significant moments on the steering wheel. Moments caused by uneven force application at the right and left hands could be observed directly in the X- and Z-axis moment data from the load cell. The mean and standard deviation of the load cell X-axis moment were -0.1 Nm and 0.35 Nm, respectively. Similarly, the moments on the load cell Z axis produced a mean of 0.0 Nm and a standard deviation of 0.93 Nm, indicating that subjects' hand forces were reasonably symmetrical. Further, the mean and standard deviation of force on the lateral (Y) load cell axis were -1.4 N and 2.2 N, respectively, indicating that there was minimal net lateral load on the steering wheel, as expected. These findings suggest that the steering wheel/hand interaction in this study can reasonably be examined using a side-view, planar analysis.

Since the hand grip position on the steering wheel was known, the Y-moment applied by the subject's hands to the steering wheel could be calculated. The diagram in Figure 6.3 shows that if the moment exerted by the hands is zero, the Y-axis moment measured by the load cell will be equal to the sum of the moments produced by the X- and Z-axis forces acting at the hand grip point. The average difference between the measured Y moment and the calculated moment due to the X and Z forces was 2.3 Nm

(standard deviation 0.7 Nm). This suggests that, on average, the subjects exerted a small moment on the steering wheel tending to rotate the wheel toward them around the lateral axis (clockwise in Figure 6.3). This is consistent with the informal observation that the pressure in the hand grip on the wheel tends to concentrate under the first and second fingers on the side of the wheel away from the subject, and under the base of the palm of the hand on the side of the wheel toward the subject. The result is a small positive moment on the steering wheel (M_{yh} in Figure 6.3).

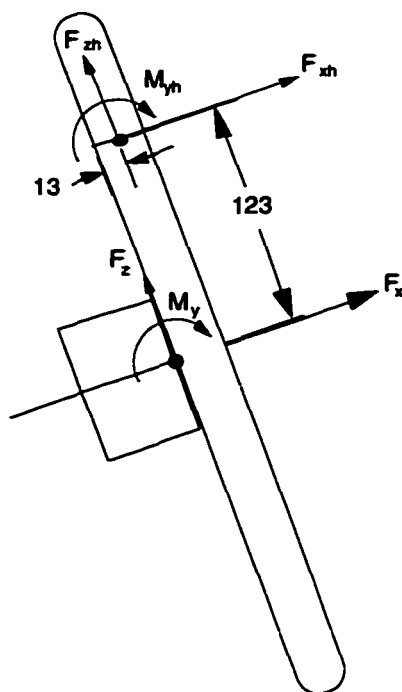


Figure 6.3. Diagram for determination of Y-axis hand moment. Forces and moments positive as shown. Subscript h denotes hand forces and moments.

For ease of presentation and interpretation of the results, the forces exerted on the steering wheel were expressed in the vehicle coordinate system, in which the X axis is horizontal and the Z axis is vertical. Table 6.2 presents summary statistics on the side-view forces and moments. On average, the subjects pushed downward on the steering wheel with about 38.2 N and pulled the wheel toward them with about 8.4 N. The horizontal force in the subjects' preferred driving postures (trial one) averaged 8.1 N at an average elbow angle of 126 degrees.

Table 6.2
Average Forces and Moments Exerted by the Hands On the Steering Wheel

Variable	Mean	Standard Deviation
F_x^*	8.4 N	16.5 N
F_z^{**}	-38.2 N	7.5 N
M_y	2.3 Nm	0.7 Nm

* Positive F_x is pulling on wheel, from driver's perspective.

** Negative F_z is pushing downward on the wheel, from the driver's perspective.

Figures 6.4, 6.5, and 6.6 show the F_x , F_z , and M_y data for all subjects, along with second-order polynomial fits to each subject's data. The second-order fit was chosen because it conveyed with reasonable accuracy the trends in most subject's data. The extent of each fit curve indicates the range of elbow angles in the subject's data. The vertical force does not show a significant effect of arm posture, and the Y-moment data appear to be relatively constant across elbow angles. However, Figure 6.4 suggests a relationship between the horizontal force and elbow angle, but most of the apparent relationship arises from the negative force values, which were generally measured at elbow angles exceeding 120 degrees. These negative values indicate that some subjects began to push against the steering wheel when their elbows were more extended. Six of ten subjects produced a net forward force on the steering wheel in at least one test condition. One subject pushed against the wheel in all conditions. Three subjects pushed against the wheel in their preferred driving posture (the first trial). As Figure 6.4 makes clear, the subject's horizontal forces became more varied at larger elbow angles, suggesting that the subjects' posture stabilization tactics diverged when the steering wheel was further away.

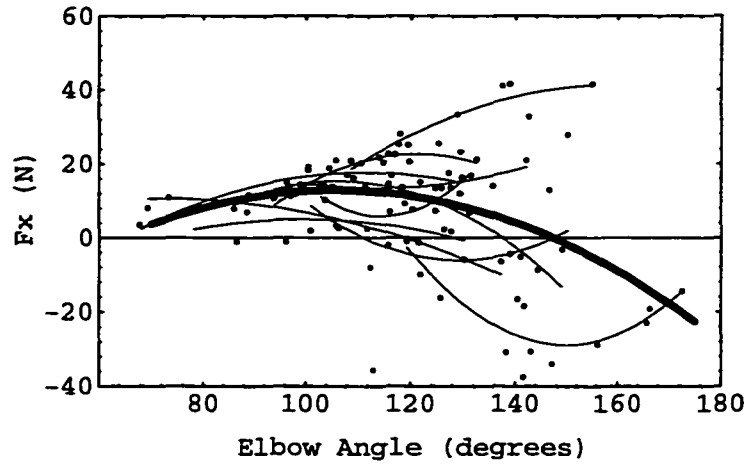


Figure 6.4. Horizontal force on the steering wheel for 10 subjects. Positive values indicate pulling on the steering wheel from the subject's perspective. Thin lines are second-order fits to each subject's data. Thick line is second-order fit to aggregate data.

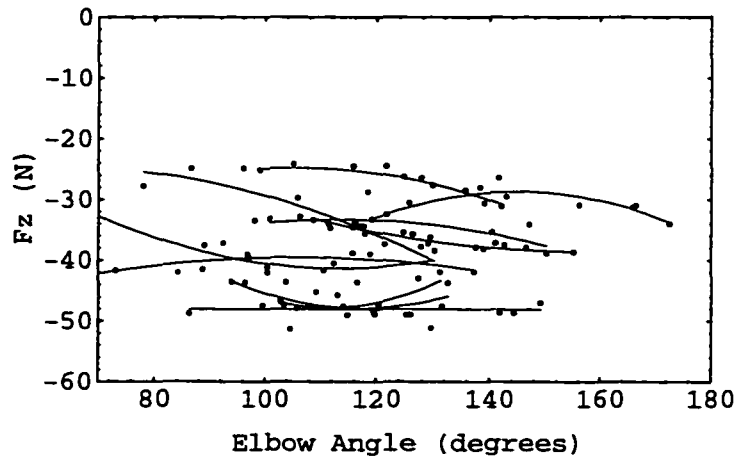


Figure 6.5. Vertical force on the steering wheel for 10 subjects. Negative values indicate downward force on the steering wheel. Lines are second-order fits to each subject's data.

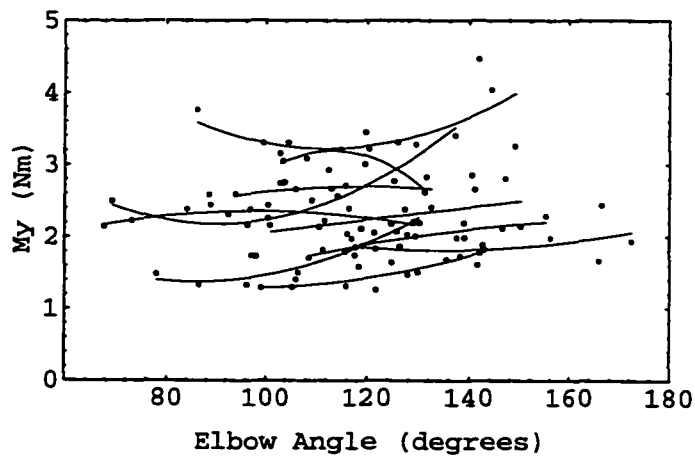


Figure 6.6. Y-axis moment on the steering wheel for 10 subjects. Positive values indicate moments tending to produce clockwise rotation of the wheel as viewed in Figure 6.3. Lines are second-order fits to each subject's data.

A planar biomechanical model of the upper extremity was developed to assist in the interpretation of the data. The model, depicted schematically in Figure 6.7, consists of rigid hand, forearm, arm, and thorax segments, connected by one-degree-of-freedom joints. The locations of the centers of mass relative to the segments were developed from the interpretation of data from McConville et al. (1908) by Robbins (1985). Hand-, forearm-, and arm-segment masses for each subject were estimated from subject anthropometric data using equations provided by McConville et al. (1980). The segment lengths for each subject were calculated using joint-location estimation techniques reported in Chapter 2.

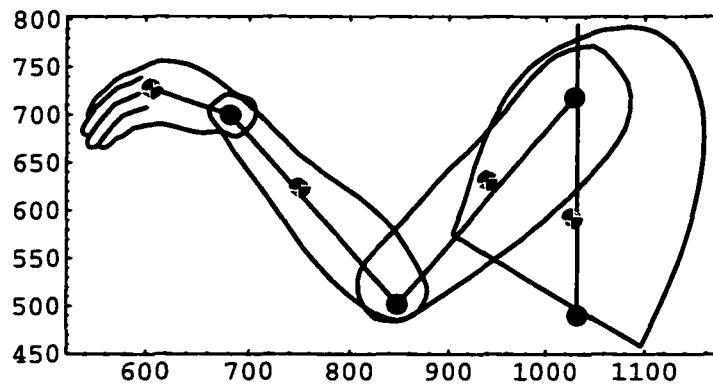


Figure 6.7. Schematic of planar, rigid-body upper-extremity model (scale in mm).

An initial simulation was conducted to predict the steering wheel forces that would result if drivers did not supply active moments at the hand, elbow, or shoulder, i.e., if they let their arms hang loosely between the shoulders and wheel. A pin joint at the hand center of mass (no transmitted moment) simulated the hand grip on the steering wheel. The model segment lengths and segment masses were set equal to the mean values for the ten subjects, summarized in Table 6.3.

Table 6.3
Estimated Mean Segment Lengths and Masses

Segment	Length (mm)	Mass (kg)
Hand	80	0.52
Forearm	259	1.52
Arm	283	1.86

The hand grip point and shoulder were set in a horizontal line. The hand position relative to the shoulder was then translated to produce a range of elbow angles, and forces at the hand grip were calculated. The simulated vertical force on the steering wheel (multiplied by two to reflect the forces generated by both arms) is shown in Figure 6.8, along with the subject data from Figure 6.4. The loose-arm-hang simulation predicts horizontal (pulling) hand forces on the steering wheel that are greater than those observed. The simulated horizontal force on the steering wheel also rises sharply as the elbow angle increases, in contrast to the trend in the measured forces. The difference between the simulation results and the data suggests that the subjects supported their upper extremities in part by moments at the shoulder and elbow. For several subjects, these moments were large enough to result in a net forward force against the steering wheel.

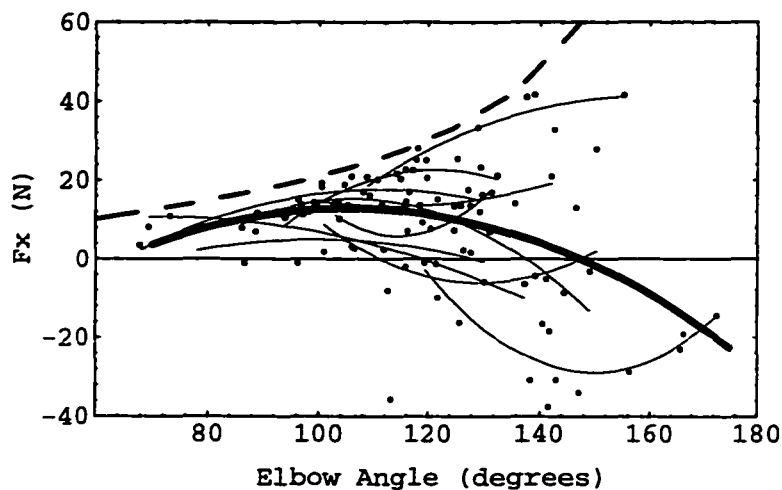


Figure 6.8. Simulated horizontal forces on the steering wheel from both arms for loose-arm-hang (dashed) along with subject data from Figure 6.4.

The elbow and shoulder moments that would be required to produce the observed average steering wheel forces and moments were calculated from the model. Force values as a function of elbow angle obtained from the second-order polynomial fit to the aggregate horizontal force data were applied to the hand grip point, along with the average observed vertical force of 38 N and the average grip moment of -2.3 Nm. (Note

that the signs are reversed compared to Table 6.2 because these forces are applied to the hand.) The net moments required for static equilibrium were calculated for the elbow and shoulder joints for a range of elbow angles. Figure 6.9 shows the predicted elbow and shoulder moments for one limb. The shoulder moment remains fairly constant in flexion, indicating that the shoulder is helping to support the upper extremity. At the elbow, the moment is minimal until the elbow angle exceeds about 115 degrees, after which it becomes positive, indicating a net extension moment at the elbow.

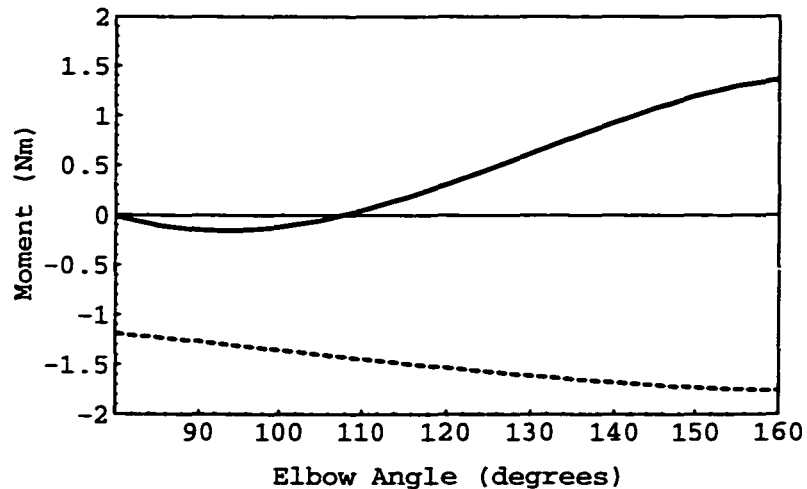


Figure 6.9. Predicted elbow (—) and shoulder (- - -) moments when average observed steering wheel forces are applied to the model of average upper-extremity segment lengths and masses (single arm). Negative shoulder moment indicates a flexion moment. Positive elbow moment indicates an extension moment.

The predicted net extension moment at the elbow should be accompanied by muscle activity in the elbow extensors, namely the triceps. Figure 6.10 shows a plot of the surface electromyography (SEMG) data collected from each subject at 5 different elbow angles, along with second-order curve fits. Although there is considerable variance in the data, the trends suggest increasing muscle activity with increasing elbow angle, consistent with the results of the simulation. SEMG from the anterior deltoid showed low levels of muscle activity and no trends with elbow angle.

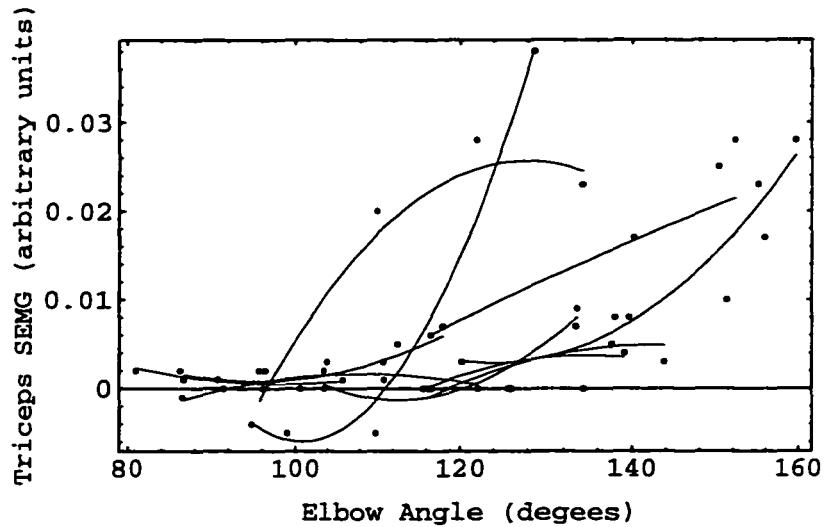


Figure 6.10. Triceps muscle activity versus elbow angle (five data points per subject), including second-order curve fits to each subject's data. Data are zeroed to the levels measured with the subject's hands resting on his thighs, and are displayed in arbitrary units linear in RMS SEMG.

One reason that drivers may choose to push against the steering wheel when sitting with large elbow angles is to reduce the moment applied by the upper extremities to the thorax. In a typical driving posture, the shoulder (glenohumeral) joints are located almost directly above the T12/L1 joint at the base of the thorax (Robbins 1985). As a consequence, vertical forces applied by the arms to the thorax at the shoulders do not result in appreciable thorax moments. However, horizontal forces applied at the shoulder act with a moment arm of about 228 mm about the T12/L1 joint for the average body dimensions of the current subjects (Robbins, 1985). Hence, the horizontal force and moment applied at the shoulder are the two primary determinants of the contribution of the upper extremities to the net moment at the base of the thorax.

With a loose-arm-hang interaction, no moment is generated at the shoulder, but large horizontal forces develop at the hands and shoulders with large elbow angles, as shown in Figure 6.8. Figure 6.11 illustrates the large resulting increase in the portion of thorax moment due to the upper extremities. In contrast, pushing against the steering wheel causes a net positive thorax moment, countered in part by the negative moment generated by the shoulder flexors. The solid line in Figure 6.11 illustrates that one effect

of the average measured hand forces on the upper-extremity model is to maintain the net forward thorax moment due to the upper extremities at a level less than about 6 Nm. The difference in hand force tactics produces substantial differences in thorax moment at elbow angles larger than about 115 degrees.

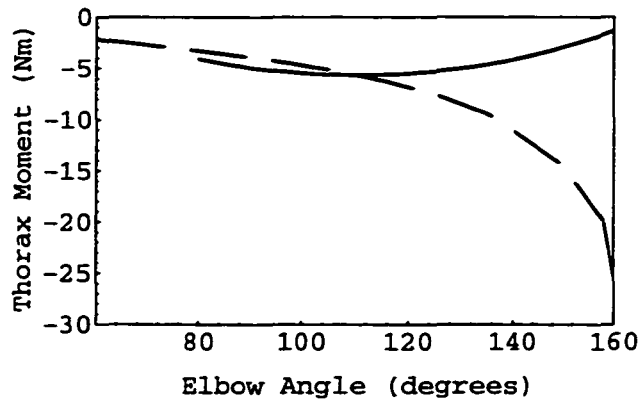


Figure 6.11. Comparison of thorax moments due to upper extremities in loose-arm-hang simulation (—) and in simulation with average measured hand forces (---). Negative moment is a forward moment on the thorax (counter-clockwise in Figure 6.7).

6.5 Discussion and Conclusions

This small-scale study was primarily intended to develop an understanding of the manner in which drivers interact with the steering wheel in normal driving postures and to facilitate the development of biomechanical models of the driver. Ten midsize male subjects exerted an average downward force on the steering wheel equal to about 38 N and exerted a pulling force on the steering wheel of about 8 N over a range of elbow angles. The average total upper extremity weight for these subjects was 38.3 N per limb, indicating that the steering wheel supported about half of the upper-extremity weight, on average. The average horizontal force was about ten percent of the upper-extremity weight.

Unexpectedly, a majority of subjects exerted a net pushing force on the steering wheel as the elbow angle increased beyond 120 degrees. A comparison of the data with the predicted forces for a loose-arm-hang steering wheel interaction suggests that the subjects were actively supporting their extremities with moments at the shoulder and

elbow even at smaller elbow angles. The results of biomechanical simulations indicate that small extension moments at the elbow account for the net pushing force on the steering wheel. Surface electromyography data from a range of elbow angles in another driving-posture experiment with the same subjects (Chapter 7) shows increasing levels of triceps activity at higher elbow angles, consistent with the steering wheel force and simulation observations.

This study is limited by the small sample size and the relative homogeneity of the subject pool. Further, the experiments were conducted using a single seat height and a fixed, subject-selected seatback angle. Different seatback angles and other differences in vehicle or seat geometry may affect the steering-wheel interaction. Elderly drivers, or those who have reduced upper body strength, may also interact differently with the steering wheel than these subjects. Because the forces were measured in a laboratory vehicle mockup without an actual driving task, the forces may not be generally representative of forces that would be exerted in vehicles during actual driving. However, the measurements demonstrate that the steering wheel interaction can be fairly complex.

In choosing to support their postures in part with elbow extension moments, drivers are apparently trading off the increased discomfort that might be associated with continuous, low-level triceps activity with reductions in other muscle activity requirements. The observed interaction strategy reduces the net forward moment on the thorax, potentially reducing back extensor activity, and also reduces grip strength requirements. At elbow angles greater than about 115 degrees, the net moment acting at the base of the thorax due to forces and moments at the shoulder in the loose-arm-hang simulation diverges from the thorax moment predicted using the measured hand-force data. At the subject's mean preferred elbow angle of 131 degrees, the estimated thorax moment due to the upper extremities is about 50% of the moment predicted for the loose-arm-hang interaction. It is possible that the steering-wheel-pushing tactic is preferred by

some drivers because it reduces the spine extension moments required to stabilize the thorax with extended-elbow postures. More research will be necessary to determine if this steering-wheel-interaction pattern is observed for torso postures other than the driver's preferred recline.

6.6 References

- McConville, J.T., Churchill, T.D., Kaleps, I., Clauser, C.E., and Cuzzi, K. (1980). *Anthropometric relationships of body and body segment moments of inertia*. Report no. AMRL-TR-80-119. Wright Patterson Air Force Base, OH: Aerospace Medical Research Laboratories.
- Robbins, D.H. (1985). *Anthropometric specifications for mid-sized male dummy, Volume 2*. Final report DOT-HS-806-716. Washington, D.C.: U.S. Department of Transportation, National Highway Traffic Safety Administration.
- Sanders, M.S. (1981). Peak and sustained isometric forces applied to a truck steering wheel. *Human Factors* 23(6): 655-660.
- Woodson, W.E. (1971). *Motor vehicle driver eye position and control reach anthropometrics. Volume 1: Static eye position, control reach and control force studies*. Report DOT HS-800-618. Washington, D.C.: U.S. Department of Transportation, National Highway Traffic Safety Administration.

CHAPTER 7

BIOMECHANICAL ANALYSIS AND PREDICTION OF NORMAL AUTOMOBILE DRIVING POSTURE

7.1 Abstract

A quantitative, biomechanical model of driver posture-selection behavior is presented in which the driver trades off static muscle exertion with the physical requirements of the driving task. The driving postures and postural muscle activity of ten men were recorded in a laboratory vehicle mockup using five different seatback angles and two different sitting procedures. The effects of perturbing the driver's preferred head and hand positions were also recorded. The analysis supports the hypothesis that, on average, drivers select the posture with the highest eye height above the hips that can be maintained without substantial back extensor exertion, and choose head and neck postures to reduce neck muscle exertion. The findings demonstrate the kinematics of the spine during recline motions induced by changes in seatback angle, and suggest that passive flexion stiffness in the lumbar region of the torso may help to stabilize the thorax in driving postures.

7.2 Introduction

Automobile driving is one of the most common interactions with a workspace that has been designed using ergonomic tools. The layout of the vehicle interior, including the control, seat, and mirror locations, is guided by statistical models based on several decades of investigation (Roe, 1993). The standard vehicle design tools, documented in Society of Automotive Engineers Recommended Practices (SAE, 1997), are task-oriented percentile models that predict parameters of the distributions of particular driving posture characteristics of interest. These practices, and more recently developed posture

prediction methods (Chapter 5), predict how and where a driver will sit, but do not provide any insight into *why* they choose particular postures. This research presents laboratory investigations and biomechanical simulations leading to the development of a quantitative model of the process by which drivers select torso, head, and neck postures.

Figure 7.1 shows a schematic of the proposed posture-selection process. Driving requires a continuous view of the environment surrounding the vehicle and the ability to manipulate the hand and foot controls, physical requirements that impose substantial kinematic restrictions on driving posture. The body dimensions and physical capabilities of a driver interact with the kinematic constraints of the task to determine a range of feasible driving postures. Drivers do not select postures randomly within this range, but rather have distinct posture preferences. Some of these posture characteristics, for example, fore-aft hip location, can be explained well by a combination of anthropometric variables and vehicle dimensions (Flannagan et al., 1996; Chapter 3). Torso posture, however, is poorly predicted by any conventional anthropometric variables, and is only slightly affected by vehicle and seat geometry, when drivers are

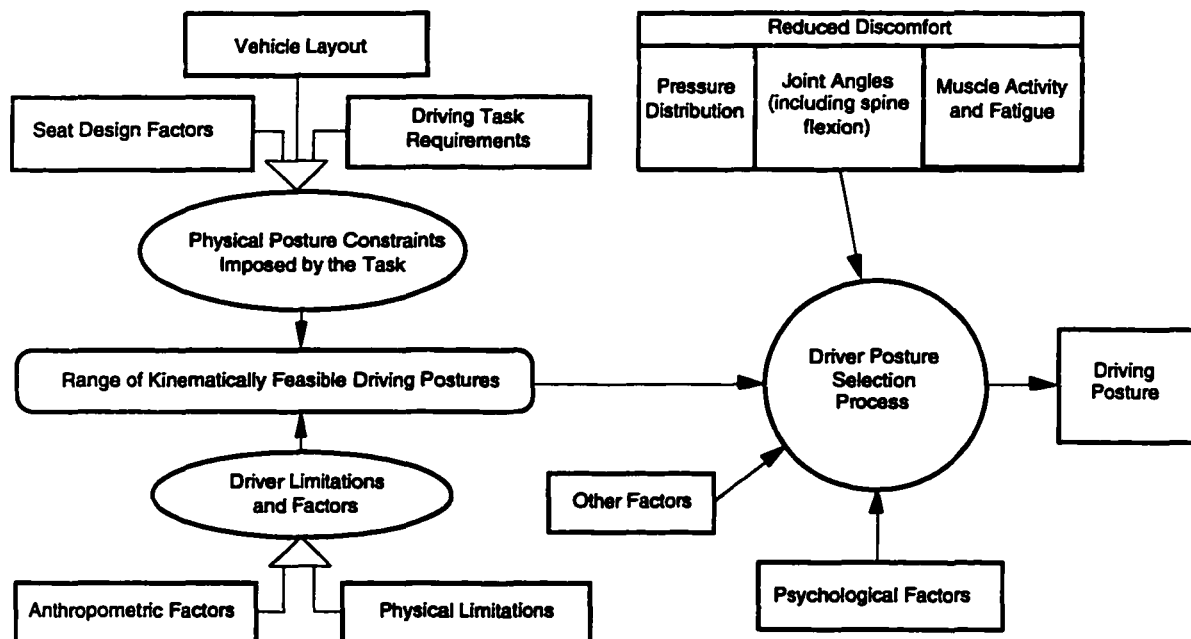


Figure 7.1. Schematic of proposed posture selection process.

free to adjust the seatback angle (Chapter 3; Reed and Schneider, 1996). Further, torso posture varies substantially among drivers, and yet is fairly consistent for an individual driver (Chapter 3, Chapter 4). The experimental evidence indicates that drivers have a distinct preference for torso posture that is only slightly affected by changes in vehicle and seat geometry. The focus of this research is on the process by which drivers select their torso, head, and neck postures.

In the proposed model, the driver is assumed to a torso posture that minimizes the static muscle exertion required to maintain the posture. The relationships between muscle activity and posture have been examined in many ergonomic studies relating to general seating situations (see Chaffin and Andersson, 1991 for a review), but relatively few studies have examined muscle activity in driving postures (Andersson et al., 1974b; Hosea et al., 1986; Sheridan et al., 1991). In general, low muscle activity is assumed to be a desirable attribute of work postures, and seat designs and orientations that produce lower muscle activity levels are recommended (Andersson et al., 1974b; Hosea et al., 1986). Sheridan et al. (1991) found evidence of fatigue in postural muscle activity during four-hour driving sessions. Other researchers have documented fatigue associated with sustained, low-level static exertions (Jorgensen et al., 1988), suggesting that driving postures with less muscle activity may be less fatiguing and more comfortable, particularly for long-duration driving.

The previous research on muscle activity in seated postures has demonstrated that muscle activity in the lumbar and thoracic regions of the back decreases to low, near-resting levels as the seatback is reclined (Akerblom, 1948; Andersson et al., 1974a, 1974b; Floyd and Silver, 1955; Hosea et al., 1986). Reductions in lumbar spine flexion associated with changes in lumbar support have relatively small effects on back muscle exertion. For near-vertical seatback angles, decreasing lumbar spine flexion tends to increase back muscle exertion (Andersson et al., 1974a), while increased lumbar support prominence, assumed to reduce lumbar spine flexion, decreases muscle activity at more

reclined seatback angles (Andersson et al., 1974a, 1974b; Hosea et al., 1986). Cleaver (1954), while presenting no data, used a biomechanical analysis to suggest that discomfort in vehicle postures could be reduced by designing seats to support postures that required no static muscle exertion.

There are two important limitations to existing research on trunk muscle activity in sitting for application to driving postures. First, the postures associated with the muscle activity measurements have generally not been characterized in detail (Andersson et al., 1974b; Hosea et al., 1986; Sheridan et al., 1991). Recent research has demonstrated that, in driver seats, the torso does not recline with seatback angle as a unit, but rather experiences changes in spine flexion as the seatback angle is changed (Manary et al., 1994; Chapter 3). Seatback angle is, therefore, not an adequate measure of torso posture for vehicle seats without addition description of the relationship between seatback angle and posture.

Second, testing has been conducted using the seatback angle as a test variable, rather than as a dependent measure. Andersson et al. (1974b) in testing in a driver seat, used seatback angles of 0, 10, 20, and 30 degrees with respect to vertical, while Hosea et al. (1986) used 10, 20, 30, and 40 degrees. The postures at seatback angles preferred by the drivers, and muscle activity in those postures, were not reported in either study. Almost all current passenger cars are equipped with reclining driver seatbacks, which allow the sitter to obtain posture support in any of a wide range of torso postures, so any particular imposed seatback angle may have a different relationship to preferred seatback angles for different drivers. While the previous research demonstrates well the effects of changes in seatback orientation on muscle activity, it does not illuminate how drivers use seatback angle adjustment in selecting their postures, and the relationships between that adjustment and muscle activity.

In other areas of biomechanical ergonomics, researchers have suggested muscle-activity related criteria as part of schemes to predict the muscle recruitment strategies

associated with various work tasks and postures. Researchers have proposed that muscle recruitment strategies follow a global optimization model (Crowninshield and Brand, 1981). Bean et al. (1988) proposed an optimization-based procedure for allocating muscle effort in lifting tasks. There is an intuitive appeal to the idea that postures and movements should be performed in such a manner that the effort expended, whether in terms of muscle force, stress, or energy, is minimized. However, it has been demonstrated that muscle recruitment patterns, particularly in the trunk, often do not follow simple minimization criteria for a range of lifting-type tasks. In particular, concurrent contraction in antagonists and the involvement of muscles with a range of efficacies for a particular movement have been observed, and new models accounting for these relationships have been developed (Nussbaum, 1994; Raschke, 1994).

In spite of the known limitations of simple optimization criteria for predicting muscle recruitment patterns in lifting tasks, the less-strenuous seated driving task may be amenable to a simpler analysis. In this research, muscle activity reduction is proposed as a general selection criterion for driving postures. Within the constraints of the task, the chosen posture is hypothesized to be the one requiring the least muscle exertion. This hypothesis will be refined further in relation to the specific considerations and restrictions of the driving task, but the central premise is that the reduction of static muscle exertion is of paramount importance in driving posture selection.

The advantages of muscle activity reduction are a decrease in metabolic cost, avoidance of fatigue, and the reduction in control requirements. A posture that is maintained through static muscle exertion will eventually lead to fatigue in the involved muscles, even at low levels of exertion (Jorgensen et al., 1988). While metabolic cost may not be an important issue for seated postures, the control requirements for an actively maintained posture may be significant, particularly in a moving vehicle environment. If a posture is maintained primarily through active muscle exertion, the

muscle forces must be modulated dynamically as the postural loads change due to accelerations transmitted through the seat.

One immediate objection to a muscle-activity reduction criterion for posture selection is that even a casual observer can note muscle activity requirements in typical driving postures. Maintaining the head in an alert posture without external support clearly requires dynamic muscle control, as does manipulating the steering wheel with the hands and operating the pedals. These observations prompt a necessary refinement of the hypothesis to suit the driving task. Specifically, the chosen posture of the torso, neck, and head is hypothesized to be the posture that best meets the task objectives while requiring muscle exertion that is as low as possible among the feasible postures. Among the kinematically feasible driving postures, some postures are better than others with respect to the requirements of the driving task. Postures that allow better vision to the environment and displays, and postures that allow better reach for manipulation of the controls, are preferred. In general, more upright postures with higher eye locations relative to the hips and greater forward reach will be preferred from the standpoint of task performance. In contrast, more reclined postures with direct support for the entire body will allow minimal muscle activity.

A conceptual illustration of the proposed torso posture selection process is as follows. The driver starts very reclined, with support for the entire back and head. No muscle activity in the trunk or neck is required to sustain the posture. However, the task requirements are poorly met, as the driver cannot see the road in front of the vehicle and cannot readily manipulate the steering wheel. As the seatback is moved to a more upright angle, the head is no longer supported by the headrest, but the suitability of the posture for the driving task improves continuously. When the driver is able to see the road in front of the vehicle and manipulate the steering wheel, the posture becomes feasible for driving. At some point in the movement toward an upright posture, the driver will begin to require thoracolumbar extensor muscle activity to maintain the torso posture. Previous

research suggests that this transition point occurs when the seatback is somewhere between 20° and 30° with respect to vertical (Andersson et al., 1974a, 1974b). The current model proposes that drivers will select postures at this transition point, because these postures are the best tradeoff between the task requirements and static muscle exertion.

This general hypotheses leads to some specific predictions concerning muscle activity in driving postures:

1. Driving postures will be characterized by near-resting levels of thoracolumbar extensor, neck flexor, and neck extensor muscle activity (<10 percent of normalized maximal exertion).
2. Perturbing driving postures toward more upright postures will cause an increase in thoracolumbar extensor activity (>10 percent of normalized maximal exertion).
3. Perturbing driving postures toward more reclined postures will result in the same low levels of thoracolumbar extensor activity measured in preferred postures (<10 percent of normalized maximal exertion).
4. Perturbing head and neck posture away from the preferred posture will cause increases in neck muscle activity.

Expressing the overall concept as a single predictive hypothesis,

5. Driving posture is predicted to be the posture that is kinematically consistent with the task requirements and has the highest eye location with respect to the hips that can be obtained while thoracolumbar extensor activity is near-resting levels.

In this study, these hypotheses concerning posture selection behavior were tested by observing the effects of perturbing drivers' preferred postures. The postures and muscle activity of ten male subjects were measured at five different seatback angles, centered on their preferred seatback angles. Preferred driving postures were measured along with postures obtained using a sitting procedure intended to minimize lumbar spine flexion. Preferred head and hand positions were also perturbed to determine the effects on muscle activity.

The first step in the analysis of data from the study was the determination of the effects of the test variables on posture (Section 7.4). The experimental muscle activity

data were then assessed in relation to the experimental hypotheses and simulation findings (Section 7.5). Finally, a biomechanical model of the driver was developed to facilitate the exploration of the hypotheses and the interpretation of the data (Section 7.6). The findings were assessed to evaluate the validity of the proposed model of posture-selection behavior.

7.3 Methods

Ten male drivers ranging in age from 21 to 50 years were selected to participate in the study. Table 7.1 summarizes a number of anthropometric measures taken from each subject. These limb dimensions were used to estimate body segment masses for biomechanical modeling (Section 7.6).

The subjects' driving postures were recorded using a Science Accessories Corp. GP8-3D sonic digitizer equipped with a measuring probe. The experimenter palpated body landmarks and recorded their positions individually. The body landmarks and posture representation methods are reported elsewhere (Chapter 2).

Table 7.1
Subject Anthropometric Measures

Measure (mm or kg)	Mean	Standard Deviation
Stature	1729.2	51.3
Mass (kg)	78.6	7.3
Erect Sitting Height	906.8	35.4
Elbow Circumference	264.6	14.5
Hand Circumference	207.9	10.0
Biceps Circumference	305.7	24.7
Acromion-Radiale Length	324.1	25.2

Vehicle sitting trials were conducted using a laboratory vehicle mockup, shown in Figure 7.2. The specially modified seat includes a manual fore-aft seat adjuster on a 3-degree track and a motorized seatback recline adjuster. The seat is equipped with an adjustable lumbar support that was set to a 35-mm prominence, measured relative to the



Figure 7.2. Laboratory vehicle mockup.

flat seatback (Reed and Schneider, 1996). The seat height (SAE H30) is 334 mm (see Appendix A for a discussion of the SAE terminology). The center of the steering wheel is 709 mm above the heel surface, and the steering wheel fore-aft position is adjustable over a wide range using a motorized control. A simplified instrument panel is located in front of the steering wheel. The accelerator pedal and brake pedal are located in typical positions relative to the seat and steering wheel and have realistic travel.

Each subject's posture was recorded in a laboratory hardseat that allows access to the thoracic and lumbar spinous processes. These data are used in conjunction with landmarks on the upper thorax to estimate the location of the T12/L1 joint when the thoracic spinous processes are not accessible (Chapter 2). For each subject, body landmark data from a relaxed standing posture were also available from another study. Standard anthropometric data and measures from toe-touch and leg-raise flexibility tests were obtained.

Each subject's muscle activity was monitored at seven body regions using surface electromyography (SEMG). Self-adhesive, pre-gelled infant ECG electrodes (Baxter Plia-Cell) were located in pairs on the right side of the body after cleaning and lightly abrading the skin at each site. Electrodes were placed on the subject's back 50 mm lateral to the midline at the L3, T12, and T8 levels, as shown in Figure 7.3. An electrode pair was located adjacent to the spine at about the C5 level, and on the anterior neck over the sternocleidomastoid. Interelectrode spacing for each pair was approximately 40 mm. Electrodes were positioned over the maximum prominence of the anterior deltoid and over the triceps at approximately the middle of the humerus. A ground electrode was located over the right acromion process of the scapula. The electrodes were connected to preamplifiers on a fabric belt worn by the subject, which were in turn connected to an amplifier and filter unit that applied a total gain of 2000 and an analog root-mean-square (RMS) filter with a time constant of 55 ms. The RMS signals from all seven channels were sampled digitally at 100 Hz and stored for subsequent analysis. These data, from nominally static exertions, were digitally low-pass filtered at 1 Hz to reduce cardiac



Figure 7.3. Posterior electrode locations.

artifacts. Unfiltered data from every trial were reviewed visually as they were collected to ensure that the muscle activity was reasonably constant. Samples with unstable signals were rejected and new samples obtained.

SEMG was recorded for several standardized exercises to provide normalization data. For the three back electrode locations, the subject sat in the laboratory hardseat and buckled a seatbelt around his hips. The seatbelt length was adjusted so that the subject had to slide forward slightly, away from the backrest, to make firm contact. The subject was instructed to keep his back straight while contacting the backrest only via a padded load cell that was positioned at approximately the T4 level. Figure 7.4 shows the subject preparing for a trial. At a signal from the investigator, the subject began to push backward against the load cell, ramped up over three seconds to maximum force, held for three seconds, then released. The subject was instructed to use the seatbelt to resist the rearward force, rather than bracing with his legs. The trial was conducted three times while SEMG and the force on the load cell were recorded.



Figure 7.4. Back SEMG normalization trial.

For the neck electrode locations, normalization trials were conducted with the subject sitting on another laboratory chair. With the subject in an upright, unsupported sitting posture, the subject pressed his forehead (anterior neck normalization) or the back of his head (posterior neck) against the load cell while maintaining his thorax, neck, and head orientations constant. Figure 7.5 shows the postures for the posterior and anterior neck normalization trials. The subject performed the ramping procedure to maximum force three times for each site while SEMG and force data were recorded. Data from the anterior deltoid and triceps locations were not normalized.

Following the normalization trials, the subject's posture was recorded as he sat in an unsupported, slumped posture. A typical slumped posture is shown in Figure 7.6. The subject sat on a flat platform looking straight forward with his arms hanging loosely from the shoulders. An oscilloscope monitoring the SEMG signals was positioned in front of the subject to provide visual feedback on back muscle activity. The subject was instructed to slump fully, relaxing his back muscles until low activity levels were observed at the three back electrode sites. All subjects were able to accomplish this relaxation. A ten-second sample of SEMG was recorded, and the subject's body landmark data were collected with the sonic digitizer.



Figure 7.5. Posterior (left) and anterior (right) neck normalization trials.



Figure 7.6. Typical unsupported slump posture.

The subject was tested in four different types of trials in the vehicle mockup: Preferred, Prescribed, Neck, and Arm. At each of the conditions within each trial type, the subject's posture was recorded using the sonic digitizer and a 10-second SEMG sample was taken. The SEMG data were recorded for each condition with the subject's hands on the steering wheel (On) and with the subject's hands resting on his thighs (Lap). The Lap trials are interpreted as representing a passenger posture.

Preferred Trials

In the preferred trials, the subject first sat in the vehicle mockup and adjusted the seatback angle to obtain the posture he would prefer as a passenger in a vehicle. The subject was instructed to place his hands on his thighs with the thumbs at the thigh-abdomen junction. The steering wheel was moved away from the subject and the subjects did not manipulate either the steering wheel or pedals while selecting a passenger posture. The subject maintained this posture while body landmark and SEMG data were collected. The subject was then instructed to select his preferred driving posture by adjusting the fore-aft seat position, seatback angle, and fore-aft steering wheel position. The subject was encouraged to manipulate the steering wheel and pedals and to

adjust each control several times. This posture was recorded and SEMG samples were taken.

The subject then exited the vehicle mockup. The next five trials were conducted with the seatback set to -10° , -5° , 0° , 5° and 10° of recline, relative to the subject's preferred seatback angle. The order of presentation was randomized within subject, and the subject stood with his back to the mockup as the seat was adjusted between trials. For each seatback angle condition, the subject sat in the seat, attempting to obtain a comfortable posture without adjusting the seat track or seatback angle. With the subject's hands on the steering wheel at the 10-o'clock and 2-o'clock positions, the experimenter adjusted the fore-aft steering wheel position to obtain the same elbow angle as was measured in the subject's preferred driving posture. Posture and SEMG were recorded for each seatback angle trial.

Prescribed Trials

The prescribed trials were identical to the preferred trials, except that the subject was instructed to sit each time in a manner intended to minimize rearward pelvis rotation. The subject sat on the seat while leaning forward at the hips, and slid his hips rearward on the seat until firm contact was made with the seatback. This procedure was intended to result in a reduction in lumbar spine flexion relative to the preferred trials. Data were recorded for passenger and driver postures, followed by the five imposed seatback angles, set relative to the seatback angle preferred by the subject when sitting with the prescribed procedure.

Neck Trials

In these trials, the subject's head position relative to the thorax was perturbed using a head position probe mounted on the seatback. Starting with the subject in his preferred driving posture, the head probe was adjusted to make light contact with back of the subject's head. The subject then flexed his neck forward while the probe was adjusted to a position -40 , -20 , 0 , 20 , or 40 mm fore-aft relative to the preferred position.

The subject was instructed to return his head to the upright position and move it slowly rearward until making light contact with the head probe, while maintaining forward-directed vision. Posture and muscle activity were recorded for each of the conditions, which were presented in random order.

Arm Trials

In these trials, the steering wheel position was varied to produce a range of arm postures. Starting with the steering wheel and seatback in the positions preferred by the subject, the steering wheel was moved -50, -25, 0, 25, and 50 mm relative to the preferred position, with the conditions presented in random order. Posture and SEMG were recorded for each condition.

SEMG Normalization

For each normalization trial, the force and RMS SEMG time histories were filtered using a digital eighth-order Butterworth low-pass filter with a cutoff frequency of 2 Hz. The value of the filtered RMS SEMG signal at the time of peak filtered force was selected as the maximum amplitude for SEMG scaling. The minimum level observed during all trials for each electrode site was selected as the minimum amplitude for scaling. RMS SEMG data from the test conditions were then expressed as a fraction of the difference between these two amplitudes. This normalization procedure is somewhat different from the commonly used Maximum Voluntary Contraction (MVC), because the trials did not necessarily result in maximum exertions of the muscles underlying each electrode site, and the minimum observed levels may not represent minimal activity. However, the standardized postures and procedures provide a means of comparing exertion levels between postures and across subjects. The normalized RMS EMG values are multiplied by 100 and referred to as NEMG. The NEMG values are approximately equivalent to percentages of the more commonly referenced MVC, but are probably higher than the corresponding percent-MVC values for the back extensor sites, because

the seated posture used in the normalization trials probably restricted the exertion to levels below the true maximum.

Posture Data Analysis

The body landmark data were used to fit a kinematic body linkage model, as described in Chapter 2. The orientations of the body segments are analyzed in the sagittal plane only, since the postures are largely sagittally symmetric. Arm postures with the hands on the steering wheel resulted in the plane formed by the wrist, elbow, and shoulder being approximately vertical, so the arm postures could reasonably be subjected to a planar analysis.

Seatback angle was calculated by using the angular offset of the seatback frame from a 23-degree seatback orientation with respect to vertical, as measured by the SAE J826 manikin and procedures (Appendix A). The seatback angle was calculated for each trial from two reference points on the seat frame that were digitized along with each posture recording.

7.4 Effects of Seatback Angle and Sitting Procedure on Trunk Posture

Each subject experienced different seatback angles that were calculated as offsets from his preferred seatback angle in a driving posture. Analysis of variance (ANOVA) was conducted to compare sitter-selected seatback angles for driver and passenger postures in both the preferred and prescribed trials. The sitter-selected seatback angles did not differ significantly between the passenger and driver postures, and there was no interaction between the hand position (on the steering wheel vs. in the lap) and the trial type (preferred vs. prescribed sitting procedure). However, sitter-selected seatback angles averaged two degrees more reclined in the prescribed sitting trials than in the preferred trials. For the preferred trials, the sitter-selected, driver-posture seatback angle ranged from 15 to 26 degrees, with a mean of 21.8 degrees. Since the test conditions were based on each subject's preferred seatback angle, the tested seatback angles ranged from 6.5 to 38.7 degrees. (The discrepancy between the minimum seatback angle of 6.5

degrees and the minimum preferred driver-posture seatback angle of 15 degree, minus 10 degrees, is likely due to flexion of the seatback under subject loading after the seatback angle was set with the subject standing. The reported seatback angles are the angles measured with the subject sitting in the seat, not the angles of the unloaded seat.)

ANOVA and regression were used to examine the relationships between seatback angle and posture variables. The primary concerns were the effects of changes in seatback angle on the torso body segment orientations, and in particular lumbar spine flexion, cervical spine flexion, overall torso recline, and thorax orientation. Table 7.2 and Figure 7.7 summarize the variables that represent these posture characteristics.

Table 7.2
Posture Variables

Posture Characteristic	Variables
Segment Orientations	Head Angle, Neck Angle, Thorax Angle, Abdomen Angle, Pelvis Angle
Lumbar Spine Flexion	Pelvis Angle minus Thorax Angle
Cervical Spine Flexion	Thorax Angle minus Head Angle
Overall Recline	Hip-to-Eye Vector Angle

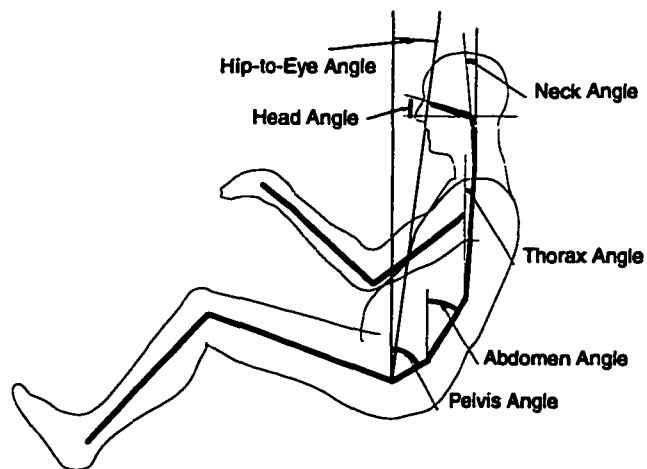


Figure 7.7. Schematic illustration of posture variables.

Table 7.3 summarizes the effects of seatback angle and sitting procedure (preferred vs. prescribed) on posture variables. Using a within-subjects ANOVA with seatback angle as a fixed, five-level effect, seatback angle was found to significantly affect all of the listed variables except head angle. The mean difference between the -10° and +10° seatback angle condition is listed. The sitting procedure (preferred vs. prescribed) affected only pelvis angle and lumbar flexion, reducing each by about 6 degrees. In no case was there a significant interaction between seatback angle and sitting procedure. A second estimate of the effect of seatback angle on these variables was obtained using a linear regression on the residuals after accounting for intersubject differences in mean response and mean differences between sitting-procedure trials. In all cases, the linear model is a reasonable fit to the data, and provides a significant estimate of the effects of seatback angle on all variables ($p < 0.001$). The estimates for a 20-degree change in seatback angle are similar to the mean differences between the -10°

Table 7.3
Effects of Seatback Angle and Sitting Procedure on Driving Posture*

Variable	Mean Response (degrees)	Seatback Angle (-10° to +10°) mean difference	Seatback Angle (-10° to +10°) linear fit	Sitting Procedure (preferred-prescribed)
Head Angle	-7.6	n.s.	5.0	n.s.
Neck Angle	-1.9	5.9†	4.6	n.s.
Thorax Angle	8.8	13.5	13.2	n.s.
Abdomen Angle	22.5	22.1	22.2	n.s.
Pelvis Angle	60.6	5.9	6.2	6.4
Hip-to-Eye Angle	11.3	13.7	13.4	n.s.
Lumbar Flexion††	51.8	-7.5	-7.1	-6.8
Cervical Flexion†††	16.3	10.6	8.2	n.s.

*Values indicate mean change in posture variable across the levels of the experimental variable.

n.s. = not significant ($p > 0.05$).

† Effect significant with $p < 0.05$; all other listed effects significant with $p < 0.01$

†† Value of pelvis angle minus thorax angle.

††† Value of thorax angle minus head angle.

and +10° conditions, with the greatest discrepancies in the head and neck variables, where the angle changes were smallest.

The reduction in lumbar spine flexion of about 7 degrees resulting from the prescribed sitting procedure was due almost entirely to a reduction in rearward pelvis rotation. This effect was approximately the same at all seatback angle conditions (the interaction was not significant).

On average, the head, neck, and pelvis segments reclined at about one quarter of the change in seatback angle while the abdomen segment reclined about the same amount as the seatback (Table 7.3). The thorax, and the overall torso, reclined at about half the rate of the seatback. The different rates of movement of the torso segments with changes in seatback angle resulted in changes in average spine flexion. The lumbar spine flexion (difference between pelvis and thorax orientations) was reduced about 7 degrees by a 20-degree increase in seatback angle, while cervical spine flexion increased about 11 degrees. The relative motions of the torso segments also suggest a change in the distribution of spine flexion. Using the two-joint lumbar model depicted in Figure 7.7, the 20-degree increase in seatback angle increased flexion at the upper lumbar joint by 8.6 degrees (change in abdomen angle minus change in thorax angle), while reducing flexion at the lower lumbar joint by 16.2 degrees (change in pelvis angle minus change in abdomen angle). In the cervical spine, the change in flexion due to changes in seatback angle was represented in the two-joint model almost entirely by motion at the lower neck joint. The head and neck segments changed angle at approximately the same rate, which was less than half the thorax motion.

The magnitudes of these effects varied significantly between subjects on most variables (subject-x-seatback and subject-x-trial interactions). In general, subjects exhibited similar trends, but the magnitudes of the effects were different. Figure 7.8 illustrates the intersubject variability in the abdomen angle and the head angle, which show the most- and least-consistent effects of seatback angle, respectively. These are

also the variables showing the greatest and smallest mean effects, respectively. Subjects who exhibited relatively large changes in one posture variable tended also to show large changes in other variables. Overall, the sensitivity of subjects to changes in seatback angle and sitting procedure varied, but the directional trends were consistent. Consistency was greatest for variables that were strongly affected by the test conditions.

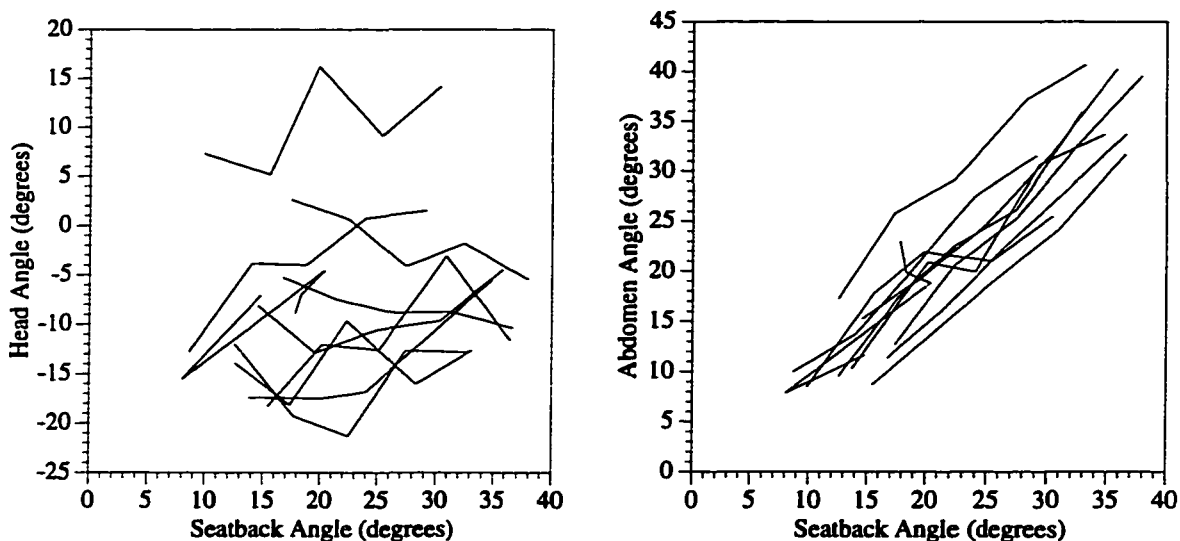


Figure 7.8. Between subjects comparison of seatback angle effects on head angle and abdomen angle. In each plot, one line for each subject connects data from the -10° , -5° , 0° , $+5^{\circ}$, and $+10^{\circ}$ conditions, in order.

7.5 Muscle Activity Analysis

Effects of Seatback Angle, Hand Position, and Sitting Procedure

Values of normalized SEMG (NEMG, %) varied widely between subjects, body sites, and conditions. For the initial analysis, the effects of the seatback angle, sitting procedure, and hand position (On and Lap) were examined for each electrode site. Figure 7.9 shows NEMG for the three back electrode locations and two hand positions. Data from the preferred- and prescribed-sitting procedure trials are pooled, since the postures for the two trial types were only slightly different (see Table 7.3). Each subject's data are shown with a thin line, and the mean at each seatback angle condition is shown with a thick line and symbols.

Two subjects produced consistently higher NEMG values than the other subjects at all three back electrode sites and both hand positions. Normalization trials and minimum values for these subjects are within the range of the other subjects, so normalization anomalies do not appear to account for the large differences between these two subjects and the other subjects.

The remaining eight subjects produced NEMG values below 5 percent, but there were trends with seatback angle condition analogous to those readily seen with the two higher-responding subjects. Figure 7.10 reproduces Figure 7.9 without the two high-responding subjects, including recalculated means. Similar trends with seatback angle are noted with the remaining subjects.

Figures 7.9 and 7.10 illustrate trends toward higher back muscle activity when the seatback angle is more upright, consistent with previous research (e.g., Anderson et al., 1974a). Looking in particular at the activity in the T12 region, muscle activity is generally below 5% NEMG at preferred seatback angles, and remains low for more reclined angles, but most subjects show increasing muscle activity at more upright seatback angles. There is, however, a wide range of response, with some subjects showing an increase of less than 2% NEMG and others changing by more than 20%. Because the variance of NEMG across subjects was influenced by the seatback angle, a log transform of the NEMG responses was made prior to further statistical analyses.

A linear statistical model was used to examine the effects of the test variables on muscle activity. After the log transform, the nonlinear trends in muscle activity with seatback angle observed in Figure 7.10 are approximately linear, so normalized seatback angle was entered as a one-degree-of-freedom, continuous effect. Hand position (On and Lap) and sitting procedure (Preferred and Prescribed) were coded as fixed, two-level effects. A within-subjects analysis was performed, including consideration of potential interactions between the test variables.

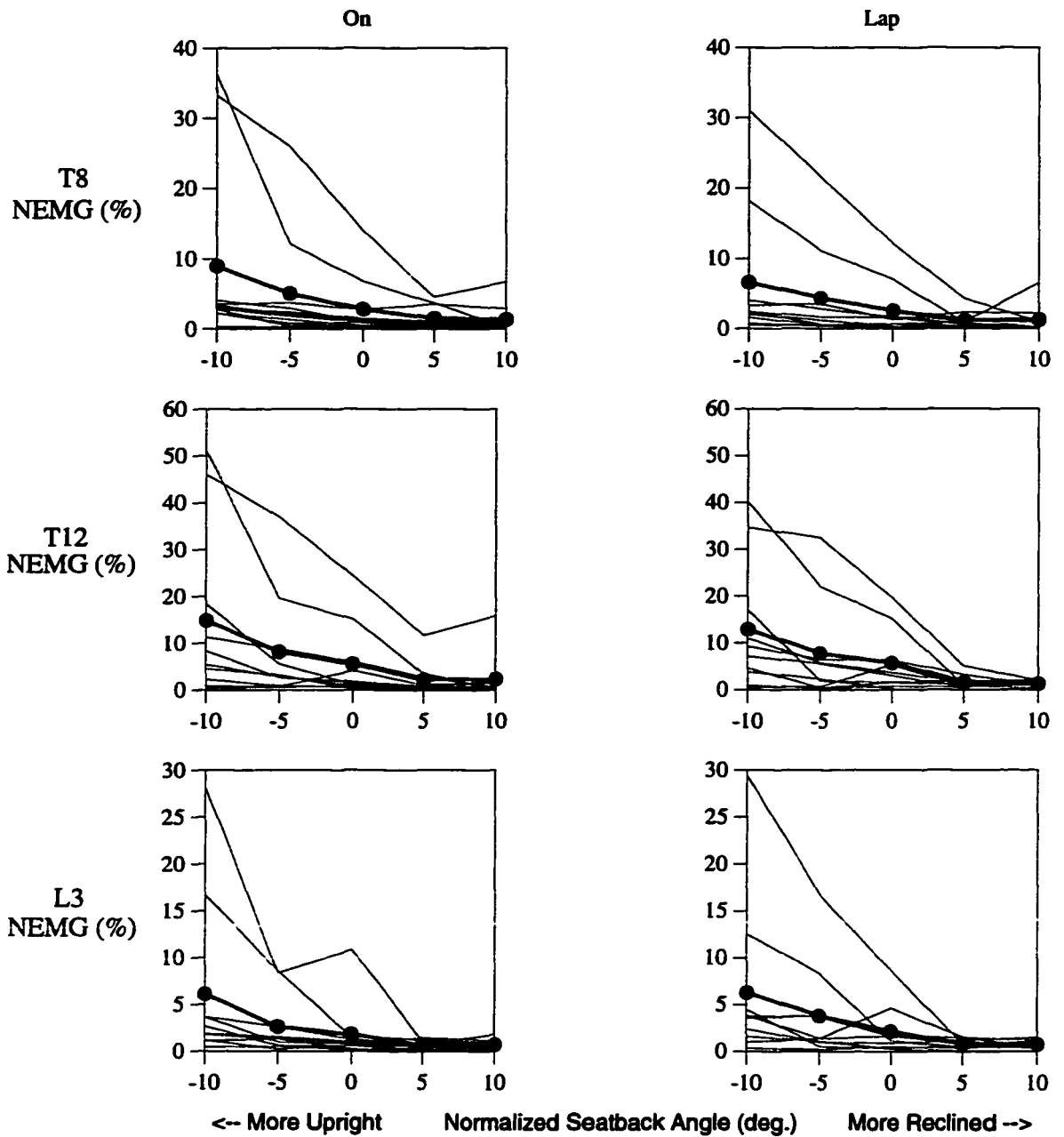


Figure 7.9. NEMG from three back sites with two hand positions. Seatback angles are normalized to each subject's preferred seatback angle (average 22.5 degrees). Dots indicate condition means. Note differing vertical axis scales.

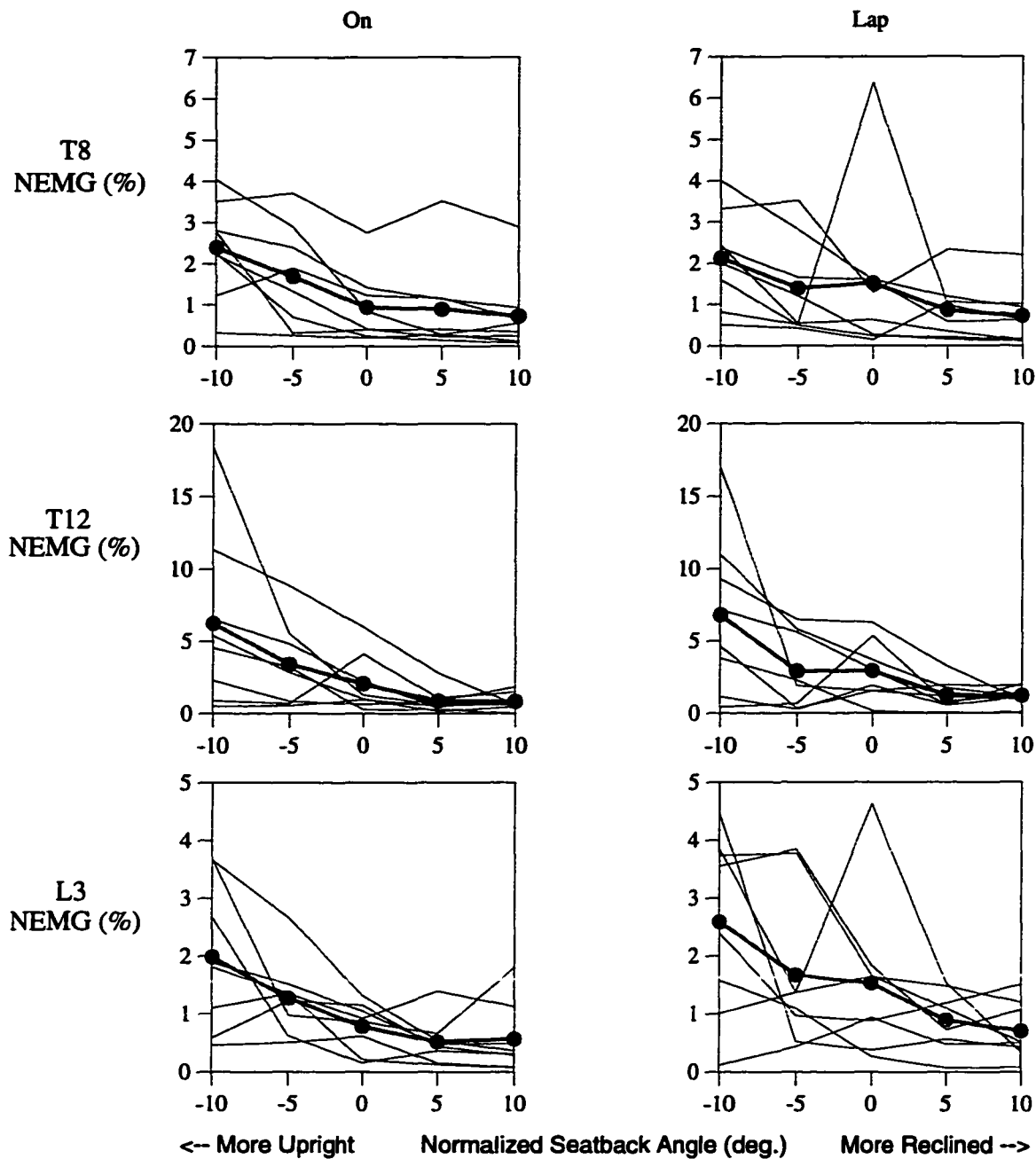


Figure 7.10. NEMG from three back sites with two hand positions versus seatback angle, with two high-responding subjects excluded. Seatback angles are normalized to each subject's preferred seatback angle (average 22.5 degrees). Dots indicate condition means. Note differing vertical axis scales.

Table 7.4 lists the results of the analysis. Seatback angle had a highly significant effect ($p < 0.001$ in all cases) on muscle activity at the L3, T12, and T8 sites, as expected. Seatback angle also had a small but significant effect on posterior neck activity, with slightly increased activity noted at more upright seatback angles. Surprisingly, hand position (On versus Lap) did not significantly affect the back muscle activity. The effects of hand position were observed only at the anterior deltoid site, where the activity dropped from a low level to an essentially resting level when the hands were lowered from the steering wheel to the lap. The prescribed sitting procedure, which resulted in a reduction in lumbar spine flexion of about 7 degrees (see Table 7.3), did not significantly affect muscle activity at any site. In no case was an interaction significant, indicating that the effects of the test variables were independent of the other variables. For example, Figure 7.11 demonstrates the small differences in mean NEMG (%) at the T12 site between the preferred and prescribed trials.

Table 7.4
Test Variable Effects on Log NEMG by Electrode Site (all subjects)

Electrode Site	Seatback Angle*	Hand Position (On/Lap)**	Preferred vs. Prescribed Sitting Procedure**
L3	5.6	n.s. †	n.s.
T12	12.4	n.s.	n.s.
T8	7.2	n.s.	n.s.
Anterior Deltoid	n.s.	1.0	n.s.
Anterior Neck	n.s.	n.s.	n.s.
Posterior Neck	2	n.s.	n.s.

*Difference in mean NEMG (%) between least and greatest normalized seatback angle (-10 and +10 degrees), when linear relationship with seatback angle is significant with $p < 0.01$ in log-transformed data.

**Mean difference in NEMG (%); Prescribed minus Preferred, or On minus Lap.

†n.s. = not significant ($p > 0.01$).

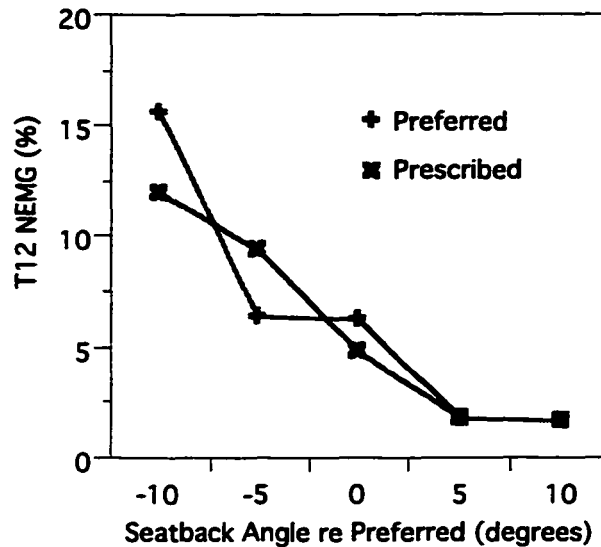


Figure 7.11. NEMG (%) at the T12 electrode site by seatback angle for preferred and prescribed sitting procedure trials. Seatback angles are normalized to each subject's preferred seatback angle (average 22.5 degrees).

The pretest hypotheses predicted that back extensor activity would increase as the seatback angle was made more vertical, but would remain at low levels as the seatback angle was reclined. Figure 7.12 shows a plot of log NEMG (log %) at the T12 site for driving postures with the hands on the steering wheel. A Duncan multiple-range comparison with $p = 0.05$ shows that the condition means at zero, +5, and -10 degrees are not significantly different, while conditions at -5 and -10 degrees are both significantly different from 0, +5, and +10 conditions. The mean trend in Figure 7.12 shows that the muscle activity in the T12 region was slightly elevated compared to the more reclined conditions, but suggests that the point in the nonlinear relationship between muscle activity and recline at which the extensor activity reaches a near-resting level lies somewhere between the preferred seatback angle and 5 degrees more reclined. Review of the plots in Figures 7.9 and 7.10 shows that most subjects showed some influence of seatback angle on back muscle activity, and many showed trends consistent with the hypothesis and the average trend.

Additional statistical analyses were performed in an attempt to determine the sources of intersubject variability in response, but no convincing explanations were

found, in part because of the small sample size. No important trends were noted with anthropometric variables or standard measures of flexibility (toe-touch and leg-raise).

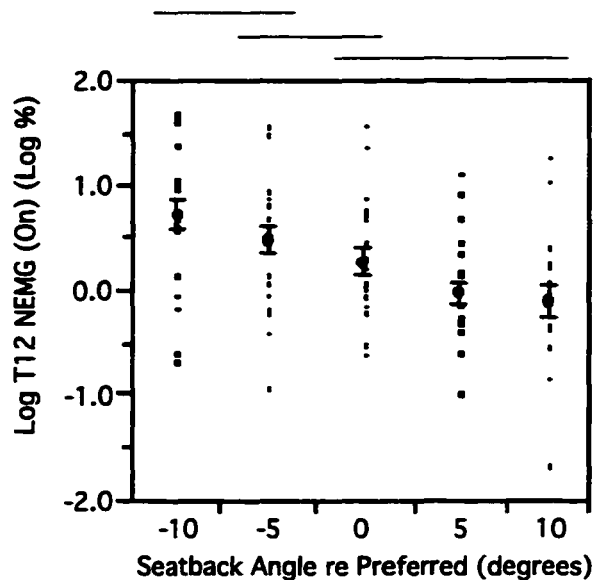


Figure 7.12. Log NEMG at the T12 electrode site, showing means and standard error bars. Lines at the top of the plot span conditions that are not significantly different, using a Duncan multiple range comparison with $p = 0.05$.

Effects of Perturbing Preferred Neck and Arm Postures

As with the back EMG sites, activity in the neck was widely variable between subjects. However, the effects of perturbing the head and neck posture were visible in the neck muscle activity patterns. Figure 7.13 shows the posterior and anterior NEMG values for the five neck conditions. The neck condition level (-40 to +40 mm) is the amount the head position was perturbed relative to the subject's preferred position (negative = rearward). When the head was perturbed forward by 20 or 40 mm, posterior neck activity increased significantly (Duncan multiple range test, $p < 0.05$). Perturbing the head rearward did not significantly increase the anterior neck muscle activity, however. Observations from the posture data collected during the trials suggests that subjects moved their heads forward primarily through neck motion, but were unable to move their heads substantially rearward, while keeping the head level as instructed, without rocking their thoraxes backward in the seat. This had the effect of protecting the anterior neck

muscles from substantial load. Nonetheless, there was a trend toward increasing anterior neck activity among some subjects as the head position was perturbed rearward.

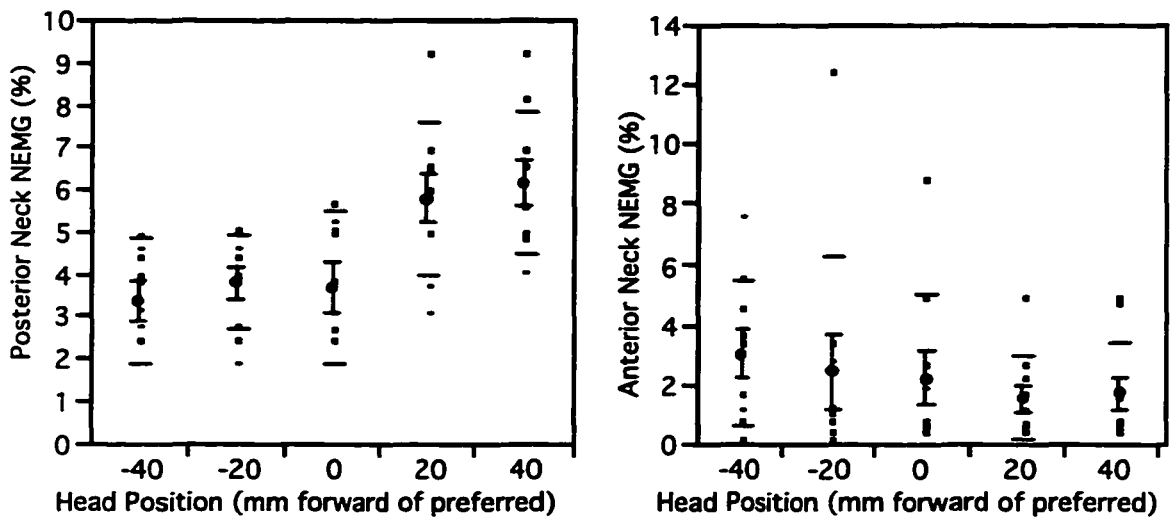


Figure 7.13. Neck muscle NEMG by head position condition. Negative head positions indicate the head position was perturbed rearward (mm). Plots show condition means, standard error bars, and standard deviation bars.

Perturbing the preferred upper-extremity postures by changing the fore-aft steering wheel position did not produce clear changes in upper-extremity muscle activity. Figures 7.14 and 7.15 show the muscle activity at the anterior deltoid and triceps sites, expressed in arbitrary units (normalization data were not available for the triceps). Comparing across steering-wheel-position conditions does not show systematic differences. When plotted against elbow angle, there is a trend toward greater triceps activity at larger elbow angles, but there is no trend observed in the anterior deltoid data. The relationship between the triceps activity and the force interaction with the steering wheel is addressed in Chapter 6.

geometry of the model links was set to the average that was obtained from the subjects in this study using the methods described in Chapter 2. As noted above, normal driving postures are largely sagittally symmetric, and the arm postures examined in this study are also largely planar, allowing a two-dimensional analysis of the body above the hips. Segment masses and centers of mass were set to the averages determined using regression equations based on McConville et al. (1980) with anthropometric data from the current subjects (Table 7.1). The model can be configured to any specified posture, forces and moments can be applied, and the reaction moments at each joint due to the action of gravity and external loads can be calculated.

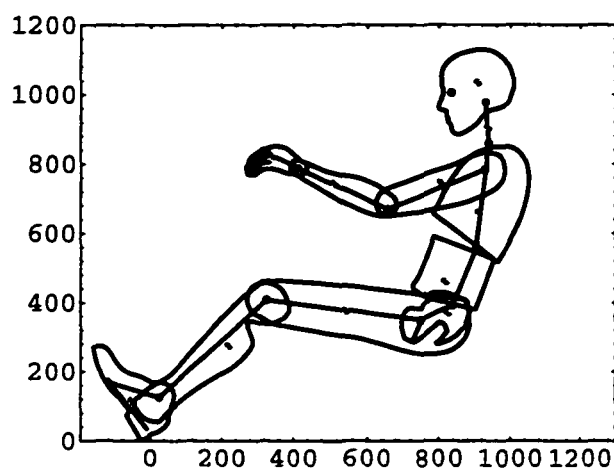


Figure 7.16. Schematic of planar linkage model of driver, showing segments and centers of mass. External contours are for visualization only and do not affect the analysis. Scales in mm.

The primary consideration in the biomechanical analysis of driving postures is the moment balance in the torso, particularly at the upper and lower lumbar joints (T12/L1 and L5/S1, respectively). Figure 7.17 shows a free-body diagram of the thorax segment, illustrating the forces and moments applied by the seat and adjacent segments. The posture in the illustration is constructed from the average preferred segment orientations in the driver posture. The head and neck apply a vertical force equal to their combined weight to the top of the thorax segment at the lower neck joint. A small moment at the

joint accounts for the action of the muscles countering the slightly forward head center of mass (CM) location. Note that the head, neck and thorax CMs are all slightly rearward of the upper lumbar joint (T12/L1) but considerably rearward of the lower lumbar (L5/S1) joint. The result is that the gravity induced moment at T12/L1 is near zero, while the moment at L5/S1 is positive, i.e., tends to rotate the abdomen segment rearward, into the seat. Because the L5/S1 joint is usually further forward than the T12/L1 joint in driving postures, the gravity induced moments at T12/L1 are the first to become negative (tending to cause a forward rotation of the thorax) as the seatback angle is made more upright.

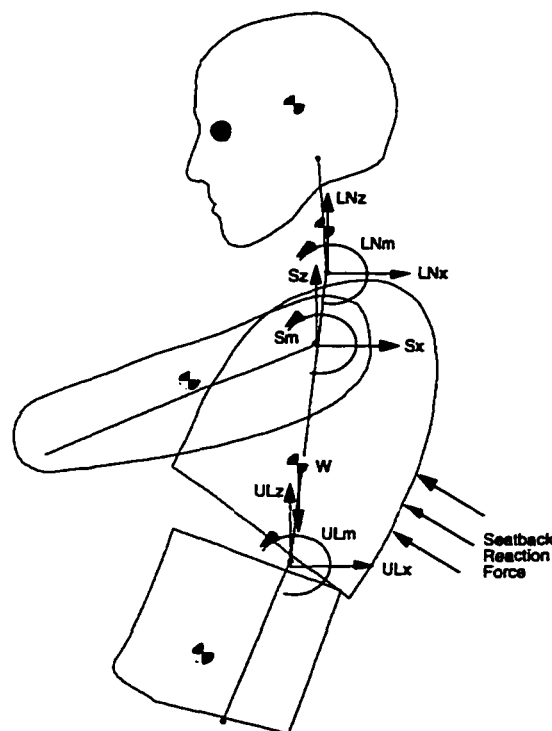


Figure 7.17. Free-body diagram of the thorax in the average preferred driving posture.

The upper extremities apply forces and moments to the thorax through the shoulder joints. As noted in Chapter 6, the drivers' interactions with the steering wheel include active moments at the shoulders and elbow, along with horizontal and vertical forces. In these simulations, the average steering wheel interaction (38 N upward, 8.1 N forward force, 2.3 Nm counter-clockwise moment) was applied to the hands of the model.

To simplify the analysis, the seatback is assumed to exert forces on the thorax only in reaction to applied loads. So, if the sum of the moments at T12/L1 due to gravity and steering wheel interaction is positive (tending to rotate the thorax into the seat), the reaction moment required to stabilize the thorax results from seatback interaction. In contrast, if the net moment on the thorax due to gravity and steering wheel interaction is negative, tending to rotate the thorax forward, then the posture must be stabilized by internally generated moments acting on the thorax. These can result from activity in the back extensors or from passive stresses in the muscles and paraspinal tissues.

The use of the model to simulate the test conditions was facilitated by including the observed patterns of torso segment motion. When the seatback angle was changed, the orientations of the segments between the pelvis and head changed at varying rates. The estimates of the seatback angle effects on each segment were used to calculate a motion distribution parameter value. The parameter values, listed in Table 7.5, are multiplied by a seatback angle change to determine the body segment angle change. Using this approach, the torso kinematics are reduced to a single degree of freedom (seatback angle). The average segment orientations in the subjects' preferred driver postures, also listed in Table 7.5, were used as the starting posture for the simulations.

Figure 7.18 illustrates the torso kinematics by exercising the model through the tested range of seatback angle, centered on the average preferred seatback angle of 22.5

Table 7.5
Starting Segment Orientations and Motion Distribution Parameters

Segment	Starting Angle (degrees re vertical)	Motion Distribution Parameter *
Pelvis	64.3	0.30
Abdomen	22.0	1.11
Thorax	6.7	0.68
Neck	-4.6	0.30
Head	-6.6	0

* Ratio of segment angle change to seatback angle change obtained from fixed effect magnitudes in Table 7.3.

degrees. Upper extremity posture is maintained at the subjects' mean preferred angles. Note that the head remains level through the recline motion, while the neck flexes in a manner that tends to keep the head approximately over the base of the neck. The lumbar spine flexes slightly at more upright postures, but note that the distribution of flexion changes. The flexion at the lower lumbar joint is reduced with increasing recline, while the flexion at the upper lumbar joint is increased (see Table 7.3).

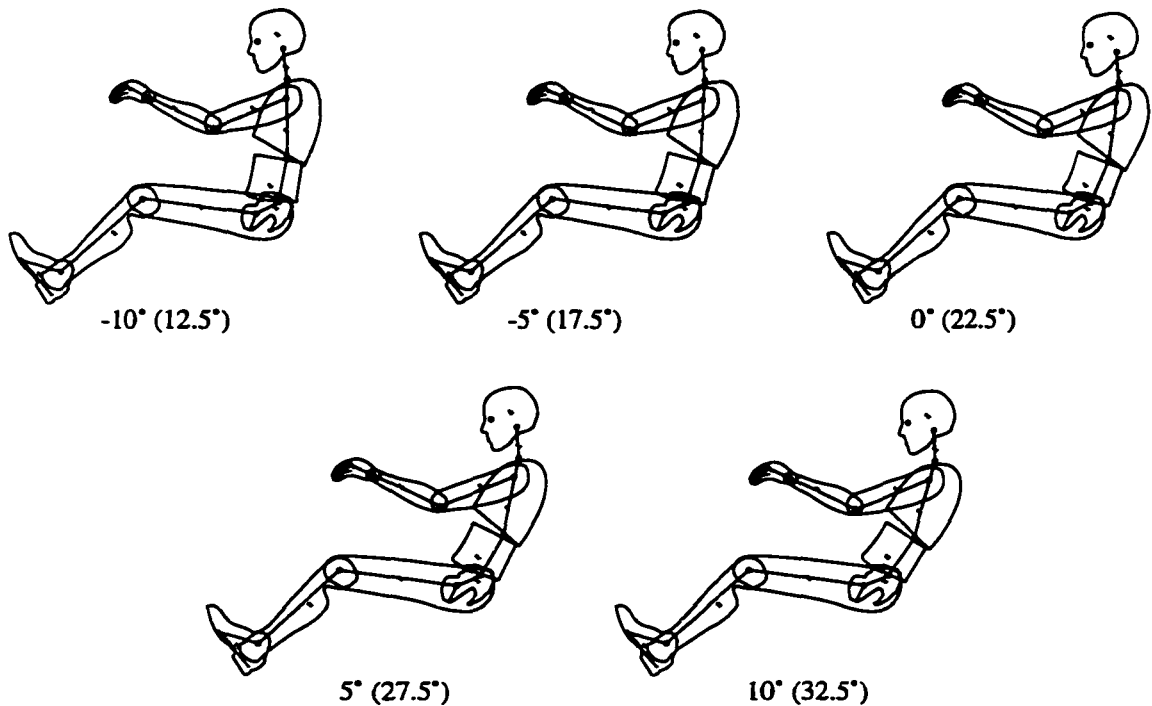


Figure 7.18. Illustration of average torso segment kinematics with changes in seatback angle, from -10 degrees with respect to the mean preferred seatback angle (22.5 degrees) to +10 degrees. Actual seatback angles are listed in parentheses.

The pre-test hypothesis was that drivers would select the most upright posture (highest eye height) that could be achieved low levels of back extensor exertion. Back extensor exertion should be related to the amount of extension moment required at the lumbar joints to stabilize the torso posture. Figure 7.19 plots the eye height in the postures in Figure 7.18 against the moment at T12/L1 due to steering wheel interaction and the action of gravity on the upper body. Positive moments would be countered by

seatback reaction, while negative moments would require passive or active, internally generated moments to stabilize the thorax.

Figure 7.20 shows the muscle activity measured at the T12 electrode site (T12 NEMG) plotted against the T12/L1 moment predicted by the model. The average muscle activity increases as the moment becomes negative, consistent with the predicted need for extensor moment in the thoracolumbar region.

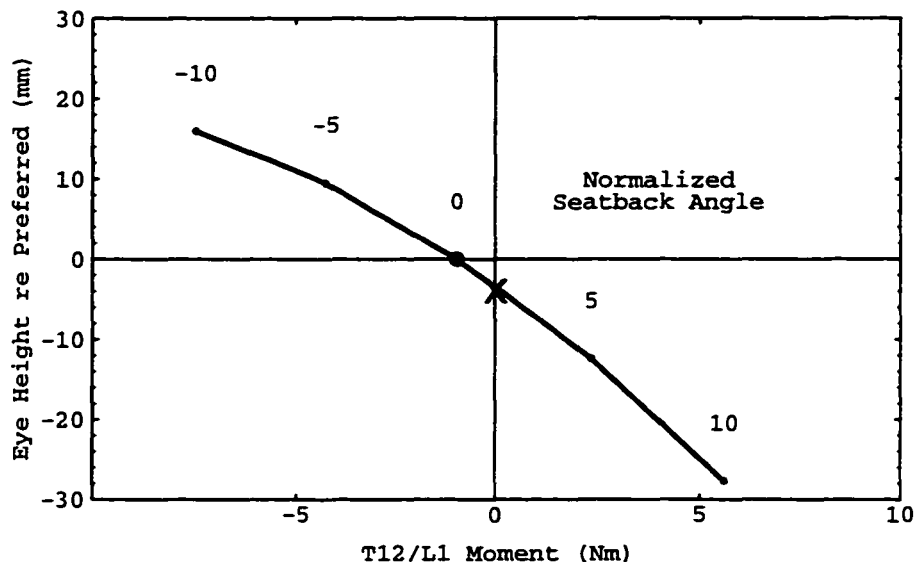


Figure 7.19. Eye height versus net moment at T12/L1 due to steering wheel interaction and upper-body mass. Large dot is mean preferred posture. Posture marked with an "X" is the posture with the greatest eye height and positive or zero moment.

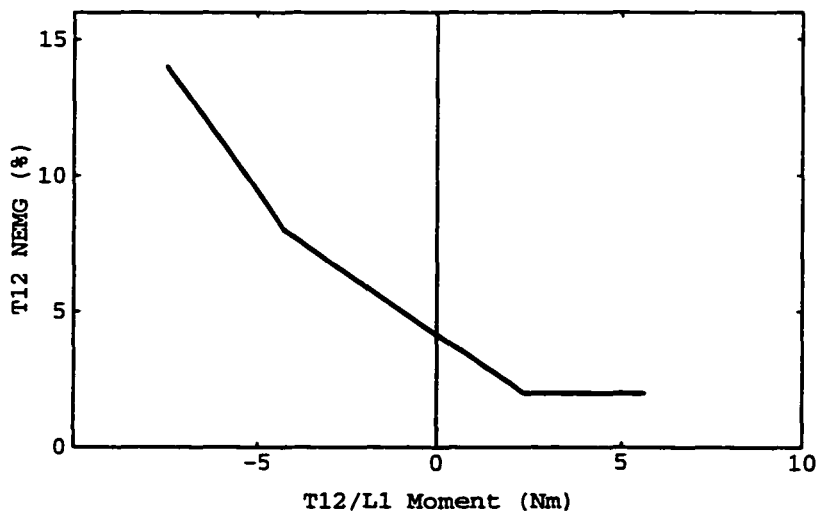


Figure 7.20. Thoracolumbar extensor activity (T12 electrode site) versus T12/L1 moment predicted by the biomechanical model.

In Figure 7.19, the mean preferred driver posture is shown with a large dot and is compared to the posture with the greatest eye height for which the moment at T12/L1 is zero or positive, i.e., for which no internally generated extensor moment is required. These postures are clearly very similar. Figure 7.21 compares the mean preferred driver posture with this balanced posture, denoted by an X in Figure 7.19, showing that they are very similar. A similar analysis could be conducted for the preferred passenger postures (hands in the lap). Figure 7.22 shows the mean preferred driver and passenger postures overlaid, indicating that the preferred passenger postures are also characterized by an approximately balanced body above T12/L1.

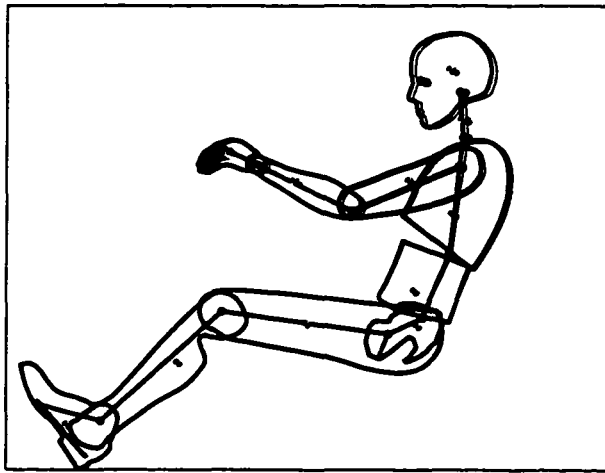


Figure 7.21. Preferred driver posture (thick lines), contrasted with posture X from Figure 7.19 (thin lines).

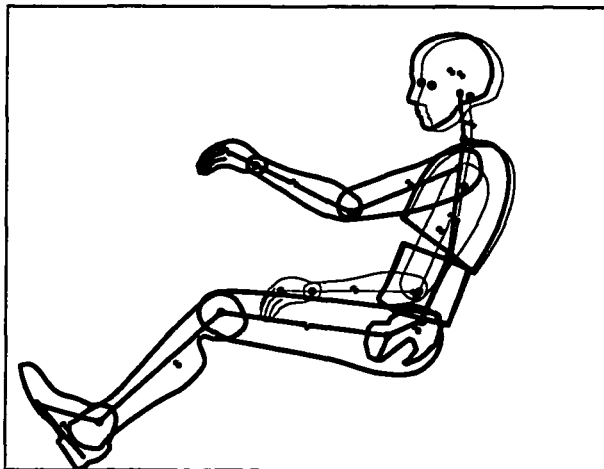


Figure 7.22. Preferred driver posture (thick lines) contrasted with preferred passenger posture (thin lines).

The preceding simulations demonstrated that, on average, the internally or externally generated moments required to stabilize the thorax in preferred driver or passenger postures are likely to be small. When more reclined seatback angles are chosen, the net upper-body moment will tend to rotate the thorax into the seatback, allowing the seatback to stabilize the thorax with reaction forces. However, when the seatback is more upright than preferred, an internally generated extension moment is required. If this moment is supplied by muscle exertion, the EMG data from the electrode sites on the back should show increased activity at more upright seatback angles. Indeed, the data show a significant increase in activity at the T12 electrode site for more upright seatback angles, and no significant change for more reclined seatback angles.

However, there was a wide range of response among the subjects. While some subjects showed substantial increases in back extensor activity as the seatback angle was made more upright, other showed only minimal increases. Additional simulations were performed to determine if passively generated extension moments could be providing thorax stabilization in lieu of back extensor muscle activity.

A number of researchers have documented the “flexion-relaxation” phenomenon that is frequently observed in lifting tasks (Floyd and Silver, 1955; Kippers and Parker, 1984). When a person bends over to lift an object from the floor, the back extensor activity rises sharply as the trunk is inclined forward. However, as the lumbar spine reaches its flexion limit, the muscle activity, measured by EMG, often decreases to a resting level, even though the flexion moment on the lumbar spine remains high, because the lumbar moment due to the weight of the body and the lifted object is balanced largely by passively generated moments created as tissues in the trunk are stressed by the flexion motion. Researchers have variously identified the spine, paraspinal ligaments, extensor muscles and fascia, and skin as important contributors to the passive moment (Dolan et al., 1993). Researchers have also documented flexion-relaxation in sitting. Akerblom

(1948) and Floyd and Silver (1955) both found considerably lower levels of back extensor activity in sitting fully slumped than in sitting erect. In the current study, subjects were able to sit fully slumped without a backrest and with no appreciable back extensor activity, based on visual examination of the EMG signal on an oscilloscope.

Several studies have quantified the passive bending stiffness of the trunk. Nyquist and Murton (1975) placed six volunteers in a fixture by which measured moments could be applied as the posture was measured. McGill et al. (1994) used an analogous but more sophisticated system with 37 men and women to measure passive lumbar stiffness while monitoring EMG to ensure low levels of actively generated moment. Dolan et al. (1994) used an innovative strategy to infer the passive moment from the lumbar moment/EMG relationship during lifting-type static exertions. Approaching the problem from a different perspective, Nussbaum and Chaffin (1996) created a three-dimensional model of the torso that included passively generated moments from the spine and muscles.

The findings from each of these sources were evaluated to develop a relationship between lumbar spine flexion and passive moment appropriate for use in the current analysis. Although each study used different posture definitions and moment locations, data from three of the sources could be adjusted to express the flexion with respect to erect standing and the moment at L5/S1. Figure 7.23 shows passive moment at L5/S1 versus lumbar flexion relative to standing. Information from Dolan et al. was obtained directly from regression equations provided in the paper. The curve for Nyquist and Murton was developed by fitting an exponential function of the form recommended by McGill et al. to the aggregate data for passive flexions. A flexion limit of 56.4 degrees reported as an average value for males (Dolan and Adams, 1993) was used to scale the Nussbaum and Chaffin model output.

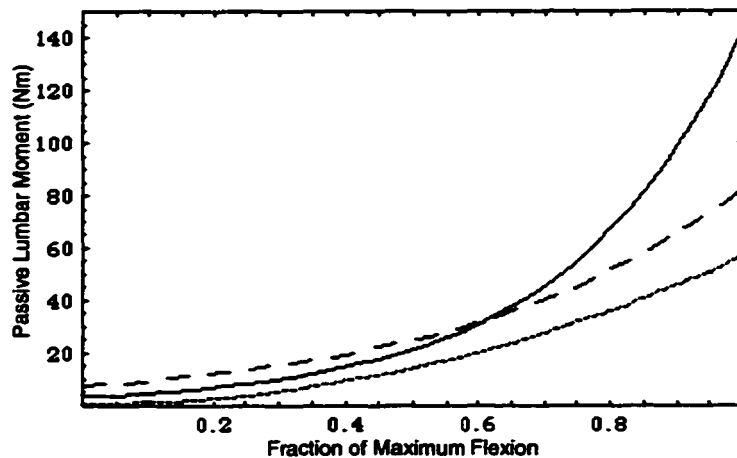


Figure 7.23. Passive lumbar moments relative to lumbar flexion adapted from Nyquist and Murton (—), Dolan et al. (---), and Nussbaum and Chaffin (-·-).

The passive flexion stiffness curves in Figure 7.23 are fairly similar, particularly up to about 80% flexion. All of the curves show increasing stiffness as the limit of motion is approached. The Nyquist and Murton data, which show the largest passive moments, also had much higher maximum flexions, averaging 96 degrees, compared with the 56-degree average for males reported by Dolan and Adams. This difference likely rises from a difference in definition of maximum flexion. Nyquist and Murton produced maximum flexion by applying substantial external moments, while the Dolan et al. maximum flexion was obtained during a voluntary toe-touch exercise. Since the three curves obtained using an entirely different method are reasonably similar, the Dolan et al. curve, which is based on the largest number of male subjects (23), was used to develop a passive stiffness function for use in the current study.

The passive stiffness function given by Dolan et al. represents L5/S1 moment, but the moments at T12/L1 are usually different from those at L5/S1. Particularly in lifting, when the torso is extended approximately horizontally, the moments at T12/L1 due to body weight can be about half of those at L5/S1. In general, the relationship between the T12/L1 and L5/S1 moments due to body weight vary depending on the posture. Figure 7.24 shows the average unsupported slump posture measured with the subjects in this study (mean segment lengths and orientations). This posture represents an average

lumbar flexion of 59.7 degrees relative to standing, measured by the relative change in orientation of the pelvis and thorax. The lumbar segment of the two-joint lumbar model is approximately vertical, so that the moments about the two joints due to gravity are similar (-40 Nm for L5/S1, -34 Nm for T12/L1). Since the subjects reduced their back extensor activity to a low level using visual feedback, the posture is likely supported primarily by passively generated moments about the upper lumbar spine. For these subjects, the trunk in the area of T12 can create an average, passive extension moment of around 34 Nm in an unsupported, slumped posture.

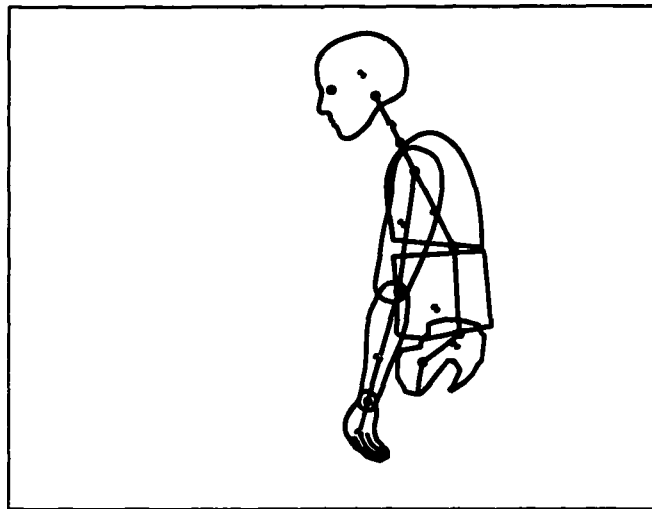


Figure 7.24. Average unsupported slump posture (sitting).

A generic passive flexion/moment relationship for the T12/L1 joint was created by assuming that the form of the Dolan *et al.* relationship is applicable and scaling the function so that the function value is 34 Nm at 100% lumbar flexion (59.7 degrees, based on the average difference between standing and unsupported slump). Figure 7.25 shows this flexion/moment relationship. The non-zero intercept is an artifact of the form of the fitting function given by Dolan *et al.* and is not important for this analysis because only flexions of greater than 40 degrees are of interest. The function is extended beyond the maximum flexion observed in the unsupported slump condition (*i.e.*, beyond the current definition of 100% flexion) to allow use of the function in a wider range of simulation

conditions. Figure 7.25 also includes two alternative stiffness relationships used to evaluate the importance of the stiffness function shape. A linear function is compared to a bilinear function that simulates zero stiffness through 40 degrees of flexion with high stiffness near the end of the flexion range of motion. All three stiffness functions produce 34 Nm of passive moment at 59.6 degrees of flexion.

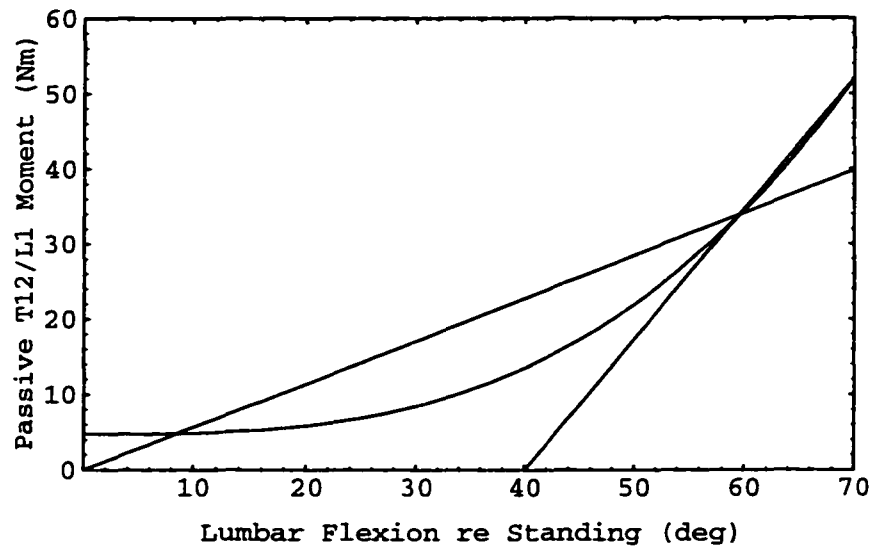


Figure 7.25. Three alternative relationships between lumbar flexion relative to standing and passive T12/L1 moment. The curve is the scaled Dolan et al. relationship, contrasted with linear and bilinear functions.

Lumbar flexion in the average preferred driving posture is about 65% of the maximum flexion (unsupported slump minus standing), or about 39 degrees. The scaled Dolan et al. relationship in Figure 7.25 suggests that at 39 degrees of flexion about 12 Nm of passively-generated extension moment is available to stabilize the thorax. This moment magnitude is relatively large compared to the gravity induced moments at T12/L1 for a range of potential driving postures (cf. Figure 7.19), indicating that passively generated moments could potentially play an important role in supporting driving postures.

Figure 7.26 shows the driving posture analysis originally presented in Figure 7.19, except that the T12/L1 moment in the figure is the net moment after subtracting the available passive moment from the gravity induced moment, yielding the extension

moment that would be required from muscle exertion. (Negative moments in the figure are required active muscle moments while positive moments would be produced by seatback reaction.) The three curves in the figure correspond to the three flexion/moment relationships depicted in Figure 7.25. Each curve shows the net moment at T12/L1, including the action of gravity on the upper body, the interaction with the steering wheel, and available passive extension moments at T12/L1.

The passive moments based on the scaled Dolan et al. flexion/moment relationship are sufficient to eliminate the need for active extensor moments in the thoracolumbar spine throughout the tested range of seatback angles. Because the moment available from the linear stiffness function exceeds the Dolan et al. value throughout the flexion range, the net moment is even larger in extension. However, the bilinear moment relationship shows an interesting divergence. Because no passive moment is available until the net lumbar spine flexion exceeds 40 degrees, some active muscle moment would be required to stabilize the thorax when the seatback angle is made more upright than preferred. However, with increasing spine flexion at more upright angles, the available passive moments match the increase in gravity generated moment.

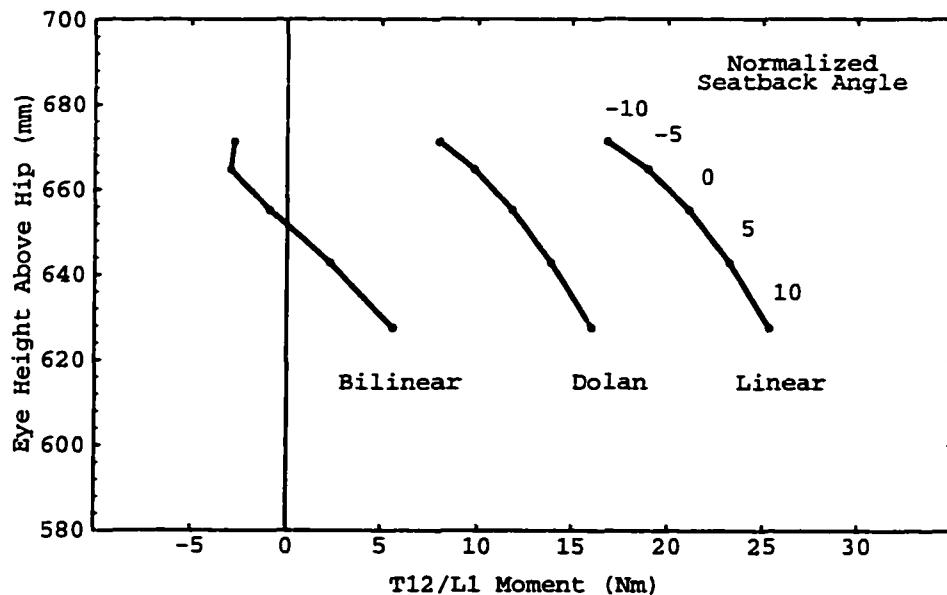


Figure 7.26. Driving posture analysis presented in Figure 7.19 with available passive extension moment included, using the scaled Dolan et al. flexion/moment relationship (center), the linear relationship (right), and the bilinear relationship (left).

This analysis demonstrates that passive lumbar flexion stiffness may contribute to thorax stability in vehicle driver and passenger postures, and may help to explain the wide range of muscle activity responses to seatback angle changes observed in testing. Other researchers, notably Nyquist and Murton (1975), have demonstrated that there is considerable intersubject variability in the shape of the torso flexion stiffness curve, and the current analysis shows that differences in the flexion/moment relationship can affect the need for back extensor exertion to stabilize the thorax.

7.7 Discussion and Conclusions

This research was conducted to explore a general hypothesis concerning the selection of driving postures. An overall posture-selection framework was proposed, in which the physical constraints of the task interact with the driver's body dimensions and physical capabilities to determine the range of kinematically feasible postures. Within this range, the driver is proposed to select a posture by trading off static muscle exertion against the adequacy of the posture for the driving task. Task suitability is represented by eye height, because higher eye locations provide better vision to the surrounding environment and position the upper extremities for better reach. But more upright postures are also associated with greater requirements for muscle exertion, particularly in the back extensors.

Previous research (e.g., Andersson et al., 1974a, 1974b) demonstrated that, as the seatback angle is made more reclined, back extensor activity decreases to a near-resting level and remains at low levels with increasing recline. The presence of this relationship between recline angle and muscle activity suggests a simple form for the trade-off between task suitability (eye height) and muscle activity. By giving priority to reducing muscle activity, the selected posture is predicted to be the most upright posture that can be achieved with back extensor activity in the thoracolumbar area near resting levels.

In previous research, experimenters have imposed the same seatback angles, in 10-degree increments, for all subjects (Andersson et al. 1974a, 1974b; Hosea et al.,

1986). The results show the average shape of the recline vs. EMG relationship, but do not provide useful information about the muscle activity at sitter-selected postures. In the current study, seatback angles were varied over a 20-degree range centered on each subject's preferred seatback angle, which ranged from 15 to 26 degrees. This normalization of seatback angles allowed characterization of muscle activity in subject-preferred postures and examination of the effects of perturbing each subject's preferred posture.

When the seatback angle was changed, sitters responded with differential movement among the torso, neck, and neck segments. Rather than the torso reclining as a unit, the lumbar and cervical spine flexion changed with the seatback angle. The effect of the cervical spine flexion was to maintain the head approximately level and over the base of the neck. Most interesting, the distribution of flexion in the lumbar spine appeared to be affected by the seatback angle. The relative movements of the thorax and pelvis indicate that increasing recline decreased flexion in the lower part of the lumbar spine but increased flexion in the upper lumbar spine.

Normalized EMG levels (NEMG) at the L3, T12, and T8 levels were generally below about 5% NEMG at the subjects' preferred driving postures, consistent with the pre-test hypotheses. Further, muscle activity at the T12 level increased significantly as the seatback angle was made more upright, and did not change significantly as the seatback reclined, supporting the hypothesis that preferred driving postures are the most upright postures consistent with near-resting-level thoracolumbar extensor exertion. There was, however, considerable variability among the subjects in muscle activity response.

The nature of the muscle-activity relationship with seatback angle makes it difficult to determine precisely the point at which muscle activity reaches a resting level. In particular, the muscle activity signal is bounded on the lower end, so that any measurement error will tend to bias the reading upward, as will any electrical noise or

movement artifacts. Further, the variance in the measurement is related to the mean value, so a transformation of the data is necessary to use standard statistical techniques. In spite of these problems, the pre-test hypotheses were supported by the statistical analyses of the EMG data.

When the driver's preferred head positions were perturbed forward, posterior neck muscle exertion increased from the low levels measured in the drivers' preferred postures. Perturbing the head rearward did not significantly increase anterior neck muscle exertion, apparently because the subjects accomplished much of the rearward head movement by rotating their thoraxes rearward, avoiding a substantial gravity induced moment on the neck. These findings suggest that neck postures are also selected to minimize the static muscle exertion required to maintain the posture.

A planar, rigid-segment biomechanical model was developed to examine the subjects' postures from an internal perspective. Configuring the model to match the subjects' average anthropometry and preferred driving postures demonstrated the net moment at T12/L1 due to the steering wheel interaction and the action of gravity on the upper body was low when the subjects were allowed to choose their seatback angle. The torso, head, and neck postures were very similar in passenger postures (no steering wheel interaction), suggesting that the posture-selection mechanism operates somewhat independent of the hand-task requirements. Indeed, other research (Chapter 3) has demonstrated that large changes in hand-location requirements change torso postures only slightly.

The trends in the model-predicted moments at the T12/L1 joint were matched well by the observed muscle activity in the thoracolumbar region (T12 electrode site). The muscle activity increased as the seatback angle was made more upright, conditions for which the model predicted that increasing thoracolumbar extension moment was required.

A net rearward gravity induced moment at T12/L1 can be balanced by the seatback reaction, but a net forward (lumbar flexion) moment must be balanced by internally generated moments. The pre-test hypotheses implicitly suggested that these moments would be generated by the back extensor muscles, yielding a measurable increase in EMG. However, the variability in muscle-activity response to more upright seatback angles indicates that some subjects supported their upper bodies using primarily passive moments.

A typical passive flexion stiffness relationship was developed from the literature to determine if such moments could contribute substantially to thorax stability in sitting postures. In fact, the passive flexion magnitudes obtained by scaling a generic stiffness function were comparable in size to the gravity induced moments. An examination of the effects of different passive stiffness function shapes indicated that the observed range of muscle-activity responses to changes in seatback angle could result from intersubject differences in this passive lumbar flexion stiffness relationship.

The differences in subject behavior may be due to alternative strategies of stabilizing the thorax with more upright seatback angles. Some subjects clearly chose to use muscle exertion to maintain thorax stability at more upright seatback angles, while others were able to obtain sufficient passive extension moments, possibly by increasing lumbar spine flexion slightly. Examination of individual subjects' data with the model was not fruitful, in part because of uncertainties concerning body segment masses and CM locations and the lack of information concerning individual subjects' passive flexion stiffness relationships. A more detailed model and more complete data will be required to explore these relationships further.

The current findings provide a more detailed understanding of seated posture selection than previous studies. Researchers have previously reported trends of increased muscle activity as the seatback angle is made more vertical (Andersson et al., 1974a, 1974b; Hosea et al., 1986). Andersson et al. (1974a) examined concurrently the effects of

changes in spine flexion, and found that reductions in spine flexion tended to increase the back muscle activity for fairly upright seatback angles. Several studies have examined muscle activity in car seats (Andersson et al., 1974b; Hosea et al., 1986; Sheridan et al., 1991), but none of the previous research has addressed the relationship between muscle activity and preferred seatback angles, examined the kinematic response of the spine to changes in vehicle seatback angle, or quantified the potential contribution of passive stiffness to postural stability in sitting. Akerblom (1948) and Floyd and Silver (1955) both identified the potential importance of passively generated moments in supporting sitting postures, but did not extend their findings to understanding posture selection behavior. Cleaver (1954) presented a biomechanical analysis of vehicle-seated postures that was more advanced much of the later research, but considered only comfort and not posture prediction.

The experimental and analytical findings generally support the proposed posture-selection model, but suggest some revisions to account for the observed contribution of passive support moments. Under the revised model, drivers are predicted to select the posture with the highest eye height that results in no net forward moment at the base of the thorax. For sitters with relatively flexible torsos, who would require back-extensor exertion to maintain a more upright posture, this hypothesis is identical to the preceding model. However, changing the criterion from muscle activity to moment accounts for subjects who are able to obtain substantial passive support moments.

From the biomechanical analysis, one might expect that a driver with a relatively flexible torso could increase his eye height without an increase in muscle activity by reducing lumbar spine flexion. Yet, substantial reductions in lumbar spine flexion in driving postures do not appear to be feasible. When drivers were instructed to sit in a manner intended to minimize lumbar spine flexion, they were able to reduce it by only about seven degrees, even in a seat with a prominent lumbar support. A previous study led to similar observations (Reed and Schneider, 1996). Apparently, pelvis orientation in

vehicle seated postures is substantially constrained, possibly by the effects of hamstring tension resulting from extended-knee lower extremity postures (Reed et al., 1995). Since drivers cannot gain substantial increases in eye height by reducing lumbar spine flexion, torso posture selection is essentially reduced to a single degree of freedom, represented by overall torso recline or seatback angle. As the results of this study demonstrate, preferred seatback angles, and hence torso postures, can be predicted by the choosing the most upright posture for which the upper lumbar spine experiences a net extension moment due to the action of gravity on the upper body.

There are some important limitations to this research, most notably that the small sample size restricts the generality of the findings. The posture and muscle-activity measurements were recorded after only a short sitting period. A longer-duration sitting session might have resulted in different behavior, particularly at the extreme seatback angle conditions. The study also considered only relatively young, healthy subjects. Elderly subjects, or those with low-back-pain, might exhibit different posture selection behavior. Each of these limitations to the current study highlights an avenue for future research to expand the understanding of torso posture selection.

7.8 References

- Åkerblom, B. (1948). Standing and sitting posture with special reference to the construction of chairs. Ph.D. dissertation, Karolinska Institutet, A.B. Nordiska Bokhandelin, Stockholm.
- Andersson, G.B.J., Örtengren, R., Nachemson, A., and Elfström, G. (1974a). Lumbar disc pressure and myoelectric back muscle activity during sitting. I. Studies on an experimental chair. *Scandinavian Journal of Rehabilitation Medicine* 6(3): 104-114.
- Andersson, G.B.J., Örtengren, R., Nachemson, A., and Elfström, G. (1974b). Lumbar disc pressure and myoelectric back muscle activity during sitting. IV. Studies on a car driver's seat. *Scandinavian Journal of Rehabilitation Medicine* 6(3): 128-133.
- Bean, J.C., Chaffin, D.B., and Schultz, A.B. (1988). Biomechanical model calculation of muscle contraction forces: A double linear programming method. *Journal of Biomechanics* 21(1): 59-66.
- Chaffin, D.B., and Andersson, G.B.J. (1991). Guidelines for seated work. In *Occupational Biomechanics, Second Edition*, 335-375. New York: John Wiley and Sons, Inc.

- Cleaver, G. E. (1954). Driving seats: An appraisal of the mechanical basis of comfort. *Automobile Engineer* 44:237-241.
- Crowninshield, R.D., and Brand, R.A. (1981). A physiologically based criterion of muscle force prediction in locomotion. *Journal of Biomechanics* 14(11): 798-801.
- Dolan, P., and Adams, M.A. (1993). Influence of lumbar and hip mobility on the bending stresses acting on the lumbar spine. *Clinical Biomechanics* 8:185-192.
- Flannagan, C.A.C., Schneider, L.W., and Manary, M.A. (1996). Development of a new seating accommodation model. SAE Technical Paper 960479. In *Automotive Design Advancements in Human Factors: Improving Drivers' Comfort and Performance (SP-1155)*, 29-36. Warrendale, PA: Society of Automotive Engineers, Inc.
- Floyd, W. F., and Silver, P. H. S. (1955). The function of the erector spinae muscles in certain movements and postures in man. *Journal of Physiology* 129: 184-203.
- Hosea, T.M., Simon, S.R., Delatizky, J., Wong, M.A., and Hsieh, C.-C. (1986). Myoelectric analysis of the paraspinal musculature in relation to automobile driving. *Spine* 11(9): 928-936.
- Jørgensen, K., Fallentin, N., Krogh-Lund, C., and Jensen, B. (1988). Electromyography and fatigue during prolonged low-level static contractions. *European Journal of Applied Physiology* 57:316-321.
- Kippers, V., and Parker, A. W. (1984). Posture related to myoelectric silence of erector spinae during trunk flexion. *Spine* 9(7): 740-745.
- Manary, M.A., Schneider, L.W., Flannagan, C.C., and Eby, B.H. (1994). *Evaluation of the SAE J826 3-D manikin measures of driver positioning and posture*. SAE Technical Paper 941048. Warrendale, PA: Society of Automotive Engineers, Inc.
- McConville, J.T., Churchill, T.D., Kaleps, I., Clauser, C.E., and Cuzzi, K. (1980). *Anthropometric relationships of body and body segment moments of inertia*. Report no. AMRL-TR-80-119. Wright Patterson Air Force Base, OH: Aerospace Medical Research Laboratories.
- McGill, S., Seguin, J., and Bennett, G. (1994). Passive stiffness of the lumbar torso in flexion, extension, lateral bending, and axial rotation: Effect of belt wearing and breath holding. *Spine* 19(6): 696-704.
- Nussbaum, M.A. (1994). Artificial neural network models for analysis of lumbar muscle recruitment during moderate static exertions. Ph.D. dissertation, University of Michigan, Ann Arbor.
- Nyquist, G.W., and Murton, C.J. (1975). Static bending response of the human lower torso. In *Proc. of the 19th Stapp Car Crash Conference*, 513-541. Warrendale, PA: Society of Automotive Engineers, Inc.
- Nussbaum, M.A. and Chaffin, D.B. (1996). Development and evaluation of a scalable and deformable geometric model of the human torso. *Clinical Biomechanics* 11(1): 25-34.

- Raschke, U. (1994). Lumbar muscle activity prediction under dynamic sagittal plane lifting conditions: Physiological and biomechanical modeling considerations. Ph.D. dissertation, University of Michigan, Ann Arbor.
- Reed, M.P., Schneider, L.W., and Eby, B.A.H. (1995). *The effects of lumbar support prominence and vertical adjustability on driver postures*. Technical Report UMTRI-95-12. Ann Arbor: University of Michigan Transportation Research Institute.
- Reed, M.P. and Schneider, L.W. (1996). Lumbar support in auto seats: Conclusions from a study of preferred driving posture. SAE Technical Paper 960478. In *Automotive Design Advancements in Human Factors: Improving Drivers' Comfort and Performance (SP-1155)*, 19-28. Warrendale, PA: Society of Automotive Engineers, Inc.
- Roe, R.W. (1993). Occupant packaging. In *Automotive Ergonomics*, ed. B. Peacock and W. Karwowski, 11-42. London: Taylor and Francis.
- Sheridan, T.B., Meyer, J.E., Roy, S.H., Decker, K.S., Yanagishima, T., and Kishi, Y. (1991). *Physiological and psychological evaluations of driver fatigue during long term driving*. SAE Technical Paper 910116. Warrendale, PA: Society of Automotive Engineers, Inc.
- Society of Automotive Engineers (1997). *Automotive Engineering Handbook*. Warrendale, PA: Society of Automotive Engineers, Inc.

CHAPTER 8

SUMMARY AND RECOMMENDATIONS

8.1 Review of Objectives

The research presented in this dissertation has the following principal goals, repeated here from Chapter 1:

1. Develop a method of representing whole-body vehicle occupant posture using a kinematic linkage based on joint locations calculated from external body landmarks.
2. Determine the effects of anthropometric variables and changes in seat height, steering wheel position, instrument panel height, and seat cushion angle on driving posture over the relevant range for passenger vehicles.
3. Develop whole-body driving posture prediction models from laboratory data and assess their accuracy using in-vehicle posture data from a large number of drivers.
4. Analyze driving posture from a biomechanical perspective, using muscle activity measurements and biomechanical simulations to determine if driving postures are consistent with a muscle-activity reduction hypothesis.

All of these objectives have been met through the research presented in the preceding chapters. The following sections summarize the findings, highlight the principal contributions of this research, and suggest avenues for further work.

8.2 Summary of Findings

The central objective of this research is to develop a greater understanding of driving posture and to develop tools with which that new knowledge can be applied to vehicle design. A qualitative framework of the posture selection hypothesis, shown in Figure 8.1, was developed to guide the work. The key concept underlying this framework is that driving posture represents a process operating within kinematic constraints imposed by the task, the vehicle geometry, and the driver's anthropometric

and physical limitations. Although there are other factors that may affect posture, such as psychological state, the driver is assumed to act to select the least uncomfortable posture among those that are feasible.

The research in this dissertation develops a quantitative analog to the quantitative model depicted in Figure 8.1. The research proceeded along two lines. First, the effects of changes in several of the key vehicle and seat factors were quantified, without regard to the underlying mechanisms of the observed effects. These observations formed the foundation for three whole-body posture-prediction models, combining statistical and kinematic submodels. Second, an intensive study of ten drivers was used to explore the mechanisms behind the observations.

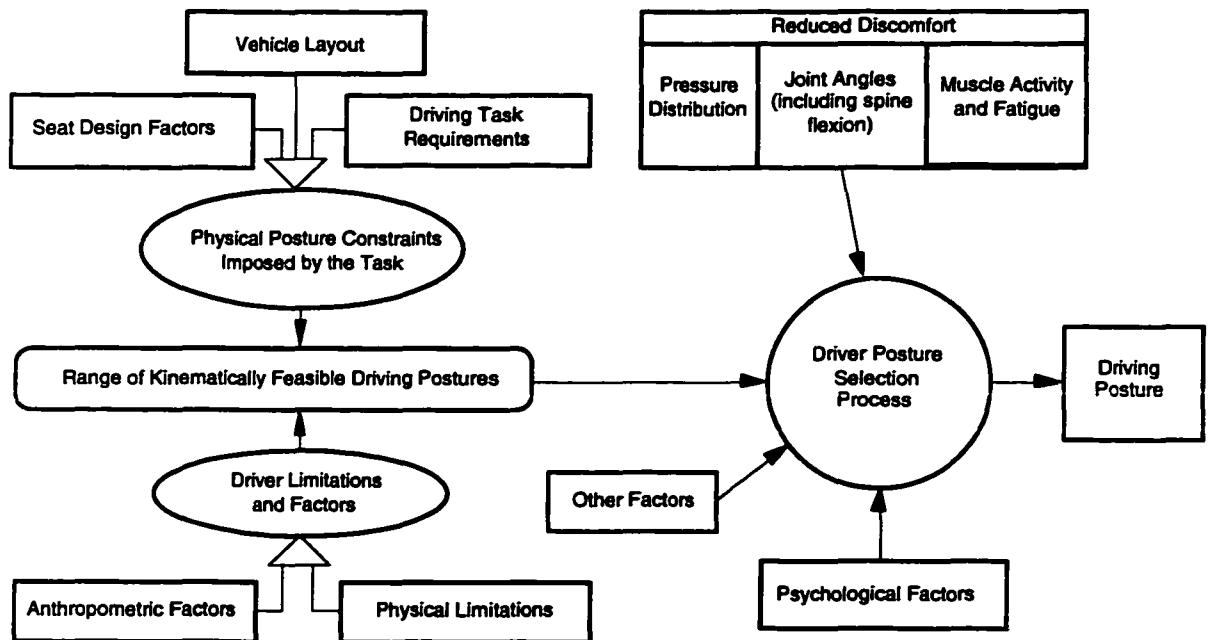


Figure 8.1. Schematic of proposed posture-selection process.

The experimental manipulation of vehicle and seat geometry led to several important conclusions. Seat height, fore-aft steering wheel position, and seat cushion angle have important, independent effects on driving posture. Steering-wheel position is by far the most important of these, in part because it can potentially be varied over a large

range in production vehicles (see Figure 3.3). Moving the steering wheel position forward by 100 mm produced a forward movement of the hips of about 45 mm and a 1.5-degree decrease in overall torso recline. Importantly, the effects of seat height, steering wheel position, and seat cushion angle were also largely independent of body size and each other. The finding of no important interactions among the test variables, including anthropometry, considerably simplifies the formulation and interpretation of posture prediction models.

Statistical Prediction of Driving Posture

Computer software representations of humans, which are increasingly used in vehicle interior design, are currently hampered by the lack of accurate posture prediction. A reach or vision analysis can be invalid if the starting posture of the simulated occupant is inaccurate. In this research, three alternative posture-prediction models were developed. The Cascade Prediction Model (CPM), so named because a number of submodels are used in sequence, was developed with the requirements of vehicle interior ergonomic analysis in mind. The CPM is intended to produce optimally accurate hip and eye location estimates, while potentially sacrificing accuracy in some other postural degrees of freedom. The Independent Prediction Model (IPM) is intended primarily as a contrast to the CPM. The IPM uses multiple independent predictions, although some of the inverse kinematics from the CPM were included to ensure that the IPM produced postures that were kinematically consistent with the task constraints. In practice, the CPM and IPM produced torso postures that were slightly different but both reasonable representations of the data.

The Optimization Prediction Model (OPM) uses an entirely different approach to posture prediction, based largely on the model presented by Seidl (1994). The OPM uses the empirical, joint distribution of posture variables to determine the likelihood of any particular posture and selects the posture that is empirically most likely. There are several important distinctions between the OPM and the Seidl approach. Foremost, the

Seidl model optimization includes many more degrees of freedom than were used in the OPM. The findings from the vehicle mockup study allowed torso recline to be reduced to a single degree of freedom without compromising the accuracy of prediction. While the Seidl technique uses exclusively internal joint angles, the OPM uses the angle of the torso with respect to vertical, rather than the hip angle. The orientation of the torso with respect to gravity, in light of the findings from the biomechanical analysis of driving posture (Chapter 7), is likely to be more meaningfully related to posture selection than hip angle. The OPM further differs in using within-subject angle distributions, and considering the joint distribution, rather than assuming independence. The large number of degrees of freedom in the Seidl model precluded considering the correlations among joint angles, but the test conditions used to develop the model also did not allow those correlations to be observed. Changes in steering wheel position, while maintaining seat height constant, produce correlated changes in elbow and knee angles (Chapter 3). The Seidl experiment, however, did not include these effects, reducing the possibility of exposing these correlations. Using the within-subject angle distributions in the OPM led to the finding of normality, simplifying the optimization process. The within-subject angle distributions are also more directly interpreted as resulting from the driver's internal posture selection process than are the aggregate distributions.

The OPM produced less accurate posture predictions than the other models, mainly because of increasing errors at extreme vehicle geometries. The model could be adjusted to improve the performance, but there are important limitations to the kinematic optimization approach that favor the use of alternative methods like the CPM. The optimization approach is dependent on the definitions of the kinematic constraints at the hands and feet to define the posture. These positions must be identical to those in the input data set, or errors will result. Further, the success of the approach is strongly dependent on the scope of the input data set. For example, if seat height and steering wheel position are not manipulated independently in the input data, the variance in the

elbow and knee angles, relative to torso angles, will be substantially reduced. When these restricted data are used in the optimization, the cost of deviations from the mean elbow and knee angles will be overvalued, resulting in inaccurate tradeoffs between extremity and torso postures. Restrictions in range would also affect the regression models, but to a lesser extent. While the OPM predictions vary with any change in the range of the experimental variables in the input data set, the regression approach used with the CPM is stable once the range of test variables is reasonably large (about 90 mm for seat height and 100 mm for steering wheel position).

The accuracy of the CPM for predicting mean eye location in novel vehicle situations is excellent for the small number of comparisons made. Importantly, the prediction errors in the vehicles also follow the same patterns as in the laboratory, simplifying the process of specifying confidence in the predictions. In general, the CPM can accurately predict the average driving posture of a group of people, whether with the same or different anthropometry, but none of the models can produce accurate predictions of an individual's posture. This appears to be an insurmountable limitation, due to variance in driving postures that is not related to anthropometric variables. Adding additional descriptors does not improve the prediction substantially, and would be of limited practical value in any case. The use of CAD human models for vehicle design is constrained by this limitation. Because there is a substantial amount of variance remaining unaccounted for by the posture prediction models, an accurate representation of the distribution of driving postures will not be obtained by simply running the posture prediction algorithm on a suitable anthropometric distribution. Instead, new techniques of incorporating the error variance into the predictions must be developed in future work.

A New Model of the Posture Selection Process

The effects of steering wheel position on posture lead to some interesting observations concerning the posture-selection process. Almost all of the adaptation to the change occurs in the limb postures, with elbow angles increasing and knee angles

decreasing as the steering wheel is moved forward. The regression coefficient for the hip location (0.45) indicates that just about half of the steering wheel movement is accommodated by the upper extremities and half by the lower. In contrast, torso posture remains nearly constant as the steering wheel position is changed.

These findings indicate that changes in vehicle geometry not only set bounds on the range of feasible postures, but also enter into the posture-selection process. Using the observations that there are only small relative movements among the torso, neck, and head segments between different driving postures, the driving posture can be described using elbow angle, knee angle, and torso recline (note that these are the variables used with the Optimization Prediction Model in Chapter 5). When the steering wheel position is changed, a driver could respond by changing any of these three variables individually, or could change them in some combination. On average, drivers adapt by changing both elbow and knee angles substantially, but the torso angle only slightly. If there were no comfort or driving-effectiveness cost to a change in elbow extension, one might expect changes in steering wheel position to be accommodated entirely by changes in arm posture. Instead, there is an apparent willingness to change the lower-extremity posture in order to decrease the amount of upper-extremity posture change. It seems unlikely, however, that this tradeoff is related directly to discomfort in the elbows or knees. The difference in internal stresses within a 20- or 30-degree band at the center of the range of motion are probably unimportant.

The conflicting requirements that lead to the observed trade-off behavior in limb postures are unknown, but some of the potential factors can be identified. When the seat position is changed, the pressure distribution on the thighs is likely to change, and, in general, the manner in which the thighs are supported by the seat will change. For the upper extremities, moving the steering wheel forward increases the amount of gravity-induced moment that must be managed. The experiments in Chapter 6 demonstrate that drivers use a strategy to interact with the steering wheel that is consistent with stabilizing

the contribution to torso flexion moment imposed by the upper extremities. Moving the steering wheel rearward would seem to decrease these problems, but also decreases the free space in front of the driver. Preferred steering wheel positions appear to be located at the point in the elbow-angle curve at which the shoulder forces in an arm-hang posture begin to mount rapidly, suggesting that preferred steering wheel positions represent a tradeoff between keeping the steering wheel as far forward as possible and controlling the contribution of the upper extremities to torso flexion moment. Perhaps, then, drivers tolerate some discomfort related to pressure distribution and thigh support to maintain moderate muscle exertion requirements for steering wheel interaction.

While drivers use their extremities to adapt to changes in vehicle geometry, the findings show that drivers do not adapt to changes in steering wheel position with substantial changes in torso posture. In fact, torso posture is poorly predicted by any anthropometric or task variables, yet an individual's torso posture is very stable across different seat and vehicle conditions. This observation, along with the finding from a previous study that lumbar supports have only a small effect on drivers' spine flexion (Reed and Schneider, 1996), led to a more intensive, biomechanical study of torso posture (Chapter 7).

Drivers are hypothesized to use a muscle-activity reduction criterion in selecting a posture. In general, postures that minimize muscle activity requirements are reclined, but more upright postures facilitate the driving task through an improved visual field and greater forward reach. If muscle activity varied continuously throughout a wide range of recline, it would be necessary to infer a continuous trade-off between the task requirements and muscle activity, making it necessary to develop a cost function to determine the optimal recline. However, a number of researchers have previously shown that back extensor activity varies non-linearly with seatback angle (Andersson et al., 1974a, 1974b; Hosea et al., 1986). On average, back extensor activity reaches a resting level with seatback angles of 20 to 30 degrees (Andersson et al., 1974b), when the weight

of the thorax creates a net extension moment on the lumbar spine, and remains at low levels as the seatback angle is reclined further. This pattern of muscle activity places an inflection point, at which the thoracolumbar extensor activity begins to rise, at approximately the average seatback angles preferred by drivers. The trade-off can then be accomplished using one continuous measure (driving efficacy increasing with more upright postures), and one binary measure (back extensors on/off). Drivers are hypothesized to choose the most upright posture, characterized by the greatest eye height above the hips, that can be achieved with near resting-level back extensor exertion.

Although such transition points are notoriously difficult to determine experimentally, two hypotheses serve to test whether preferred driving postures lie at this point in the back-extensor activity curve. First, back extensor activity in preferred driving postures is hypothesized to be low. Second, muscle activity is hypothesized to increase for seatback angles more upright than preferred, but remain at consistently low levels for more reclined seatback angles.

Both hypotheses were supported by the research findings. Thoracolumbar extensor activity in preferred driving postures was typically below 5% of a standardized maximal exertion. At the T12 electrode site, muscle activity increased significantly for more upright seatback angles and did not change for more reclined seatback angles. There was, however, considerable intersubject variability in response. All subjects had low levels of muscle activity in their preferred driving postures, and all showed decreasing or constant, low activity for more reclined postures, but some did not show substantial increases for more upright postures. The findings from the biomechanical simulations suggest a possible reason why some subjects could tolerate decreases in seatback recline without increases in back extensor activity.

The biomechanical model of driving posture was created to facilitate an understanding of the forces and moments that are experienced in driving postures, and to observe how these change with posture (Chapter 7). Two important findings were made

simply by configuring the model to match the average anthropometry and preferred driver and passenger postures. First, the average preferred driver and passenger postures are very similar, suggesting that when drivers are free to choose the fore-aft position of the steering wheel, the presence of the hand task does not affect torso, neck, and head posture. Since changes in steering wheel position in a separate study only slightly affected torso posture (Chapter 3), torso postures appear to be, to a reasonable approximation, independent of the hand task location. Second, preferred driver and passenger postures are characterized by an approximately vertical alignment of the key joints and centers of mass in the thorax, neck, and head. Moment calculations show that this alignment results in the upper body being nearly balanced with respect to gravity, effectively eliminating the need for substantial active or passive support moments.

If the segments of the torso moved independently between alternative driving postures, there would be considerably greater complexity to evaluating the effects of posture change on gravitational loading. However, torso kinematics in driving postures can be adequately represented using only a single degree of freedom (Chapter 7). When the seatback angle is changed, imposing a range of torso recline, the angle change is distributed unequally among the torso segments, but the pattern is fairly consistent across subjects and seatback angles. The neck and head articulate to maintain the head approximately level, and also maintain the head center of mass approximately over the lower neck joint. The lumbar spine extends slightly as the torso is reclined, but, more importantly, the distribution of flexion in the lumbar spine appears to change. Based on the observed positions and orientations of the pelvis and thorax, recline appears to be accompanied by a reduction in flexion at the lower levels of the lumbar spine together with an increase in flexion at the upper levels. This pattern is observed whether the change in recline is induced by changing the steering wheel position (Chapter 3) or by changing the seatback angle (Chapter 7). Although the reasons for this redistribution of

lumbar flexion with recline are unknown, the analysis of the potential effects of torso flexion stiffness on posture stability suggest a potential explanation.

Based on a synthesis of data from the literature, the passive flexion resistance of the torso appears to be able to contribute substantially to the support of the upper body in driving postures. Using a scaled stiffness function intended to be typical, a 12-Nm passive moment at T12/L1 was estimated to be available when the spine was flexed 65%, the average value for these subjects. Importantly, the shape of the passive stiffness curve was found to affect the relationships between posture change and muscle activity requirements. If the stiffness is great enough near the end of the range of spine flexion, then the increases in flexion moment due to decreases in torso recline are fully compensated by increases in the available passive moment, allowing the driver to sit more upright without increased back extensor activity. This pattern of minimal increases in back extensor activity at more upright seatback angles was observed with several subjects. For these subjects, the posture-selection hypothesis might be revised to choose the most upright posture characterized by low passive or active extension moments.

The change in the distribution of motion in the lumbar spine with changes in recline may result from a stiffness gradient in the lumbar area, combined with changes in moment distribution with recline. Because the lumbar spine, in aggregate, is approximately aligned with the seatback angle, the flexion moments at the lower lumbar spine are lower and decrease more rapidly with recline than those at T12/L1. This decrease in moment may cause the lower lumbar spine to return passively to a less flexed posture. However, decreasing the flexion in the lower lumbar spine may reduce the passive stiffness of the upper lumbar area, via decreases in muscle length, allowing flexion to increase in the upper lumbar spine even as the flexion moment in that area is decreasing. More study and more sophisticated models will be necessary to understand these effects.

Applications of the New Posture Selection Model

The findings from this research and several preceding studies (Reed et al., 1991; Reed and Schneider, 1996), indicate that some prevailing concepts of seating, particularly for automobile occupants, should be revised. Since the 1950s, the literature of ergonomic seating has focused on lumbar lordosis as the ultimate goal of seat design. Åkerblom (1948), in pioneering work, identified three “rest” postures in which muscle activity was minimal, including a forward slumped posture. He also noted that a seatback can effectively support the torso while providing support force to only a small area of the back. Support in other areas might improve comfort and stability, but was not necessary to the essential function of the seatback of holding the torso in a comfortable work posture and reducing, or eliminating, muscle activity. Keegan (1953) was responsible, more than any other researcher, for bringing lumbar spine posture to the forefront of seating ergonomics. Using radiography, he demonstrated that changes in sitting posture are accompanied by changes in spine flexion. He noted, anecdotally, that patients with low-back pain achieved some relief by sitting in a supportive chair with reduced spine flexion, and concluded that healthy people could likewise benefit from sitting with a lordotic lumbar spine contour. He later applied his recommendations to automobile seats, suggesting that a longitudinally convex lumbar support could induce lordosis and thereby improve comfort (Keegan, 1964).

Meanwhile, Floyd and Silver (1955) and others demonstrated that muscle activity varied widely in sitting postures, noting that reclined, supported postures, as well as slumped, unsupported postures were both characterized by near-resting-level back extensor exertion. Andersson et al. (1974a, 1974b), in the most influential work since Åkerblom, studied both muscle activity and the pressure inside the lumbar intervertebral disks for a wide range of seated postures and tasks. Andersson, whose work included a study on a car seat, found that disk pressure increased with spine flexion and with activity in the back extensors. Concluding that higher disk pressures increased the risk of low-

back injury, he recommended prominent lumbar supports and reclined postures (Andersson et al., 1974b). These findings have had great appeal to seat designers, because they apparently establish a link between posture and a health outcome. In more recent years, however, Adams and Hutton (1985) have questioned whether the low pressure levels in quiescent sitting can contribute to spine injury, and suggest a number of advantages to sitting with a flexed lumbar spine. More importantly, longitudinally convex lumbar supports have been found to be ineffective for inducing lordosis, both in auto seats and office chairs (Reed et al., 1995; Reed and Schneider, 1996; Bendix et al., 1996). Although sitters can, when instructed, actively maintain a lordosis around a lumbar support, sitter-preferred postures usually include a flexed lumbar spine. One can conclude that there are physiological reasons, most likely related to discomfort, that lead people to choose flexed-spine sitting postures.

The analyses in the current work suggest that the answer may be that sitters strive for passive torso stability. By flexing the lumbar spine, a sitter's thorax can be supported in an upright posture, suitable for many tasks, without appreciable muscle exertion. Importantly, because of the nonlinear characteristic of the passive flexion/moment curve, increase in moment due to posture perturbations can potentially be offset passively, without requiring muscle activity to re-balance the posture. In auto seats, there appears to be a further limit on lumbar spine extension in sitting postures arising from restrictions on pelvis orientation. Even when instructed to sit in a manner intended to minimize posterior pelvis rotation, the ten drivers in the current research were able to reduce their lumbar spine flexion by only 6 degrees. In a study with 32 subjects, the average change was 10 degrees using an identical procedure (Reed and Schneider, 1996). Given these apparent restrictions on pelvis orientation, likely due in part to hamstring muscle tension, an upright thorax orientation suitable for driving can only be achieved with substantial lumbar spine flexion.

These findings do not suggest that lumbar support in sitting is unimportant, but rather that its function should be reassessed. Andersson et al. (1974a, 1974b) demonstrated clearly that stresses in and near the spine are reduced when spine flexion is reduced. Dolan and Adams (1993) and others have demonstrated that stiffness in the spine and paraspinal tissues is nonlinear, with stresses increasing more rapidly as the end of the range of motion is approached. Consequently, relatively small reductions in flexion can substantially change the tissue stresses when the lumbar spine is flexed considerably. So, although Reed and Schneider (1996) noted only a 10% reduction in lumbar spine flexion with a 45-mm change in lumbar support prominence, this 10%, occurring at 60 to 70 percent of full flexion, probably results in a large decrease in tissue stress. The challenge for the seat designer is to accomplish these small, but potentially important changes in posture, without imposing uncomfortably high pressure concentrations in the lower back. The goal of inducing lordosis in automobile driving postures should be discarded, because sitters do not choose lordotic postures. However, small, potentially important reductions in lumbar spine flexion can be achieved through seatback design that recognizes, as sitters unconsciously do, the stability advantages of flexed postures.

Although the experimental scope in this research does not directly support generalization of the posture-selection model, there are a number of observations that indicate applicability beyond vehicle environments. First, passenger postures were observed to be very similar to driving postures, for a range of steering wheel locations. This suggests that the hand task location may not strongly affect torso posture, which may therefore be determined primarily by the hypothesized internal discomfort minimization. For tasks with fairly neutral hand location restrictions and forward, approximately horizontally directed vision, the same posture selection process may apply, and the same hypotheses may hold. In particular, VDT operation may be amenable to a similar analysis. Grandjean et al. (1983) and Bendix et al. (1996) both found that VDT

operators tend to choose reclined postures, rather than the upright, lordotic postures. The posture-selection hypothesis explored in the current research, that drivers choose postures to maximize eye height while maintaining low back extensor exertion, may also be successful in predicting postures for other quiescent seated tasks.

Limitations

The experiments in this dissertation each have important limitations that affect the generality of the findings. For all of the studies, the subjects were relatively fit, adult drivers, generally representative of the population. However, the findings may not be applicable to some groups of people, such as the very elderly, those with physical disabilities, or those who are obese. In the electromyographic study (chapter 7), the small number of subjects and their homogeneity may restrict the applicability of the findings to other subject groups. In several of the studies, some additional factors might be considered in future studies. For example, additional seat geometry factors might be examined in relation to torso posture, and the effects of task difficulty on driving posture in the presence of forward vision restriction could be examined. The fact that the subjects were aware that their postures were to be measured should also not be overlooked.

Other potential influences on the posture selection process that were not directly addressed in this work include vibration and the task duration. While these two factors were not manipulated experimentally, the potential effects of normal on-road vibration were implicit in the comparison of posture predictions developed from static, vehicle-mockup data with postures measured in vehicles driven over a road route. With regard to driving duration, a previous study found that driving postures do not change substantially over a one-hour driving simulation (Reed et al., 1995), so short-term measurements of posture are likely to be adequate for most vehicle design tasks.

8.3 Principal Contributions

The research in this dissertation, summarized in the preceding paragraphs, resulted in a number of substantial contributions to the knowledge of driving posture.

1. Development of methods for representing three-dimensional driving postures using a kinematic model. The methods presented in Chapter 2 are a synthesis of information from a number of literature sources, combined with new data and analysis. This represents the first time that such methods have been developed specifically for representing normal vehicle occupant postures. The techniques are intended to be generally consistent with previous work, with particular connection to the work of Robbins (1985), which comprises the anthropometric standards for the new generation of crash dummies. A minimal set of body landmark locations is used to calculate internal joint locations that define a kinematic linkage. The positions and orientations of these kinematic links are the basic variables used to describe and predict driving posture.

2. Determining the quantitative effects of anthropometric, vehicle, and seat variables on driving posture. Experiments in laboratory mockups, confirmed in part by in-vehicle testing, demonstrated the effects of seat height, fore-aft steering wheel position, seat cushion angle, and forward vision restriction on driving posture. Using subjects from a large anthropometric range allowed determination of the direct and interactive effects of anthropometric variability.

3. Quantifying the kinematics of torso recline in driving. Torso recline, over the range of interest for driving postures, was found to involve a fairly complex distribution of motion throughout the spine. A quantitative description of the motion distribution patterns reduced the torso recline to a single degree of freedom without compromising the essential characteristics of the movement.

4. Developing a new biomechanical model to predict driving posture using a muscle-activity-reduction hypothesis. A qualitative model of the posture selection process was developed to examine specific quantitative hypotheses concerning posture-selection behavior. Driving posture was proposed to result from balance between physical task requirements and the driver's comfort. Drivers were hypothesized to select the torso postures that provided the highest eye location with respect to the hips while

maintaining resting-level back extensor exertion. Head and neck postures were similarly balanced to reduce static neck muscle exertion. Biomechanical simulations and experimental perturbations of drivers' preferred postures provided results largely consistent with the hypotheses.

5. Developing and assessing three alternative statistical posture-prediction models applicable to CAD human models. Using data from experiments in a vehicle mockup, three alternative techniques of posturing a three-dimensional kinematic representation of a driver were developed and evaluated. The Cascade Prediction Model, a new approach to posture prediction intended to produce optimal accuracy for the most important postural degrees of freedom, was found to be highly accurate for predicting average in-vehicle driving postures.

8.4 Recommendations for Future Research

The findings of this research, in the context of previous work related to seated postures, suggest several areas for future investigation.

1. Integration of additional seat and vehicle factors into the posture prediction models. While the posture prediction models presented in this work include several of the most important vehicle and seat factors, other potentially important factors are not yet included. Seatback contour (lumbar support), already known to have significant effects, should be included as soon as adequate measurements are available. Other factors that should be investigated include transmission type (effects of clutch and shifter location), headroom restriction, seatback angle (for fixed seatbacks), and censoring (seat track length and seatback angle).

2. Investigations of the effects of additional adjustments on driving posture. The current posture-prediction models are applicable only to the situation where the driver is provided with a fore-aft seat adjustment and an adjustable-recline seatback. When additional adjustments are provided, such as seat height or seat cushion angle, the preferred driving postures may be different. Research into these effects should

also include other factors, such as adjustable steering wheel positions and lumbar support prominences. In general, a coherent theory of postural response in the presence of adjustable components is needed.

3. Study of dynamic posture selection in extended-duration driving. The generality of the findings from the current research could be extended by examining dynamic postures in driving, particularly under long-term driving conditions. Drivers shift their postures regularly during driving, and quantification of these posture changes would allow broader application of the posture selection models developed in the current work.

4. Examination of the role of discomfort in posture selection. Muscle activity minimization was proposed as a possible mechanism of posture selection, providing a potential explanation for the predictive ability of back extensor activity. Muscle exertion reduction might be part of a general process of discomfort reduction, which would include simultaneously minimizing other types of discomfort-causing stresses. A study combining muscle activity measurement with subjective discomfort assessment and pressure distribution measurement could be conducted to examine the relationships among these potential sources of discomfort, the sitter's perception, and posture selection.

5. Application of the experimental and analysis methods to other seated work. The biomechanical methods developed in this work should be applied to the study of other types of seated work. The most direct application, because of similarities in task requirements, would be VDT operation, which is also an increasingly prevalent work task. The investigations should focus on the postural responses to changes in the workstation geometry, and should use the biomechanical analysis to determine if the hypotheses concerning torso posture selection explored in the current research are also valid for VDT operation.

6. In-depth investigation of the role of passive torso stiffness in stabilizing seated postures. The experiments and analyses in this dissertation suggest that passive torso stiffness may be a more important contributor to seated posture stability, and a more important part of the posture-selection process, than previously considered. Further in-depth investigation of the character and function of torso flexion stiffness should be conducted and the results reflected in the development of more complete biomechanical models of the torso for use in analysis of seated work.

8.5 References

- Adams, M.A., and Hutton, W.C. (1985). The effect of posture on the lumbar spine. *Journal of Bone and Joint Surgery* 67-B(4): 625-629.
- Åkerblom, B. (1948). Standing and sitting posture with special reference to the construction of chairs. Ph.D. dissertation, Karolinska Institutet, A.B. Nordiska Bokhandeln, Stockholm.
- Andersson, G.B.J., Örtengren, R., Nachemson, A., and Elfström, G. (1974a). Lumbar disc pressure and myoelectric back muscle activity during sitting. I. Studies on an experimental chair. *Scandinavian Journal of Rehabilitation Medicine* 6(3): 104-114.
- Andersson, G.B.J., Örtengren, R., Nachemson, A., and Elfström, G. (1974b). Lumbar disc pressure and myoelectric back muscle activity during sitting. IV. Studies on a car driver's seat. *Scandinavian Journal of Rehabilitation Medicine* 6(3): 128-133.
- Bendix, T., Poulsen, V., Klausen, K., and Jensen, C.V. (1996). What does a backrest actually do to the lumbar spine? *Ergonomics* 39(4): 533-542.
- Floyd, W. F., and Silver, P. H. S. (1955). The function of the erectores spinae muscles in certain movements and postures in man. *Journal of Physiology* 129: 184-203.
- Grandjean, E., Hünting, W., and Pidermann, M. (1983). VDT workstation design: preferred settings and their effects. *Human Factors* 25(2): 161-175.
- Hosea, T.M., Simon, S.R., Delatizky, J., Wong, M.A., and Hsieh, C.-C. (1986). Myoelectric analysis of the paraspinal musculature in relation to automobile driving. *Spine* 11(9): 928-936.
- Keegan, J.J. (1953). Alterations of the lumbar curve related to posture and seating. *Journal of Bone and Joint Surgery* 35-A(3): 589-603.
- Keegan, J.J. (1964). *The medical problem of lumbar spine flattening in automobile seats.* SAE Technical Paper 838A. New York, NY: Society of Automotive Engineers, Inc.

- Reed, M. P., Saito, M., Kakishima, Y., Lee, N. S., and Schneider, L. W. (1991). *An investigation of driver discomfort and related seat design factors in extended-duration driving*. SAE Technical Paper 910117. (Also in *1991 SAE Transactions* 100.) Warrendale, PA: Society of Automotive Engineers, Inc.
- Reed, M.P., Schneider, L.W., and Eby, B.A.H. (1995a). Some effects of lumbar support on driver seated posture. SAE Technical Paper 950141. In *Human Factors in Vehicle Design: Lighting, Seating and Advanced Electronics (SP-1088)*, 9-20. Warrendale, PA: Society of Automotive Engineers, Inc.
- Reed, M.P. and Schneider, L.W. (1996). Lumbar support in auto seats: Conclusions from a study of preferred driving posture. SAE Technical Paper 960478. In *Automotive Design Advancements in Human Factors: Improving Drivers' Comfort and Performance (SP-1155)*, 19-28. Warrendale, PA: Society of Automotive Engineers, Inc.
- Seidl, A. (1994). *Das Menschmodell RAMSIS: Analyse, Synthese und Simulation dreidimensionaler Körperhaltungen des Menschen [The man-model RAMSIS: Analysis, synthesis, and simulation of three-dimensional human body postures]*. Ph.D. dissertation, Technical University of Munich, Germany.

APPENDIX

VEHICLE PACKAGING TERMINOLOGY AND PRACTICES

Like any other technical field, automobile interior packaging has its own terminology and practices that can make the literature inaccessible to an interested person lacking background in the field. The purpose of this appendix is to provide some basic information on occupant packaging to assist in the understanding of the work presented in this thesis. For a more complete presentation of contemporary practices, see Ron Roe's excellent chapter in *Automotive Ergonomics* (Roe, 1993) or consult the *Society of Automotive Engineers Handbook* (SAE, 1997).

The Society of Automotive Engineers (SAE) has developed, through committees of interested auto industry practitioners, a large number of standard practices published annually in the *SAE Handbook*. Several of these practices are important to vehicle occupant packaging, among them:

- Driver Hand Control Reach, SAE J287
- Devices for Use in Defining and Measuring Vehicle Seating Accommodation, SAE J826
- Motor Vehicle Driver's Eye Range, SAE J941
- Motor Vehicle Driver and Passenger Head Position, SAE J1052
- Motor Vehicle Dimensions, SAE J1100
- Accommodation Tool Reference Point, SAE J1516
- Driver Selected Seat Position, SAE J1517

Figure A1 shows several of the key reference points used to define the vehicle occupant space. All three are defined and measured using tools specified in SAE J826. The SAE H-point machine is a weighted manikin that defines and is used to measure a point relative to the seat known as the H-point (for hip point). Figure A1 depicts the SAE 2-D template, a planar representation of the contours of the H-point machine. The H-

point moves with the seat, defining a travel path as the seat is moved throughout its range of adjustment. For a seat on a flat, two-way track, the path is a line in side view. The angle that the H-point travel path forms with the horizontal is called the seat track angle (or rise). There is a particular point on this travel path known as the design H-point, also called the Seating Reference Point (the abbreviated form is SgRP to distinguish it from a previous seating reference point defined using a different procedure). The SgRP is intended to be the rearmost normal driving position, but manufacturers locate the point in different ways. Some place the point at the expected 95th percentile of the driver-selected seat position distribution. Others select the rearmost position on the seat track. When a seat is equipped with a height-adjustable seat, the definition of the SgRP is even more variable. Some manufacturers define the SgRP using the middle seat height to define the fore-aft travel path, while others use the full-down/full-rear position. This difference in definitions may not pose problems for the designers, who have adjusted their accommodation tools to suit to their definitions, but it does create difficulty for cross-vehicle comparisons and standards development. Efforts are currently underway to define a more consistent standard.

When the H-point manikin or 2-D template are installed according to the procedures specified in SAE J826, and the seat is located in the design position, the heel and ball-of-foot locations on the manikin foot define two reference points, called the Accelerator Heel Point (AHP) and the Ball of Foot (BOF). The AHP defines the horizontal plane from which vertical package measurements are made, while the BOF defines a vertical plane to which most horizontal measurements are referenced.

Many interior dimensions have standardized definitions given in SAE J1100, and many of these measurements are made with respect to the three reference points (SgRP, AHP, and BOF) defined using the J826 H-point machine. In J1100, dimensions are specified using a letter and a number. Dimensions beginning with "H" are vertical measurements, those beginning with "L" are fore-aft horizontal measurements (or

angles), and those beginning with “W” are lateral horizontal measurements. Seat height is defined by SAE H30, and is the vertical distance from AHP to SgRP. A typical value for a midsize sedan is 250 mm. Steering wheel position is measured with respect to AHP and BOF as well. In the present research, the fore-aft distance from BOF to the center of the steering wheel is an important package dimension. Unfortunately, this measurement is not defined in SAE J1100, which instead defines L11, the fore-aft distance from AHP to the center of the steering wheel. The measure to BOF is preferred for posture prediction because the horizontal distance between AHP and BOF varies with seat height, potentially confounding the two variables. In addition to defining and measuring the H-point, the H-point machine is used to define and measure seat cushion angle (L27). This measure of the seat independent of the package is an important determinant of posture and seat position.

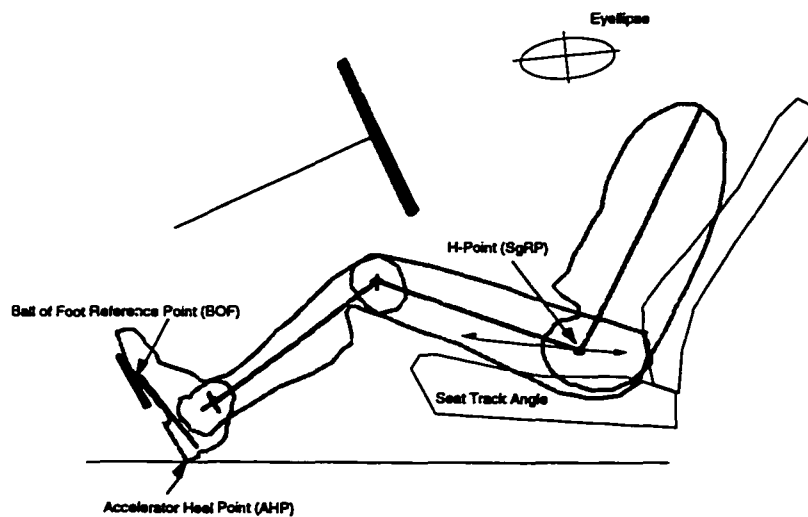


Figure A1. Side-view schematic of driver's station.

SAE practices provide several task-oriented percentile models that define functional characteristics of driving postures. SAE J1517 gives second-order polynomials that predict a number of percentiles of the driver-selected seat position distribution as a function of seat height. J941 defines the eyellipse, a statistical construct

predicting the distribution of driver eye locations. The centroid of the eyellipse is the predicted mean eye location. The ellipse is constructed so that any line tangent to the ellipse in side-view plane divides the eye location distribution according to the percentile specification of the ellipse. So, a line tangent to the 95th-percentile eyellipse divides the eye location distribution into 5% and 95% parts. This construction has been found to be more useful than a density ellipse, which would contain a specified percentage of the distribution. The driver's eyellipse in current SAE practice is a function of SgRP location, design seatback angle, and seat track length. The inclusion of seatback angle is a holdover from a time when few driver seats had adjustable-angle seatbacks. Now that almost all do, the accuracy of the eyellipse location is dependent on the designer's ability to select an accurate design seatback angle.

This brief summary is intended to assist the reader in the interpretation of this thesis. For a more detailed treatment of current packaging practices, see Roe (1993), which includes references to the research studies used to develop the current practices.

References

Roe, R.W. (1993). Occupant Packaging, in Karwowski and Peacock, eds., *Automotive Ergonomics*, London:Taylor and Francis.

Society of Automotive Engineers (1997). *1997 Automotive Engineering Handbook*. Warrendale, PA:Society of Automotive Engineers.

BIBLIOGRAPHY

- Abraham, S., Johnson, C. L., and Najjar, M. F. (1979). *Weight by height and age for adults 18-74 years: United States, 1971-74, Vital and health statistics, Series 11, No. 208*. DHEW Publication No. 79-1656. Hyattsville, MD: U.S. Department of Health, Education, and Welfare.
- Adams, M.A., and Hutton, W.C. (1985). The effect of posture on the lumbar spine. *Journal of Bone and Joint Surgery* 67-B(4): 625-629.
- Åkerblom, B. (1948). Standing and sitting posture with special reference to the construction of chairs. Ph.D. dissertation, Karolinska Institutet, A.B. Nordiska Bokhandelin, Stockholm.
- Andersson, G.B.J., and Örtengren, R. (1974). Lumbar disc pressure and myoelectric back muscle activity during sitting. II. Studies on an office chair. *Scandinavian Journal of Rehabilitation Medicine* 6(3): 115-121.
- Andersson, G.B.J., Murphy, R.W., Örtengren, R., and Nachemson, A.L. (1979). The influence of backrest inclination and lumbar support on lumbar lordosis. *Spine* 4(1), 52-58.
- Andersson, G.B.J., Örtengren, R., Nachemson, A., and Elfström, G. (1974). Lumbar disc pressure and myoelectric back muscle activity during sitting. I. Studies on an experimental chair. *Scandinavian Journal of Rehabilitation Medicine* 6(3): 104-114.
- Andersson, G.B.J., Örtengren, R., Nachemson, A., and Elfström, G. (1974). Lumbar disc pressure and myoelectric back muscle activity during sitting. IV. Studies on a car driver's seat. *Scandinavian Journal of Rehabilitation Medicine* 6(3): 128-133.
- Arnold, A.J., Ferrara, R.A., and Kuechenmeister, T.J. (1985). Driver eyellipses produced by minimum deflection seats and by U.S. adult population changes. In *Proc. of the 29th Annual Meeting of the Human Factors Society, Volume I*, ed. R.W. Swezey, L.B. Strother, T.J. Post, and M.G. Knowles, 447-451. Santa Monica, CA: Human Factors Society.
- Asano, H., Yanagishima, T., Abe, Y., and Masuda, J. (1989). *Analysis of primary equipment factors affecting driving posture*. SAE Technical Paper 891240. Warrendale, PA: Society of Automotive Engineers, Inc.
- Babbs, F.W. (1979). A design layout method for relating seating to the occupant and vehicle. *Ergonomics* 22(2): 227-234.
- Backaitis, S.H., and Mertz, H.J., eds. (1994) *Hybrid III: The first human-like crash test dummy*. Special Publication PT-44. Warrendale, PA: Society of Automotive Engineers, Inc.

- Bean, J.C., Chaffin, D.B., and Schultz, A.B. (1988). Biomechanical model calculation of muscle contraction forces: A double linear programming method. *Journal of Biomechanics* 21(1): 59-66.
- Bell, A.L., Pedersen, D.R., and Brand, R.A. (1990). A comparison of the accuracy of several hip center location prediction methods. *Journal of Biomechanics* 23(6): 617-621.
- Bendix, T., Poulsen, V., Klausen, K., and Jensen, C.V. (1996). What does a backrest actually do to the lumbar spine? *Ergonomics* 39(4): 533-542.
- Bohlin, N., Hallen, A., Runberger, S., and Aasberg, A. (1978). *Safety and comfort--Factors in Volvo occupant compartment packaging*. SAE Technical Paper 780135. Warrendale, PA: Society of Automotive Engineers, Inc.
- Boughner, R. L. (1991). A model of average adult male human skeletal and leg muscle geometry and hamstring length for automotive seat designers. Master's thesis, Michigan State University, Department of Metallurgy, Mechanics, and Material Science, East Lansing.
- Box, G.E.P., and Draper, N.R. (1987). *Empirical model-building and response surfaces*. New York: Wiley and Sons, Inc.
- Branton, P. (1969). Behaviour, body mechanics and discomfort. *Ergonomics* 12(2): 316-327.
- Bush, N.J. (1993). Two-dimensional drafting template and three-dimensional computer model representing the average adult male in automotive seated postures. Master's thesis, Michigan State University, East Lansing.
- Chaffin, D.B. (1973). Localized muscle fatigue-definition and measurement. *Journal of Occupational Medicine* 15:346.
- Chaffin, D.B., and Andersson, G.B.J. (1991). Guidelines for seated work. In *Occupational Biomechanics, Second Edition*, 335-375. New York: John Wiley and Sons, Inc.
- Cleaver, G. E. (1954). Driving seats: An appraisal of the mechanical basis of comfort. *Automobile Engineer* 44:237-241.
- Crowninshield, R.D., and Brand, R.A. (1981). A physiologically based criterion of muscle force prediction in locomotion. *Journal of Biomechanics* 14(11): 798-801.
- Dempster, W.T. (1955). *Space requirements of the seated operator: Geometrical, kinematic, and mechanical aspects of the body with special reference to the limbs*. WADC Technical Report 55-159. Wright-Patterson AFB, OH: Wright Air Development Center.
- Devlin, W.A., and Roe, R.W. (1968). *The eyellipse and considerations in the driver's forward field of view*. SAE Technical Paper 680105. New York, NY: Society of Automotive Engineers, Inc.
- Dolan, P., and Adams, M.A. (1993). Influence of lumbar and hip mobility on the bending stresses acting on the lumbar spine. *Clinical Biomechanics* 8:185-192.

- Drillis, R., and Contini, R. (1966). *Body segment parameters* (PB174 945). University Heights, NY: New York University, School of Engineering and Science.
- Ewing, C.L., and Thomas D.J. (1972) *Human head and neck response to impact acceleration*. NAMRL Monograph 21. Pensacola, FL: Naval Aerospace Medical Research Laboratory.
- Flannagan, C.A.C., Schneider, L.W., and Manary, M.A. (1996). Development of a new seating accommodation model. SAE Technical Paper 960479. In *Automotive Design Advancements in Human Factors: Improving Drivers' Comfort and Performance (SP-1155)*, 29-36. Warrendale, PA: Society of Automotive Engineers, Inc.
- Floyd, W. F., and Silver, P. H. S. (1955). The function of the erector spinae muscles in certain movements and postures in man. *Journal of Physiology* 129: 184-203.
- Geoffrey, S.P. (1961). *A 2-D mannikin--The inside story. X-rays used to determine a new standard for a basic design tool*. SAE Technical Paper 267A. New York, NY: Society of Automotive Engineers, Inc.
- Grandjean, E. (1980). Sitting posture of car drivers from the point of view of ergonomics. In *Human Factors in Transport Research. Volume 2 - User Factors: Comfort, the Environment and Behaviour*, ed. D.J. Osborne and J.A. Levis, 205-213. New York: Academic Press.
- Grandjean, E., Hünting, W., and Pidermann, M. (1983). VDT workstation design: preferred settings and their effects. *Human Factors* 25(2): 161-175.
- Gross, C.M., Goonetilleke, R.S., Menon, K.K., Banaag, J.C.N., and Nair, C.M. (1993). The biomechanical assessment and prediction of seat comfort. In *Hard Facts About Soft Machines: The Ergonomics of Sitting*, ed. R. Lueder and K. Noro, 231-253. London: Taylor and Francis.
- Haas, W.A. (1989). Geometric model and spinal motions of the average male in seated postures. Master's thesis, Michigan State University, East Lansing.
- Hammond, D.C., and Roe, R.W. (1972). *Driver head and eye positions*. SAE Technical Paper 720200. New York, NY: Society of Automotive Engineers, Inc.
- Hosea, T.M., Simon, S.R., Delatizky, J., Wong, M.A., and Hsieh, C.-C. (1986). Myoelectric analysis of the paraspinal musculature in relation to automobile driving. *Spine* 11(9): 928-936.
- Jørgensen, K., Fallentin, N., Krogh-Lund, C., and Jensen, B. (1988). Electromyography and fatigue during prolonged low-level static contractions. *European Journal of Applied Physiology* 57:316-321.
- Judic, J.M., Cooper, J.A., Truchot, P., Effenterre, P.V., and Duchamp, R. (1993). *More objective tools for the integration of postural comfort in automotive seat design*. SAE Technical Paper 930113. Warrendale, PA: Society of Automotive Engineers, Inc.
- Kaptur, V., and Myal, M. (1961). *The General Motors comfort dimensioning system*. SAE Technical Paper 267B. New York, NY: Society of Automotive Engineers, Inc.
- Keegan, J.J. (1953). Alterations of the lumbar curve related to posture and seating. *Journal of Bone and Joint Surgery* 35-A(3): 589-603.

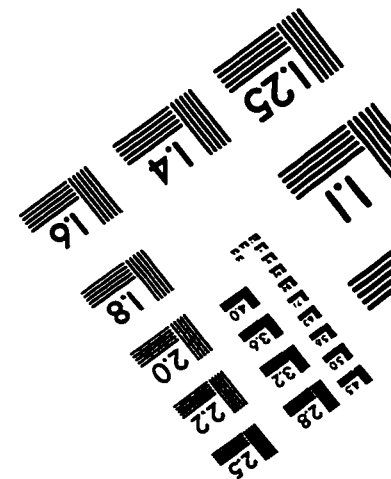
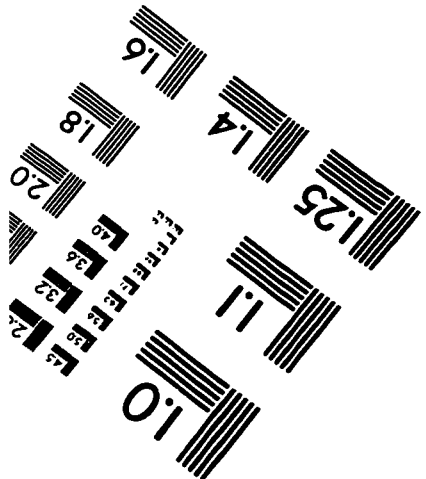
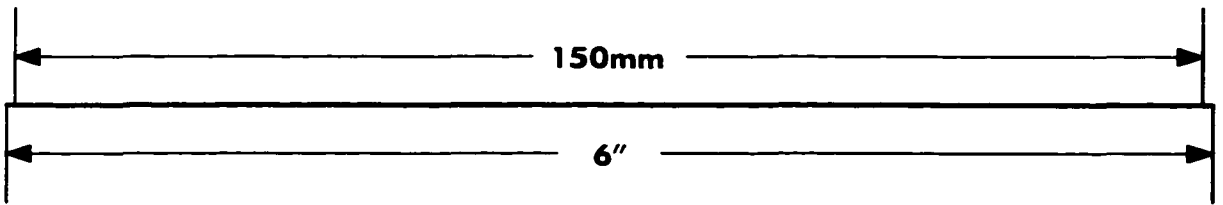
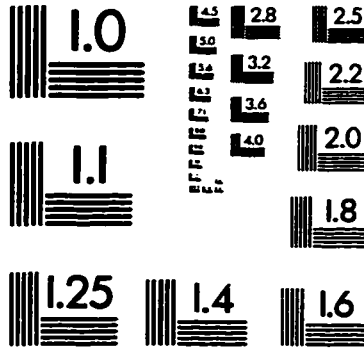
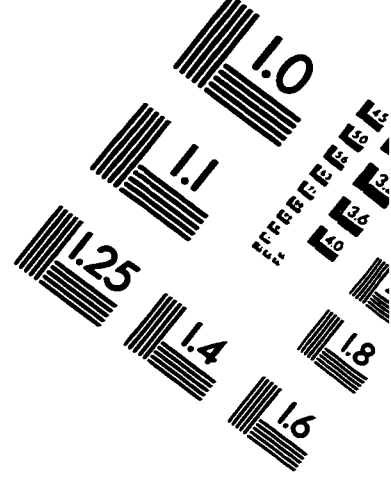
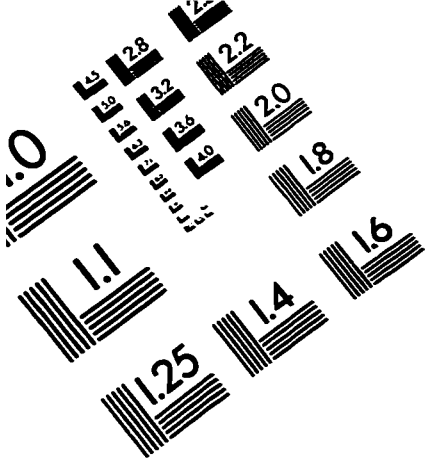
- Keegan, J.J. (1964). *The medical problem of lumbar spine flattening in automobile seats*. SAE Technical Paper 838A. New York, NY: Society of Automotive Engineers, Inc.
- Kippers, V., and Parker, A. W. (1984). Posture related to myoelectric silence of erectors spinae during trunk flexion. *Spine* 9(7): 740-745.
- Lay, W.E., and Fisher, L.C. (1940). Riding comfort and cushions. *SAE Journal* 47(5): 482-496.
- MacAdam, C.C., Green, P.A., and Reed, M.P. (1993). An overview of UMTRI driving simulators. *UMTRI Research Review* 24(1): 1-8.
- Maltha, J., and Wismans, J. (1980) MADYMO - Crash victim simulations, a computerised research and design tool. *Proc. 5th International IRCOBI Conference on the Biomechanics of Impact*, ed. J.P. Cotte and A. Charpenne, 1-13. Bron, France: IRCOBI.
- Manary, M.A., Schneider, L.W., Flannagan, C.C., and Eby, B.H. (1994). *Evaluation of the SAE J826 3-D manikin measures of driver positioning and posture*. SAE Technical Paper 941048. Warrendale, PA: Society of Automotive Engineers, Inc.
- Matsuhashi, K. (1991). Improvement of seating comfort. In *Proc. of the 6th International Pacific Conference on Automotive Engineering, Volume 1*, 625-633. Seoul: Korea Society of Automotive Engineers.
- Matsuoka, Y., and Hanai, T. (1988). *Study of comfortable sitting posture*. SAE Technical Paper 880054. Warrendale, PA: Society of Automotive Engineers, Inc.
- McConville, J.T., Churchill, T.D., Kaleps, I., Clauser, C.E., and Cuzzi, K. (1980). *Anthropometric relationships of body and body segment moments of inertia*. Report no. AMRL-TR-80-119. Wright Patterson Air Force Base, OH: Aerospace Medical Research Laboratories.
- McGill, S., Seguin, J., and Bennett, G. (1994). Passive stiffness of the lumbar torso in flexion, extension, lateral bending, and axial rotation: Effect of belt wearing and breath holding. *Spine* 19(6): 696-704.
- Meldrum, J.F. (1965). *Automobile driver eye position*. SAE Technical Paper 650464. New York, NY: Society of Automotive Engineers, Inc.
- Mourant, R.R., Pak, T., and Moussa-Hamouda, E. (1978). *Dynamic eye positions by vehicle type. Final report of the Second Generation Eyellipse Project*. Detroit, MI: Wayne State University, Department of Industrial Engineering and Operations Research.
- Myal, M. (1958). A new method of accommodation dimensioning. Unpublished report to General Motors Styling Staff and General Motors Institute, Warren, MI.
- Nussbaum, M.A. (1994). Artificial neural network models for analysis of lumbar muscle recruitment during moderate static exertions. Ph.D. dissertation, University of Michigan, Ann Arbor.
- Nussbaum, M.A. and Chaffin, D.B. (1996). Development and evaluation of a scalable and deformable geometric model of the human torso. *Clinical Biomechanics* 11(1): 25-34.

- Nyquist, G.W., and Murton, C.J. (1975). Static bending response of the human lower torso. In *Proc. of the 19th Stapp Car Crash Conference*, 513-541. Warrendale, PA: Society of Automotive Engineers, Inc.
- Parkin, S., Mackay, G.M., and Cooper, A. (1993). How drivers sit in cars. In *Proc. of the 37th Annual Conference of the Association for the Advancement of Automotive Medicine*, 375-388. Des Plaines, IL: Association for the Advancement of Automotive Medicine.
- Philippart, N.L., Kuechenmeister, T.J., Ferrara, R.A., and Arnold, A.J. (1985). *The effects of the steering wheel to pedal relationship on driver-selected seat position*. SAE Technical Paper 850311. Warrendale, PA: Society of Automotive Engineers, Inc.
- Phillipart, N.L., Roe, R.W., Arnold, A.J., and Kuechenmeister, T.J. (1984). *Driver selected seat position model*. SAE Technical Paper 840508. Warrendale, PA: Society of Automotive Engineers, Inc.
- Porter, J.M., Case, K., Freer, M.T., and Bonney, M.C. (1993). Computer-aided ergonomics design of automobiles. In *Automotive Ergonomics*, ed. B. Peacock and W. Karwowski, 43-77. London: Taylor and Francis.
- Pywell, J. F. (1993). Measuring seat comfort. *Automotive Engineering* 101(7): 25-29.
- Raschke, U. (1994). Lumbar muscle activity prediction under dynamic sagittal plane lifting conditions: Physiological and biomechanical modeling considerations. Ph.D. dissertation, University of Michigan, Ann Arbor.
- Rebiffe, R. (1980). General reflections on the postural comfort of the driver and passengers: Consequences on seat design. In *Human Factors in Transport Research. Volume 2 - User Factors: Comfort, the Environment and Behaviour*, ed. D.J. Osborne and J.A. Levis, 240-248. New York: Academic Press.
- Reed, M. P., Saito, M., Kakishima, Y., Lee, N. S., and Schneider, L. W. (1991). *An investigation of driver discomfort and related seat design factors in extended-duration driving*. SAE Technical Paper 910117. (Also in *1991 SAE Transactions* 100.) Warrendale, PA: Society of Automotive Engineers, Inc.
- Reed, M.P. and Schneider, L.W. (1996). Lumbar support in auto seats: Conclusions from a study of preferred driving posture. SAE Technical Paper 960478. In *Automotive Design Advancements in Human Factors: Improving Drivers' Comfort and Performance (SP-1155)*, 19-28. Warrendale, PA: Society of Automotive Engineers, Inc.
- Reed, M.P., Schneider, L.W., and Eby, B.A.H. (1995) *The effects of lumbar support prominence and vertical adjustability on driver postures*. Technical Report UMTRI-95-12. Ann Arbor: University of Michigan Transportation Research Institute.
- Reed, M.P., Schneider, L.W., and Eby, B.A.H. (1995). Some effects of lumbar support on driver seated posture. SAE Technical Paper 950141. In *Human Factors in Vehicle Design: Lighting, Seating and Advanced Electronics (SP-1088)*, 9-20. Warrendale, PA: Society of Automotive Engineers, Inc.
- Reed, M.P., Schneider, L.W., and Eby, B.A.H. (1995). *The effects of lumbar support prominence and vertical adjustability on driver postures*. Technical Report UMTRI-95-12. Ann Arbor: University of Michigan Transportation Research Institute.

- Reed, M.P., Schneider, L.W., and Ricci, L.L. (1994). *Survey of Auto Seat Design Recommendations for Improved Comfort*. Technical Report UMTRI-94-6. Ann Arbor, MI: University of Michigan Transportation Research Institute.
- Reynolds, H.M. (1993). Automotive seat design for sitting comfort. In *Automotive Ergonomics*, ed. B. Peacock and W. Karwowski, 99-116. London: Taylor and Francis.
- Reynolds, H.M. (1994). *Erect, neutral, and slump sitting postures: A study of the torso linkage system from shoulder to hip joint*. Final Report AL/CF-TR-1994-0151. Wright Patterson Air Force Base, OH: Air Force Material Command.
- Reynolds, H.M., Snow, C.C., and Young, J.W. (1981). *Spatial Geometry of the Human Pelvis*. Memorandum Report AAC-119-81-5. Oklahoma City, OK: Federal Aviation Administration, Civil Aeromedical Institute.
- Robbins, D.H. (1985). *Anthropometric specifications for mid-sized male dummy, Volume 2*. Final report DOT-HS-806-716. Washington, D.C.: U.S. Department of Transportation, National Highway Traffic Safety Administration.
- Robbins, D.H. (1985). *Anthropometric specifications for small female and large male dummies, Volume 3*. Final report DOT-HS-806-717. Washington, D.C.: U.S. Department of Transportation, National Highway Traffic Safety Administration.
- Roe, R.W. (1993). Occupant packaging. In *Automotive Ergonomics*, ed. B. Peacock and W. Karwowski, 11-42. London: Taylor and Francis.
- Sanders, M.S. (1981). Peak and sustained isometric forces applied to a truck steering wheel. *Human Factors* 23(6): 655-660.
- Schneider, L.W., Anderson, C.K., and Olson, P.L. (1979). *Driver anthropometry and vehicle design characteristics related to seat positions selected under driving and non-driving conditions*. SAE Technical Paper 790384. Warrendale, PA: Society of Automotive Engineers, Inc.
- Schneider, L.W., Langenderfer, L.S., Flannagan, C.A.C., and Reed, M.P. (1994). *Effects of seat height, cushion length, seatpan angle, and pedal force level on resting foot force and maximum comfortable displacement of the accelerator pedal*. Final Report. Technical Report UMTRI-94-38. Ann Arbor: University of Michigan Transportation Research Institute.
- Schneider, L.W., Robbins, D.H., Pflüg, M.A., and Snyder, R.G. (1985). *Development of anthropometrically based design specifications for an advanced adult anthropomorphic dummy family, Volume 1*. Final report DOT-HS-806-715. Washington, D.C.: U.S. Department of Transportation, National Highway Traffic Safety Administration.
- Seidl, A. (1994). *Das Menschmodell RAMSIS: Analyse, Synthese und Simulation dreidimensionaler Körperhaltungen des Menschen [The man-model RAMSIS: Analysis, synthesis, and simulation of three-dimensional human body postures]*. Ph.D. dissertation, Technical University of Munich, Germany.
- Seidl, G.K., Marchinda, D.M., Dijkers, M., and Soutas-Little, R.W. (1995). Hip joint center location from palpable bony landmarks—A cadaver study. *Journal of Biomechanics* 28(8): 995-998.

- Sheridan, T.B., Meyer, J.E., Roy, S.H., Decker, K.S., Yanagishima, T., and Kishi, Y. (1991). *Physiological and psychological evaluations of driver fatigue during long term driving*. SAE Technical Paper 910116. Warrendale, PA: Society of Automotive Engineers, Inc.
- Snyder, R.G., Chaffin, D.B., and Schutz, R. (1972). *Link system of the human torso*. Report no. AMRL-TR-71-88. Wright-Patterson Air Force Base, OH: Aerospace Medical Research Laboratory.
- Society of Automotive Engineers (1997). *Automotive Engineering Handbook*. Warrendale, PA: Society of Automotive Engineers, Inc.
- Stokes, I. A. F., and Aberly, J. M. (1980). Influence of the hamstring muscles on lumbar spine curvature in sitting. *Spine* 5(6): 525-528.
- Treaster, D.E., and Marras, W.S. (1989). *Seat pressure: Measurement and analysis*. SAE Technical Paper 890849. Warrendale, PA: Society of Automotive Engineers, Inc.
- Verriest, J.P., and Alonzo, F. (1986). A tool for the assessment of inter-segmental angular relationships defining the postural comfort of a seated operator. SAE Technical Paper 860057. In *Passenger Comfort, Convenience and Safety: Test Tools and Procedures*, 71-83. Warrendale, PA: Society of Automotive Engineers, Inc..
- Weichenrieder, A., and Haldenwanger, H.G. (1985). *The best function for the seat of a passenger car*. SAE Technical Paper 850484. Warrendale, PA: Society of Automotive Engineers, Inc.
- Wolfram, S. (1996). *The Mathematica Book, Third Edition*. Champaign, IL: Wolfram Media.
- Woodson, W.E. (1971). *Motor vehicle driver eye position and control reach anthropometrics. Volume 1: Static eye position, control reach and control force studies*. Report DOT HS-800-618. Washington, D.C.: U.S. Department of Transportation, National Highway Traffic Safety Administration.

TEST TARGET (QA-3)



APPLIED IMAGE . Inc
1653 East Main Street
Rochester, NY 14609 USA
Phone: 716/482-0300
Fax: 716/288-5989

© 1993, Applied Image, Inc., All Rights Reserved